

General Disclaimer

One or more of the Following Statements may affect this Document

- This document has been reproduced from the best copy furnished by the organizational source. It is being released in the interest of making available as much information as possible.
- This document may contain data, which exceeds the sheet parameters. It was furnished in this condition by the organizational source and is the best copy available.
- This document may contain tone-on-tone or color graphs, charts and/or pictures, which have been reproduced in black and white.
- This document is paginated as submitted by the original source.
- Portions of this document are not fully legible due to the historical nature of some of the material. However, it is the best reproduction available from the original submission.

~~REPRODUCIBILITY OF THE ORIGINAL PAGE IS POOR.~~

CR - 128526

THE THERMODYNAMIC PROPERTIES
OF NITROGEN FROM 65 TO 2000 K
WITH PRESSURES TO 10,000 ATM

RICHARD T. JACOBSEN

1972



THE THERMODYNAMIC PROPERTIES OF NITROGEN
FROM 65 TO 2000 K WITH PRESSURES TO
10,000 ATMOSPHERES

By
RICHARD T. JACOBSEN

A thesis submitted in partial fulfillment of the
requirements for the degree of
DOCTOR OF PHILOSOPHY

WASHINGTON STATE UNIVERSITY
Program in Engineering Science

1972

To the Faculty of Washington State University:

The members of the Committee appointed to examine the thesis of RICHARD T. JACOBSEN find it satisfactory as to content and form and recommend that it be accepted.

Chairman

ACKNOWLEDGMENTS

The author wishes to acknowledge the assistance of Dr. Richard B. Stewart, Professor and Chairman of the Department of Mechanical Engineering at the University of Idaho in Moscow, Idaho. His experience in data correlation and in thermodynamic property research has provided countless techniques and suggestions which contributed significantly to the success of this work.

Grateful acknowledgment is made to Associate Professor Richard W. Crain, Jr., for his suggestions and encouragement throughout this work. His experience in experimental techniques and in the formulation of equations of state has proven invaluable in providing additional insight into the experimental work which provided the basis for this study. Also acknowledged with thanks for serving on the Doctoral Committee of the author are Professors George T. Austin, Harold W. Dodgen, and David T. Pratt.

In particular, acknowledgment is made to Mr. Albert F. Myers, Research Engineer at the University of Idaho, for his assistance in the computer formulations which are an essential part of the study, and for his ingenuity in the calculations employed. Acknowledgment is made to Mr. Garry L. Rose, graduate student at the University of Idaho, for his development of a multiple stepwise regression technique for least-squares fitting.

Appreciation is expressed to Dr. Dale Everson, Professor of Agriculture at the University of Idaho and to Dr. Thomas P. Bogyo, Associate Professor of Genetics and Associate Statistician, College of Agriculture Research, at Washington State University for their assistance in the application of statistical methods.

Helpful criticisms have been received during the course of this work from many persons. Encouragement and suggestions have been received from Dr. Selby Angus, Scientific Director of the International Union for Pure and Applied Chemistry (IUPAC), Thermodynamics Tables Project Centre, Dr. Lloyd A. Weber and Mr. Robert McCarty of the Cryogenics Division of the National Bureau of Standards, Dr. A. P. Vasserman and Dr. V. A. Rabinovich in the U.S.S.R., and Dr. E. Bender of the Ruhr University in Bochem, Germany.

The present work is an extension of the investigation begun under contract no. CST-962-5-69 from the National Bureau of Standards, Office of Standard Reference Data with Dr. Howard J. White, Jr. as scientific officer. The doctoral dissertation investigation by Dr. Thomas C. Coleman at Worcester Polytechnic Institute, Worcester, Massachusetts, 1971, presented preliminary results of the study and documented the need for further work on the thermodynamic properties of nitrogen. The University of Idaho Department of Mechanical Engineering, of which the author is a faculty member, was under contract during the two year period ending July 1, 1971 with the Office of Standard Reference Data, National Bureau of Standards, U.S. Department of Commerce; to provide an improved set of tables and equations for the thermodynamic properties of nitrogen. This work has continued since July 1, 1971, under contract NAS 9-12078 to the National Aeronautics and Space Administration (NASA)--Manned Spacecraft Center, Systems Management Branch, Houston, Texas with Walter Scott, Jr. as Technical Monitor.

The facilities of the computer centers at the University of Idaho and Washington State University have been used extensively, and the staffs of these centers have contributed materially to the progress of this work. The work was partially supported by Washington State University Computer Center funds allocated to the Washington State University Department of Mechanical Engineering.

A special thanks is given to Mrs. Bonnie Lustig for her assistance in the organization and preparation of this manuscript. Her aptitude has contributed significantly to the appearance and accuracy of this manuscript.

THE THERMODYNAMIC PROPERTIES OF NITROGEN FROM 65 TO 2000 K
WITH PRESSURES TO 10,000 ATMOSPHERES

ABSTRACT

by Richard T. Jacobsen, Ph.D.
Washington State University, 1972

Chairman: Richard W. Crain Jr.

An equation of state, $P = P(\rho, T)$, is presented for liquid and gaseous nitrogen for temperatures from 65 K to 2000 K and pressures to 10,000 atmospheres. All of the Pressure-Density-Temperature ($P-\rho-T$) data available from the published literature have been reviewed, and appropriate corrections have been identified and applied to bring experimental temperatures into accord with the International Practical Temperature Scale of 1968. Comparisons of property values calculated from the equation of state to measured values are included to illustrate the accuracy of the equation in representing the data. The coefficients of the equation of state were determined by a weighted least squares fit to selected published $P-\rho-T$ data and, simultaneously, to C_V data determined by corresponding states analysis from oxygen data, and to data which define the phase equilibrium criteria for the saturated liquid and saturated vapor. The methods of weighting the various data for simultaneous fitting are presented and discussed.

A vapor pressure equation, melting curve equation, and an equation to represent the ideal gas heat capacity, C_p^0 , are also presented. Comparisons of measurements of various thermodynamic properties with values calculated using the equation of state, and the vapor pressure equation and ideal gas heat capacity equation as appropriate, are included. (e.g., specific heats

C_p and C_v , enthalpy, latent heat of vaporization, entropy of the saturated liquid, and velocity of sound.)

The extrapolation of the equation of state to the saturated liquid line and to the melting curve are discussed, and comparisons to the available measurements of density at these conditions are included. Extrapolation of the equation of state to higher and lower temperatures for the vapor is discussed.

The equation of state is estimated to be accurate to within 0.5 percent in the liquid region, to within 0.1 percent for supercritical isotherms up to 1000 atmospheres, and to within 0.3 percent from 1000 to 10,000 atmospheres. The vapor pressure equation is accurate to within ± 0.01 K between the triple point and the critical point. Tables of calculated thermodynamic properties of nitrogen are presented including values of temperature, density, internal energy, enthalpy, entropy, C_v , C_p , and velocity of sound along selected iso-bars. A separate table of the thermodynamic properties of nitrogen at saturation is also included.

TABLE OF CONTENTS

	Page
ACKNOWLEDGMENTS	iii
ABSTRACT	vi
LIST OF TABLES	x
LIST OF ILLUSTRATIONS	xii
NOMENCLATURE	xiii
Chapter	
1. INTRODUCTION	1
2. PRIOR WORK ON THERMODYNAMIC PROPERTIES OF NITROGEN	3
3. THE P- ρ -T DATA AND VAPOR PRESSURE DATA FOR NITROGEN	6
P- ρ -T Data	6
Vapor Pressure Data	6
Critical Point Parameters	6
4. PREPARATION OF THE P- ρ -T AND VAPOR PRESSURE DATA FOR USE IN LEAST SQUARES FITTING OF THE EQUATION OF STATE AND THE VAPOR PRESSURE EQUATION	12
Conversion of Units	12
Determination of Estimated Experimental Uncertainty of the Data	13
Weighting of the Data	16
Temperature Scale Corrections	19
5. THE DETERMINATION OF THE EQUATION OF STATE	27
Preliminary Fitting Procedures	27
Stepwise Multiple Regression Analysis	30
Simultaneous Fitting	32
6. THE VAPOR PRESSURE EQUATION FOR NITROGEN	36
7. COMPARISONS OF THE P- ρ -T DATA TO THE EQUATION OF STATE	39
Data Near the Critical Point	40
Low Temperature Liquid Data	41
High Pressure Data	42

	Page
8. EXTRAPOLATION OF THE EQUATION OF STATE	110
9. IDEAL GAS HEAT CAPACITY	119
10. DERIVED THERMODYNAMIC PROPERTIES	123
11. COMPARISONS OF THE EQUATION OF STATE WITH DERIVED THERMODYNAMIC DATA	126
Calculated Heat Capacity Values	126
Comparisons of the Specific Heat Data	126
Comparisons of Latent Heat Data	133
Comparison of Experimental Enthalpy Values	137
Comparisons of the Entropy of the Saturated Liquid	137
Comparison of Selected Velocity of Sound Data	141
12. CONCLUSIONS AND RECOMMENDATIONS	146
BIBLIOGRAPHY	148
References Containing Experimental Data for Nitrogen . . .	148
General References	155
APPENDIX	
A. THE SELECTION OF P-ρ-T AND VAPOR PRESSURE DATA FOR THE DETERMINATION OF EQUATIONS (22) AND (29)	158
Selection of P-ρ-T Data	159
Selection of Vapor Pressure Data	162
B. DERIVATION OF FUNCTIONS FOR THE USE OF PHASE EQUILIBRIUM CRITERIA IN SIMULTANEOUS LEAST SQUARES FITTING	163
C. HEAT CAPACITY VALUES CALCULATED USING THE PRINCIPLE OF CORRESPONDING STATES	167
D. FUNCTIONS FOR THE CALCULATION OF THERMODYNAMIC PROPERTIES FROM THE EQUATION OF STATE (22)	171
The Equation of State	172
The Isotherm Derivative	173
The Isochore Derivative	174
The Evaluation of Integrals	175
E. TABLES OF THERMODYNAMIC PROPERTIES OF NITROGEN	179

LIST OF TABLES

Table	Page
1. Summary of P- ρ -T Data for Nitrogen	8
2. Summary of Vapor Pressure Data	10
3. Constants and Conversion Factors used in Data Reduction . . .	13
4. Uncertainty Values for Data used in the Determination of the Preliminary Equation of State	15
5. Temperature Scales of P- ρ -T Data Sets	25
6. Temperature Scales of Vapor Pressure Data Sets	26
7. Coefficients for the Interim Equation of State (20)	29
8. Functions for Simultaneous Fitting	33
9. Constraints Imposed on the Equation of State	34
10. Coefficients for the Equation of State (22) for Nitrogen . . .	35
11. Coefficients for Nitrogen Vapor Pressure Equation (29) . . .	37
12. P- ρ -T Data with Density Deviations in Excess of ± 1 Percent	105
13. Root Mean Square Deviations in Density and Pressure of P- ρ -T Data from the Equation of State	109
14. Coefficients for the Ideal Heat Capacity Equation (34) for Nitrogen	120
15. Values of Ideal Gas Heat Capacity, C_p^0/R , from Baehr et al. [84]	121
16. Comparisons of Heat Capacity Data of Kruse and Mackey [54] with Values Calculated from the Equation of State (22) and the Ideal Gas Heat Capacity Equation (34)	129
17. Comparisons of Heat Capacity Data of Mage et al. [55] with Values Calculated from the Equation of State (22) and the Ideal Gas Heat Capacity Equation (34)	131

Table	Page
18. Comparisons of Isochoric Heat Capacity Data at 11.1 moles/liter of Voronel et al. [56] with Values Calculated from the Equation of State (22) and the Ideal Gas Heat Capacity Equation (34)	134
19. Comparison of Latent Heats of Evaporation from [52] and [53] to Values from Equations (22) and (29)	136
20. Comparison of Enthalpy Data by Weiner [57] with Values Calculated from the Equation of State (22) and the Ideal Gas Heat Capacity Equation (34)	138
21. Comparison of Saturated Liquid Entropy Calculated from (1) Equation of State and Ideal Gas Heat Capacity Equation, and (2) Saturated Liquid Heat Capacity Data of Clusius [50] and Wiebe and Brevoort [58]	139
22. Representative Comparisons of Calculated Sonic Velocities to Experimental Values	142

LIST OF ILLUSTRATIONS

Figure	Page
1. Map of the P- ρ -T Data used in the Determination of the Equation of State	11
2. Deviations of Nitrogen Vapor Pressure Equation (29) from Selected Vapor Pressure Data	38
3-235. Density Deviations of Equation (22) from Data of References Indicated	44-102
236-	
241. Density Deviations of Equation (22) from Isochoric Data of Weber [36]	103-104
242. Deviations of Equation of State from Liquid P- ρ -T Data at the Vapor Pressure	114
243. Deviations of Equation (22) from Liquid P- ρ -T Data on the Freezing Line from [39] (Nominal temperatures are given below each point)	115
244. Percentage Contribution of First and Second Virial Terms to Pressure from Eqn. (22) at High Temperature . .	116
245. Percentage Contribution of First and Second Virial Terms to Pressure from Eqn. (22) at Low Temperature . . .	116
246. Percentage Contribution of First Virial (ideal gas) Terms to Pressure from Eqn. (22) at Low Temperature . . .	117
247. Comparison of Second Virial Coefficient from Equation (22) to Experimental Values from the Sources Indicated .	118
248. Constant Pressure Heat Capacity (C_p) of Nitrogen Calculated from Equation of State (22) with Coefficients of Table 10	127
249. Constant Volume Heat Capacity (C_v) of Nitrogen Calculated from Equation of State (22) with Coefficients of Table 10	128
250-	
257. Comparisons of C_v Data for Fluorine from [112] with Values Predicted from Oxygen Equation of [99] using the Principle of Corresponding States (Data are for approximate isochores)	169-170

NOMENCLATURE

P pressure
T temperature
ρ density
 ρ_{STP} standard density (at 273.15 K and 1 atmosphere)
V specific volume = $1/\rho$
R universal gas constant = 0.0820539 liter-atm/g mole-K
U internal energy
H enthalpy
S entropy
L latent heat of vaporization
 C_p specific heat at constant pressure
 C_v specific heat at constant volume
 C_s specific heat at constant saturation
G Gibbs function
 $B(T)$ second virial coefficient
W (Chapter 4) . weighting factor
W (Chapter 11). velocity of sound
 σ experimental uncertainty of individual data point

Superscripts

0 ideal gas property
 ll saturated liquid property

Subscripts

c critical point value
s property at saturation
o reference state property
calc calculated property value
corr. st. . . . corresponding states
data experimental property value
eqn value calculated from specific equation
SV saturated vapor
SL saturated liquid
S saturation value
[] data values from the reference indicated

CHAPTER 1

INTRODUCTION

The increasing use of cryogenic fluids by industry in the United States has led to a considerable number of recent experimental investigations of the thermodynamic properties of nitrogen. In particular, new measurements of properties of nitrogen have extended the range of pressure-density-temperature ($P-\rho-T$) data in the liquid region and at high pressures and temperatures. The National Aeronautics and Space Administration (NASA)--Manned Spacecraft Center has clearly established a need for improved thermodynamic property formulations for nitrogen and oxygen for computer analyses in support of the Space Shuttle and Skylab programs which will employ two-gas atmospheres. In addition to the space-oriented applications for thermodynamic properties of nitrogen where precise design requires accurate property tables, there are large-scale industrial applications where improved design may result in significant reductions in costs of materials and equipment.

At present, no table of thermodynamic properties of nitrogen has been recognized as satisfactory for inclusion in the tables issued by the Office of Standard Reference Data of the National Bureau of Standards. In addition, the International Union for Pure and Applied Chemistry (IUPAC), Thermodynamic Tables Project Centre is interested in obtaining at least two independent concordant property formulations for preparation of an internationally accepted table of nitrogen properties.

The principal objectives of this work were to develop procedures of thermodynamic property formulation by computer analysis, and to prepare a table of properties of nitrogen that represented the best available compilation utilizing all existing measurements of thermodynamic data reported in the scientific literature. It was expected that the methods developed could be easily extended to similar new compilations of properties of oxygen and other atmospheric gases.

The technique used for development of the equation of state was least-squares curve fitting of the equation of state to the available experimental observations over the range of interest. Although many correlations of thermodynamic data use different equations of state to fit discrete regions of the P- ρ -T surface, it was felt that a single equation of state would adequately describe the surface for nitrogen. One of the important requirements of the formulation of an equation of state for nitrogen is ease of programming for use in design work, which is facilitated by a single equation of state. In addition to the extension of the range of values covered by the property tables to 10,000 atmospheres and 2000 degrees Kelvin, improved concordance of the equation of state and vapor pressure equation with calorimetric measurements and other thermodynamic property measurements was accomplished.

CHAPTER 2

PRIOR WORK ON THERMODYNAMIC PROPERTIES OF NITROGEN

In addition to the experimental investigations enumerated in Chapter 3, there have been several compilations and correlations of thermodynamic properties of nitrogen in recent years. Among these are Din [96], Hilsenrath et al. [100], Strobridge [119], Vasserman and Rabinovich [120], Vasserman et al. [121], and Coleman and Stewart [95]. The tables of Din and Hilsenrath et al. are presently outdated by the addition of considerable recent data in certain regions and by new developments in the formulation of the equation of state.

The compilation by Strobridge first used the procedure of fitting a modified Benedict-Webb-Rubin (B-W-R) equation to the available P- ρ -T data, a technique which has been used by others in recent years, and which this work perpetuates. The equation used by Strobridge can be traced historically to the virial form suggested by Kamerlingh Onnes [107] in 1901. This equation is

$$PV = A + \frac{B}{V} + \frac{C}{V^2} + \frac{D}{V^4} + \frac{E}{V^6} + \frac{F}{V^8} + \dots, \quad (1)$$

with $A = RT$, $B = b_1T + b_2 + \frac{b_3}{T} + \frac{b_4}{T^3}$, and C, D, E, and F expressed in the same form as B (i.e., power series expansions in temperature). An improvement of the virial equation was manifested in the Beattie-Bridgeman equation, the form of which is

$$\begin{aligned} P = \rho RT + (B_0 RT - A_0 - RC/T^2)\rho^2 + (-B_0 bRT - A_0 a - RB_0 C/T^2)\rho^3 \\ + RB_0 bC \rho^4/T^2 \end{aligned} \quad (2)$$

with coefficients A_0 , B_0 , a , b , and C determined by the data being represented. A modification of this equation designed to allow surface description at higher densities was the Benedict-Webb-Rubin equation,

$$\begin{aligned} P = & \rho RT + (B_0 RT - A_0 - C_0/T^2)\rho^2 + (bRT - a)\rho^3 + a\alpha\rho^6 \\ & + (c\rho^3/T^2)(1 + \gamma\rho^2) \exp(-\gamma\rho^2), \end{aligned} \quad (3)$$

with coefficients A_0 , B_0 , C_0 , a , b , c , α , and γ determined by fitting the data [91].

In work at the National Bureau of Standards beginning in the late 1950's, it was found that the B-W-R equation was not adequate for the vapor and liquid range of values needed for the cryogenic fluids. This led to the pressure explicit equation for nitrogen reported by Strobridge [119] which was used to calculate properties from 64 K to 300 K and between 0.1 and 200 atmospheres. This equation is

$$\begin{aligned} P = & \rho RT + (n_1T + n_2 + n_3/T + n_4/T^2 + n_5/T^4)\rho^2 \\ & + (n_6T + n_7)\rho^3 + n_8T\rho^4 \\ & + \rho^3(n_9/T^2 + n_{10}/T^3 + n_{11}/T^4) \exp(-\gamma\rho^2) \\ & + \rho^5(n_{12}/T^2 + n_{13}/T^3 + n_{14}/T^4) \exp(-\gamma\rho^2) \\ & + n_{15}\rho^6 \end{aligned} \quad (4)$$

with the values of the n_i and γ determined by fitting the data in the range of applicability.

Further development of the functional form of the equation of state led to the work of Coleman and Stewart [95]. Among the most significant is an equation of state developed for oxygen reported by Stewart [116] which suggests further modifications for higher densities and gives increased accuracy in the range near the critical state. The form of this equation is

$$\begin{aligned}
P = & \rho RT + (n_1 T + n_2 + n_3/T^2 + n_4/T^4 + n_5/T^6)\rho^2 \\
& + (n_6 T^2 + n_7 T + n_8 + n_9/T + n_{10}/T^2)\rho^3 \\
& + (n_{11} T + n_{12})\rho^4 + (n_{13} + n_{14}/T)\rho^5 \\
& + \rho^3(n_{15}/T^2 + n_{16}/T^3 + n_{17}/T^4) \exp(n_{25}\rho^2) \\
& + \rho^5(n_{18}/T^2 + n_{19}/T^3 + n_{20}/T^4) \exp(n_{25}\rho^2) \\
& + \rho^7(n_{21}/T^2 + n_{22}/T^3 + n_{23}/T^4) \exp(n_{25}\rho^2) \\
& + n_{24} \rho^{n_{28}} + 1 (\rho^{n_{28}} - \rho_c^{n_{28}}) \exp[n_{26}(\rho^{n_{28}} - \rho_c^{n_{28}})^2] \\
& + n_{27}(T - T_c)^2].
\end{aligned} \tag{5}$$

This equation was then modified by Coleman and Stewart [95] to represent the P-ρ-T data of nitrogen in the range 0.1 to 100 atmospheres from 70 K to 1000 K. The equation is

$$\begin{aligned}
P = & \rho RT + (n_1 T + n_2 + n_3/T^2 + n_4/T^4)\rho^2 \\
& + (n_5 T^2 + n_6 T + n_7 + n_8/T + n_9/T^2)\rho^3 \\
& + (n_{10} T + n_{11})\rho^4 + (n_{12} + n_{13}/T)\rho^5 \\
& + (n_{14}/T^2 + n_{15}/T^3 + n_{16}/T^4)\rho^3 \exp(-\gamma\rho^2) \\
& + (n_{17}/T^2 + n_{18}/T^3 + n_{19}/T^4)\rho^5 \exp(-\gamma\rho^2) \\
& + (n_{20}/T^2 + n_{21}/T^3 + n_{22}/T^4)\rho^7 \exp(-\gamma\rho^2).
\end{aligned} \tag{6}$$

This formulation represents the available data in the ranges indicated. However, difficulty was encountered in attempts to fit this functional form to data in the range from 1000 to 10,000 atmospheres.

The compilation by Vasserman and Rabinovich [120] covers the range 65 K to 150 K at pressures from 1 to 500 bars for liquid nitrogen. Although the property tables reported in this work appear to be of high accuracy, the formulation would be difficult to use in design work because of the procedures employed in the calculations. The later work by Vasserman et al. [121] covers the range of 70 K to 1300 K at pressures from .25 to 1000 bars for gaseous nitrogen.

CHAPTER 3

THE P- ρ -T DATA AND VAPOR PRESSURE DATA FOR NITROGEN

P- ρ -T Data

The sources of experimental P- ρ -T data that form the basis of this work are summarized in Table 1. This table includes data reported in the literature as saturation line data and measurements of the liquid on the freezing line. Details of the procedures used in data conversion and reduction are presented in Chapter 4. Figure 1 is a map of the P- ρ -T data used in the final formulation of the equation of state.

Vapor Pressure Data

The literature reporting measurements of the vapor pressure of nitrogen is summarized in Table 2. Unit conversion and temperature scale correction procedures for these data sets are also discussed in Chapter 4.

Critical Point Parameters

The values of pressure and temperature at the critical point of nitrogen were selected to be consistent with the measurement of White et al. [122] and with the vapor pressure formulation discussed in Chapter 6. The critical pressure and temperature reported in [122] determined by observing the disappearance of the meniscus at the liquid-vapor interface of a nitrogen sample in a pipet were 33.54 ± 0.02 atmospheres and 126.26 ± 0.04 degrees Kelvin respectively. The critical point density for the equation of state was determined by the method of rectilinear diameters using values of saturated liquid and saturated vapor densities calculated by the simultaneous solution of the

vapor pressure equation and the equation of state each fit to the appropriate data. The development of these equations is discussed in Chapters 5 and 6. The critical point defined in this manner was at 33.555 atmospheres, 11.21 moles/liter, and 126.20 K.

TABLE 1
SUMMARY OF P- ρ -T DATA FOR NITROGEN

Source	Temperature Range (K)	Pressure Range (atm)	Number of Data Points
Vapor			
Amagat [1]	273 - 473	1 - 1000	73
Amagat [2]	273 - 317	1 - 3000	80
Bartlett [3]	273	1 - 1000	9
Bartlett et al. [4]	273 - 673	1 - 1000	52
Bartlett et al. [5]	203 - 293	100 - 1000	42
Benedict [6]	90 - 273	99 - 1500	25
Benedict [7]	98 - 473	981 - 5879	124
Canfield [8]	133 - 273	2 - 300	152
Crain [9]	143 - 273	2 - 500	90
Friedman [10]	80 - 300	1 - 200	201
Hall and Canfield [11]	103, 113	2 - 9	8
Heuse and Otto [12]	273	0.04 - 0.1	8
Holborn and Otto [13]	273 - 373	20 - 99	32
Holborn and Otto [14]	273 - 673	20 - 99	66
Holborn and Otto [15]	143 - 273	20 - 99	24
Kamerlingh Onnes and van Urk [16]	124 - 293	30 - 50	143
Malbrunot and Vodar [17]	473 - 1273	1000 - 4000	63
Malbrunot [18]	473 - 1273	800 - 5000	191
Michels et al. [19]	273 - 423	20 - 80	56
Michels et al. [20]	273 - 423	200 - 3000	147
Miller et al. [21]	294	9 - 260	10
Otto et al. [22]	298 - 423	45 - 400	63
Roberts and Babb [23]	308 - 673	1600 - 10,000	170
Saural [4]	423 - 1073	10 - 900	87
Smith and Taylor [25]	273 - 473	34 - 319	40
Townsend [26]	298, 323	2 - 140	35
Tsiklis and Polyakov [27]	294 - 673	1500 - 10,000	69
Tsiklis [28]	323 - 423	3000 - 10,000	45
Verschouye [29]	273 - 293	25 - 205	36
Liquid			
Cockett et al. [30]	85 - 120	50 - 200	63
Gibbons [31]	72 - 77	22 - 124	17
Golubev and Dobrovolskii [32]	78 - 133	49 - 484	59
Streett and Staveley [33]	77.35 - 120.23	4.32 - 680.46	107
Van Itterbeek and Verbeke [34]	65 - 90	15 - 840	67
Van Itterbeek and Verbeke [35]	77 - 90	79 - 815	13
Weber [36]	80 - 140	30 - 266	76

TABLE 1--continued

Source	Temperature Range (K)	Pressure Range (atm)	Number of Data Points
Saturated Liquid			
Goldman et al. [37]	78 - 125	1 - 32	80
Terry et al. [38]	77 - 104	1 - 10	15
Liquid on the Freezing Line			
Grilly and Mills [39]	64 - 120	76 - 3441	10

TABLE 2
SUMMARY OF VAPOR PRESSURE DATA

Source	Temperature Range (K)	Number of Data Points
Armstrong [40]	66 - 77	74
Cath [41]	64 - 84	8
Crommelin [42]	81 - 125	9
Dodge and Davis [43]	78 - 94	15
Friedman and White [44]	77 - 123	19
Giauque and Clayton [45]	54 - 63	9
Keesom and Bijl [46]	65 - 77	18
Michels et al. [47]	96 - 125	10
Moussa et al. [48]	63 - 77	31
Porter and Perry [49]	90 - 121	12
Weber [36]	65 - 126	47

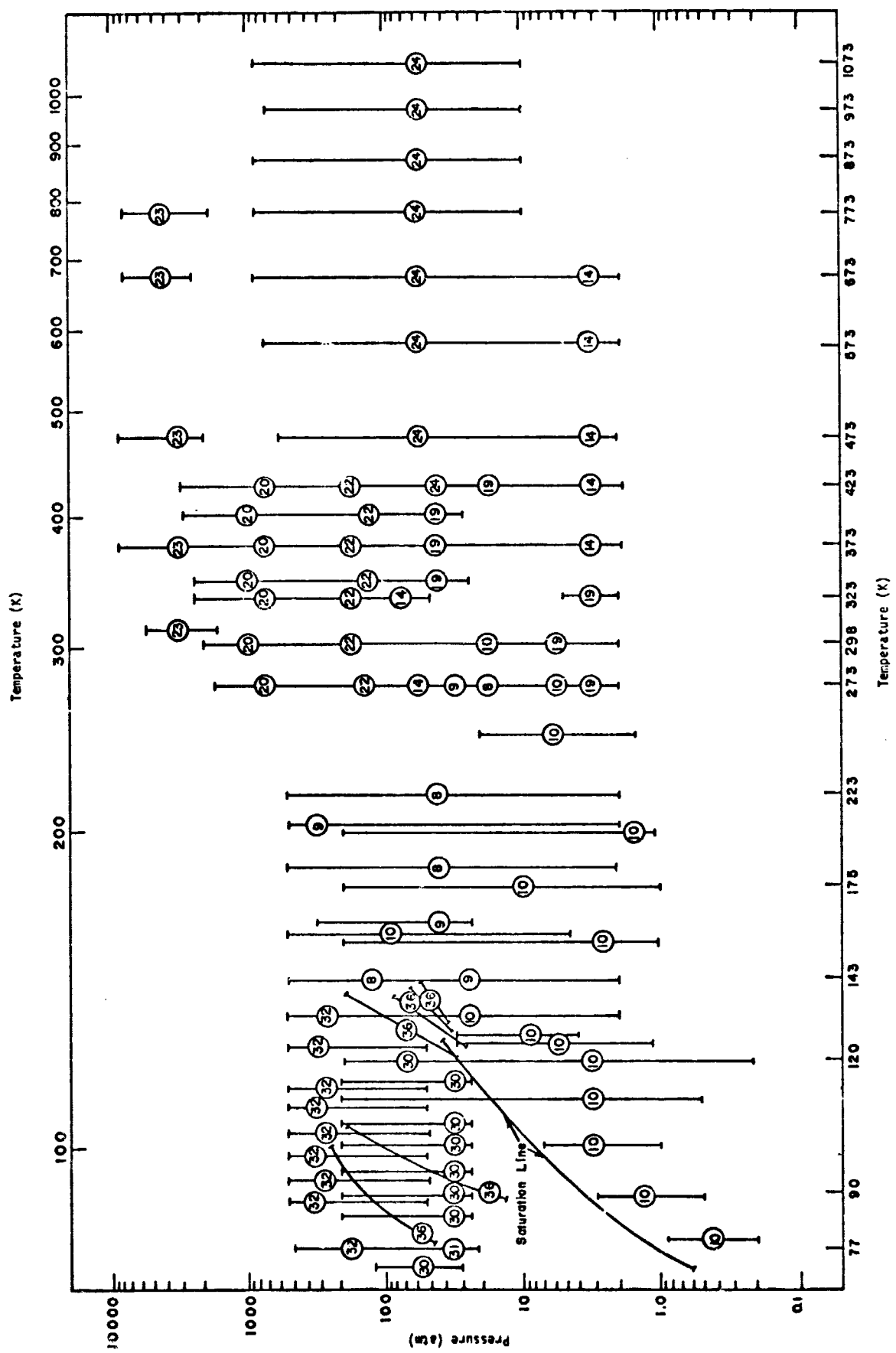


Figure 1---Map of the p - p - T Data used in the Determination of the Equation of State.

CHAPTER 4

PREPARATION OF THE P- ρ -T AND VAPOR PRESSURE DATA FOR
USE IN LEAST SQUARES FITTING OF THE
EQUATION OF STATE AND THE
VAPOR PRESSURE EQUATION

Conversion of Units

In order to facilitate comparison of the results of this investigation to the recent work of Coleman and Stewart [95] the data sets were reviewed, and the units of the experimental data were changed to the following:

Pressure - atmospheres (atm)

Density - moles per liter (moles/liter)

Temperature - degrees Kelvin, IPTS-68 (K)

Table 3 is a listing of conversion factors used in data reduction with the number of significant figures used in this work.

TABLE 3
CONSTANTS AND CONVERSION FACTORS USED IN DATA REDUCTION

Quantity	Value
Molecular Weight of Nitrogen (M)	28.0134 grams/mole
Universal Gas Constant (R)	0.0820539 liter-atm/mole-degree K
Standard Density of Nitrogen	1.25053 moles/liter
Pressure Conversion Factors	760.0 mm Hg/atm [110]
	1.01325 (10^5) $\frac{\text{N}/\text{m}^2}{\text{atm}}$ [110]
	9.80665 (10^4) $\frac{\text{N}/\text{m}^2}{\text{Kg}_f/\text{cm}^2}$ [110]
	1.00 (10^5) $\frac{\text{N}/\text{m}^2}{\text{bar}}$ [110]
Density Conversion Factor	1000.0 cm^3/liter [110]
Temperature Conversion Factor	Degrees K = Degrees C + 273.15 (IPTS-48, IPTS-68)

Determination of Estimated Experimental
Uncertainty of the Data

P-ρ-T Data

An approximate experimental uncertainty in density for each data set was used to calculate weighting factors for data points incorporated in a weighted least-squares fit of the equation of state. The results of many of the experimental investigations included estimates of the accuracy of the reported measurements, which served as a guide in the initial estimates of the uncertainty of these data. Estimated uncertainties of the various data sets given by Sengers [115], Din [96], and Vasserman and Rabinovich [120] were used when estimates by the experimenter were inadequate or unavailable. In most cases the values of experimental uncertainty were estimated as percentages in

density. When no independent estimate of uncertainty was available, an estimated uncertainty in density was based on the precision of a preliminary fit to the available data including the set being examined. The uncertainty values in Table 4 represent the estimates used in preliminary weighting of the data for investigating the functional form of the equation of state. The weighting techniques employed in this work are detailed in the following section. When data were found to be discordant in specific regions, it was necessary to select certain data for use in determining the coefficients of the equation of state as discussed in Appendix A.

Vapor Pressure Data

For the vapor pressure data, preliminary calculations indicated that an unweighted fit to selected data produced smaller deviations in temperature from data values than a weighted fit. After a careful investigation of weighting vapor pressure data points using uncertainties in temperature and in pressure, equal weights of unity were assigned to all data values used in the vapor pressure fit. As a consequence, no estimated uncertainties for the vapor pressure data are reported here. Appendix A includes a discussion of the selection of data for use in determining the vapor pressure equation.

TABLE 4

UNCERTAINTY VALUES FOR DATA USED IN THE
DETERMINATION OF THE PRELIMINARY
EQUATION OF STATE

Source	Uncertainty in Density (percent)
Vapor	
Bartlett et al. [5]2
Benedict [6]3
Benedict [7]3
Canfield [8]15
Crain [9]1
Friedman [10]1
Hall and Canfield [11]39 at 103 K .55 at 113 K
Holborn and Otto [14]05
Michels et al. [19]01
Michels et al. [20]01 below 1000 atm .1 above 1000 atm
Miller et al. [21]1
Otto et al. [22]01
Robertson and Babb [23]05
Saurel [24]1
Tsiklis and Polyakov [27]	1.0
Tsiklis [28]	1.0
Liquid	
Gibbons [31]15
Golubev and Dobrovolskii [32]1
Streett and Staveley [33]1
Van Itterbeek and Verbeke [34], [35]1
Weber [36]15

Weighting of the Data

P-ρ-T Data

Preliminary weighting for fitting the equation of state was accomplished using the estimated uncertainties in density assigned to each data set. To express the deviation of the dependent variable in the fit (in this case, pressure) as a function of the deviation of the independent variables (temperature and density) the error propagation formula was employed in the specific form below:

$$\sigma_p^2 = \left[\sigma_p \left(\frac{\partial P}{\partial \rho} \right)_T \right]^2 + \left[\sigma_T \left(\frac{\partial P}{\partial T} \right)_\rho \right]^2 \quad (7)$$

where

σ_p is the uncertainty in pressure, the dependent variable, due to the combined uncertainties in temperature and density,

σ_ρ is the estimated uncertainty in experimental density values for the data set being considered,

σ_T is the estimated uncertainty in experimental temperature for the data set,

and the partial derivatives, $(\frac{\partial P}{\partial \rho})_T$ and $(\frac{\partial P}{\partial T})_\rho$, are taken from an equation of state which is known to describe the surface.

In the preliminary work the nitrogen equation from Coleman and Stewart [95] was used for calculating these partial derivatives.

The weighting factor to be applied to each data point in performing a least squares fit to the data was calculated from the following equation:

$$W = \frac{1}{\sigma_p^{-2} + \sigma_T^{-2}} \quad (8)$$

where

W is the weighting factor,

σ_p is the uncertainty in the pressure due to uncertainty in the independent variable measurements calculated from (7),

and σ_p is the uncertainty in the pressure due to experimental inaccuracy.

The weights applied to the data using the error propagation formula were calculated by assigning an estimated uncertainty to the value of density at each data point which was then used to determine an uncertainty in pressure for each point. The weighting function used for preliminary weighting was:

$$W = \frac{1}{\sigma_p (\frac{\partial P}{\partial \rho})_T^2} \quad (9)$$

The weights used for the P- ρ -T data were reviewed and changed several times during the development of the equation of state. In addition, data sets found to be in disagreement with one another were reviewed, and the data considered less accurate were removed from the compiled data set used for establishing the equation.

After the development of the interim functional form of the equation of state (21) (further discussion of this equation is given in Chapter 5), which provided an acceptable fit to the entire range of P- ρ -T data, the behavior of the equation was further examined by calculating derived thermodynamic properties (i.e., enthalpy, entropy, and the heat capacities, C_p and C_v). The equation of state was found to exhibit the correct characteristics for these calculated properties over much of the range of pressure and temperature for which P- ρ -T data were available. (A detailed analysis of this equation is presented in [117].) However, values of heat capacity calculated

using this equation exhibit erratic behavior in the liquid region and near the critical temperature, indicating the need for further modification of the equation of state.

Weights for the further development of the form of the equation of state were, therefore, determined using the root mean square (rms) deviations in pressure along isotherms and isochores from separate fits of the interim equation (21) (Chapter 5) reported in [117] to selected data in the liquid and vapor regions. The rms deviations calculated along isotherms or isochores of data of each author is

$$\text{rms} = \frac{[\sum(P_{\text{calc}} - P_{\text{data}})^2 / N]}{P_{\text{data}}}^{1/2} \quad (10)$$

where

P_{calc} is the pressure calculated from the appropriate liquid or vapor equation of state,

P_{data} is the experimental pressure,

and N is the number of data points on the isotherm or isochore.

The weight applied to each data point was calculated from

$$WT = \frac{1}{(\text{rms} \times P_{\text{data}})} \quad (11)$$

Following the development of the functional form of the equation of state (22) (Chapter 5) using P - ρ - T data, constant volume specific heat data and data to describe the criteria for liquid-vapor equilibrium were added to the compiled P - ρ - T values used for determining the form of the equation, and new coefficients for (22) were determined by a simultaneous least squares fit of these related data as discussed in Chapter 5.

C_V and Saturation Data

The weights applied to the C_V data and to the saturation data used in fitting phase equilibrium criteria were arbitrary, and were specified to make the effects of each of the data points compatible with P- ρ -T points in the same region of temperature and pressure. The coefficients for equation (22) given in Table 10 (Chapter 5) were determined by a simultaneous least squares fit of P- ρ -T data weighted using equation (11), to calculated C_V data weighted by the relation, $WT = 10,000/(C_V)^2$, and to phase equilibrium criteria defined by saturation data weighted with the equation, $WT = 100/(P + 0.01)$.

Temperature Scale Corrections

Identification of Temperature Scales

The data sets used in this investigation span the period of the evolution of several interim uniform temperature scales terminating with the adoption of the International Practical Temperature Scale of 1968 (IPTS-68) by the *Comité International des Poids et Mesures (CIPM)* in October of 1968 [105]. Among the temperature scales identified by the various investigators in addition to the IPTS-68 were the following:

1. IPTS-48, the International Practical Temperature Scale of 1948,
2. NBS-55, the low temperature scale adopted by the National Bureau of Standards in 1955,
3. NPL-61, the scale adopted by the National Physical Laboratory in the United Kingdom in 1961,
4. PRMI-54, the scale adopted by the Physicotechnical and Radiotechnical Measurements Institute of the U.S.S.R. in 1954,
5. CCT-64, a preliminary scale which is a smoothed average reduced scale based upon the NBS-55, NPL-61, PRMI-54, and a scale in use at Pennsylvania State University in 1954, PSU-54,
6. KOL scale, the temperature scale formerly used at the Kamerlingh Onnes Laboratory in Leiden, Netherlands,

7. PTR scale, the scale formerly used at the Physikalisch Technischen Reichsanstalt in Germany, and
8. OSU scale, a helium gas thermometer scale formerly used at the Ohio State University Cryogenic Laboratory.

This list includes the temperature scales used by the experimenters in reporting the P-p-T data and the vapor pressure data.

In the following section details are presented on the temperature scale corrections made for the experimental data to convert all data points to the IPTS-68 scale.

Numerical Corrections for Temperature Scales

IPTS-48

The conversion of data point temperatures assumed to be consistent with IPTS-48 was the most frequent correction required. This correction was defined by Douglas [98]. The lower limit of definition of this scale was approximately 90 K, while the lower limit of the IPTS-68 is about 14 K. The correction is accomplished by equations from [98] in three ranges: 90.188 K to 273.15 K, 273.15 K to 903.89 K, 903.89 K to 1337.58 K.

90.188 K to 273.15 K

For the first range to 273.15 K, the equation employed is:

$$\begin{aligned} T_{68} - T_{48} = & \{[1 + 3.984517(10^{-3})(t_{48}) - 5.855019(10^{-7})(t_{48}) \\ & + 4.35717(10^{-12})(100 - t_{48})(t_{48})^3 - W] 250.97\} / \\ & [1 - 2.9389(10^{-6})(t_{48}) + 4.3741(10^{-9})(75 - t_{48})(t_{48})^2] \end{aligned} \quad (12)$$

where

T_{68} is the IPTS-68 temperature in degrees K,

T_{48} is the IPTS-48 temperature in degrees K,

t_{48} is the IPTS-48 temperature in degrees C,

and W is the standard reference function from [105] calculated by iterative solution of the equation

$$T_{48} = A_0 + \sum_{i=1}^{20} A_i [\ln W(T_{48})]^i \quad (13)$$

where the A_0 and A_i coefficients are as given in [105].

273.15 K to 903.89 K

In the range from 273.15 K to 903.89 K the calculated method is:

$$\begin{aligned} T_{68} - T_{48} &= [4.904(10^{-7})t_{48}(t_{48} - 100)/1 - 2.939(10^{-4})t_{48}] \\ &+ \phi(t_{48}) \end{aligned} \quad (14)$$

$$\begin{aligned} \text{where } \phi &= 0.045[t_{48}/100][(t_{48}/100) - 1][(t_{48}/419.58) - 1] \\ &[(t_{48}/630.74) - 1] \end{aligned} \quad (15)$$

and t_{48} , T_{68} , and T_{48} are as defined above.

903.89 K to 1337.58 K

From 903.89 K to 1337.58 K, the temperature adjustments are made by the equation:

$$\begin{aligned} T_{68} - T_{48} &= [-1.3145 + 1.5016(10^3)t_{48} + 1.5625(10^6)(t_{48})^2]/ \\ &[1 + 4.101(10^4)(t_{48})] \end{aligned} \quad (16)$$

where all parameters are as previously defined. These calculations differ from those reported in [105] and [98] by the use of t_{48} and T_{48} in place of the values t_{68} and T_{68} indicated in the references. The error introduced by this substitution is negligible when compared to the relative uncertainties of the respective definitions of the temperature scales employed, and the temperature difference calculations are considerably simplified by this approx-

imation. Calculated differences employing this procedure agree with those reported in [98] to the number of digits given.

NBS-55, NPL-61, and PRMI-54

Data temperatures reported on the NBS-55, NPL-61, and PRMI-54 scales between temperatures of 14 K and 90.188 K were adjusted by interpolation from tabulated differences given in [89]. These differences are reported for even degree intervals of the IPTS-68 scale over the range above.

CCT-64

This scale was reported to be a smoothed average of the NBS-55, NPL-61, PRMI-54, and PSU-54 scales. The triple point of oxygen was given as 54.352 K and the boiling point of oxygen was 90.1727 K [101]. These fixed points were corrected to the IPTS-68 values of 54.361 K and 90.188 K respectively, and temperatures between these values were adjusted by linear interpolation.

KOL and PTR Scales

Data points reported on both of these temperature scales between the oxygen point and the ice point were corrected by a similar procedure. The oxygen point and the ice point for the scales were taken from [101] and a fixed-point correction was applied using an equation suggested by Ziegler et al. [124].

$$T = (T^* - T_{O_2}^*) [(273.15 - 90.18)/(T_0^* - T_{O_2}^*)] + 90.18 \quad (17)$$

where

T^* is the measured temperature,

$T_{O_2}^*$ is the oxygen point corresponding to the experimental measurements,

T_0^* is the ice point corresponding to the experimental data,
and T is the adjusted temperature.

The values thus determined were assumed to be consistent with IPTS-48. The standard correction for converting these values to IPTS-68 as previously described was then applied to those values.

In correcting data taken at the Kamerlingh Onnes Laboratory (KOL), the values for the experimental oxygen boiling point for the experimental ice point as indicated by Hust [101] were used to bring data temperatures into accord with IPTS-48. These temperatures were then converted to IPTS-68 values.

For correcting temperatures of data points on the PTR scale, values for the experimental ice point and oxygen point were taken from [101] to correspond to the date of the experimental results.

Data reported on the KOL scale between the triple point and boiling point of oxygen were corrected using the following equation:

$$T = (T^* - T_t) [(90.188 - 54.361)/(T_{O_2} - T_t)] + 54.361 \quad (18)$$

where

T^* is the measured temperature,

T_t is the oxygen triple point corresponding to the experimental measurements,

T_{O_2} is the oxygen boiling point corresponding to the experimental data, and T is the corrected temperature.

The values for T_t and T_{O_2} used in the corrections were taken from [101].

OSU

Temperatures reported on the Ohio State Cryogenic Laboratory Temperature Scale were adjusted by first applying a ratio correction for the ice point discrepancy in the scale. This fixed point correction was of the form

$$T_{corr} = T_{meas} \cdot (273.15/273.16) \quad (19)$$

where T_{corr} is the adjusted temperature and T_{meas} is the experimental temperature. The values determined in this manner were assumed to be consistent with IPTS-48, and the standard correction was applied to bring them into accord with IPTS-68.

Tables 5 and 6 list the assumed temperature scales for the data sets used in this investigation. In some cases no temperature scale identification could be made, and no correction was applied, since these data were used for comparison purposes only.

TABLE 5
TEMPERATURE SCALES OF P-ρ-T DATA SETS

Source	Temperature Scale
Vapor	
Amagat [1], [2].	IPTS-48
Bartlett [3]	IPTS-48
Bartlett et al. [4], [5]	IPTS-48
Benedict [6], [7]	IPTS-48
Canfield [8]	IPTS-48
Crain [9]	IPTS-48
Friedman [10]	OSU
Hall and Canfield [11]	IPTS-48
Heuse and Otto [12]	PTR
Holborn and Otto [13], [14], [15]	PTR
Kamerlingh Onnes and van Urk [16]	KOL
Malbrunot and Vodar [17]	IPTS-48
Malbrunot [18]	IPTS-48
Michels et al. [19], [20]	IPTS-48
Miller et al. [21]	IPTS-48
Otto et al. [22]	KOL
Robertson and Babt [23]	IPTS-48
Saurel [24]	IPTS-48
Smith and Taylor [25]	Not identified
Tsiklis and Polyakov [27]	IPTS-48
Tsiklis [28]	IPTS-48
Verchoyle [29]	Not identified
Liquid	
Cockett et al. [30]	<90.18 K, NPL >90.18 K, IPTS-48
Gibbons [31]	NBS-55
Golubev and Dobrovolskii [32]	<90.18 K, PRMI-54 >90.18 K, IPTS-48
Streett and Staveley [33]	<90.18 K, NPL >90.18 K, IPTS-48
Van Itterbeek and Verbeke [34], [35]	Not identified
Weber [36]	IPTS-68
Saturated Liquid	
Goldman et al. [37]	<90.18 K, NPL >90.18 K, IPTS-48
Terry et al. [38]	IPTS-48
Liquid on the Freezing Line	
Grilly and Mills [39]	IPTS-48

TABLE 6
TEMPERATURE SCALES OF VAPOR PRESSURE DATA SETS

Source	Temperature Scale
Armstrong [40].	IPTS-48*
Cath [41].	Not identified
Crommelin [42].	Not identified
Dodge and Davis [43].	Not identified
Friedman and White [44].	OSU
Giauque and Clayton [45].	Not identified
Keesom and Bijl [46].	KOL
Michels et al. [47].	IPTS-48
Moussa et al. [48].	CCT-64
Porter and Perry [49].	Not identified
Weber [36].	IPTS-68

* After fixed point correction of -0.01

CHAPTER 5

THE DETERMINATION OF THE EQUATION OF STATE

Preliminary Fitting Procedures

After the data sets had been prepared by converting units and applying temperature scale corrections to bring the data values into accord with IPTS-68, a preliminary weighted least squares fit of the data to the 22-coefficient equation reported in [95] was made. The deviations in density of calculated values for this equation from data values above 1000 atmospheres were large, and systematic trends were noted in the deviations from data particularly in the liquid region.

Deviations of calculated densities from data values for weighted data sets for early experimental fits indicated that the several data sets in the liquid and high-pressure vapor regions were not concordant. A least squares fit to all of the data in these regions was unacceptable because of systematic trends in properties calculated from the equation. Certain data were removed from the compilation of data used to fit to the equation of state but all data were compared to the resulting equation to preserve the comprehensive nature of the data analysis. (See Appendix A.)

The experimental determination of the functional form of the equation of state utilized a combination of trial-and-error and analytical procedures. Initial forms were postulated by adding terms with higher powers of density to the nucleus of terms suggested by the formulation in [95]. Terms which contained the exponential quantity, $e^{-\gamma p^2}$, were studied to determine the signifi-

cance of the value of γ in the formulation and to evaluate the nature of the contribution of this term in fitting higher density data. It was found that the value of γ had little effect on the quality of the fit of an equation to the available data, and that values of γ between 0.001 and 0.01 produced essentially identical results for the same data. The value of 0.0056 which has been used in this work was taken from [119].

Each exponential term in the equation of state was analyzed by taking its first derivative with respect to density and equating the result to zero to locate the density at which the contribution of the term to the total pressure was a maximum. This procedure allowed the adjustment of the exponential terms to distribute the effect of the contributions of these terms over the range of densities from about 1.2 times the critical density to the maximum density of the available data, a range of from about 15 to 40 moles/liter. This analysis indicated that an equation including exponential terms containing odd powers of ρ in integers from 3 to 13 resulted in a distribution of these maxima over the range of the high density data used in determining the equation of state.

An interim form of the equation of state developed by the procedure described above contained 35 coefficients. This equation is presented below and the coefficients reprinted from [117] are listed in Table 7.

$$\begin{aligned}
 P = & \rho RT + \rho^2(N_1 T + N_2 T^{1/2} + N_3 + N_4/T^{1/2} + N_5/T + N_6/T^2 + N_7/T^3 + N_8/T^4) \\
 & + \rho^3(N_9 T^2 + N_{10} T + N_{11} + N_{12}/T + N_{13}/T^2) \\
 & + \rho^4(N_{14}/T + N_{15}) + \rho^5(N_{16} + N_{17}/T) \\
 & + \rho^3(N_{18}/T^2 + N_{19}/T^3 + N_{20}/T^4) \exp(-\gamma\rho^2) \\
 & + \rho^5(N_{21}/T^2 + N_{22}/T^3 + N_{23}/T^4) \exp(-\gamma\rho^2) \\
 & + \rho^7(N_{24}/T^2 + N_{25}/T^3 + N_{26}/T^4) \exp(-\gamma\rho^2) \\
 & + \rho^9(N_{27}/T^2 + N_{28}/T^3 + N_{29}/T^4) \exp(-\gamma\rho^2) \\
 & + \rho^{11}(N_{30}/T^2 + N_{31}/T^3 + N_{32}/T^4) \exp(-\gamma\rho^2) \\
 & + \rho^{13}(N_{33}/T^2 + N_{34}/T^3 + N_{35}/T^4) \exp(-\gamma\rho^2)
 \end{aligned} \tag{20}$$

where T is the temperature, P the pressure, and ρ the density.

TABLE 7
COEFFICIENTS FOR THE INTERIM EQUATION OF STATE (20)*

Coefficient	Numerical Value	Coefficient	Numerical Value
N_1	$0.442846853539105 \times 10^{-2}$	N_{19}	$-0.111691086112682 \times 10^6$
N_2	$-0.829417233959518 \times 10^{-1}$	N_{20}	$0.131992876308097 \times 10^7$
N_3	0.831816820844281	N_{21}	$-0.107110551745687 \times 10^2$
N_4	$0.789454995207039 \times 10^1$	N_{22}	$-0.280710075038644 \times 10^3$
N_5	$-0.519464730111641 \times 10^3$	N_{23}	$0.103571934551340 \times 10^6$
N_6	$0.486788204145566 \times 10^5$	N_{24}	$-0.324638262862371 \times 10^{-2}$
N_7	$-0.276765813270827 \times 10^7$	N_{25}	$-0.143915062954146 \times 10^1$
N_8	$0.531902528027746 \times 10^8$	N_{26}	$0.232500139742939 \times 10^3$
N_9	$-0.107038956039902 \times 10^{-6}$	N_{27}	$-0.201017505855138 \times 10^{-3}$
N_{10}	$0.274500963709232 \times 10^{-3}$	N_{28}	$0.283301453486397 \times 10^{-1}$
N_{11}	$-0.911499335271588 \times 10^{-1}$	N_{29}	$-0.255833003328750 \times 10^1$
N_{12}	$0.145051669173734 \times 10^2$	N_{30}	$0.126004937195284 \times 10^{-6}$
N_{13}	$0.277646315858169 \times 10^3$	N_{31}	$-0.159463113142953 \times 10^{-4}$
N_{14}	$-0.458649005760810 \times 10^{-6}$	N_{32}	$0.294340278758674 \times 10^{-2}$
N_{15}	$0.138049438981636 \times 10^{-2}$	N_{33}	$-0.246822376653425 \times 10^{-9}$
N_{16}	$0.821404094790335 \times 10^{-4}$	N_{34}	$0.784099910579200 \times 10^{-6}$
N_{17}	$-0.986881710201094 \times 10^{-2}$	N_{35}	$-0.108263295096092 \times 10^{-5}$
N_{18}	$0.137925677998808 \times 10^3$		

$$\gamma = 0.0056; R = 0.0820539 \text{ liter-atm/mole-K}$$

*Coefficients are for temperatures in degrees Kelvin, pressures in atmospheres, and density in moles/liter.

Stepwise Multiple Regression Analysis

Although a satisfactory equation of 35 terms had been developed, no systematic procedure had been employed to ascertain that the best 35 terms were used or that 35 was an optimum number of terms. To systematize the choice of terms to be used in the equation of state for nitrogen, a computer program developed by G. L. Rose [114] was utilized to analyze the following comprehensive equation of state.

$$\begin{aligned}
 P = & \rho RT + \rho^2(N_1T + N_2T^2 + N_3 + N_4/T + N_5/T^2 + N_6/T^3 + N_7/T^4) \\
 & + \rho^3(N_8T^2 + N_9T + N_{10} + N_{11}/T + N_{12}/T^2) \\
 & + \rho^4(N_{13}T^2 + N_{14}T + N_{15} + N_{16}/T + N_{17}/T^2) \\
 & + \rho^5(N_{18}T^2 + N_{19}T + N_{20} + N_{21}/T + N_{22}/T^2) \\
 & + \rho^6(N_{23}/T + N_{24}/T^2) \\
 & + \rho^7(N_{25}/T + N_{26}/T^2) \\
 & + \rho^8(N_{27}/T + N_{28}/T^2) \\
 & + \rho^9(N_{29}/T + N_{30}/T^2) \\
 & + \rho^{11}(N_{31}/T + N_{32}/T^2) \\
 & + \rho^3(N_{33}/T^2 + N_{34}/T^3 + N_{35}/T^4) \exp(-\gamma\rho^2) \\
 & + \rho^5(N_{36}/T^2 + N_{37}/T^4) \exp(-\gamma\rho^2) \\
 & + \rho^7(N_{38}/T^2 + N_{39}/T^3) \exp(-\gamma\rho^2) \\
 & + \rho^9(N_{40}/T^2 + N_{41}/T^3 + N_{42}/T^4) \exp(-\gamma\rho^2) \\
 & + \rho^{11}(N_{43}/T^2 + N_{44}/T^3 + N_{45}/T^4) \exp(-\gamma\rho^2) \\
 & + \rho^{13}(N_{46}/T^2 + N_{47}/T^3 + N_{48}/T^4) \exp(-\gamma\rho^2) \\
 & + \rho^{15}(N_{49}/T^3 + N_{50}/T^4) \exp(-\gamma\rho^2)
 \end{aligned} \tag{21}$$

Equation (21) includes the possible terms that previous experience had indicated might produce an equation appropriate to describe the P- ρ -T surface. The analysis of (21) was then designed to determine the relative significance of these selected 50 terms.

The technique of stepwise multiple regression was utilized to fit a selected data set for nitrogen. The first term for the equation was selected as the one which had the highest correlation coefficient for the data used. The second term was chosen from among the remaining terms to provide the highest correlation coefficient for two terms including the first term as selected above. This procedure was continued until all 50 terms with undetermined coefficients had been utilized in the final fit.

The fitting process was then repeated with 45 terms by deleting the five terms which had the lowest F-statistics of the group of 50, and repeated again with 43 terms after the deletion of two more terms with the least significant F-values. To eliminate further terms which had small or negligible contributions to the fit, the analysis of the F-statistics of the coefficients was continued by deleting one term with each successive fit. This procedure was continued until an equation was obtained with only one term with an F-statistic below the value for significance at the one percent level. This resulted in the equation (22) below, which, when fit to P-ρ-T data for the entire range of available measurements, had 31 coefficients with F-values above the level for significance.

$$\begin{aligned}
 P = & \rho RT + \rho^2(N_1 T + N_2 T^2 + N_3 + N_4/T + N_5/T^2) \\
 & + \rho^3(N_6 T + N_7 + N_8/T + N_9/T^2) \\
 & + \rho^4(N_{10} T + N_{11} + N_{12}/T) \\
 & + \rho^5(N_{13}) \\
 & + \rho^6(N_{14}/T + N_{15}/T^2) \\
 & + \rho^7(N_{16}/T) \\
 & + \rho^8(N_{17}/T + N_{18}/T^2) \\
 & + \rho^9(N_{19}/T^2)
 \end{aligned}$$

$$\begin{aligned}
 & + \rho^3(N_{20}/T^2 + N_{21}/T^3) \exp(-\gamma\rho^2) \\
 & + \rho^5(N_{22}/T^2 + N_{23}/T^4) \exp(-\gamma\rho^2) \\
 & + \rho^7(N_{24}/T^2 + N_{25}/T^3) \exp(-\gamma\rho^2) \\
 & + \rho^9(N_{26}/T^2 + N_{27}/T^4) \exp(-\gamma\rho^2) \\
 & + \rho^{11}(N_{28}/T^2 + N_{29}/T^3) \exp(-\gamma\rho^2) \\
 & + \rho^{13}(N_{30}/T^2 + N_{31}/T^3 + N_{32}/T^4) \exp(-\gamma\rho^2)
 \end{aligned} \tag{22}$$

The 32 coefficient equation fit to the P- ρ -T data alone provided an acceptable representation of the P- ρ -T surface, but further refinements in the values of coefficients N_1 through N_{32} were subsequently made for improving the calculation of derived properties, particularly of specific heats in the liquid range and at temperatures near the critical value. The functional form of the equation was fixed as that of (22).

Simultaneous Fitting

To incorporate related thermodynamic data with the P- ρ -T data in a single determination of the equation of state, procedures were developed for including values of C_V , and the criteria for phase equilibrium between saturated liquid and saturated vapor points in a simultaneous least squares fitting technique. The procedures for including the conditions of phase equilibrium with the method of least squares are described in [92]. The method used allows integration of functions for property calculation along hypothetical isotherms through the two-phase region. This is accomplished by satisfying thermodynamic relations for two-phase equilibrium of a pure substance. In the least squares formulation incorporating P- ρ -T data, heat capacity data, and these equilibrium conditions, the sums of squares of the weighted residuals of the following functions are minimized simultaneously.

Table 8 indicates the functions minimized in simultaneous fitting.

TABLE 8
FUNCTIONS FOR SIMULTANEOUS FITTING

Function	Equation Number
$P = \sum N_i P_i(\rho, T) + \rho RT$	(23)
$C_v = \sum N_i C_i(\rho, T) + C_v^0$	(24)
$\sum N_i P_i(\rho_{SL}, T_S) - \sum N_i P_i(\rho_{SV}, T_S) = (\rho_{SV} - \rho_{SL})RT_S$	(25)
$\sum N_i G_i = P_S \left(\frac{1}{\rho_{SL}} - \frac{1}{\rho_{SV}} \right) + RT \ln \left(\frac{\rho_{SL}}{\rho_{SV}} \right)$	(26)

NOTE: P , ρ , T , and C_v are respectively the pressure, density, temperature, and constant volume heat capacity of data points used in the fit, P_S , T_S , ρ_{SL} , ρ_{SV} , are the saturation pressure, saturation temperature, density of the saturated liquid, and density of the saturated vapor respectively,

the P_i are the individual terms of the equation of state,

$$\text{the } C_i(\rho, T) \text{ are given by } C_i(\rho, T) = \int_0^\rho \frac{T}{\rho^2} \left[\frac{\partial^2 P_i(\rho, T)}{\partial T^2} \right] d\rho, \quad (27)$$

$$\text{the } G_i \text{ are given by } G_i = \int_{\rho_{SL}}^{\rho_{SV}} \left[\frac{P_i(\rho, T_S)}{\rho^2} - \frac{RT_S}{\rho} \right] d\rho, \quad (28)$$

and the N_i are the coefficients of the equation of state to be determined.

The derivations of equations (25) and (26) are presented in Appendix B.

The equation for C_v for oxygen from Goodwin and Weber [99] was used with the principle of corresponding states for estimating values of C_v for nitrogen. (See Appendix C.) The C_v data were used in simultaneous fitting

primarily to give an equation which exhibited proper behavior of the first and second derivatives as evidenced by the behavior of calculated derived properties using these derivatives.

Saturated liquid and saturated vapor densities were required in the formulation of the phase equilibrium criteria. These were calculated from the simultaneous solution of the vapor pressure equation and the interim equation of state both from [117] on intervals of 0.25 degree K between the triple point and the critical point, and two equations of state determined by separate fits to the liquid and vapor regions alone.

The final coefficients for the equation of state were determined by a weighted least squares fit using the criteria outlined above, and constrained to the critical point data of Table 9 using a procedure suggested by McCarty [109].

TABLE 9
CONSTRAINTS IMPOSED ON THE EQUATION OF STATE

Constraint	Numerical Value
Pressure at the critical point.	$P_c = 33.555 \text{ atm}$
Density at the critical point	$\rho_c = 11.21 \text{ moles/liter}$
Temperature at the critical point	$T_c = 126.20 \text{ K}$
Isotherm derivative at the critical point	$(\partial P / \partial \rho)_T = 0$
Second derivative of pressure with respect to density at the critical point.	$(\partial^2 P / \partial^2 \rho)_T = 0$

The coefficients for the constrained equation of state (22) determined as discussed above are presented in Table 10. The functional form of the equation is repeated above the table to facilitate comparison of the values of the coefficients and the respective terms for which they are applicable.

The value of the isochore derivative $(\partial P/\partial T)_P$ for this equation was 1.6569 atm/K. This value was used as a constraint on the slope of the vapor pressure equation at the critical point as discussed in Chapter 6.

$$\begin{aligned}
 P = & \rho RT + \rho^2(N_1T + N_2T^{1/2} + N_3 + N_4/T + N_5/T^2) \\
 & + \rho^3(N_6T + N_7 + N_8/T + N_9/T^2) \\
 & + \rho^4(N_{10}T + N_{11} + N_{12}/T) + \rho^5(N_{13}) \\
 & + \rho^6(N_{14}/T + N_{15}/T^2) + \rho^7(N_{16}/T) \\
 & + \rho^8(N_{17}/T + N_{18}/T^2) + \rho^9(N_{19}/T^2) \\
 & + \rho^{10}(N_{20}/T^2 + N_{21}/T^3) \exp(-\gamma\rho^2) \\
 & + \rho^{11}(N_{22}/T^2 + N_{23}/T^4) \exp(-\gamma\rho^2) \\
 & + \rho^{12}(N_{24}/T^2 + N_{25}/T^3) \exp(-\gamma\rho^2) \\
 & + \rho^{13}(N_{26}/T^2 + N_{27}/T^4) \exp(-\gamma\rho^2) \\
 & + \rho^{14}(N_{28}/T^2 + N_{29}/T^3) \exp(-\gamma\rho^2) \\
 & + \rho^{15}(N_{30}/T^2 + N_{31}/T^3 + N_{32}/T^4) \exp(-\gamma\rho^2)
 \end{aligned} \tag{22}$$

TABLE 10
COEFFICIENTS FOR THE EQUATION OF STATE (22) FOR NITROGEN*

Coefficient	Numerical Value	Coefficient	Numerical Value
N_1	$0.136224769272827 \times 10^{-2}$	N_{17}	$-0.111614119537424 \times 10^{-5}$
N_2	0.107032469908591	N_{18}	$0.353796562233495 \times 10^{-3}$
N_3	$-0.243900721871413 \times 10^{-1}$	N_{19}	$-0.201317691347729 \times 10^{-5}$
N_4	$0.341007449376470 \times 10^{-2}$	N_{20}	$-0.169717444755949 \times 10^{-5}$
N_5	$-0.422374309466167 \times 10^{-4}$	N_{21}	$-0.119719240044192 \times 10^{-6}$
N_6	$0.105098600246494 \times 10^{-3}$	N_{22}	$-0.975218272038281 \times 10^{-2}$
N_7	$-0.112594826522081 \times 10^{-1}$	N_{23}	$0.554639713151823 \times 10^{-5}$
N_8	$0.142600789270907 \times 10^{-3}$	N_{24}	-0.179920450443470
N_9	$0.184698501609007 \times 10^{-5}$	N_{25}	$-0.256582926077184 \times 10^{-1}$
N_{10}	$0.811140082588776 \times 10^{-7}$	N_{26}	$-0.413707715090789 \times 10^{-3}$
N_{11}	$0.233011645038006 \times 10^{-1}$	N_{27}	-0.256245415300293
N_{12}	-0.507752586350986	N_{28}	$-0.124222373740063 \times 10^{-6}$
N_{13}	$0.485027881931214 \times 10^{-4}$	N_{29}	$0.103556535840165 \times 10^{-4}$
N_{14}	$-0.113656764115364 \times 10^{-2}$	N_{30}	$-0.538699166558303 \times 10^{-9}$
N_{15}	-0.707430273540575	N_{31}	$-0.757415412839596 \times 10^{-8}$
N_{16}	$0.751706648852680 \times 10^{-5}$	N_{32}	$0.585367172069521 \times 10^{-7}$

$$\gamma = 0.0056; \quad R = 0.0820539 \text{ liter-atm/mole-K}$$

*Coefficients are for temperature in degrees Kelvin, pressure in atmospheres, and density in moles/liter.

CHAPTER 6

THE VAPOR PRESSURE EQUATION FOR NITROGEN

The literature reporting measurements of the vapor pressure of nitrogen was summarized in Table 2. A preliminary study of the vapor pressure data, and a preliminary vapor pressure equation were reported in [95]. Following the development of the equation for the vapor pressure of oxygen using calorimetric as well as vapor pressure measurements [111], a new vapor pressure equation was developed for nitrogen. This equation is a result of a least squares fit to the nitrogen data of Armstrong [40], and Weber [36]. These data were used since they cover the range from the triple point to the critical point, have a high precision, and appear to be the most accurate measurements available. The form of the vapor pressure equation used in this work is

$$\ln(P) = N_1/T + N_2 + N_3T + N_4(T_C - T)^{1.95} + N_5T^3 + N_6T^4 + N_7T^5 + N_8T^6 + N_9 \ln(T) \quad (29)$$

where $T_C = 126.20$ K, the critical point temperature, T is the saturation temperature, and P is the vapor pressure. The coefficients for this equation for temperature in degrees Kelvin and pressure in atmospheres are given in Table 11 below.

A comparison of the vapor pressure equation (29) with the selected data sets used in determining the coefficients is given in Figure 2.

The equation has been constrained to the critical point temperature of 126.20 K, the critical pressure of 33.555 atmospheres, and the slope dP/dT of

1.6569 atm/K consistent with the value of $(\partial P/\partial T)_P$ at the critical point from the constrained equation of state reported in Chapter 5.

TABLE 11
COEFFICIENTS FOR NITROGEN VAPOR PRESSURE EQUATION (29)*

Coefficient	Numerical Value	Coefficient	Numerical Value
N_1	$0.8394409444 \times 10^{-4}$	N_6	$-0.5944544662 \times 10^{-5}$
N_2	$-0.1890045259 \times 10^{-4}$	N_7	$0.2715433932 \times 10^{-7}$
N_3	$-0.7282229165 \times 10^{-1}$	N_8	$-0.4879535904 \times 10^{-10}$
N_4	$0.1022850966 \times 10^{-1}$	N_9	$0.5095360824 \times 10^{-3}$
N_5	$0.5556063825 \times 10^{-3}$		

*Coefficients are for temperature in degrees Kelvin, and pressure in atmospheres.

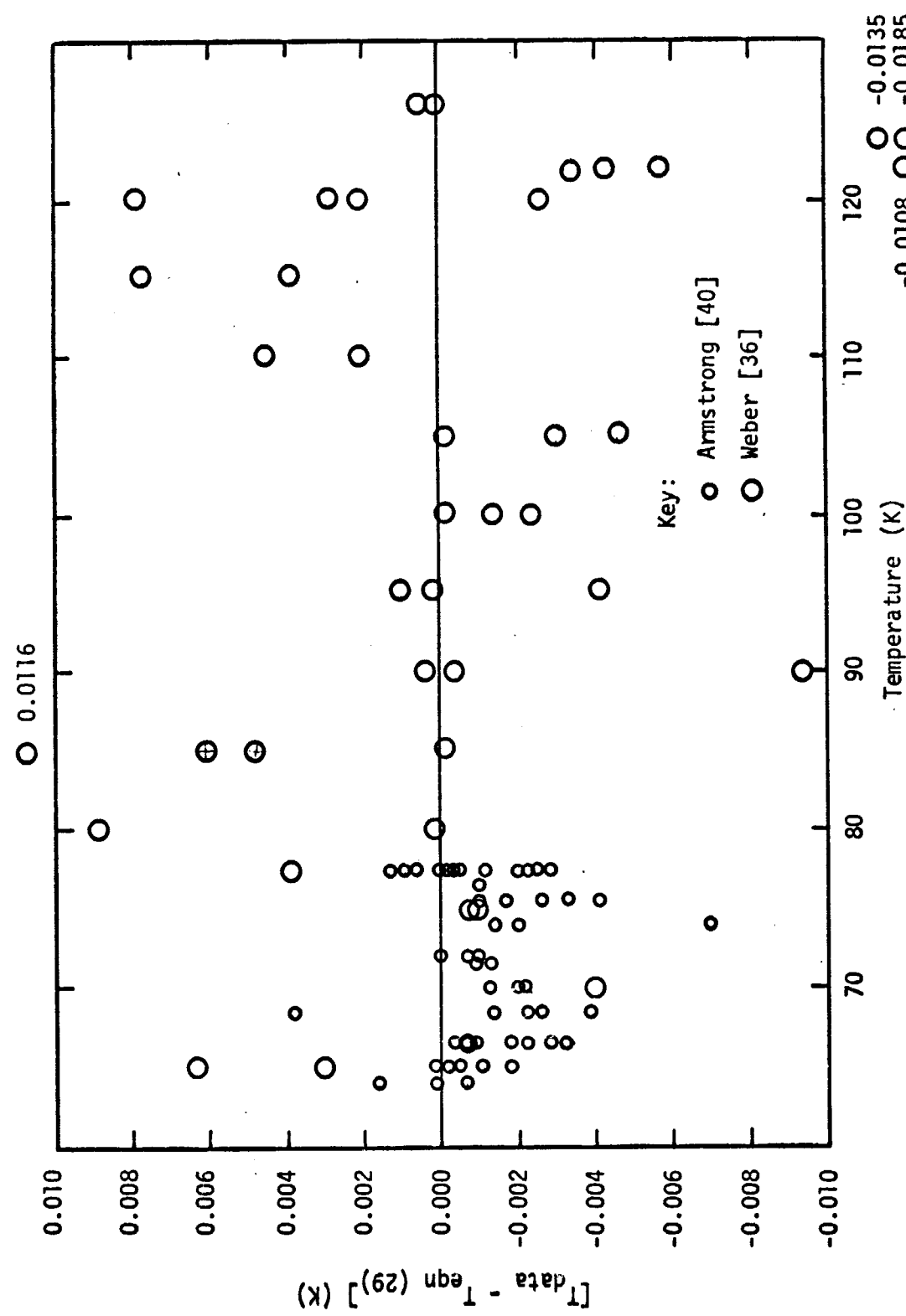


Figure 2.--Deviations of Nitrogen Vapor Pressure Equation (29) from Selected Vapor Pressure Data.

CHAPTER 7

COMPARISONS OF THE P-ρ-T DATA TO
THE EQUATION OF STATE

Figures 3 through 241 illustrate the accuracy of the equation of state (22) in representing the available experimental data for nitrogen. In the determination of the equation of state, data sets were selected based on concordance among data from various experimenters in the same region of the P-ρ-T surface, and on relative agreement with trends established by reliable data defining adjacent regions. Data found to be in disagreement in the determination of preliminary equations of state are discussed in Appendix A. The P-ρ-T data set utilized in the calculation of the coefficients in Table 10 consisted of 1247 weighted data points from [8], [30], [9], [10], [31], [32], [14], [19], [20], [22], [23], [24], and [36]. The remainder of the data illustrated in the figures are included for comparison.

Figures 3 through 130 are comparisons of the percent density deviation, $[(\rho_{\text{exp}} - \rho_{\text{calc}})/\rho_{\text{exp}}] \times 100$, along approximate isotherms for data used in the determination of the coefficients in Table 10. The quantity ρ_{exp} represents the observed density reported by the experimenter at a particular temperature and pressure, and ρ_{calc} is the density calculated from equation (22) for each experimental temperature and pressure. Figures 131 through 235 illustrate the density deviations of experimental data which were not used in the determination of the coefficients for equation (22). In addition to the data illustrated in these figures, the density deviations for some data points exceeded the value of 1 percent. Table 12 is a listing of these data including the density deviation of each point.

The equation of state generally shows agreement with P- ρ -T data within the experimental uncertainty of the measured values, except in the vicinity of the critical point, in the low temperature liquid region, and in the high pressure supercritical region where experimental uncertainties are large. Table 13 lists the root mean square deviations in pressure and in density for the various P- ρ -T data sets. The following discussions apply to the data illustrated in Figures 3 through 235 and to that listed in Table 12.

Data Near the Critical Point

The data of Friedman [10] (Figures 25 through 30), Weber [36] (Figures 120 through 125), and Kamerlingh Onnes and van Urk [16] (Figures 199 through 201) illustrate the imprecision of the data in the region of the critical point between temperatures of 120 K and 130 K. This is a difficult region for precise experimental measurements, and a difficult region for fitting the equation of state. The data of [16] were not incorporated in the development of the equation because they are limited to pressures between 35 and 63 atmospheres, and there are other data of at least equal precision in this region. Systematic deviations between the equation and the data appear to be present for isotherms above the critical temperature in the data of Canfield [8] and that of Crain [9]. This is evidenced between 30 and 60 atmospheres in Figures 3 and 4 for the data of Canfield at 133.1 K and 143.1 K, respectively, and in Figure 17 which illustrates a systematic deviation of nearly 0.5 percent at pressures between 40 and 70 atmospheres for the data of Crain at 143.1 K. With the exception of these systematic deviations the equation of state appears to fit the data within the experimental uncertainty of the measurements in this region.

Low Temperature Liquid Data

The data of Cockett et al. [30] for the low temperature liquid are shown in Figures 9 through 16. The deviations are negative at temperatures below 105 K, and are positive at 110 K and above with the exception of one value at 120 K. The deviations for isotherms between 85 K and 115 K are all within ± 0.5 percent.

The data of Golubev and Dobrovolskii [32] are illustrated in Figures 39 through 48 including one supercritical isotherm in Figure 48. The data at 77.3 K and 78.1 K in Figures 39 and 40 illustrate an apparent systematic trend with deviations up to 0.5 percent at pressures above 400 atmospheres. Systematic deviations are evident in Figures 44 through 48 for temperatures between 98.2 K and 133.1 K, where the deviations at pressures below 100 atmospheres reach about + 1.0 percent, and at pressures in excess of 400 atmospheres are as large as -0.5 percent.

The data of Gibbons [31] are illustrated in Figures 37 and 38. These data appear consistent with the equation of state for the two isotherms at 72.3 K and 77.9 K.

The density deviations of the equation of state from the data of Weber [36] are illustrated on isotherms in Figures 92 through 130. These data are also compared for approximate isochoric values between 9 and 28 moles/liter in Figures 236 through 241. (At 9.47 moles/liter the state is vapor, while all other isochores are for liquid values.) The isochoric density deviation plots show the minimum and maximum temperatures for each isochore. These data exhibit general agreement with the equation of state, although the isochoric plots indicate a systematic deviation with a maximum discrepancy of -2.4 percent for the 9.47 moles/liter vapor isochore and systematic trends are evident

in Figures 237 and 238 for the 11.2 and 16.0 moles/liter isochores, respectively. The data of [36] appear to be more precise than the other liquid data available for nitrogen.

The liquid data of Streett and Staveley [33] are illustrated in Figures 211 through 218 for isotherms between 77.4 K and 120.2 K. Systematic trends in the deviations are apparent in Figure 211 at 77.4 K and above 104 K in Figures 214 through 218, while the data at 90.6, 95.6, and 100.1 K appear to have a constant deviation from the equation of state. The data of Streett and Staveley indicate general agreement with the equation of state although these points were not used in the least squares fit to determine the equation.

The data of Van Itterbeek and Verbeke [34] shown in Figures 227 through 231 for isotherms between 65 K and 91 K exhibit systematic deviations with a maximum of ± 0.5 percent below 90.6 K. The data of [35] by the same authors illustrated in Figures 232 and 233 exhibit systematic deviations from the equation of up to 1 percent. The isotherms of [35] at 77.3 K and 90.3 K are not consistent with the isotherms at 77.9 K and 90.6 K from [34]. The data of Van Itterbeek and Verbeke were not used in the development of the equation of state.

High Pressure Data

There is a lack of concordance among the data sets above 1000 atmospheres. In general, the equation of state developed here fits the data of Saurel [24] shown in Figures 84 through 91, and that of Robertson and Babb [23] illustrated in Figures 77 through 83, which were judged to be most accurate. The high pressure data of Malbrunot [18] and Malbrunot and Vodar [17] shown in Figures 180 through 197, are not in agreement with the equation of state or with the selected data. In addition, there are inconsistencies between the data from [17] and [18], which contain results from the same experimenters.

The data of Tsiklis and Polyakov [27] and Tsiklis [28] exhibit systematic deviations from the equation of state of as much as 1 percent, as illustrated in Figures 222 through 226. The high pressure data of Benedict [7] are less precise than those of other authors as shown in Figures 157 through 168, and were not used in the determination of the equation of state.

PERCENT DENSITY DEVIATION

FIGURE 3

133.1 K

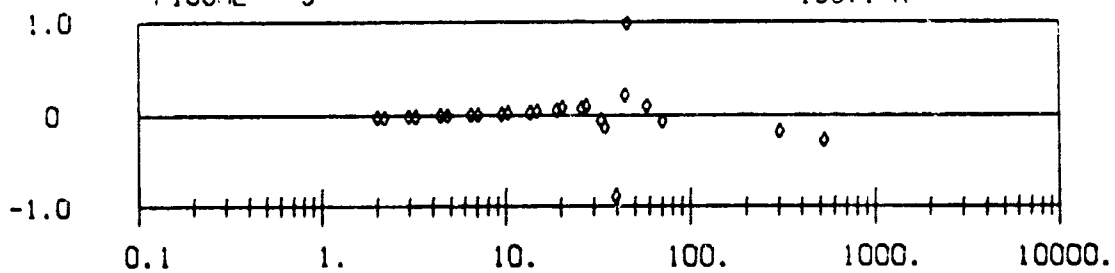


FIGURE 4

143.1 K

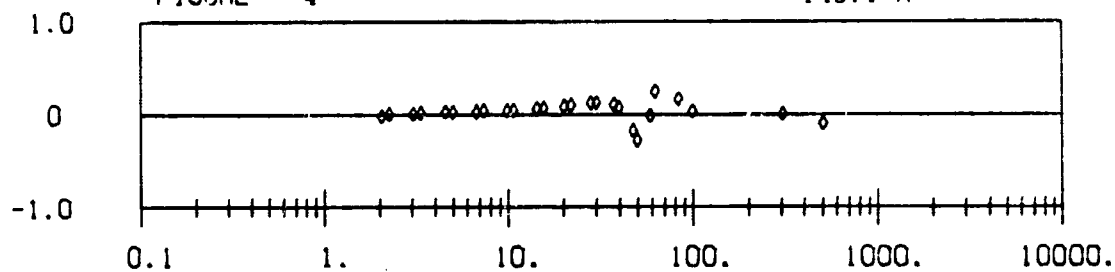


FIGURE 5

158.2 K

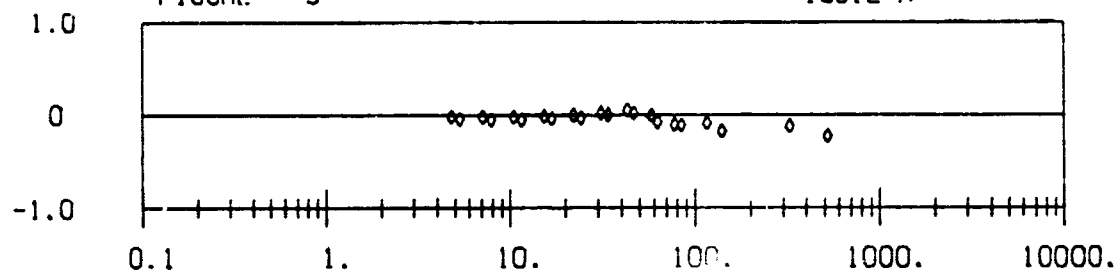
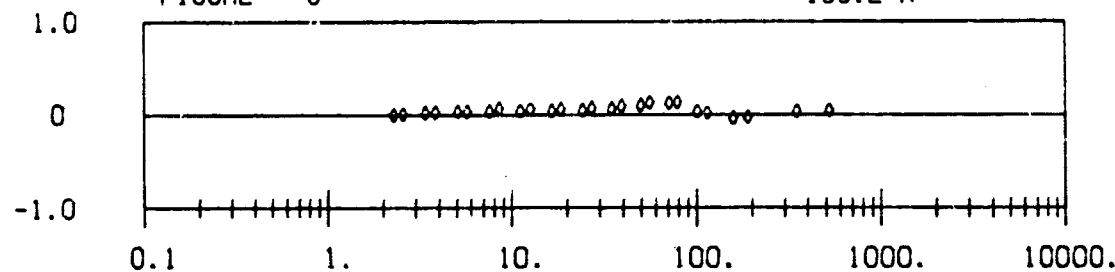


FIGURE 6

183.2 K

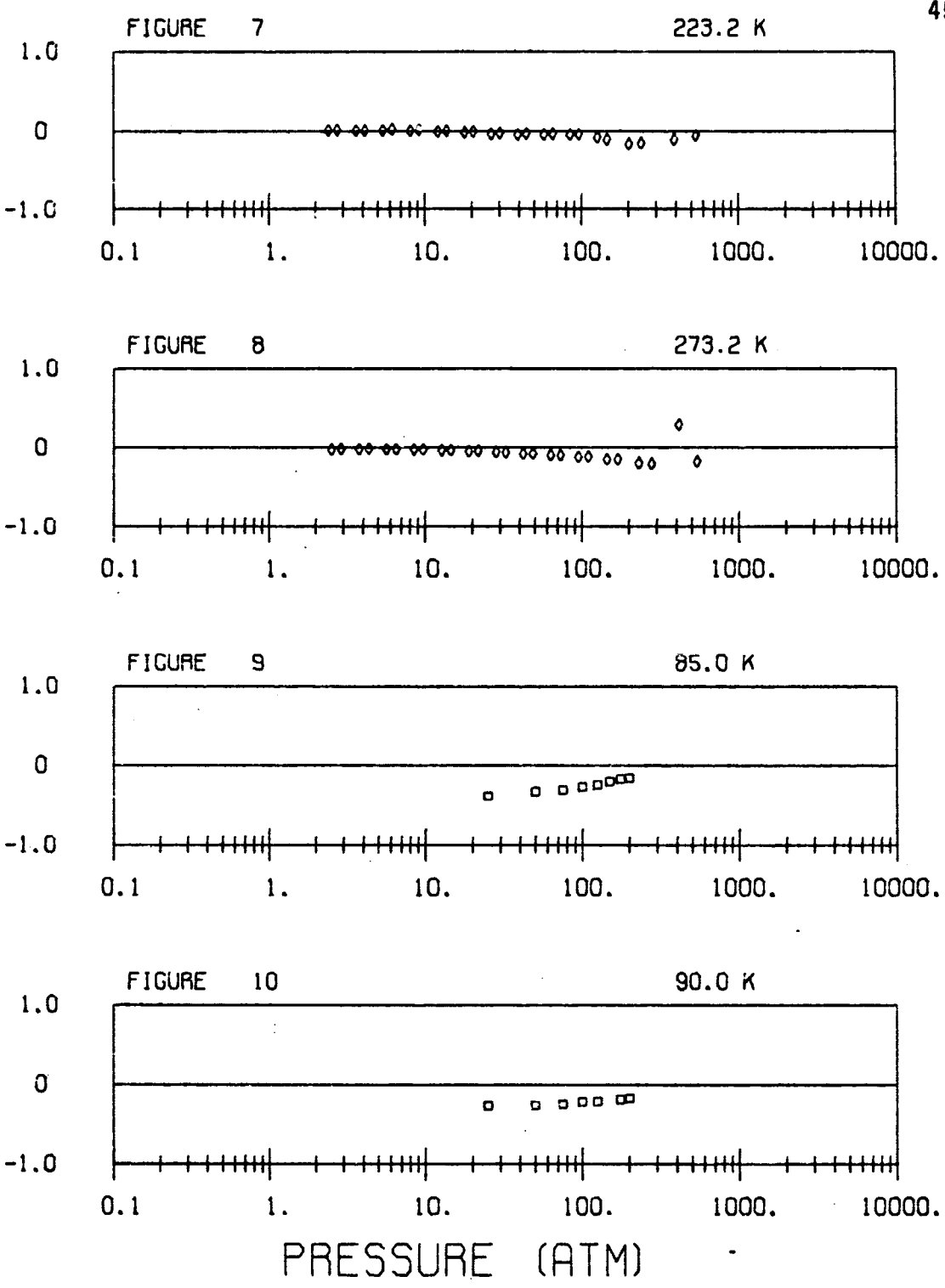


PRESSURE (ATM)

♦ CANFIELD C8]

Density Deviations of Equation (22) from Data of References Indicated.

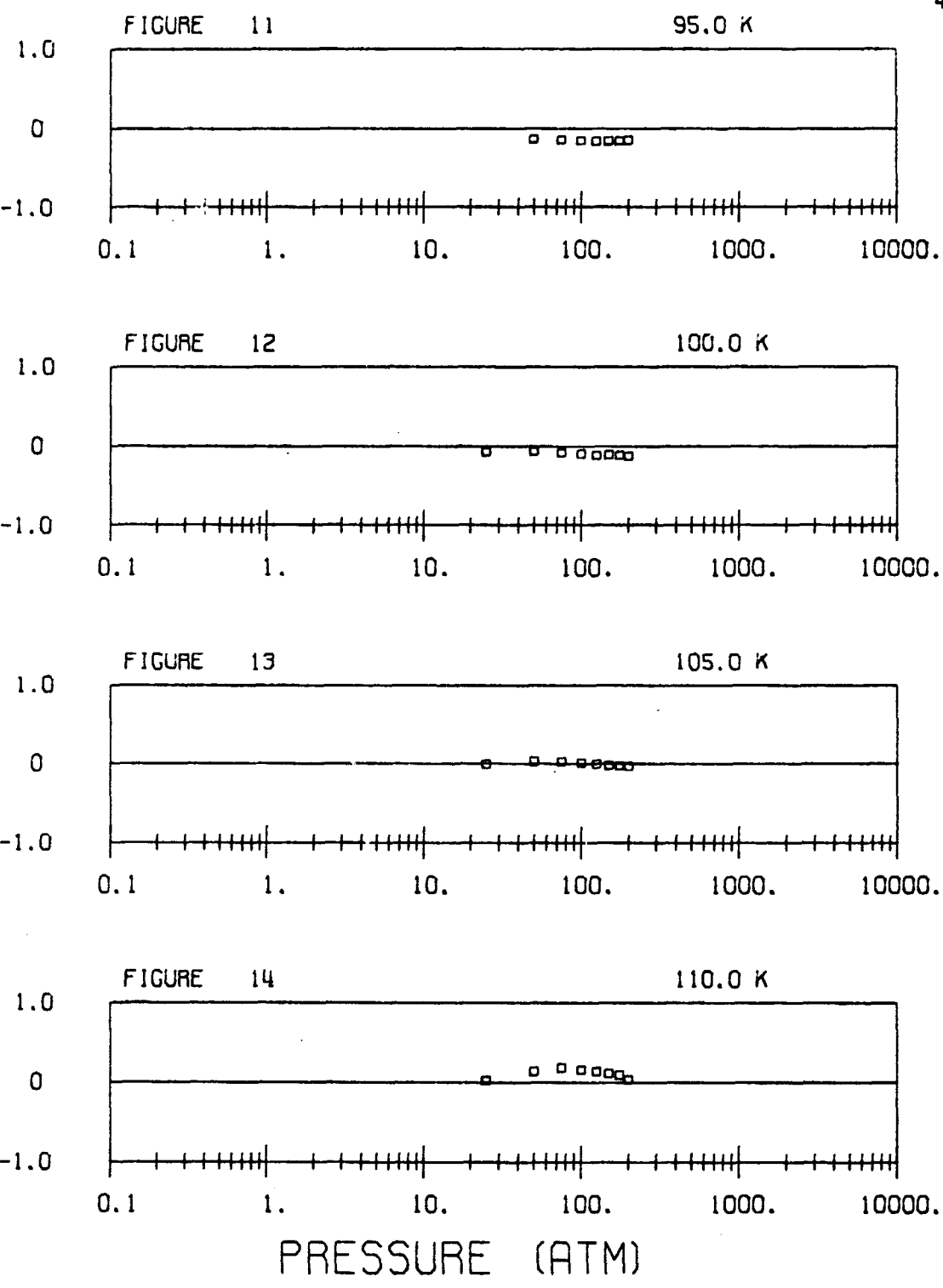
PERCENT DENSITY DEVIATION



♦ CANFIELD [8] □ COCKETT [30]

Density Deviations of Equation (22) from Data of References Indicated.

PERCENT DENSITY DEVIATION



□ COCKETT C303

Density Deviations of Equation (22) from Data of References Indicated.

PERCENT DENSITY DEVIATION

FIGURE 15

115.0 K

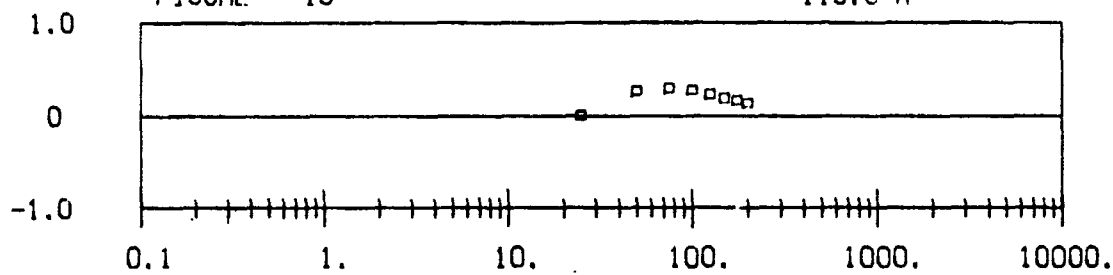


FIGURE 16

120.0 K

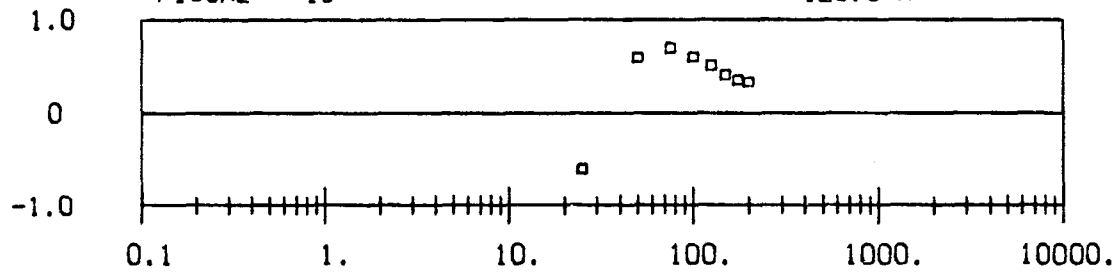


FIGURE 17

143.1 K

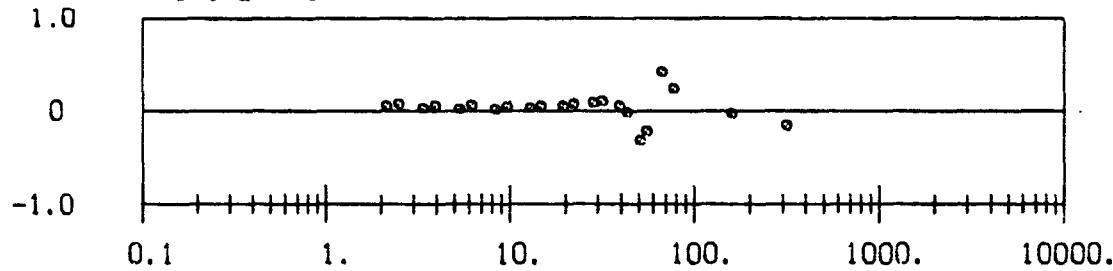
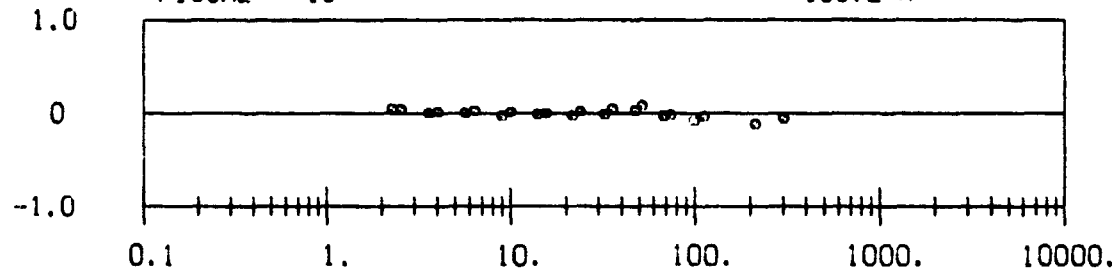


FIGURE 18

163.2 K



PRESSURE (ATM)

□ COCKETT

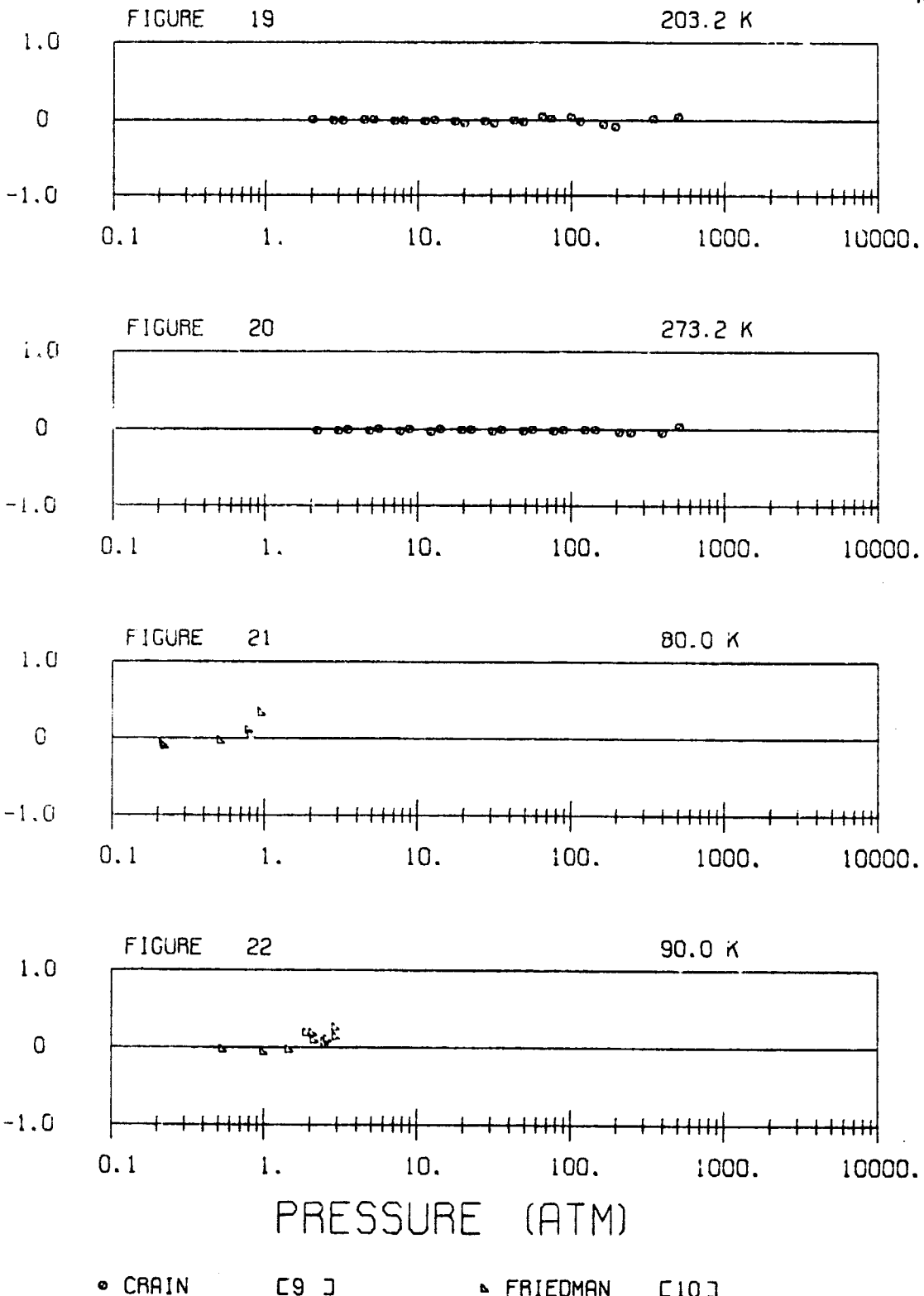
[30]

● CRAIN

[9]

Density Deviations of Equation (22) from Data of References Indicated.

PERCENT DENSITY DEVIATION



• CRAIN [9]

▲ FRIEDMAN [10]

Density Deviations of Equation (22) from Data of References Indicated.

PERCENT DENSITY DEVIATION

FIGURE 23

100.0 K

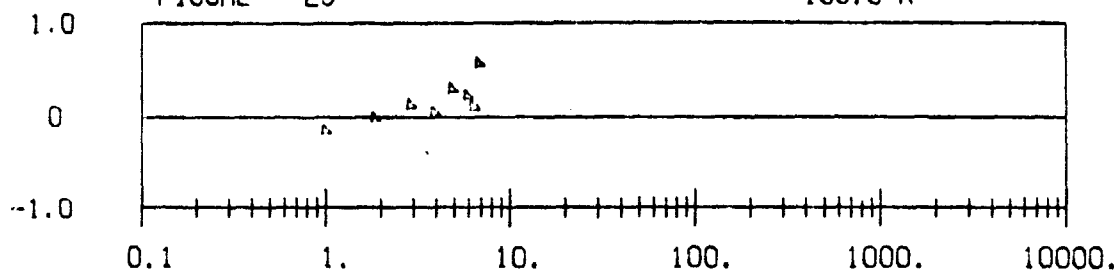


FIGURE 24

110.0 K

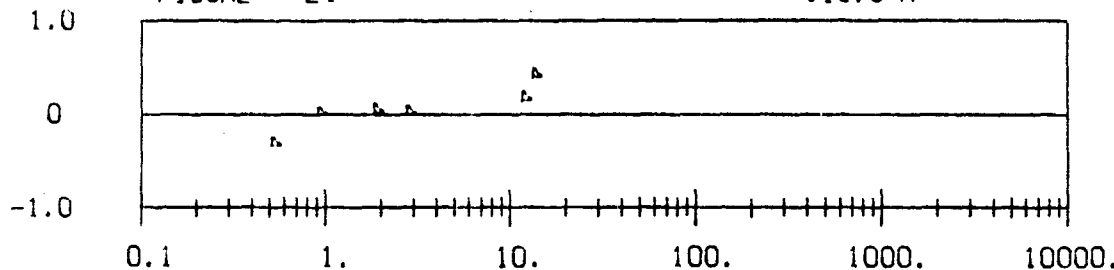


FIGURE 25

120.0 K

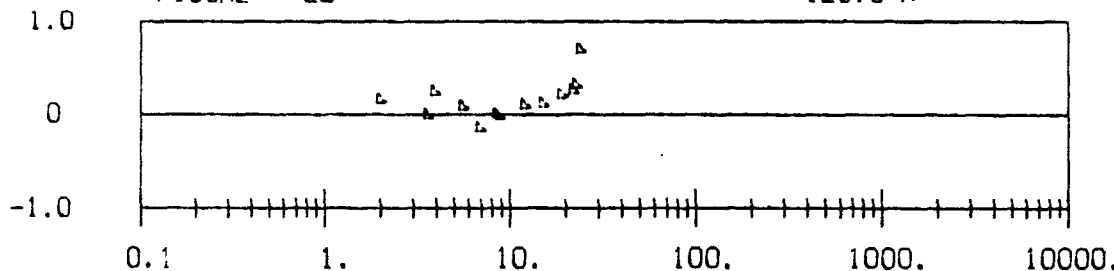
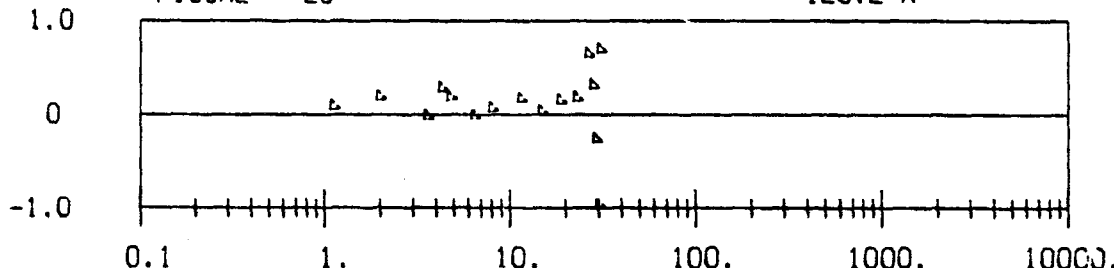


FIGURE 26

125.2 K



PRESSURE (ATM)

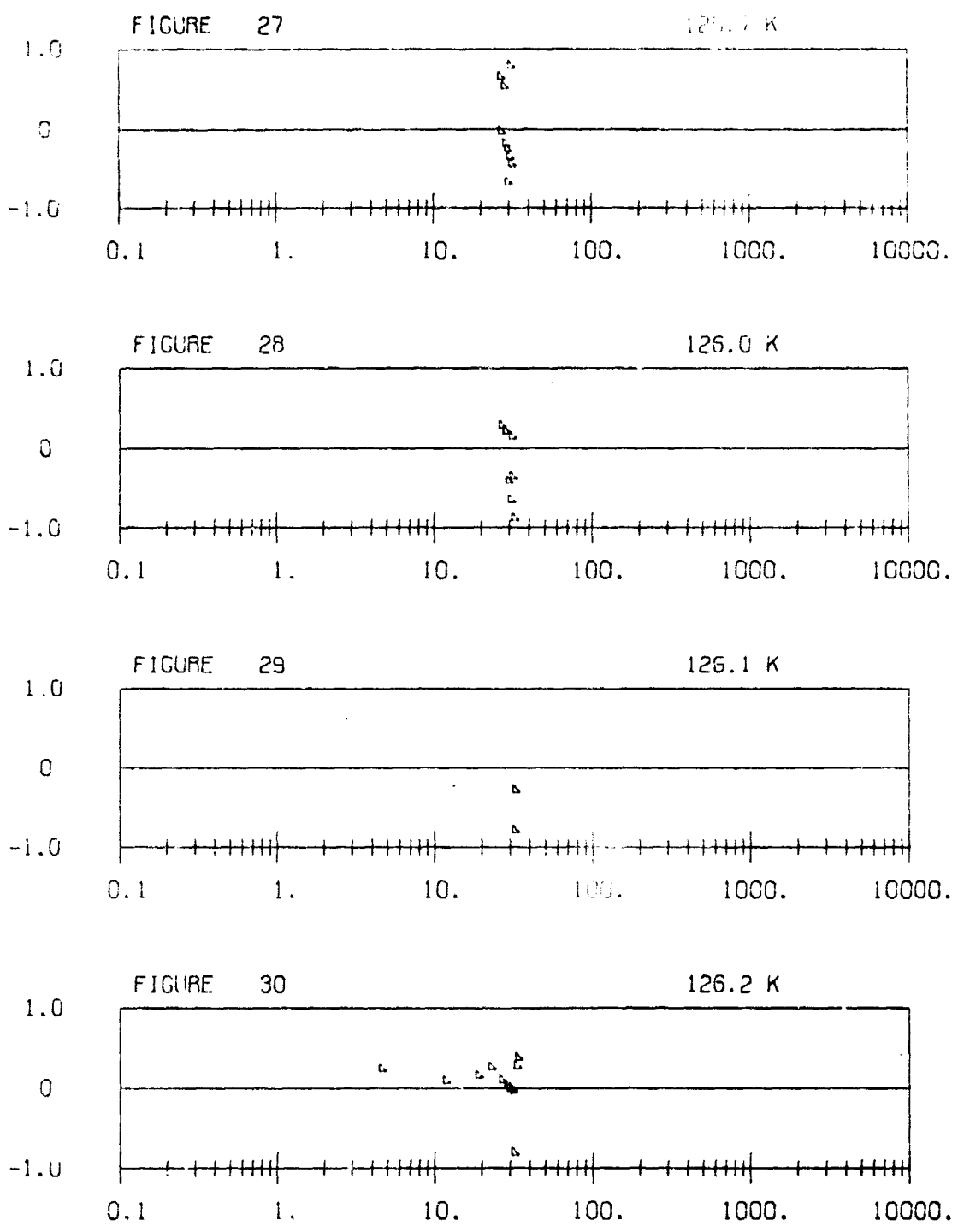
▲ FRIEDMAN [10]

Density Deviations of Equation (22) from Data of References Indicated.

REPRODUCIBILITY OF THE ORIGINAL PAGE IS POOR.

50

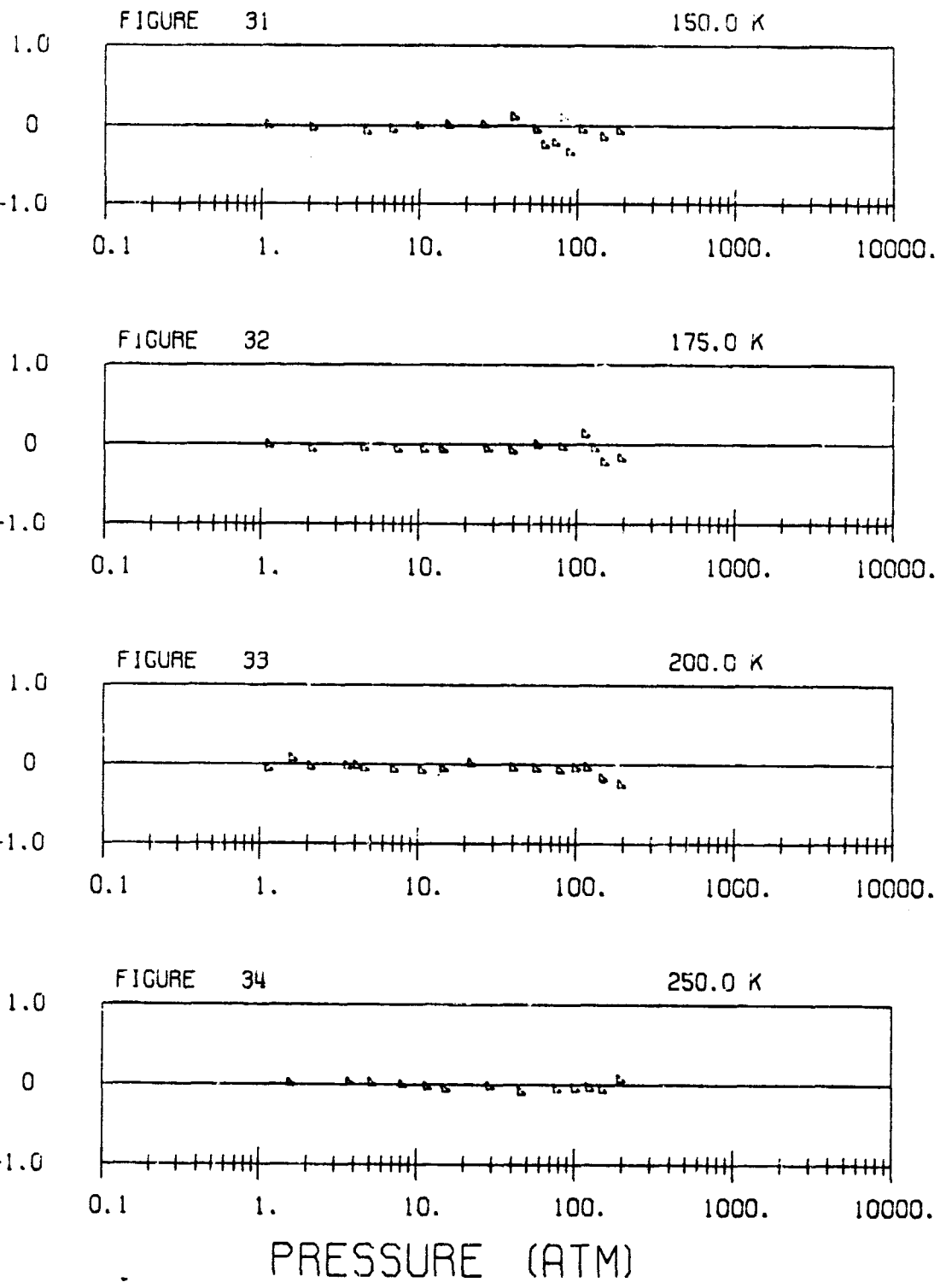
PERCENT DENSITY DEVIATION



◆ FRIEDMAN C103

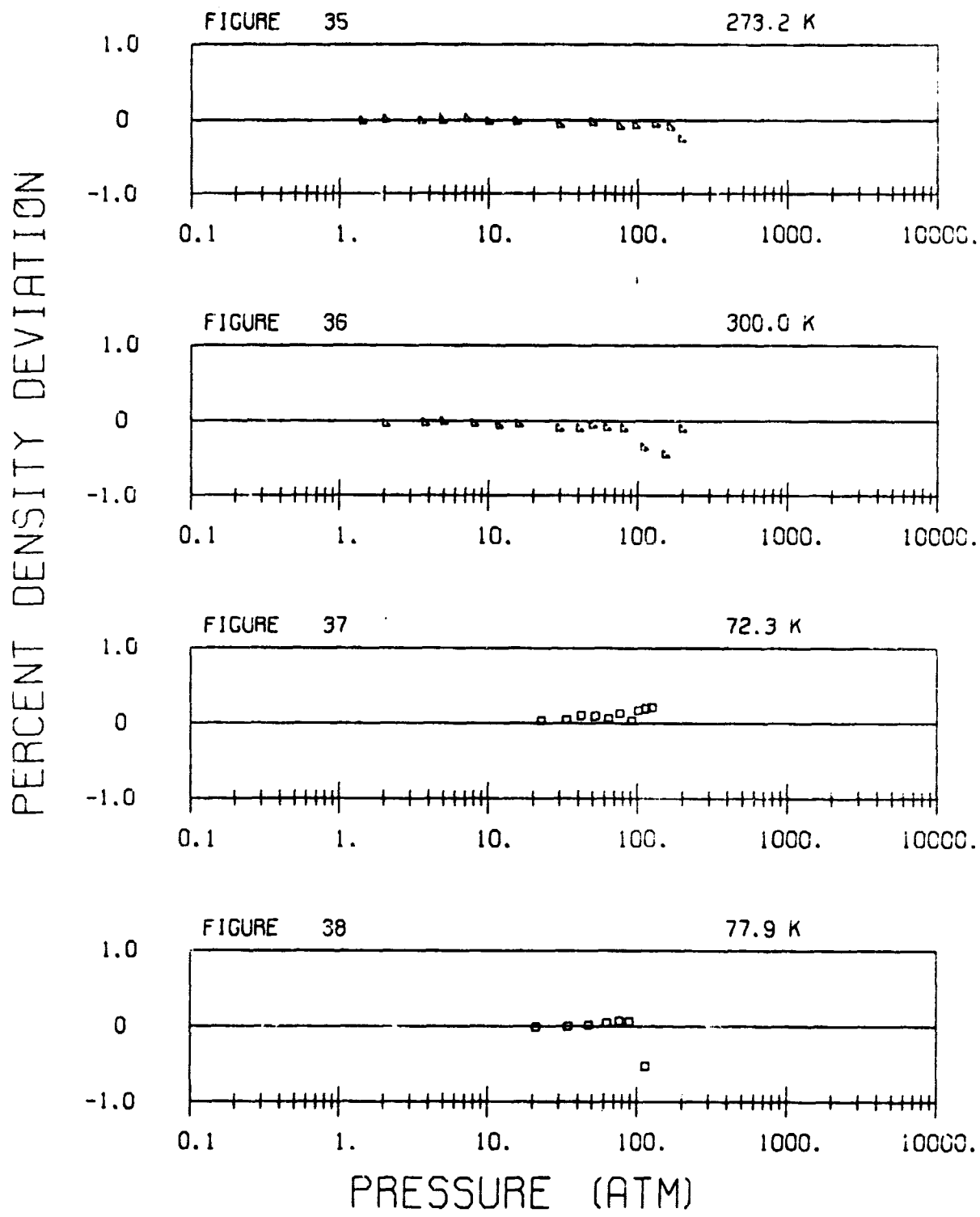
Density Deviations of Equation (22) from Data of References Indicated.

PERCENT DENSITY DEVIATION



▲ FRIEDMAN [10]

Density Deviations of Equation (22) from Data of References Indicated.



— FRIEDMA

[103]

• GIBSONS

[31]

Density Deviations of Equation (22) from Data of References Indicated.

PERCENT DENSITY DEVIATION

FIGURE 39

77.3 K

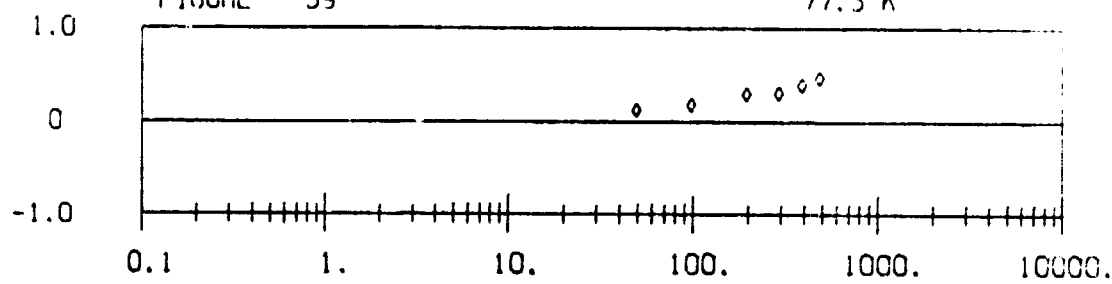


FIGURE 40

78.1 K

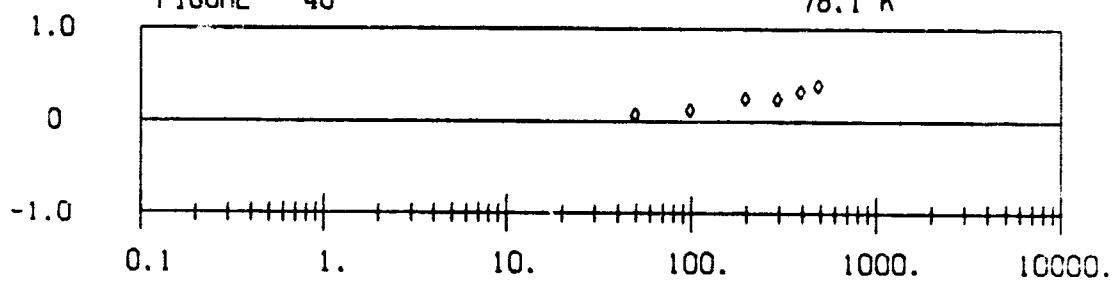


FIGURE 41

83.1 K

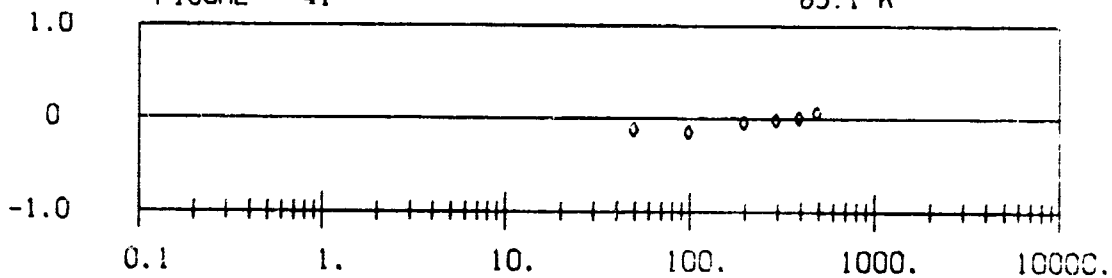
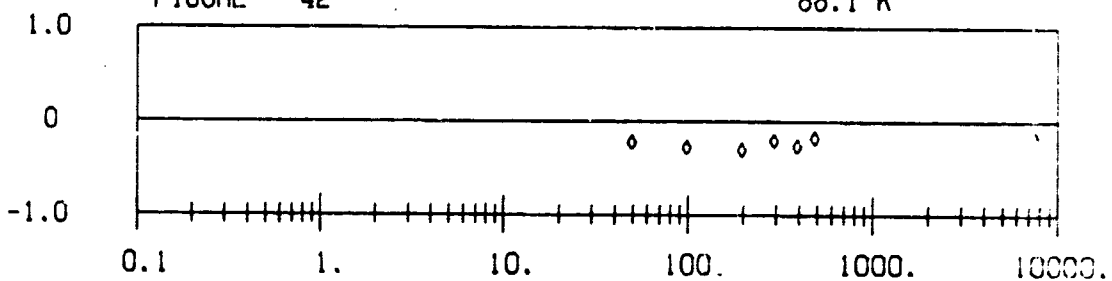


FIGURE 42

88.1 K



PRESSURE (ATM)

♦ GOLUBEV [32]

Density Deviations of Equation (22) from Data of References Indicated.

PERCENT DENSITY DEVIATION

FIGURE 43

93.2 K

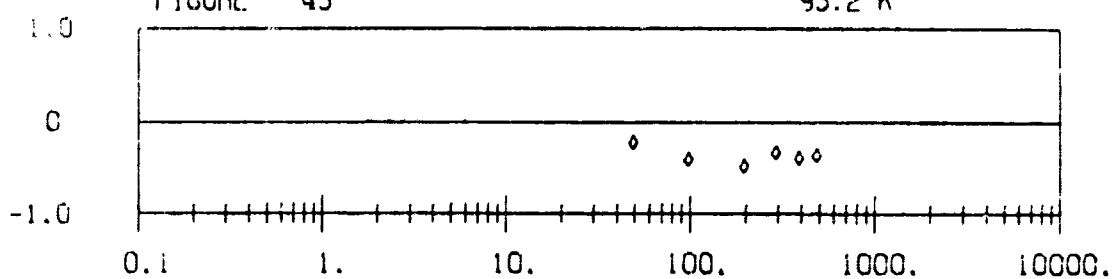


FIGURE 44

98.2 K

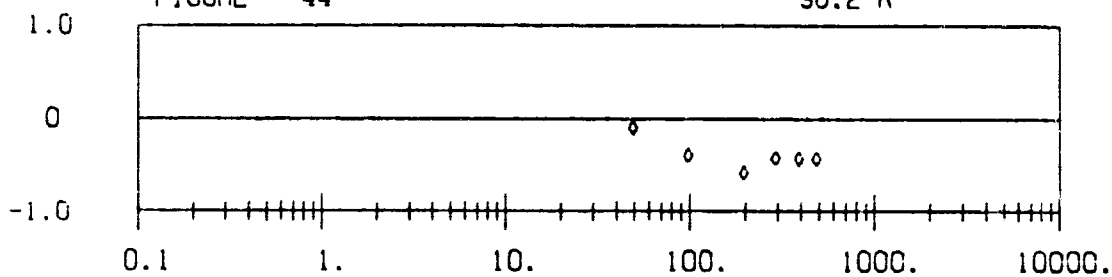


FIGURE 45

103.2 K

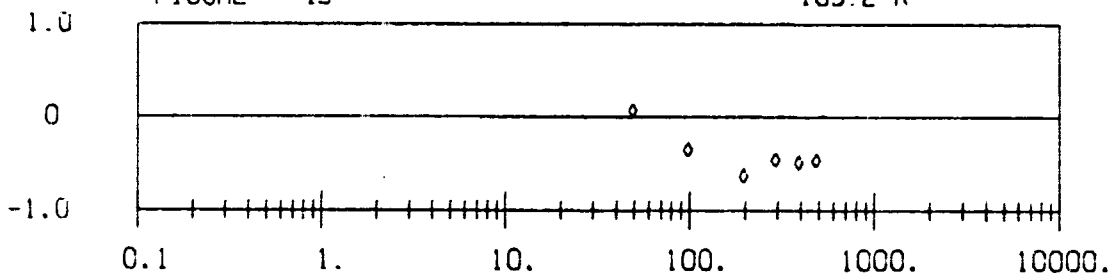
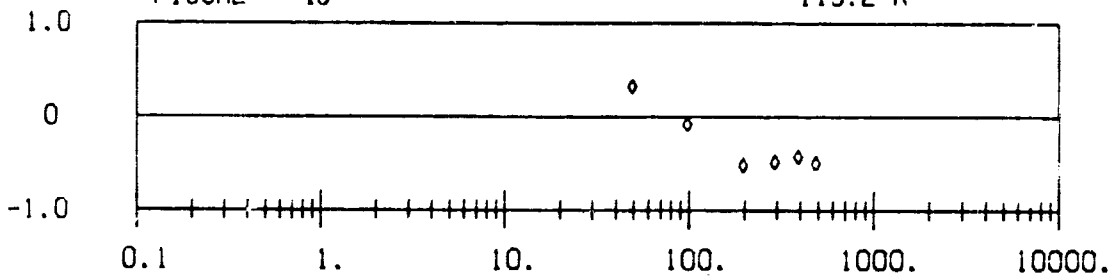


FIGURE 46

113.2 K

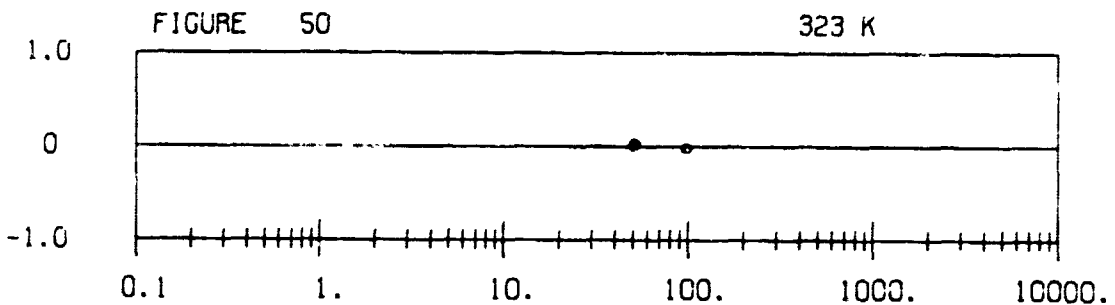
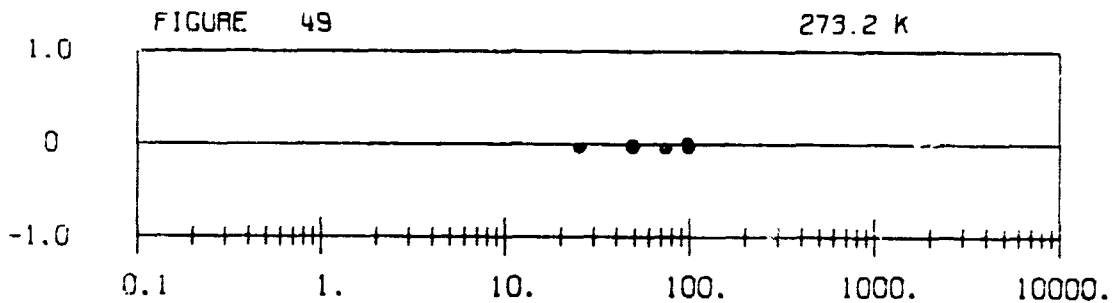
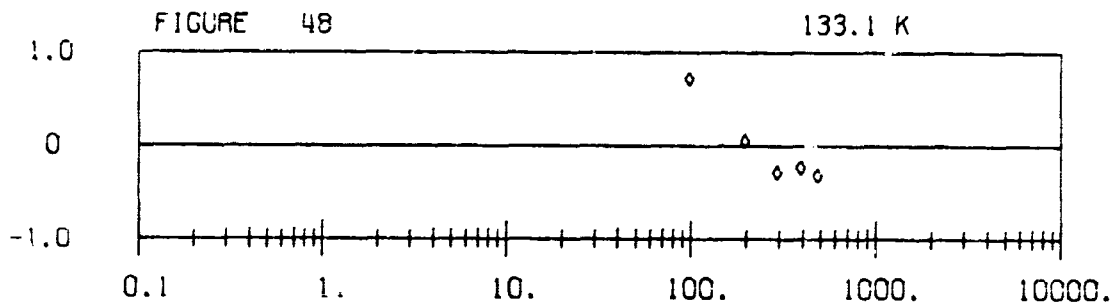
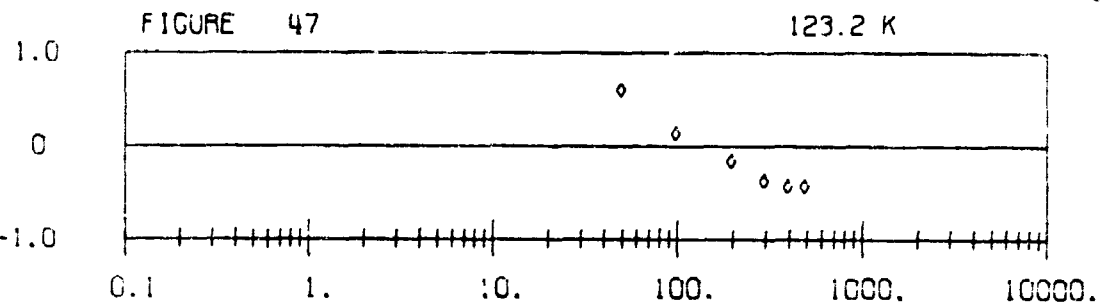


PRESSURE (ATM)

♦ GOLUBEV [32]

Density Deviations of Equation (22) from Data of References Indicated.

PERCENT DENSITY DEVIATION



PRESSURE (ATM)

◆ GOLUBEV [32]

◆ HOLBORN [14]

Density Deviations of Equation (22) from Data of References Indicated.

PERCENT DENSITY DEVIATION

FIGURE 51

373 K

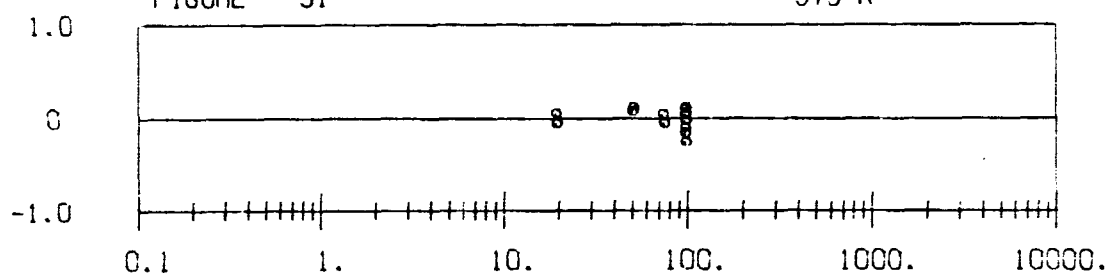


FIGURE 52

423 K

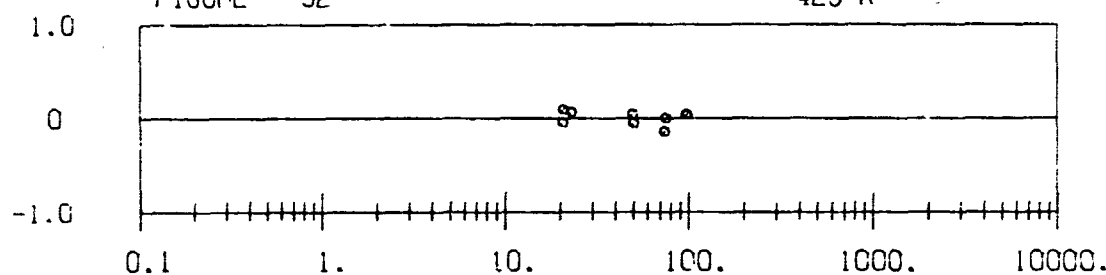


FIGURE 53

473 K

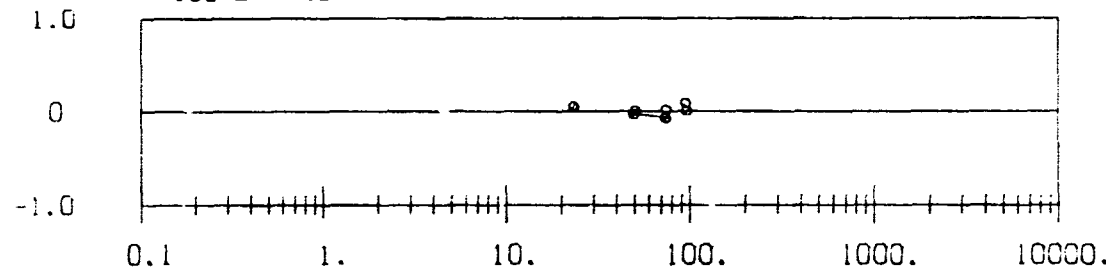
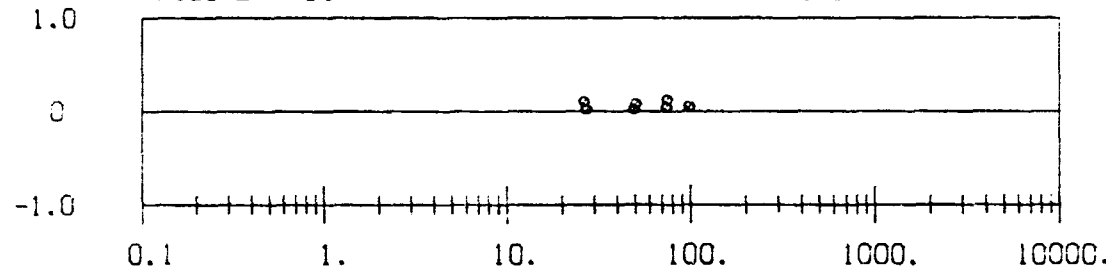


FIGURE 54

573 K

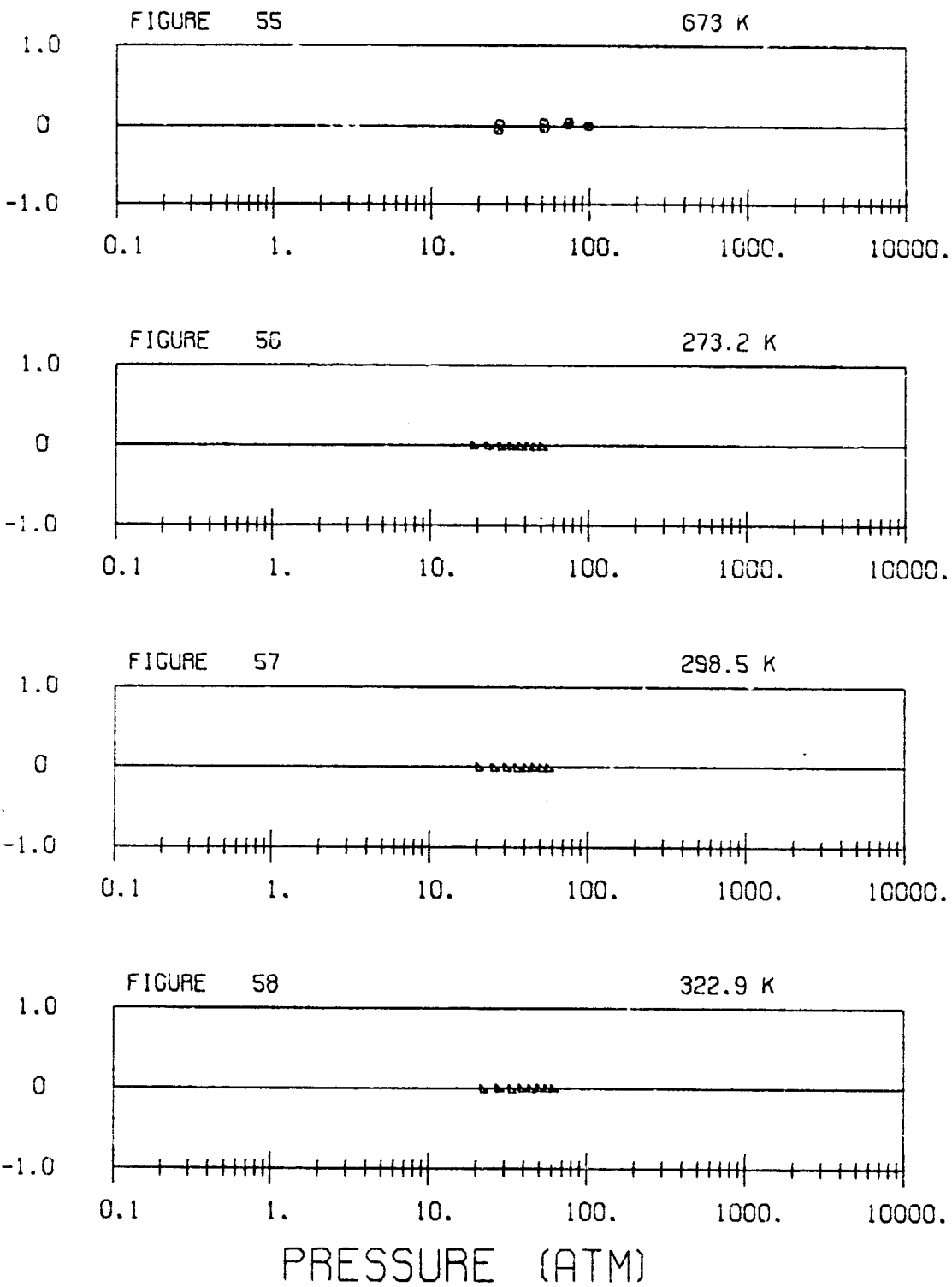


PRESSURE (ATM)

• HOLBORN [14]

Density Deviations of Equation (22) from Data of References Indicated.

PERCENT DENSITY DEVIATION



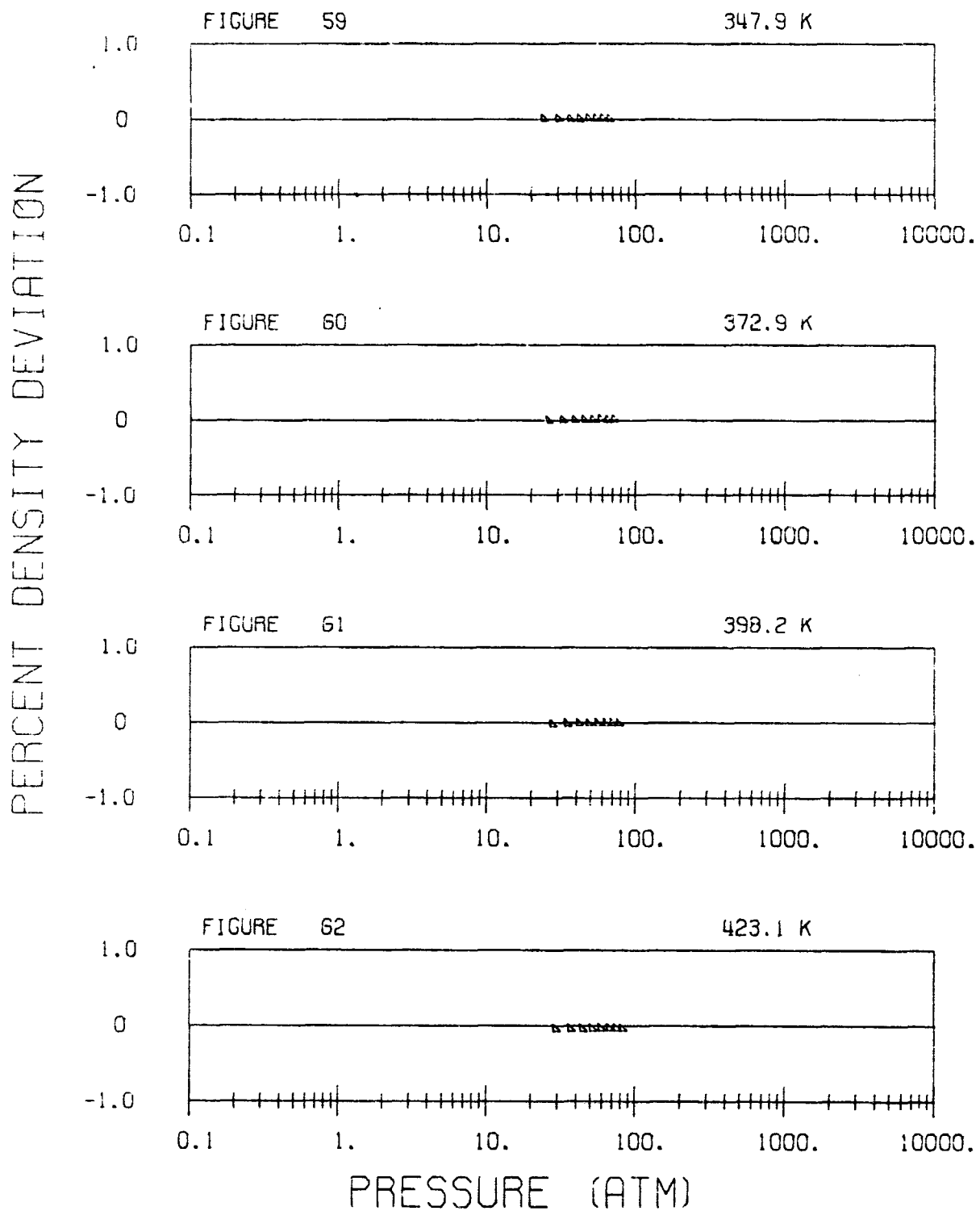
• HOLBORN

[14]

▲ MICHELS

[19]

Density Deviations of Equation (22) from Data of References Indicated.



• MICHELS [19]

Density Deviations of Equation (22) from Data of References Indicated.

PERCENT DENSITY DEVIATION

FIGURE 63

273.2 K

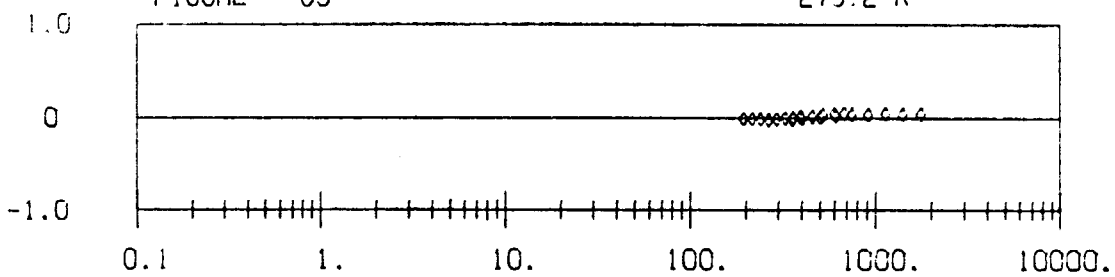


FIGURE 64

298.1 K

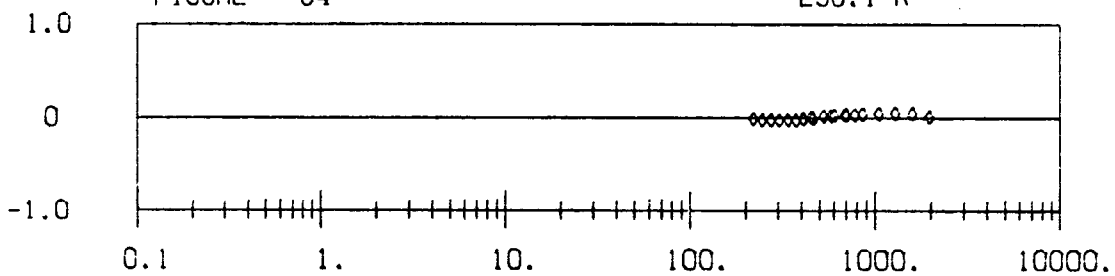


FIGURE 65

323.1 K

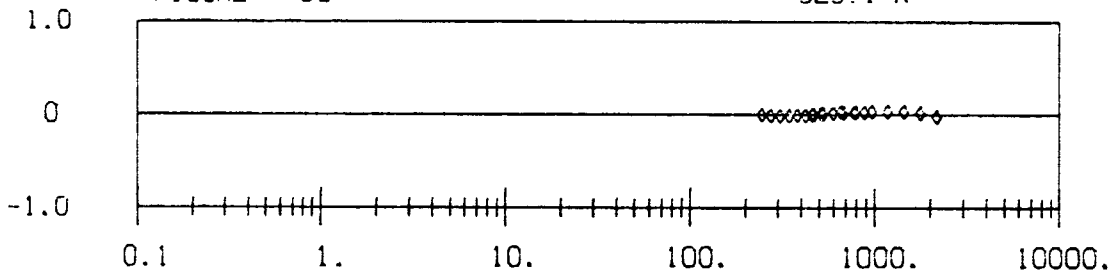
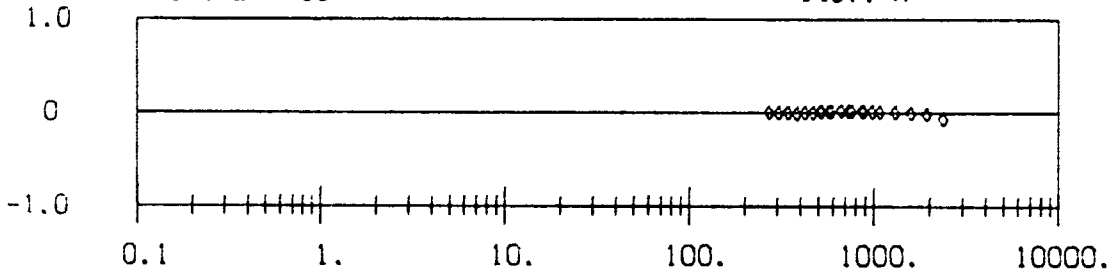


FIGURE 66

348.1 K



PRESSURE (ATM)

◆ MICHELS [20]

Density Deviations of Equation (22) from Data of References Indicated.

PERCENT DENSITY DEVIATION

60

FIGURE 67

373.2 K

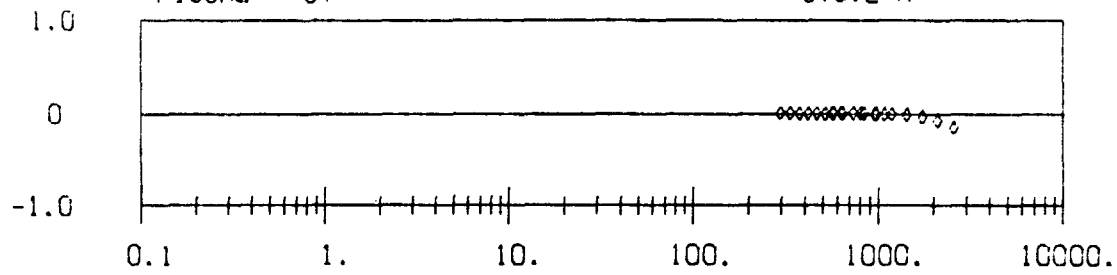


FIGURE 68

398.6 K

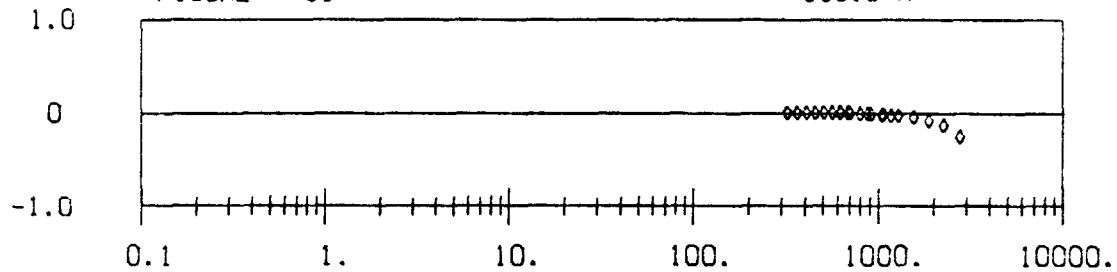


FIGURE 69

423.2 K

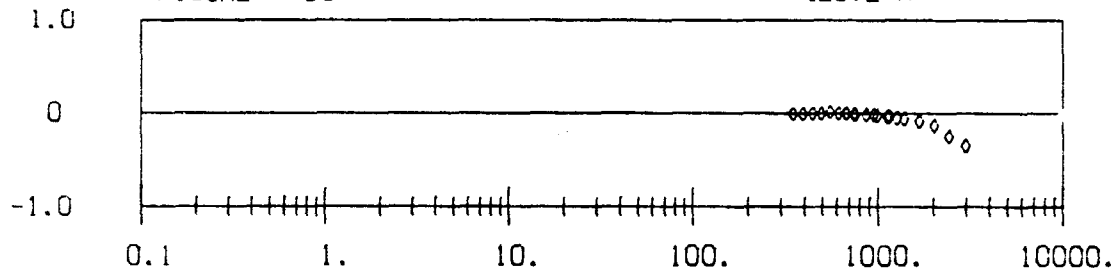
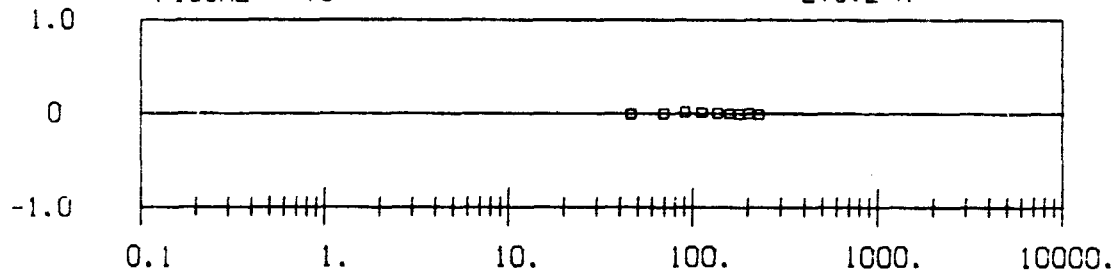


FIGURE 70

273.2 K



PRESSURE (ATM)

◊ MICHELS

[20]

□ OTTO

[22]

Density Deviations of Equation (22) from Data of References Indicated.

PERCENT DENSITY DEVIATION

FIGURE 71

298.5 K

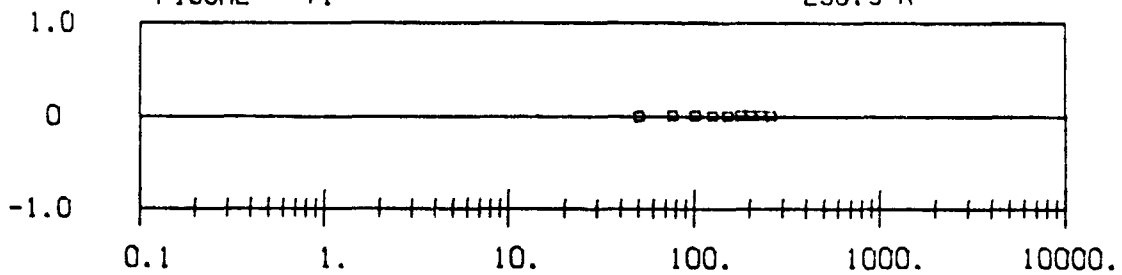


FIGURE 72

322.9 K

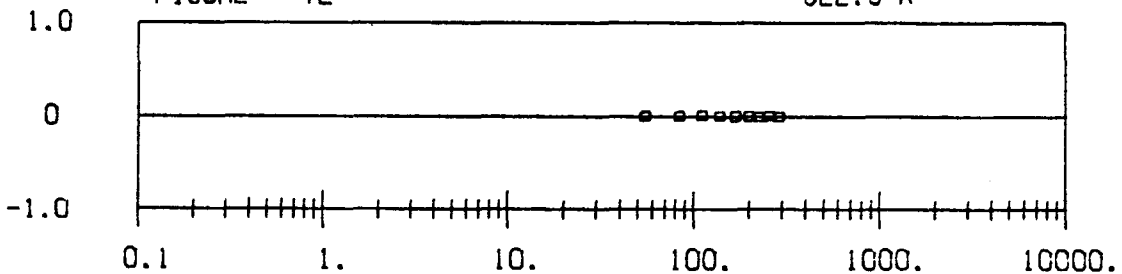


FIGURE 73

348.4 K

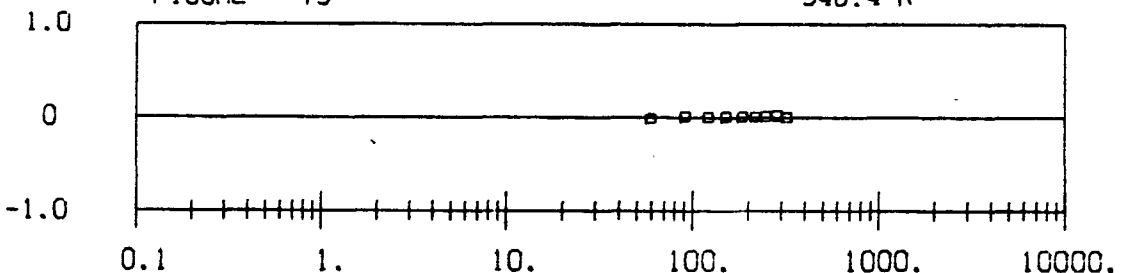
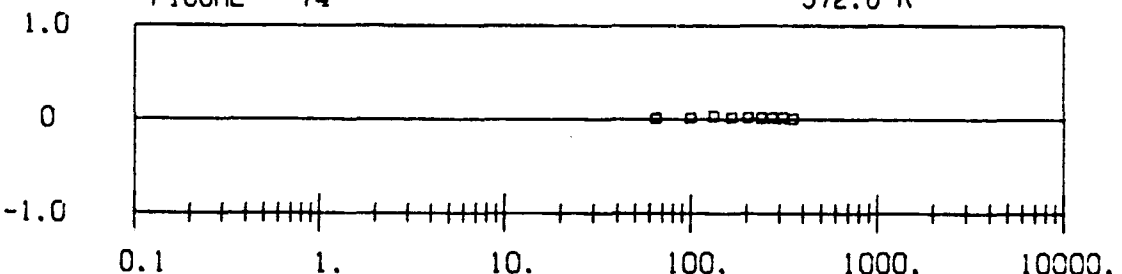


FIGURE 74

372.8 K

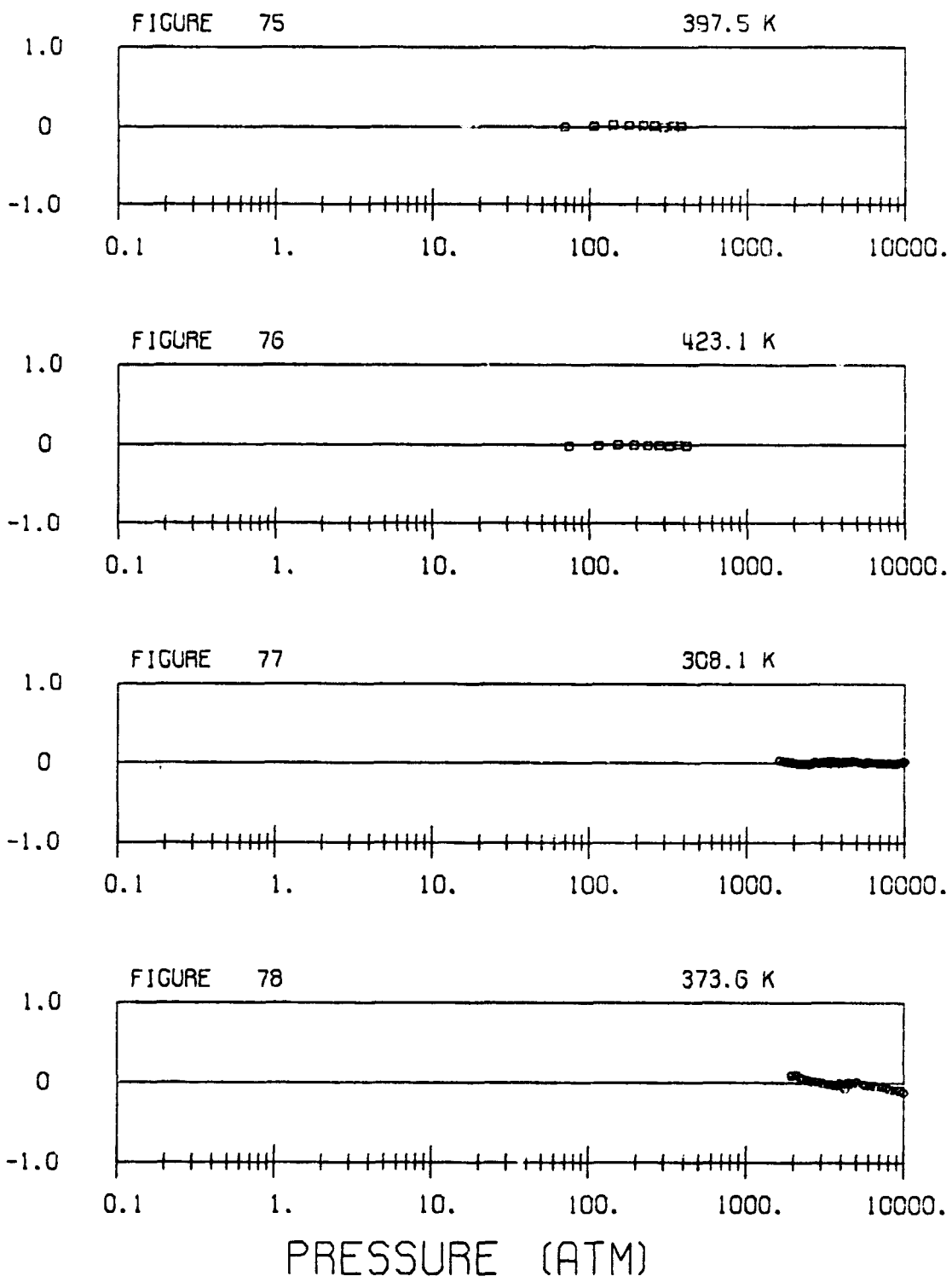


PRESSURE (ATM)

□ OTTO □ C223

Density Deviations of Equation (22) from Data of References Indicated.

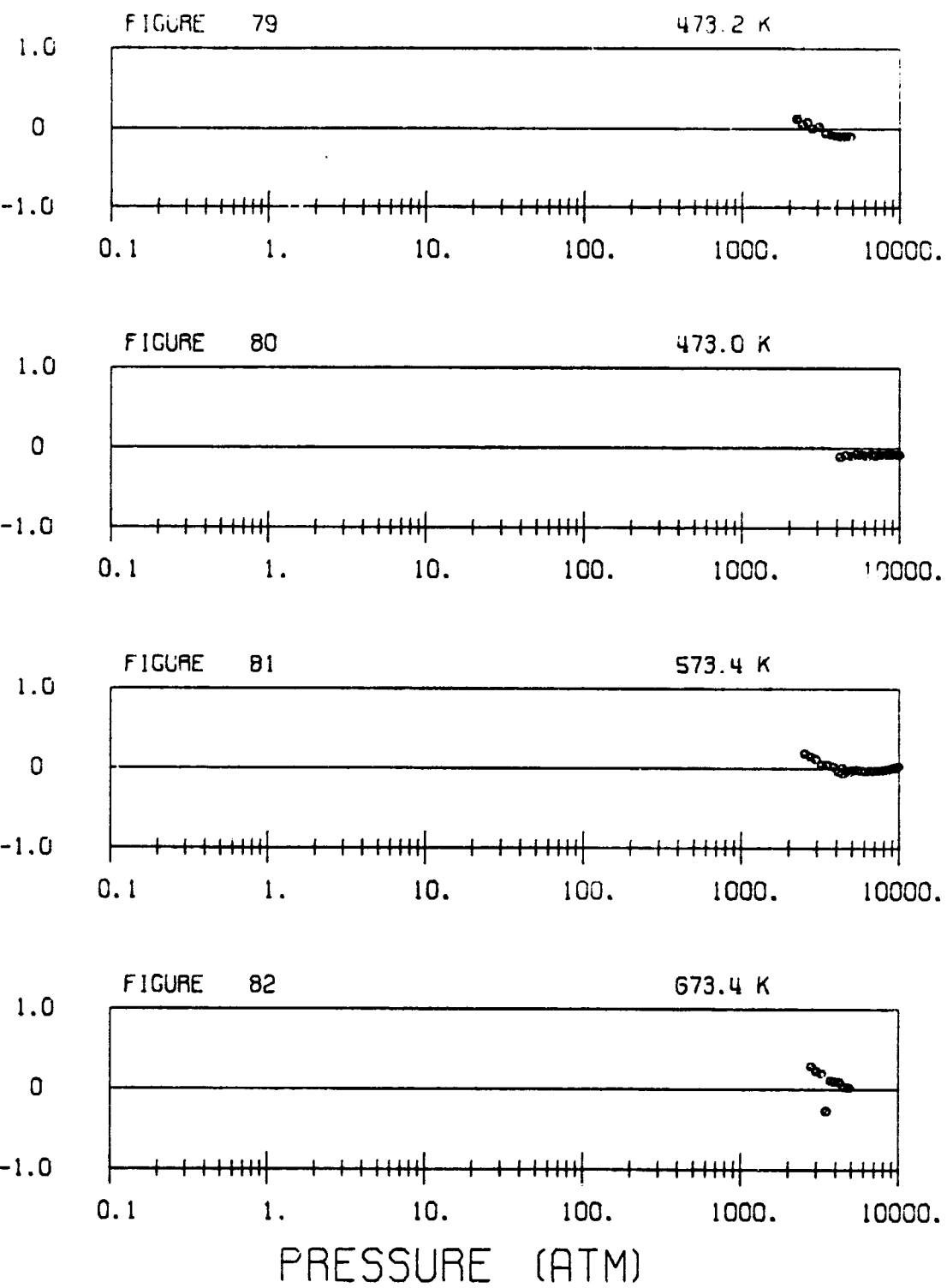
PERCENT DENSITY DEVIATION



△ OITO [22] ◇ ROBERTSON [23]

Density Deviations of Equation (22) from Data of References Indicated.

PERCENT DENSITY DEVIATION



• ROBERTSON [23]

Density Deviations of Equation (22) from Data of References Indicated.

PERCENT DENSITY DEVIATION

FIGURE 83

673.1 K

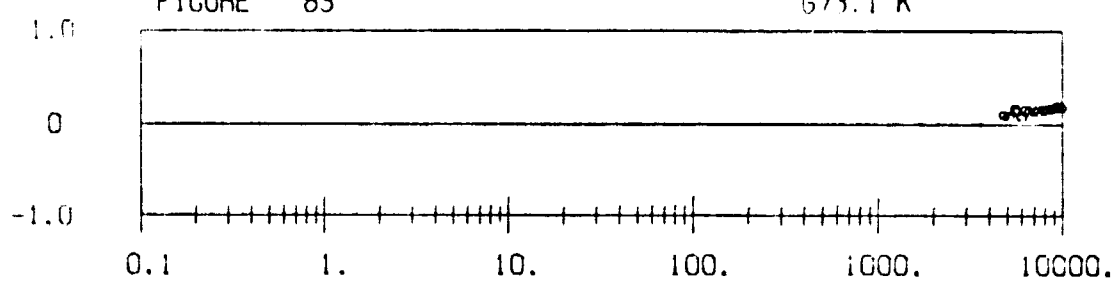


FIGURE 84

423.2 K

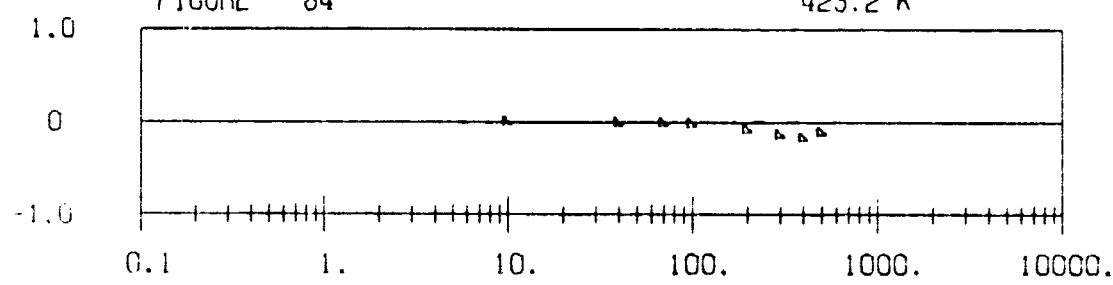


FIGURE 85

473.2 K

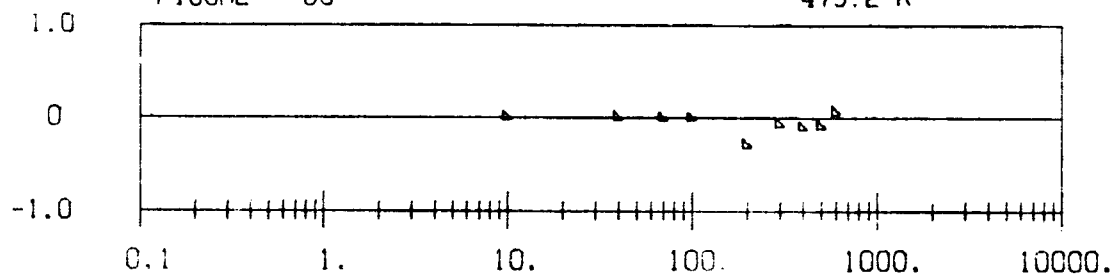
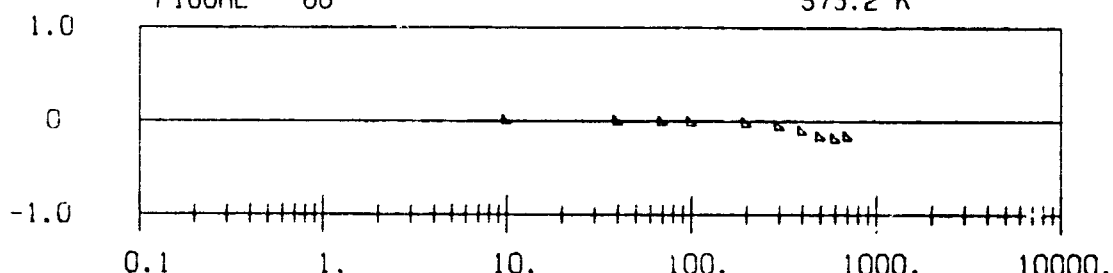


FIGURE 86

573.2 K

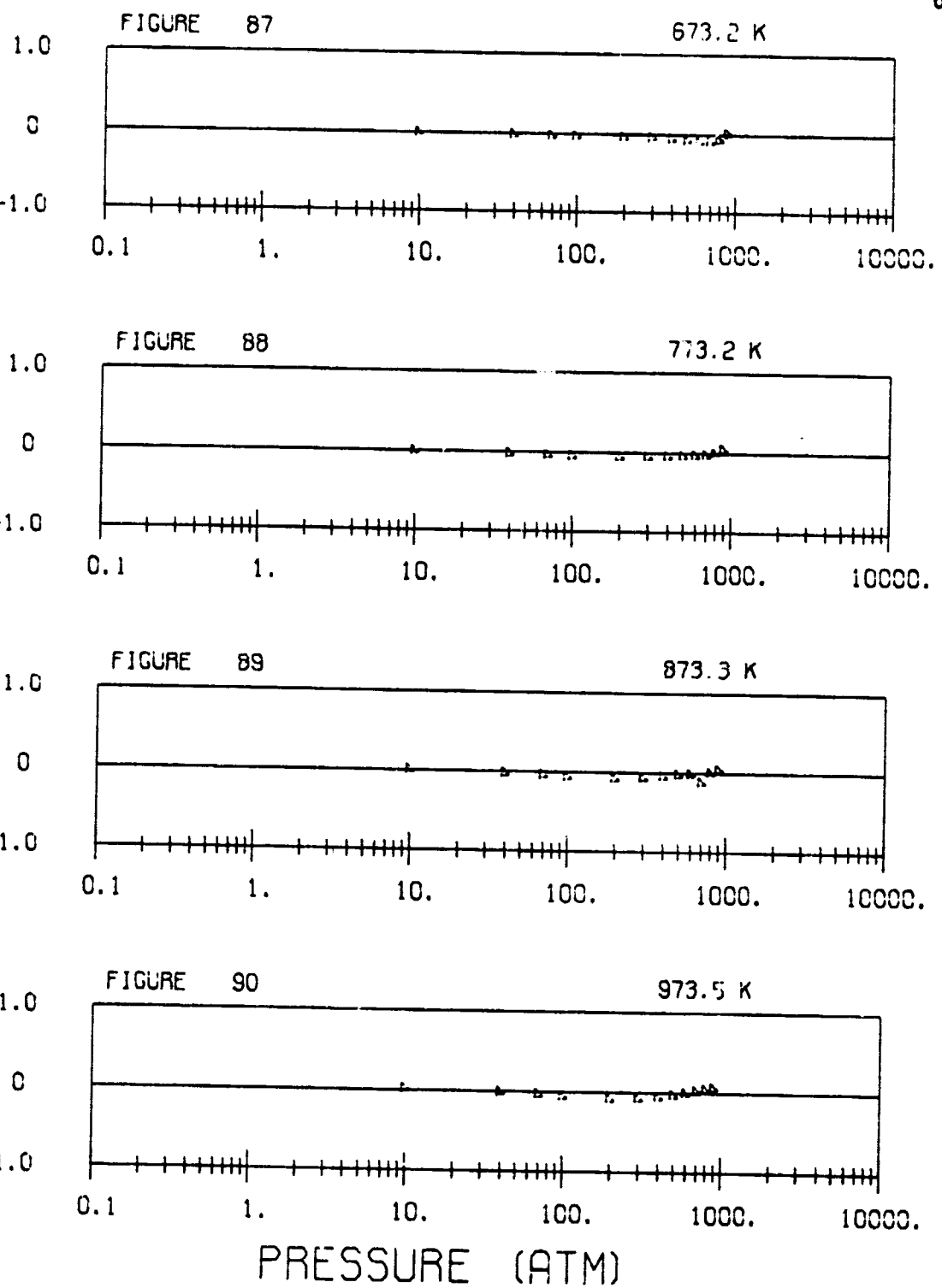
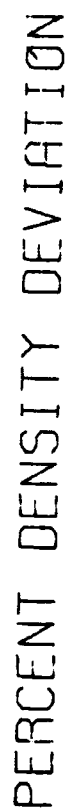


PRESSURE (ATM)

• ROBERTSON [23]

▲ SAUREL [24]

Density Deviations of Equation (22) from Data of References Indicated.



SAUREL C24

Density Deviations of Equation (22) from Data of References Indicated.

PERCENT DENSITY DEVIATION

FIGURE 91

1073.8 K

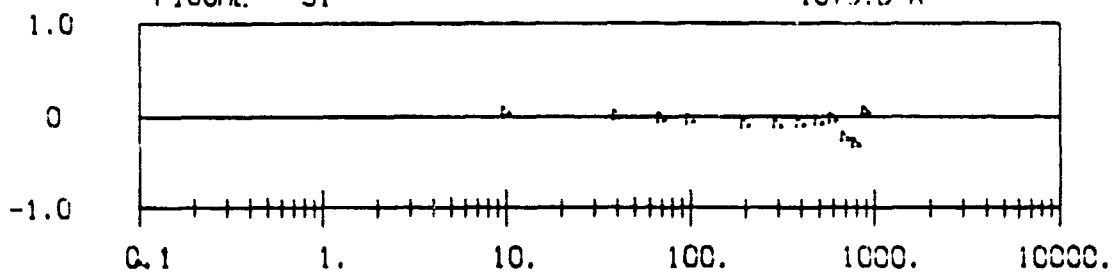


FIGURE 92

80.0 K

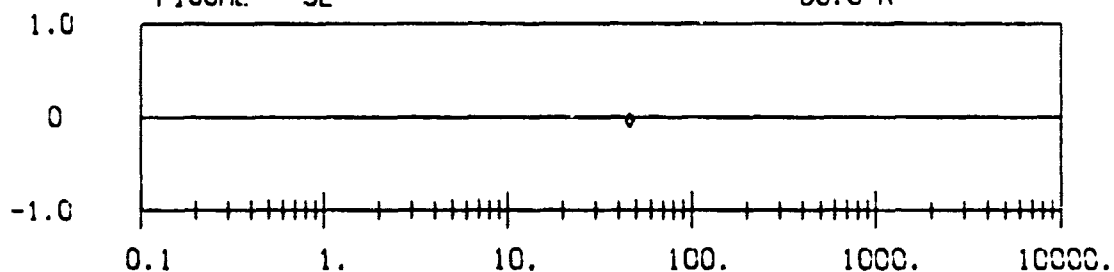


FIGURE 93

81.0 K

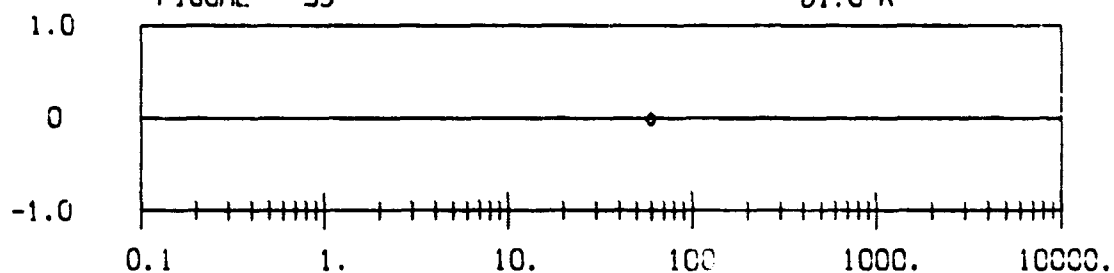
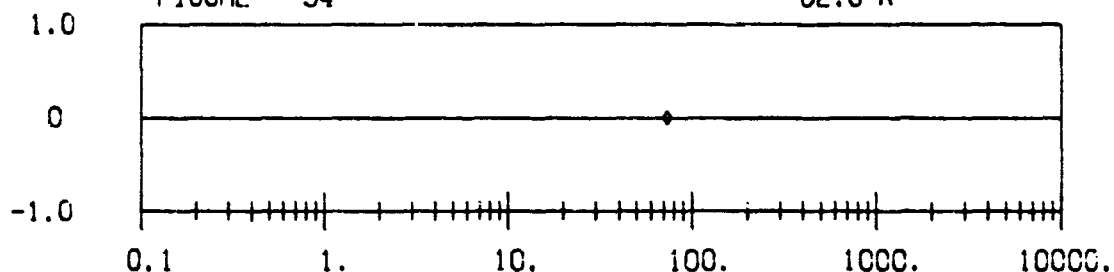


FIGURE 94

82.0 K



PRESSURE (ATM)

▲ SAUREL

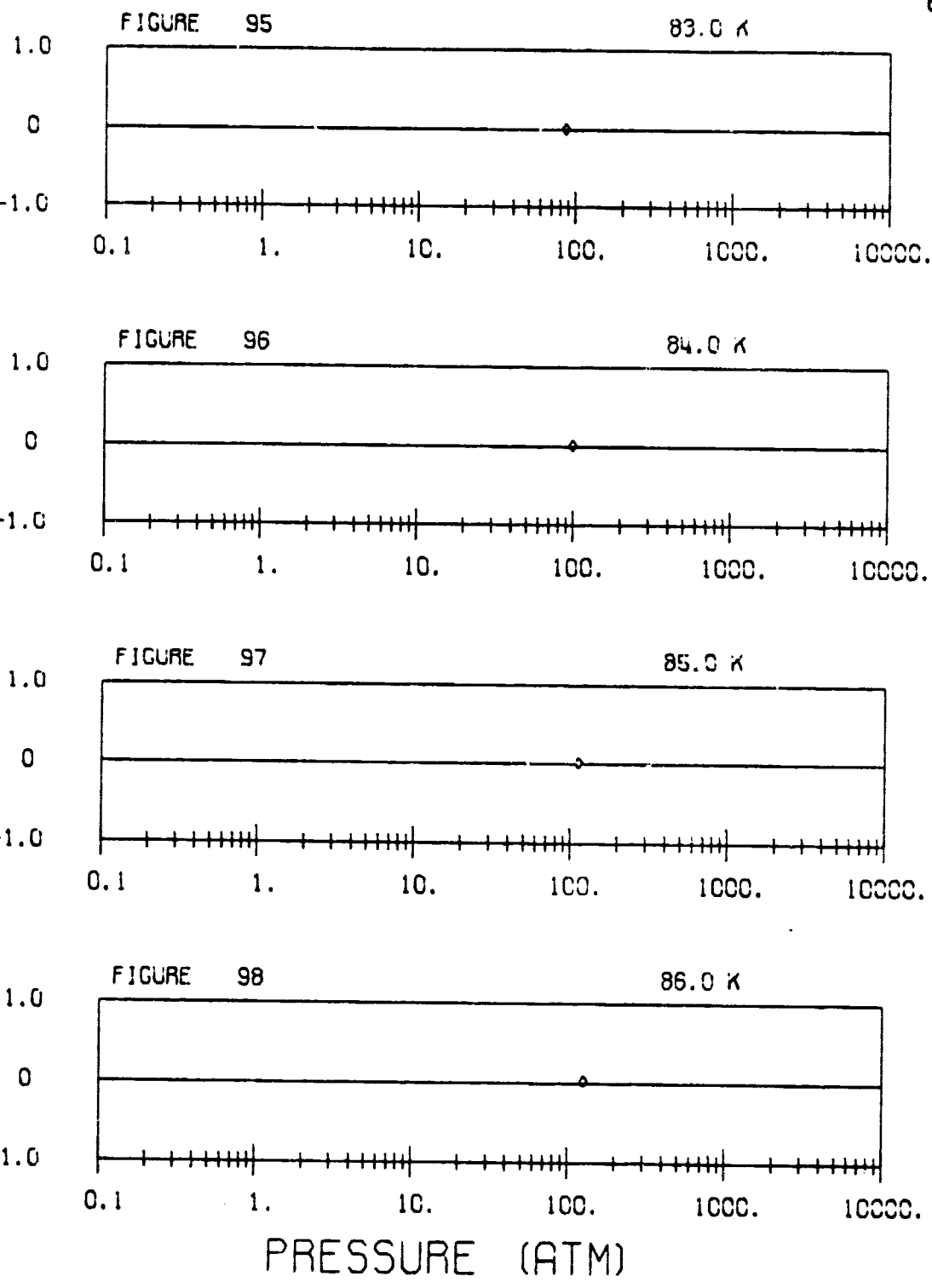
[24]

◆ WEBER

[36]

Density Deviations of Equation (22) from Data of References Indicated.

PERCENT DENSITY DEVIATION



♦ WEBER

[36]

Density Deviations of Equation (22) from Data of References Indicated.

PERCENT DENSITY DEVIATION

FIGURE 99

87.0 K

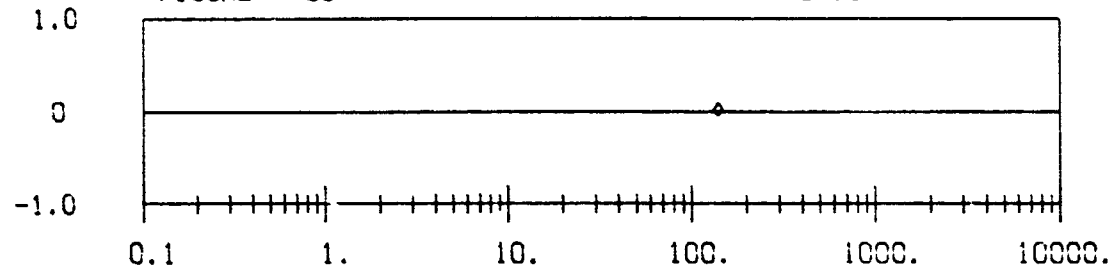


FIGURE 100

88.0 K

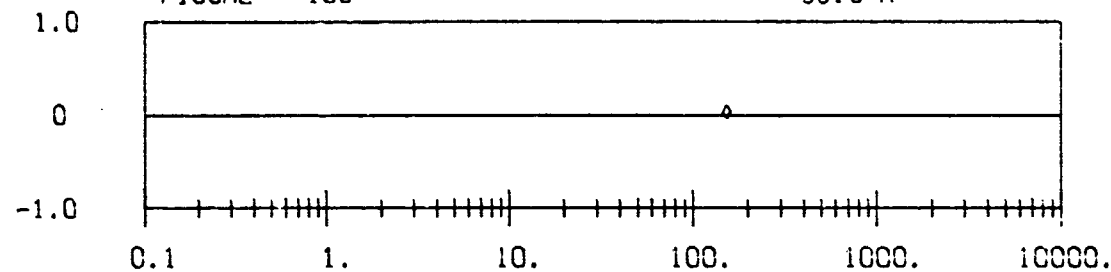


FIGURE 101

89.0 K

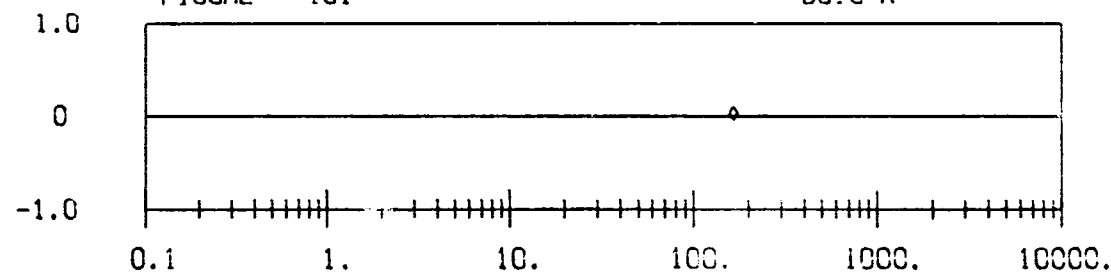
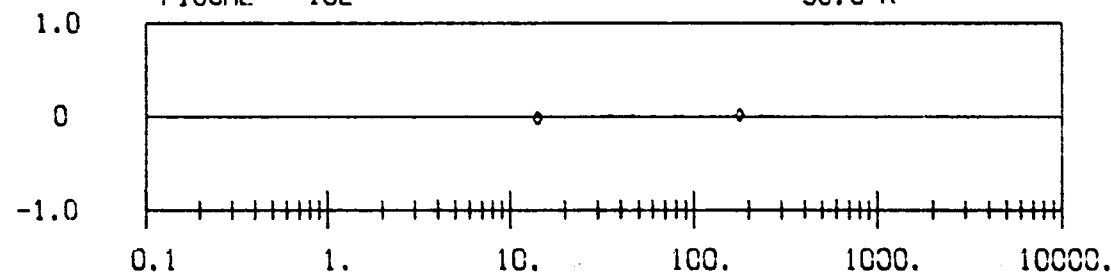


FIGURE 102

90.0 K



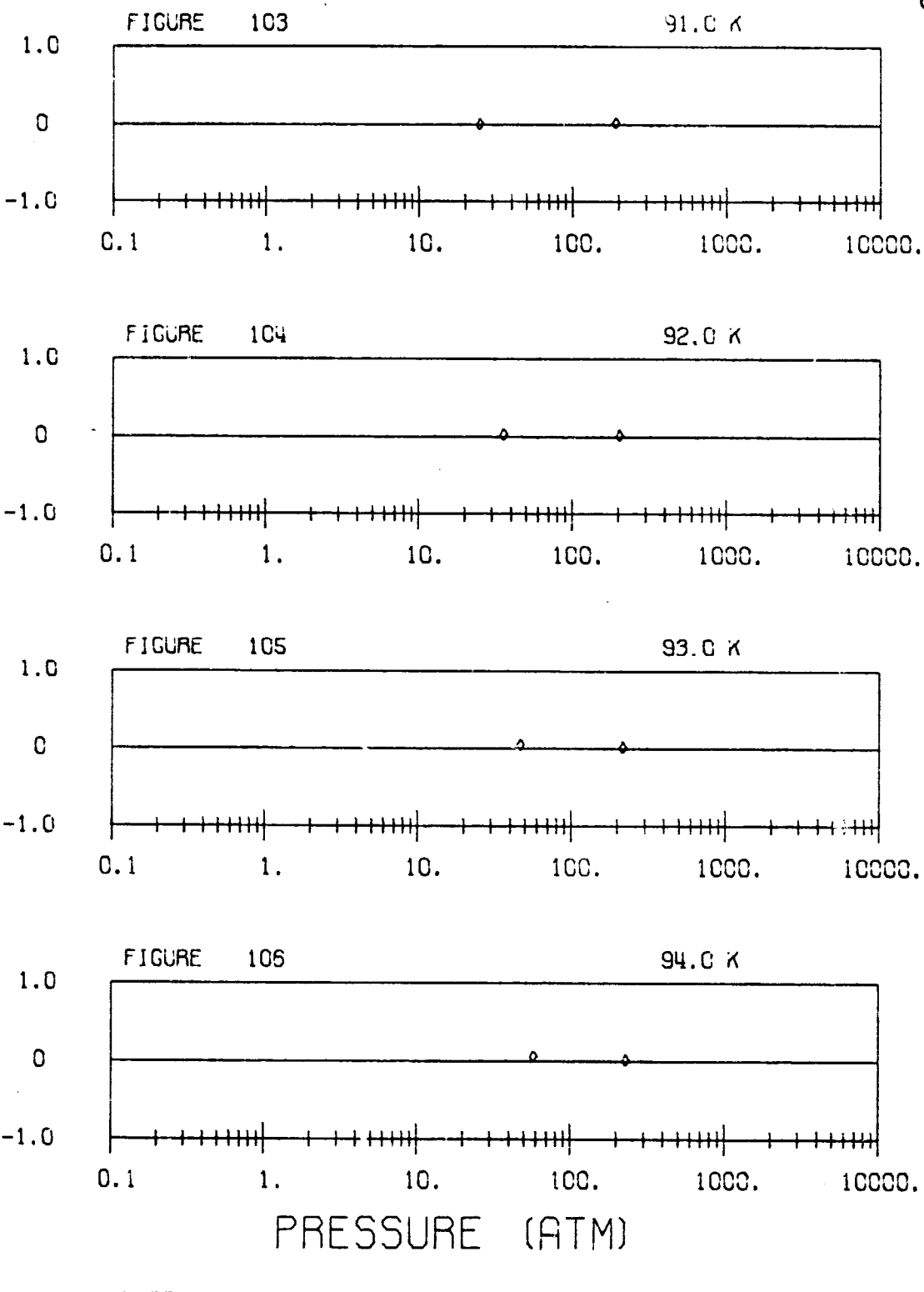
PRESSURE (ATM)

◊ WEBER

[36]

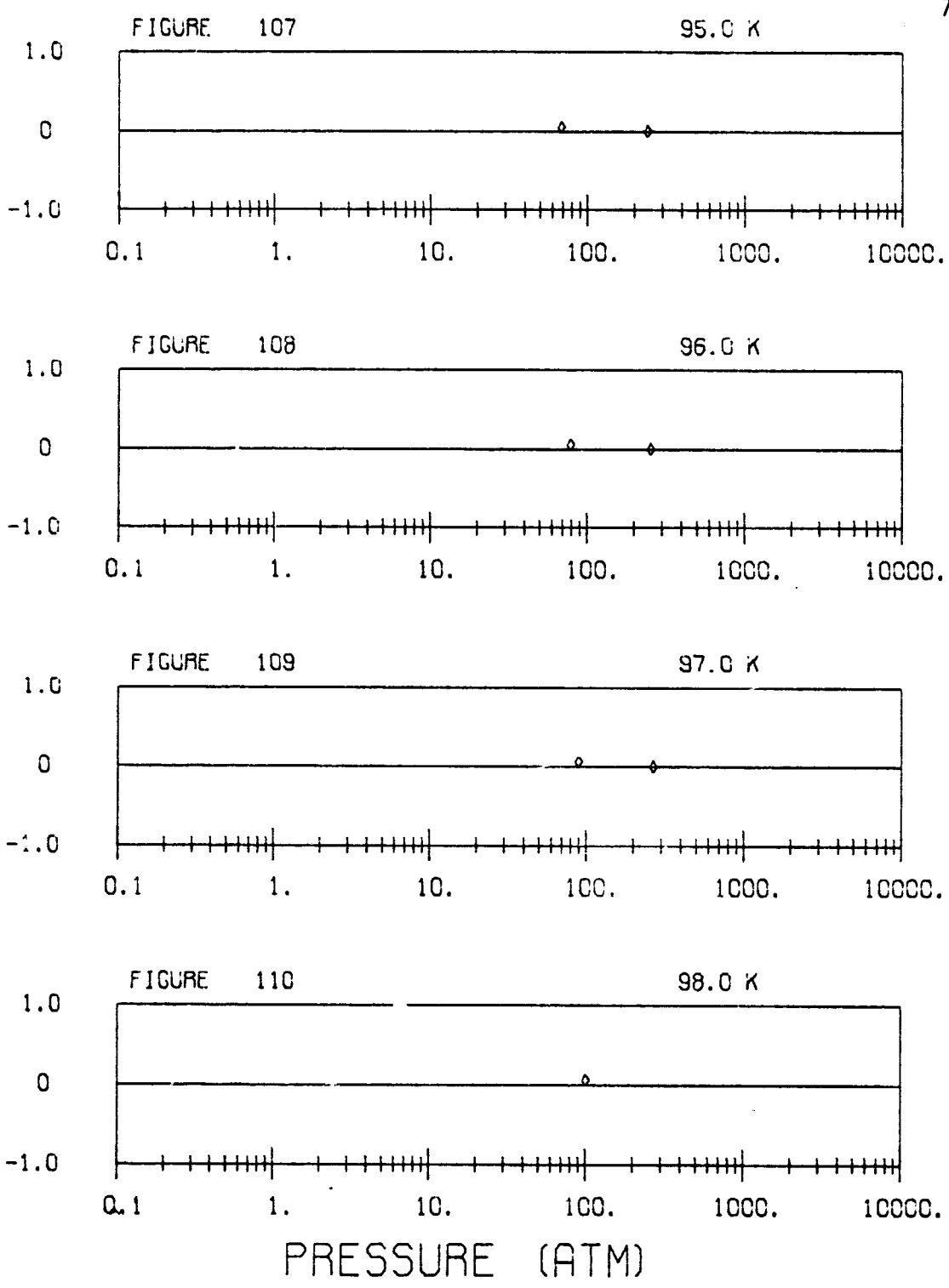
Density Deviations of Equation (22) from Data of References Indicated.

PERCENT DENSITY DEVIATION



Density Deviations of Equation (22) from Data of References Indicated.

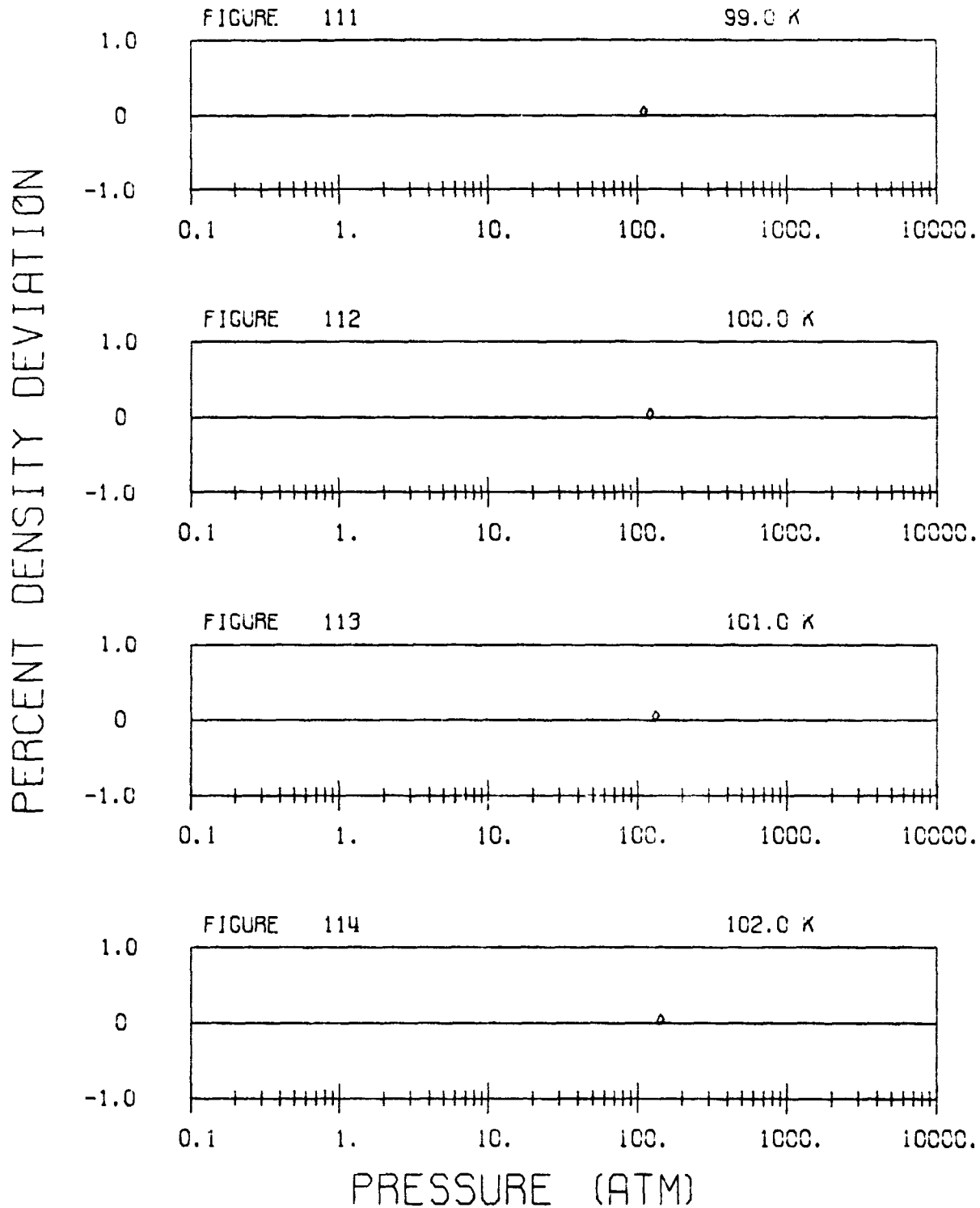
PERCENT DENSITY DEVIATION



◊ WEBER

[36]

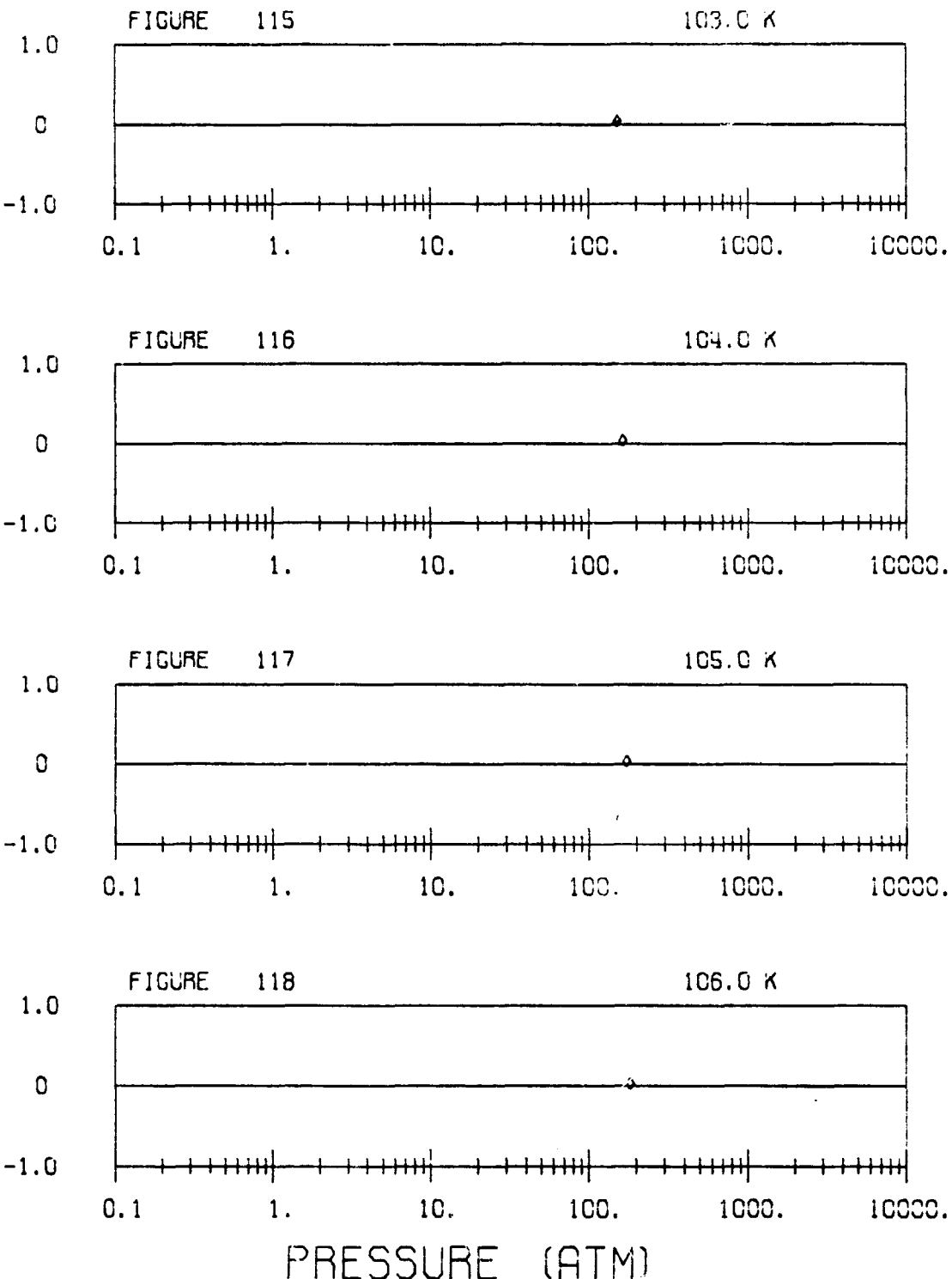
Density Deviations of Equation (22) from Data of References Indicated.



◆ WEBER ◆ 36 ◆

Density Deviations of Equation (22) from Data of References Indicated.

PERCENT DENSITY DEVIATION

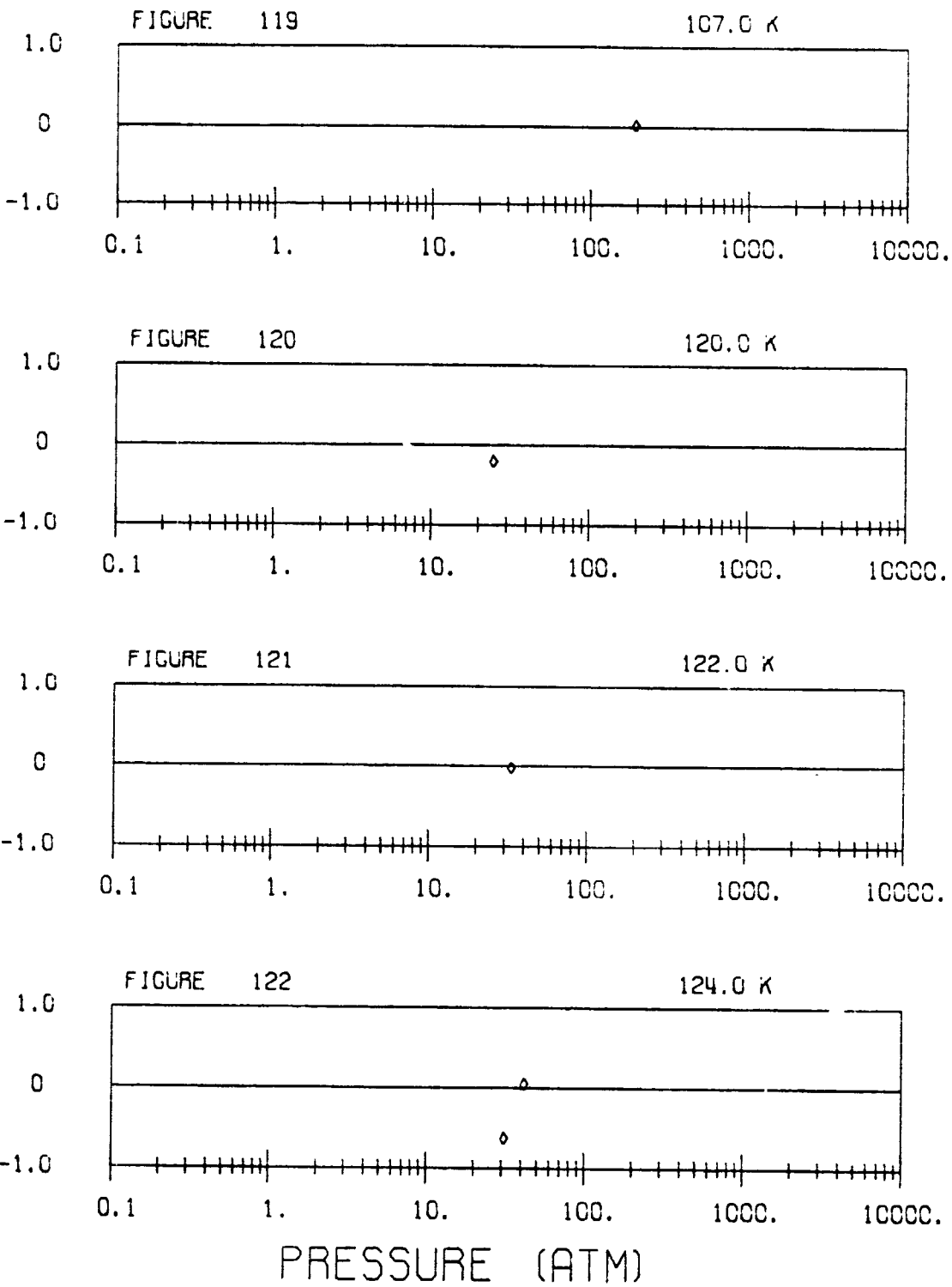


◆ WEBER

[36]

Density Deviations of Equation (22) from Data of References Indicated.

PERCENT DENSITY DEVIATION



♦ WEBER

[36]

Density Deviations of Equation (22) from Data of References Indicated.

PERCENT DENSITY DEVIATION

FIGURE 123

126.0 K

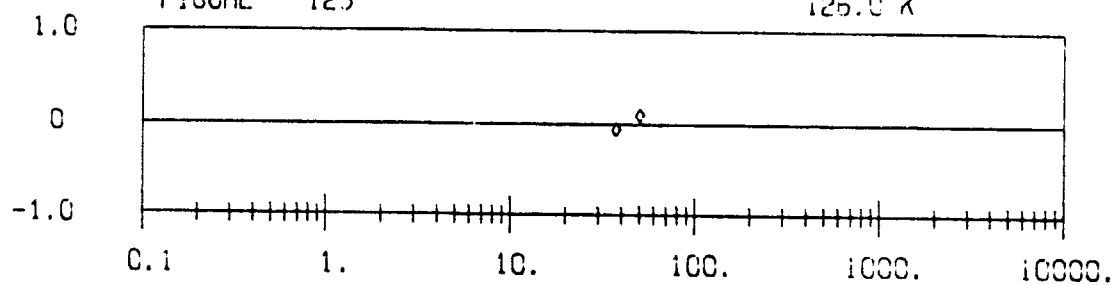


FIGURE 124

128.0 K

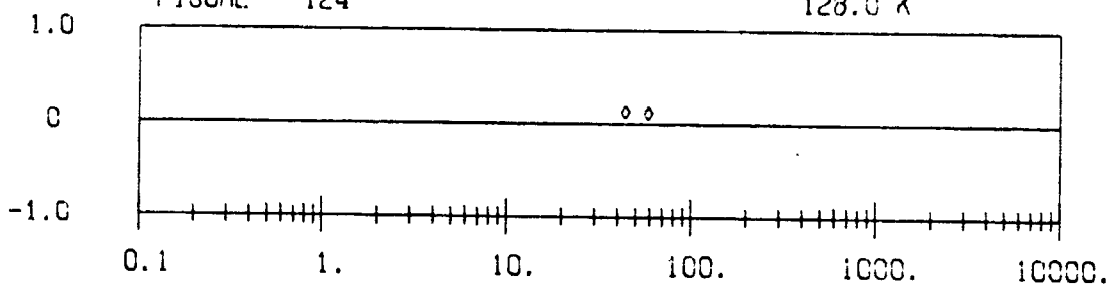


FIGURE 125

130.0 K

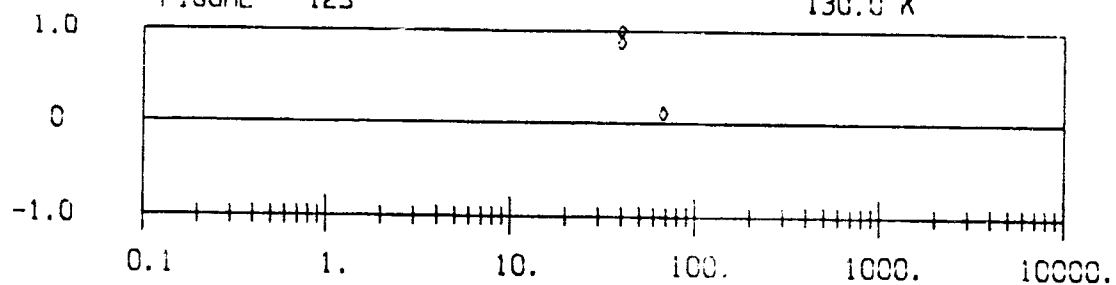
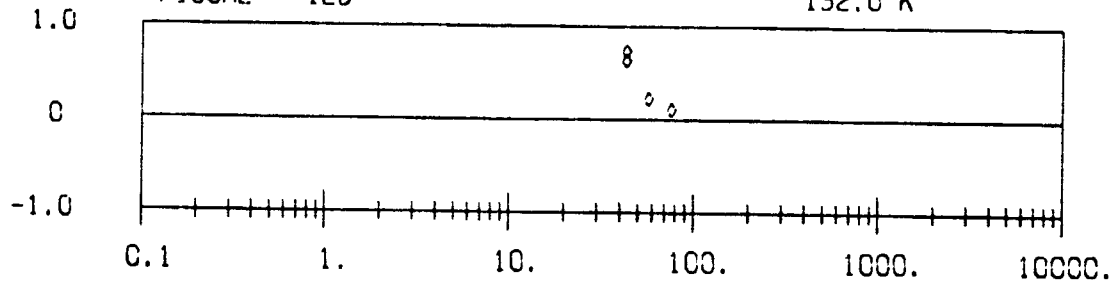


FIGURE 126

132.0 K



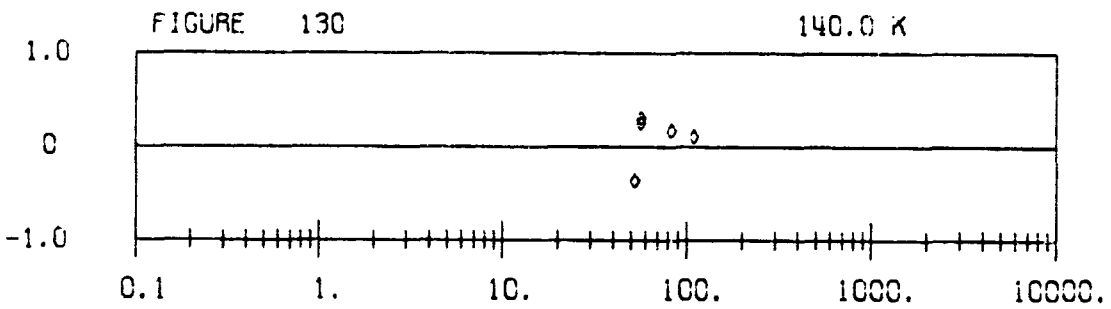
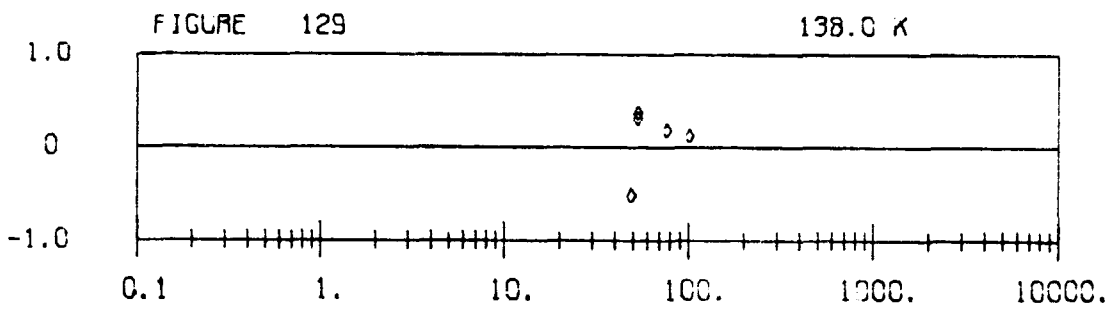
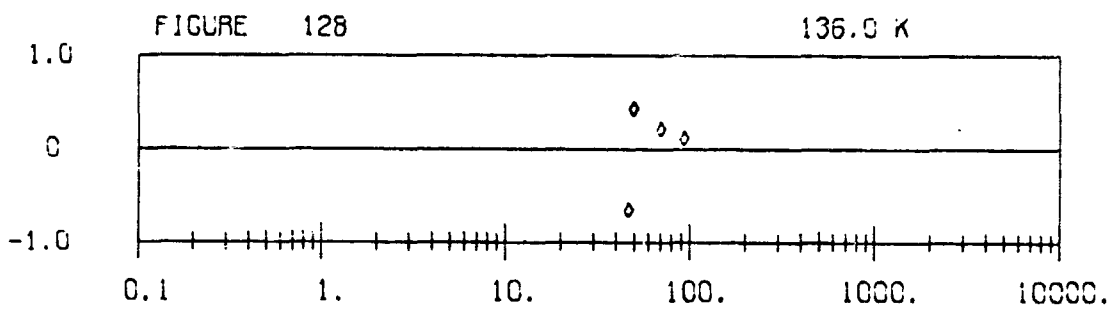
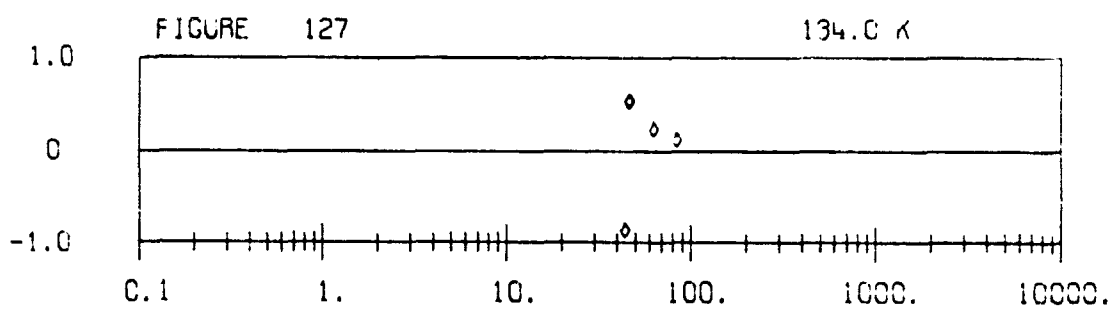
PRESSURE (ATM)

♦ WEBER

E36

Density Deviations of Equation (22) from Data of References Indicated.

PERCENT DENSITY DEVIATION



PRESSURE (ATM)

◊ WEBER

□ E36 □

Density Deviations of Equation (22) from Data of References Indicated.

PERCENT DENSITY DEVIATION

FIGURE 131

273.2 K

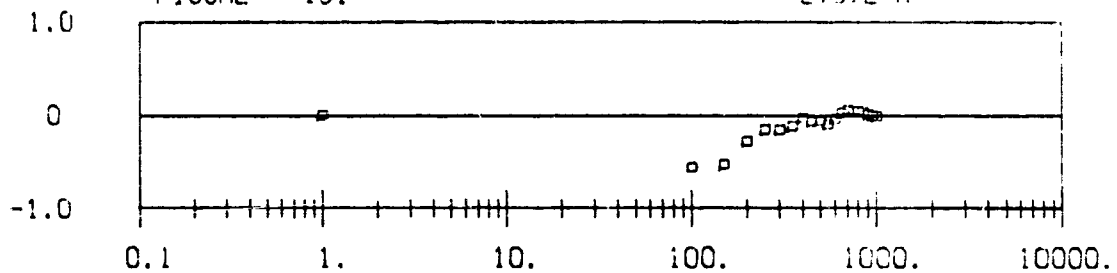


FIGURE 132

289.2 K

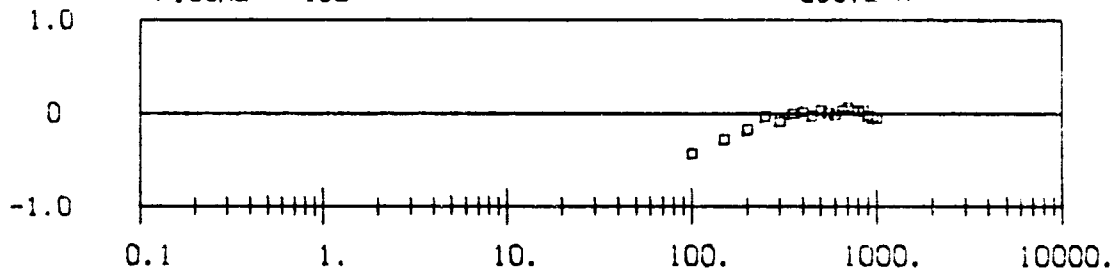


FIGURE 133

372.6 K

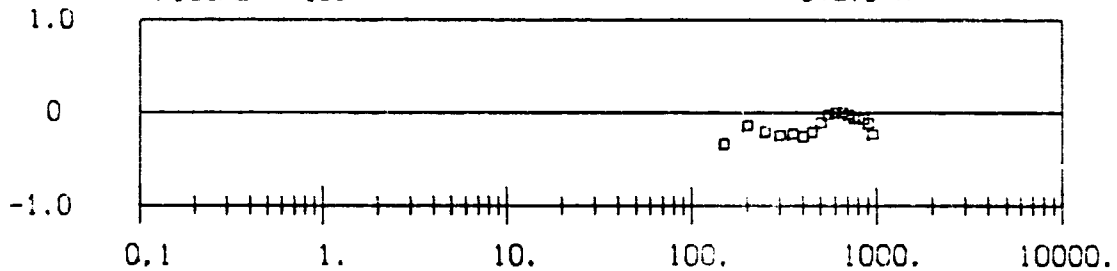
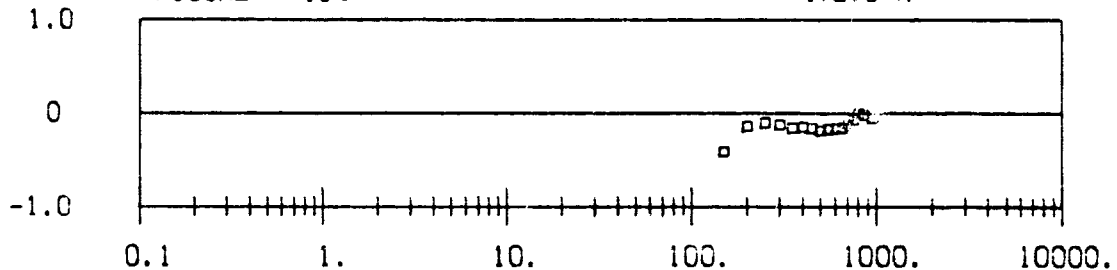


FIGURE 134

472.6 K

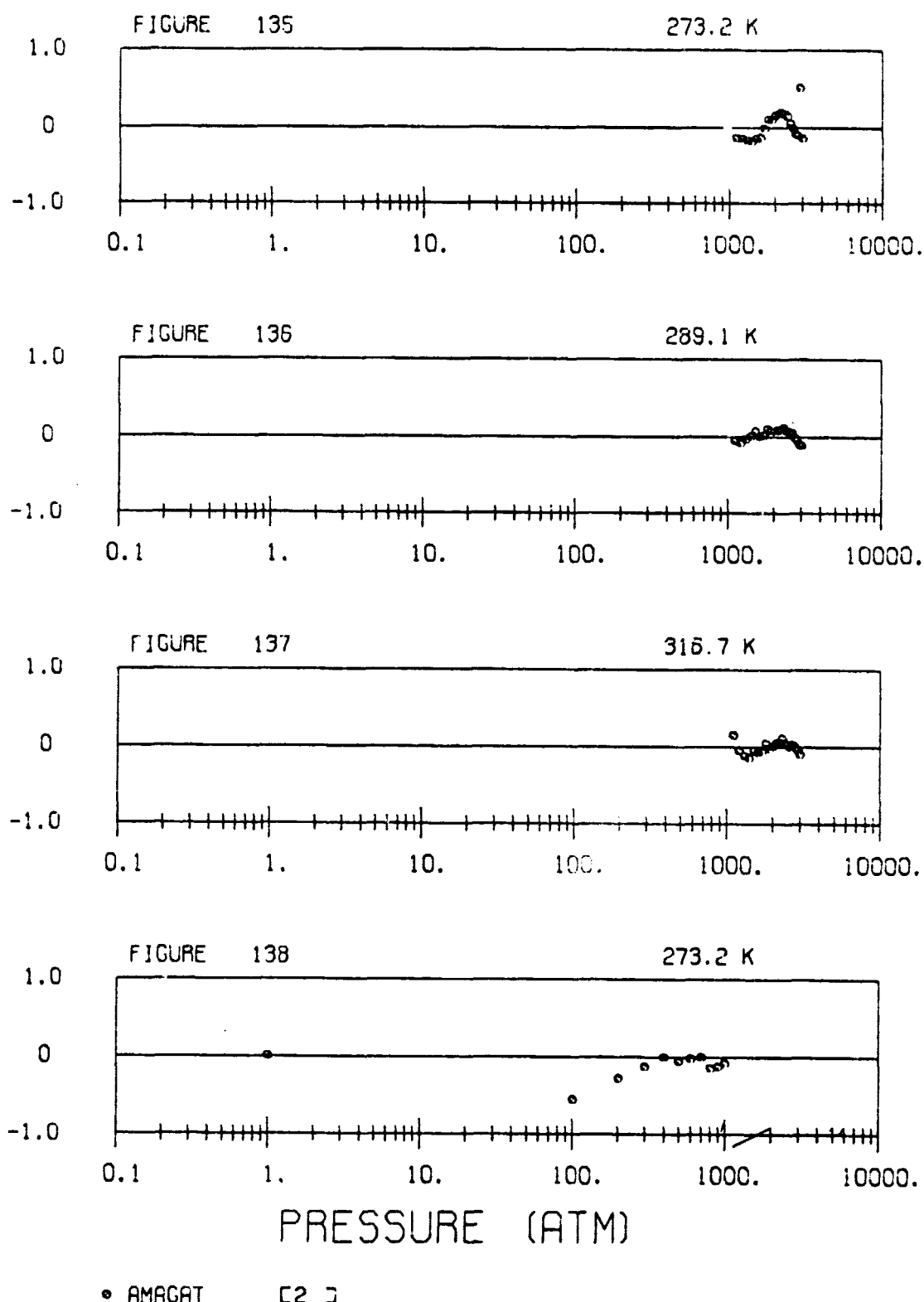


PRESSURE (ATM)

□ AMAGAT C1 □

Density Deviations of Equation (22) from Data of References Indicated.

PERCENT DENSITY DEVIATION



• AMAGAT C2 □

Density Deviations of Equation (22) from Data of References Indicated.

PERCENT DENSITY DEVIATION

FIGURE 139

289.1 K

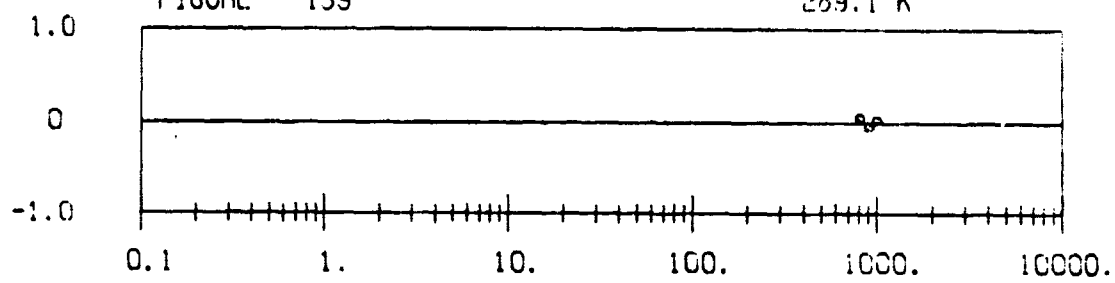


FIGURE 140

316.7 K

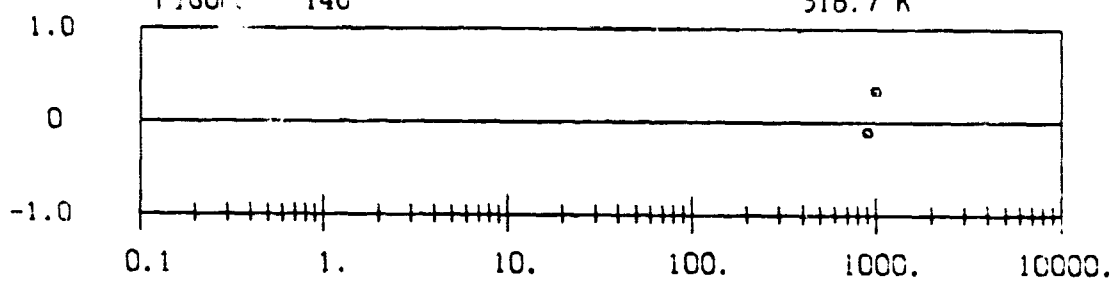


FIGURE 141

273.2 K

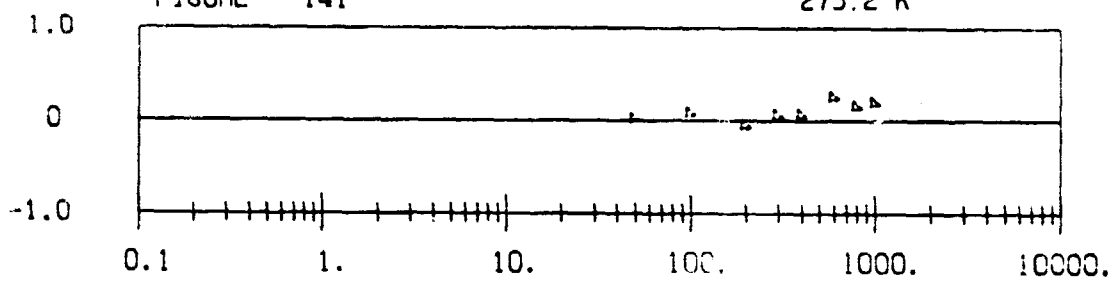
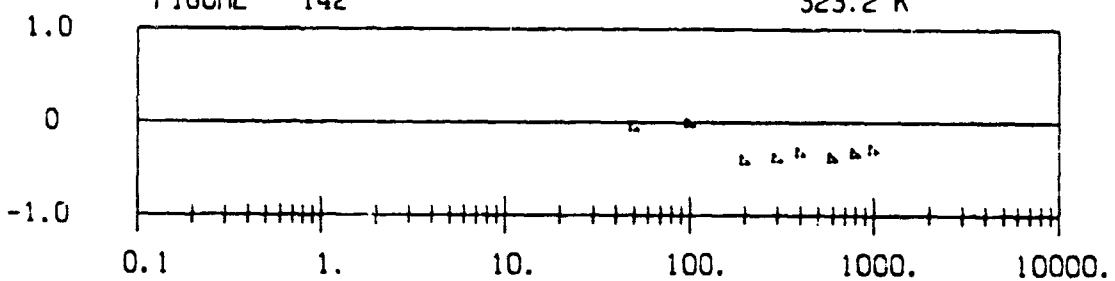


FIGURE 142

323.2 K



PRESSURE (ATM)

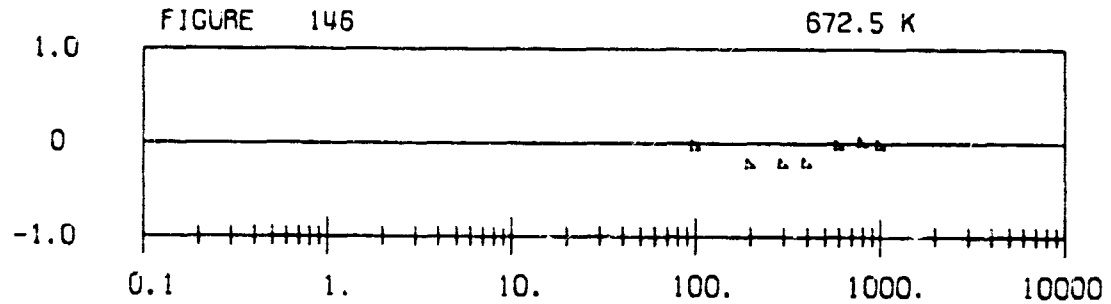
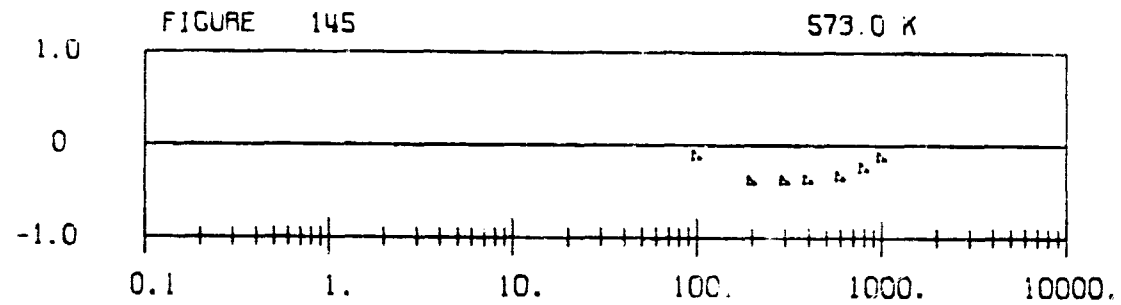
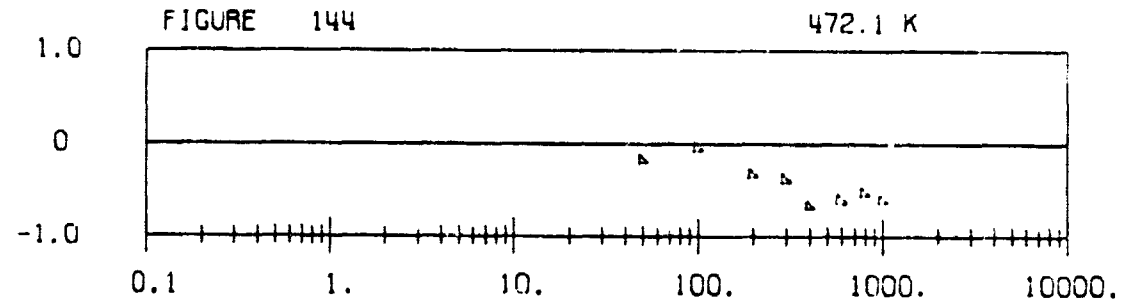
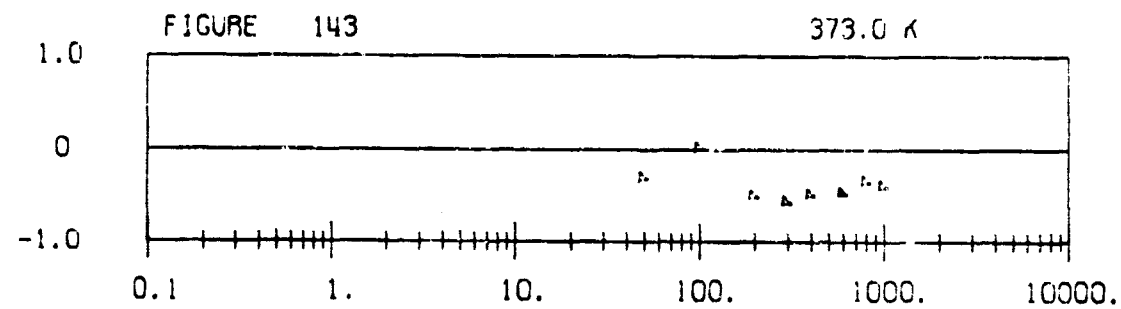
• AMAGAT

E2 □

▲ BARTLETT E4 □

Density Deviations of Equation (22) from Data of References Indicated.

PERCENT DENSITY DEVIATION

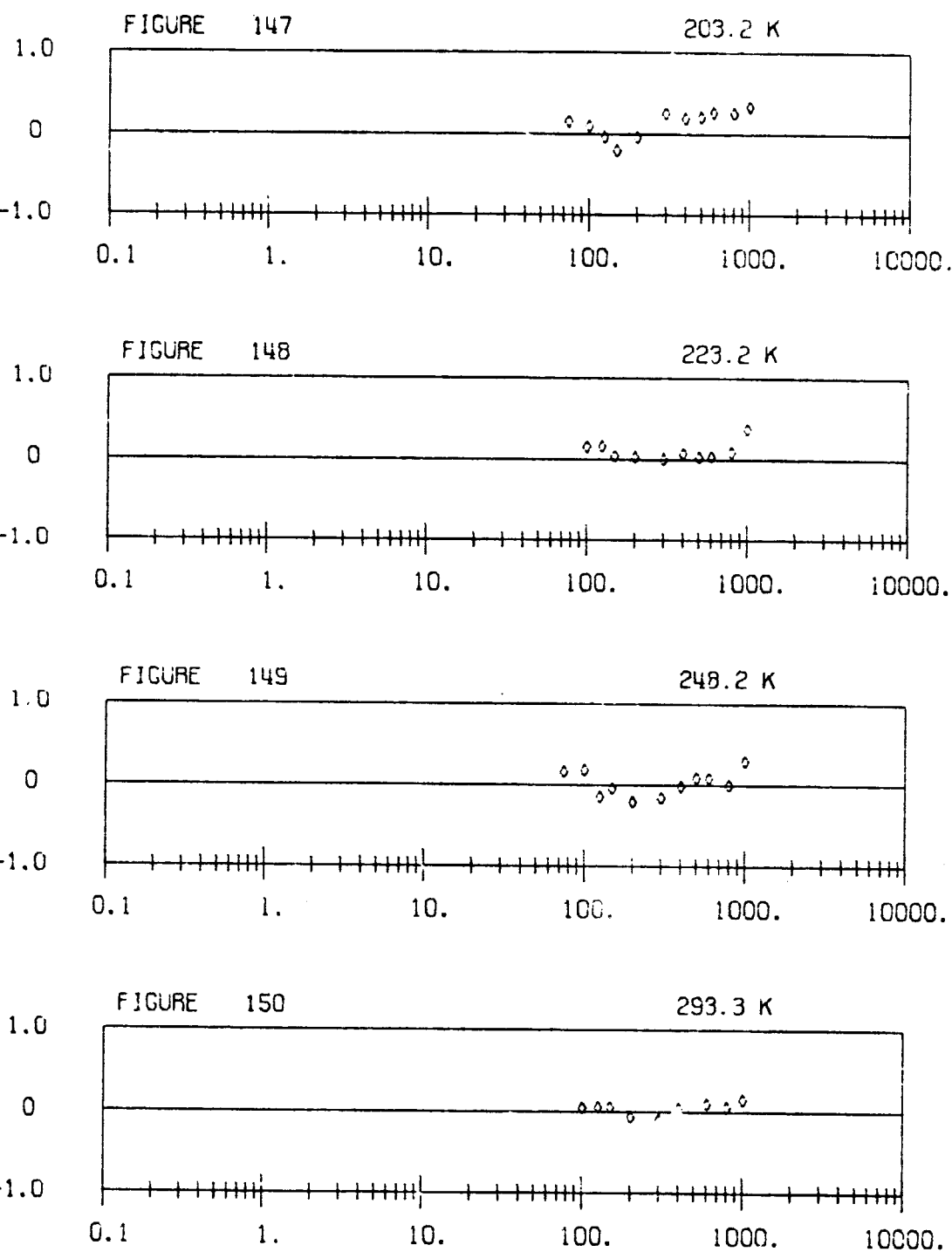


PRESSURE (ATM)

▲ BARTLETT C4 □

Density Deviations of Equation (22) from Data of References Indicated.

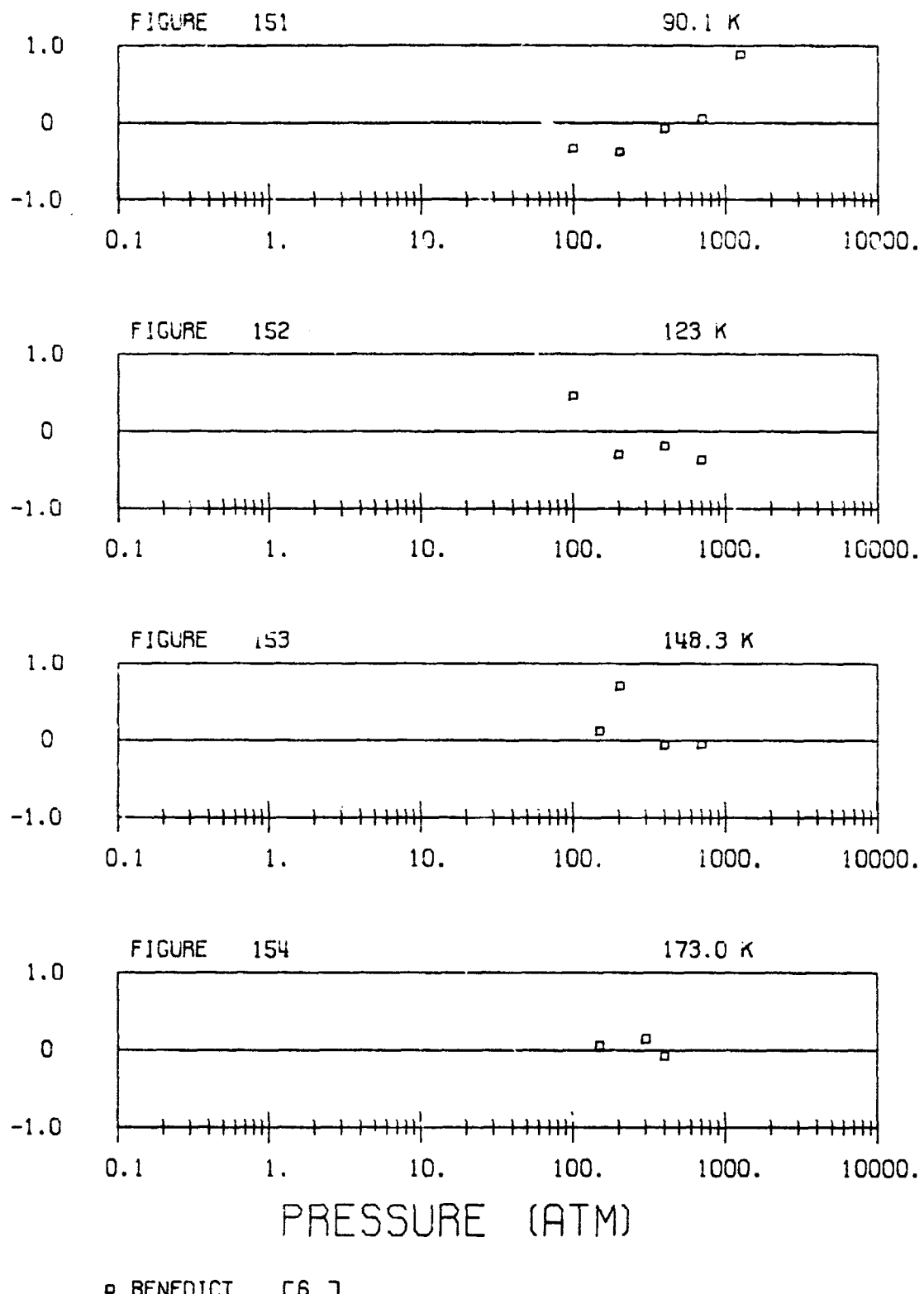
PERCENT DENSITY DEVIATION



♦ BARTLETT C5 □

Density Deviations of Equation (22) from Data of References Indicated.

PERCENT DENSITY DEVIATION



Density Deviations of Equation (22) from Data of References Indicated.

PERCENT DENSITY DEVIATION

FIGURE 155

173.2 K

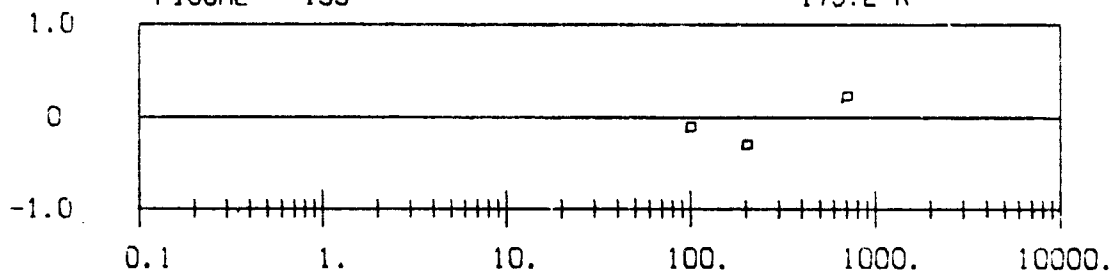


FIGURE 156

273.2 K

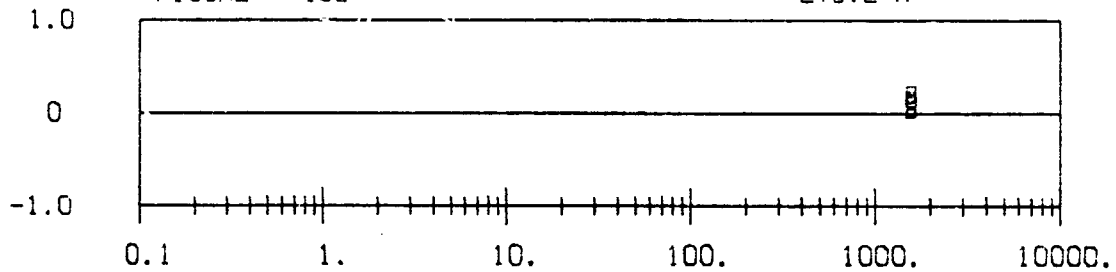


FIGURE 157

98.2 K

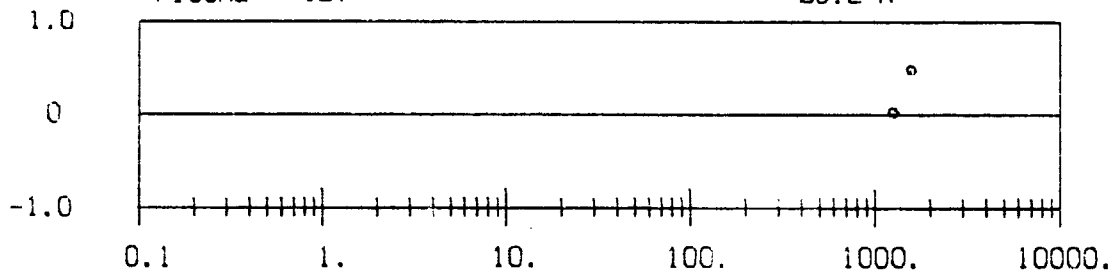
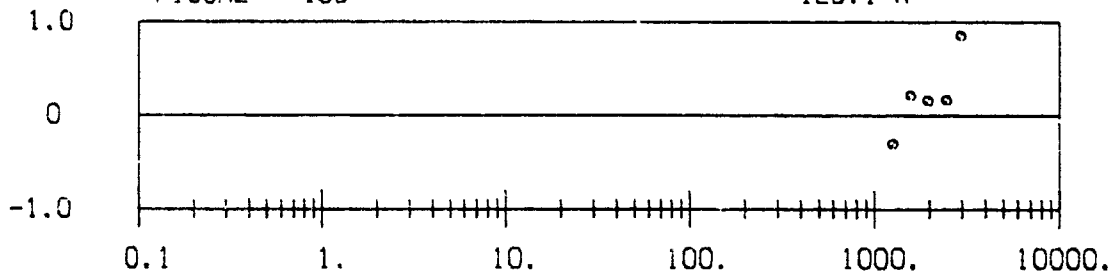


FIGURE 158

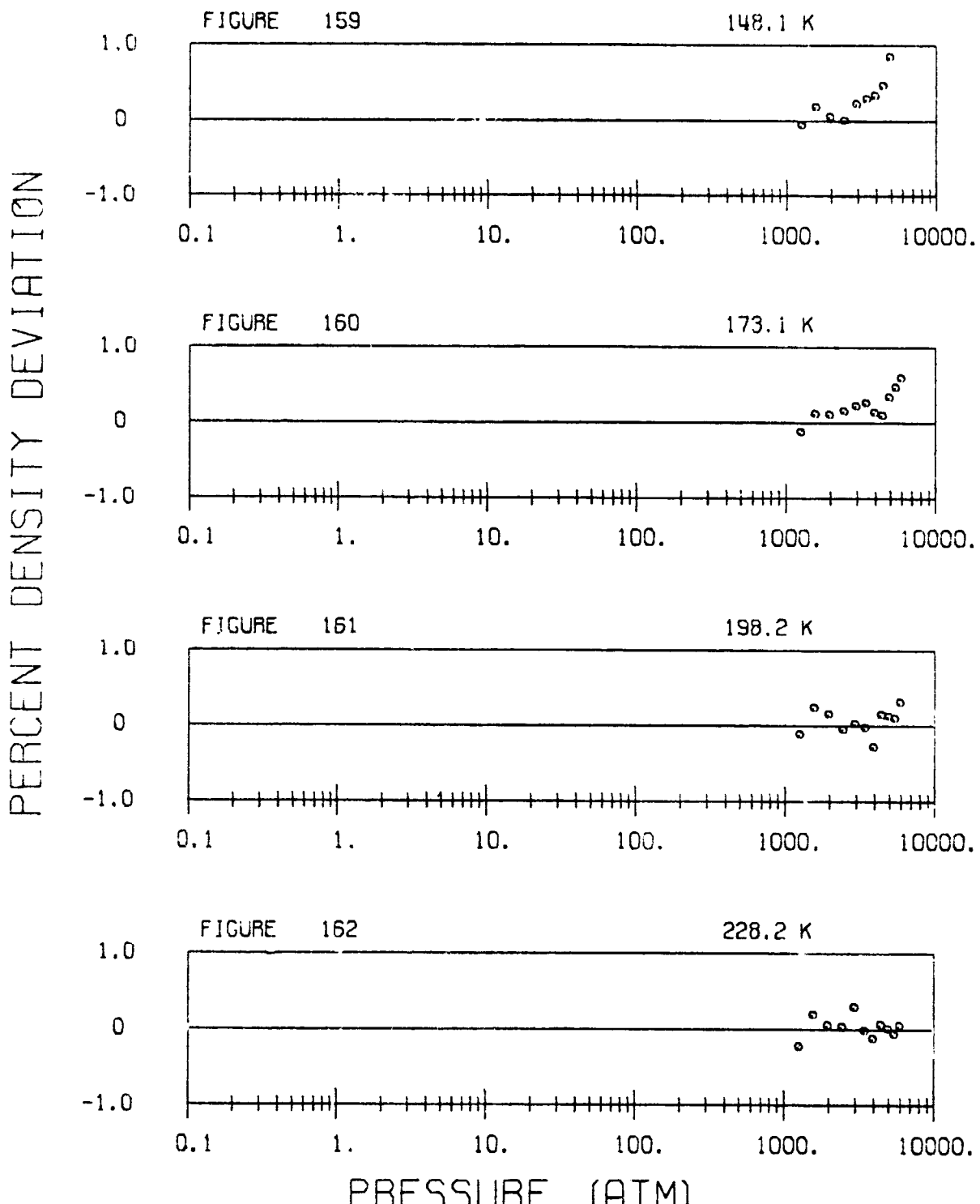
123.1 K



PRESSURE (ATM)

□ BENEDICT C6 □ • BENEDICT C7 □

Density Deviations of Equation (22) from Data of References Indicated.



Density Deviations of Equation (22) from Data of References Indicated:

PERCENT DENSITY DEVIATION

FIGURE 163

273.2 K

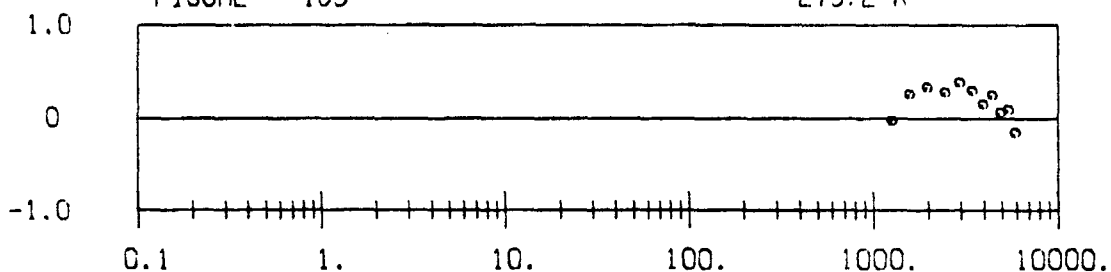


FIGURE 164

298.1 K

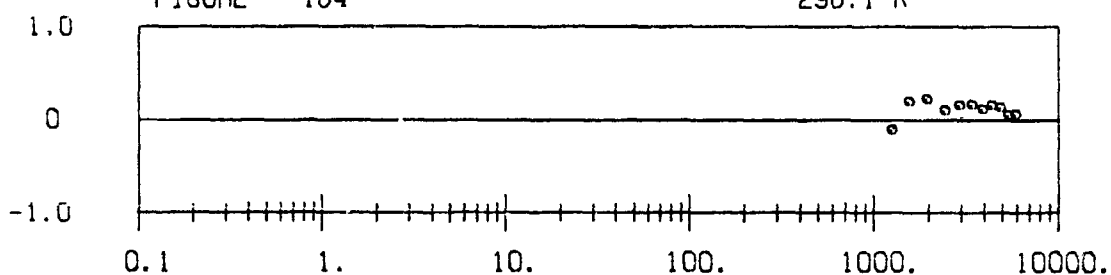


FIGURE 165

323.1 K

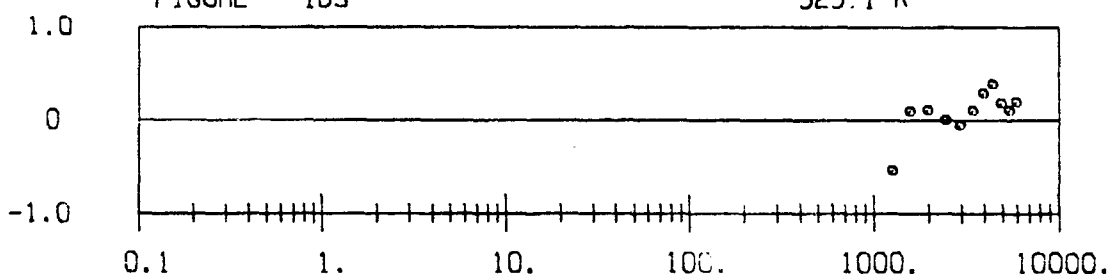
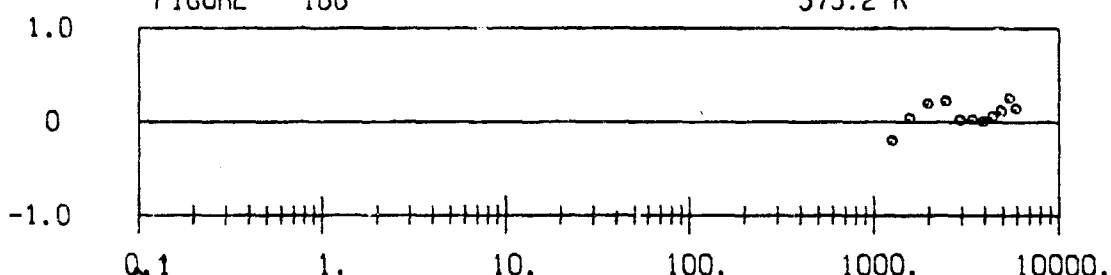


FIGURE 166

373.2 K

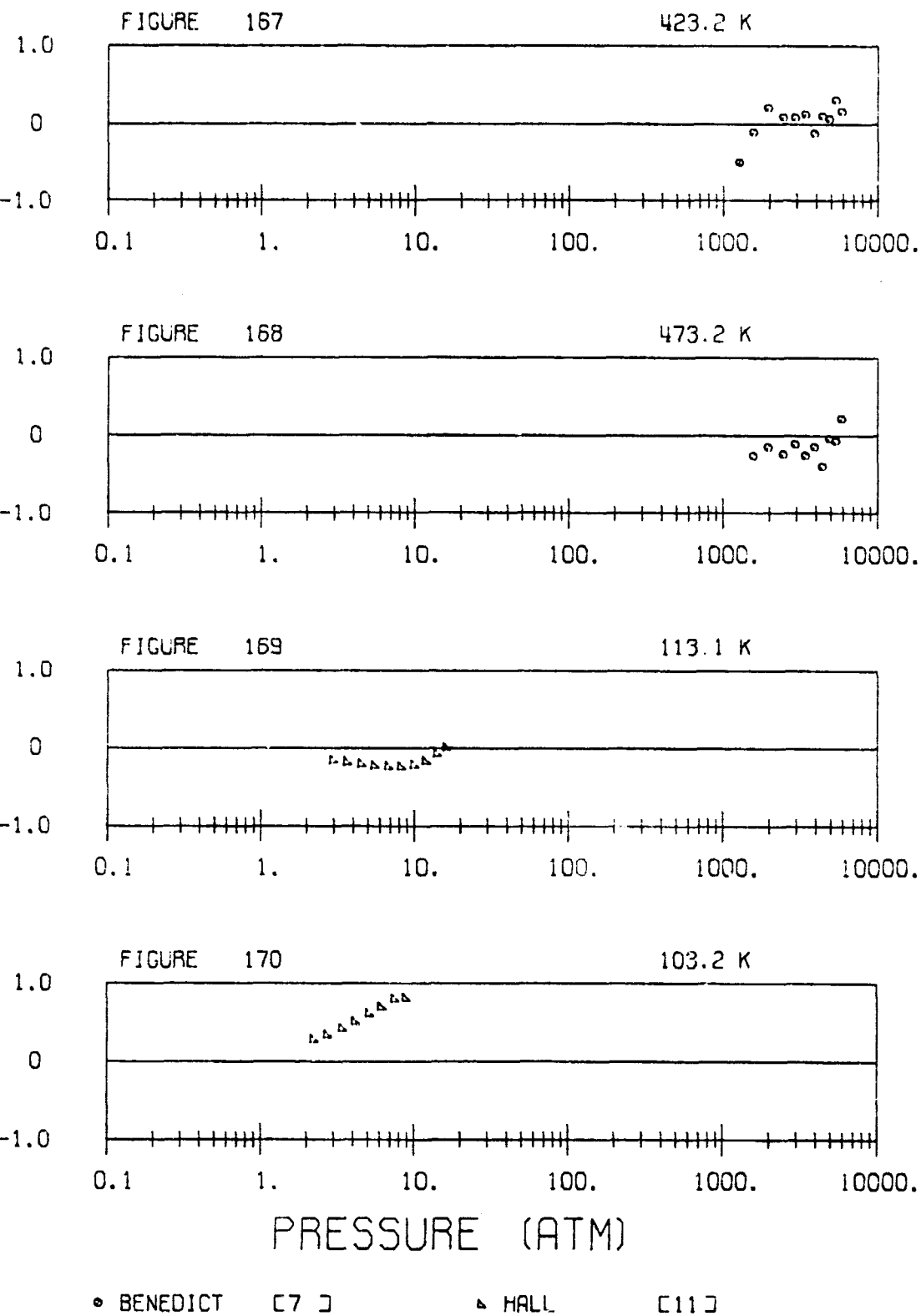


PRESSURE (ATM)

• BENEDICT [7]

Density Deviations of Equation (22) from Data of References Indicated.

PERCENT DENSITY DEVIATION



• BENEDICT [7]

△ HALL [11]

Density Deviations of Equation (22) from Data of References Indicated

PERCENT DENSITY DEVIATION

FIGURE 171

273.2 K

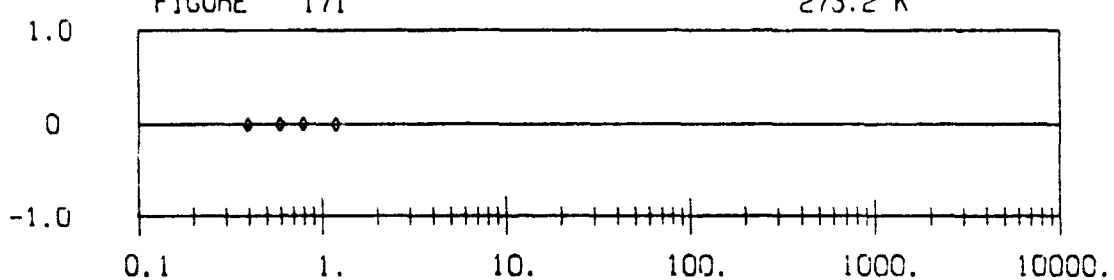


FIGURE 172

215.2 K

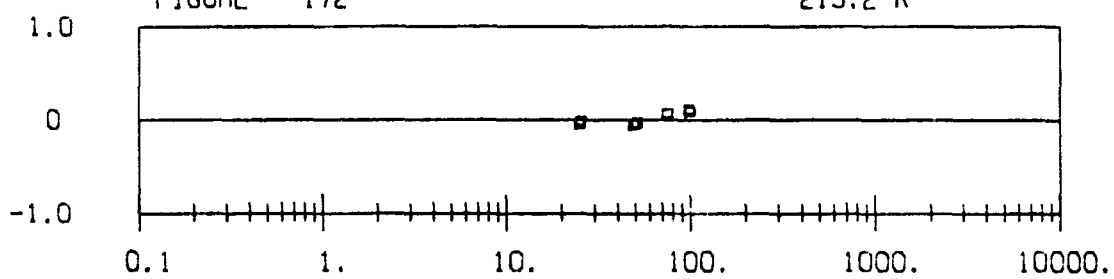


FIGURE 173

323.2 K

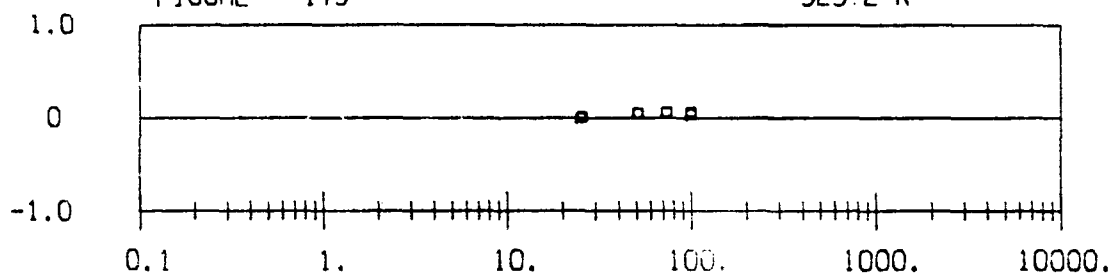
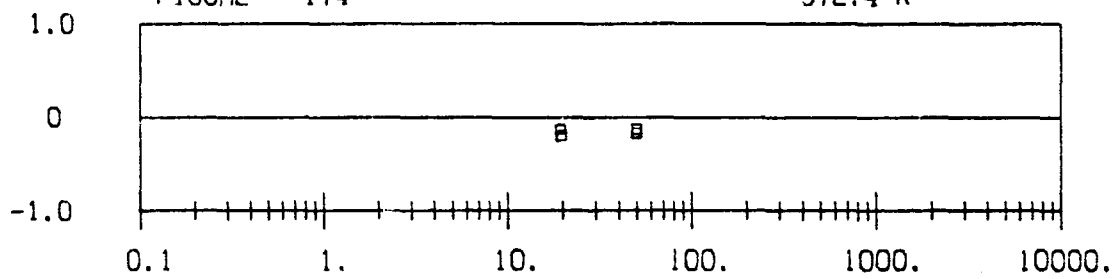


FIGURE 174

372.4 K



PRESSURE (ATM)

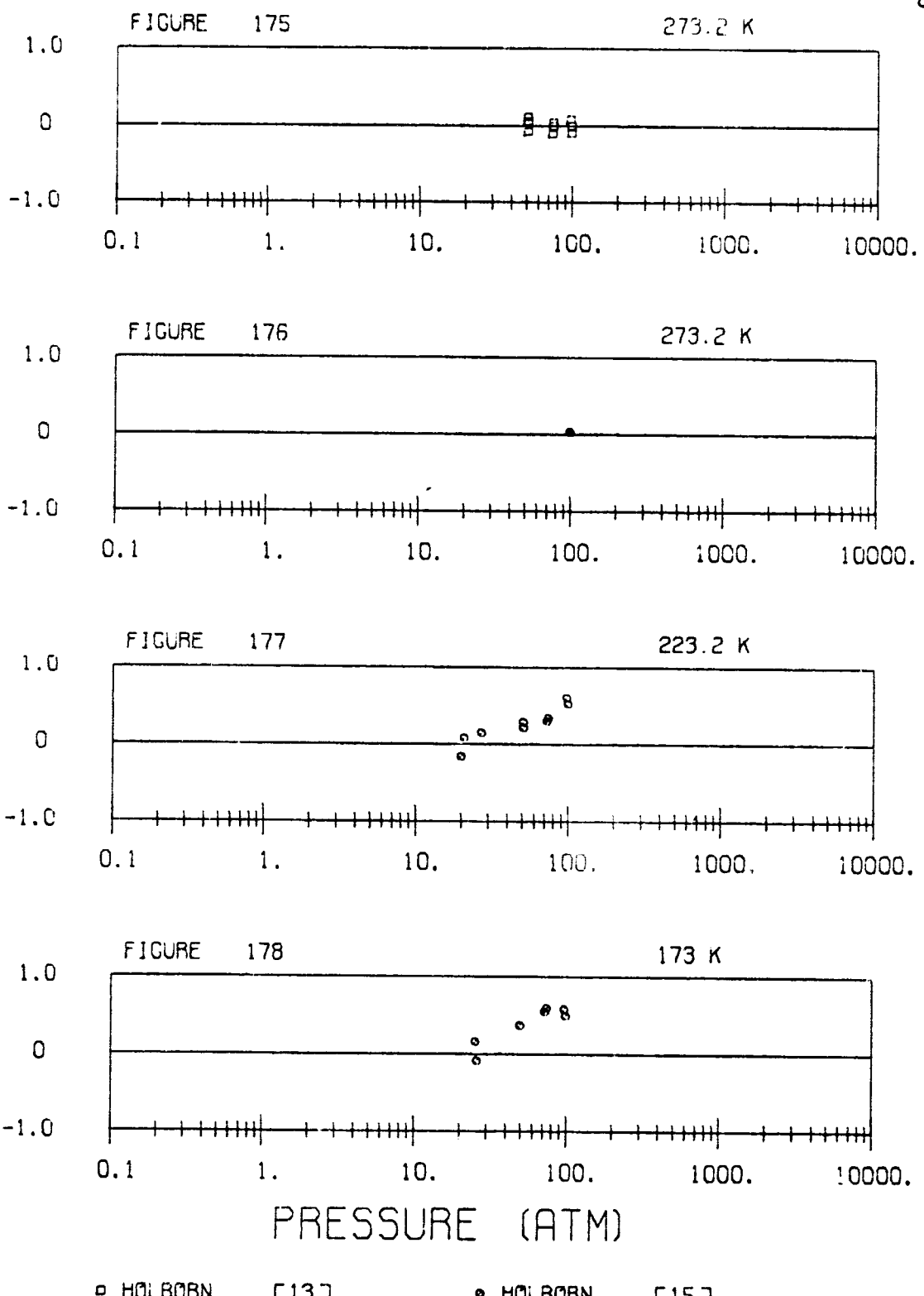
◊ HEUSE

□ HOLBORN

□ HOLBORN

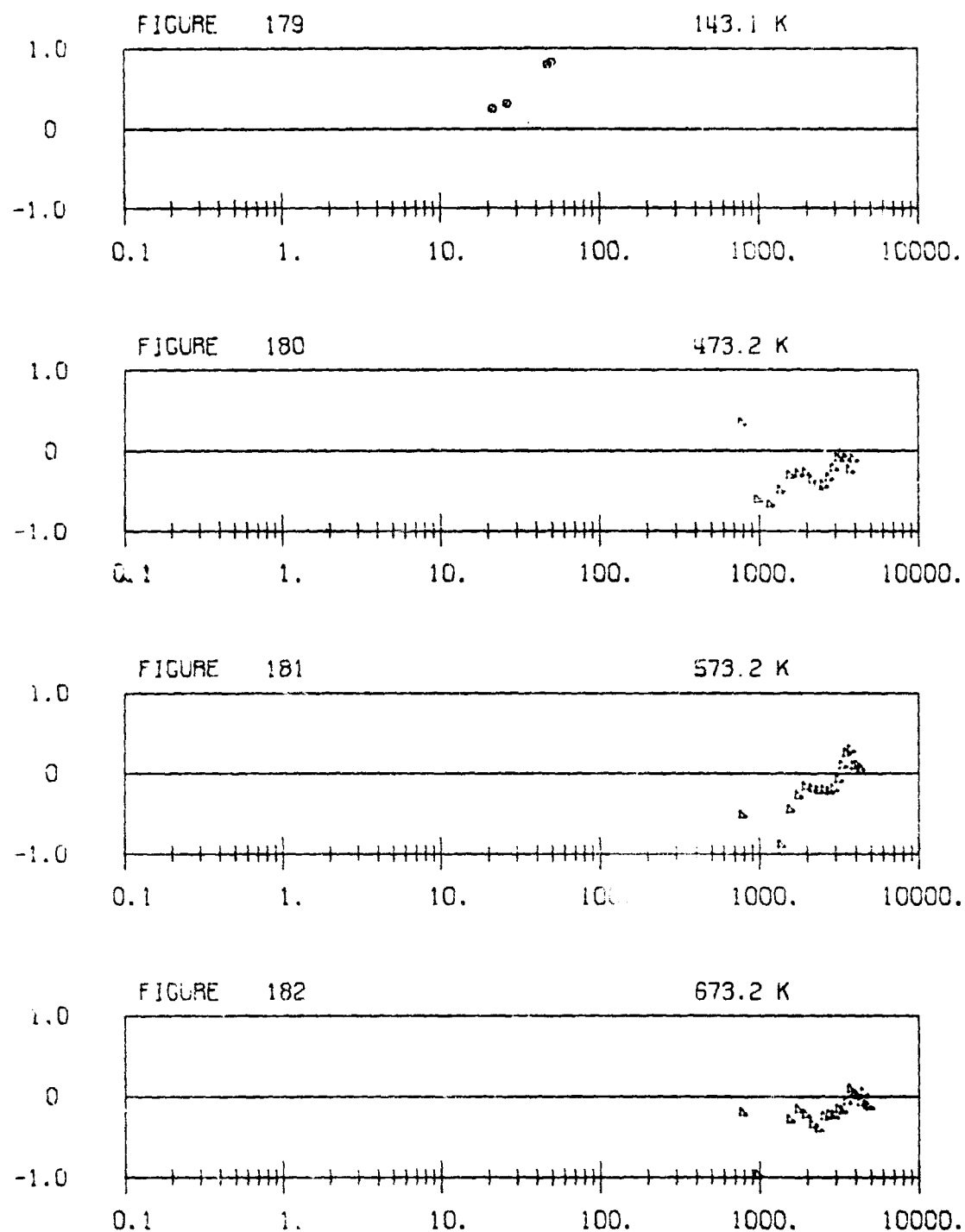
Density Deviations of Equation (22) from Data of References Indicated.

PERCENT DENSITY DEVIATION



Density Deviations of Equation (22) from Data of References Indicated

PERCENT DENSITY DEVIATION



PRESSURE (ATM)

• HOLBORN [15] ▲ MALBRUNOT [17]

Density Deviations of Equation (22) from Data of References Indicated.

PERCENT DENSITY DEVIATION

FIGURE 183

873.3 K

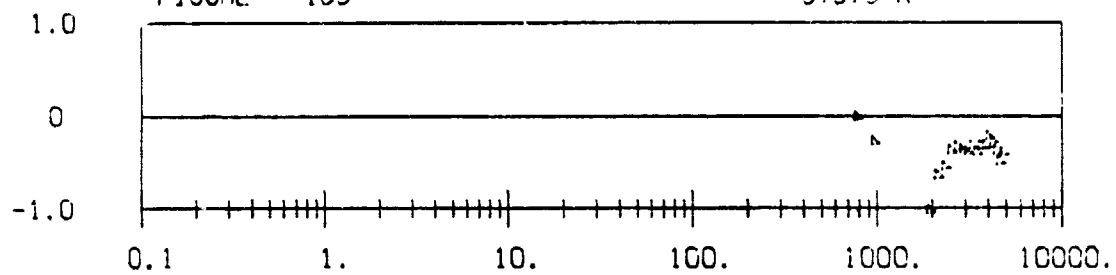


FIGURE 184

873.3 K

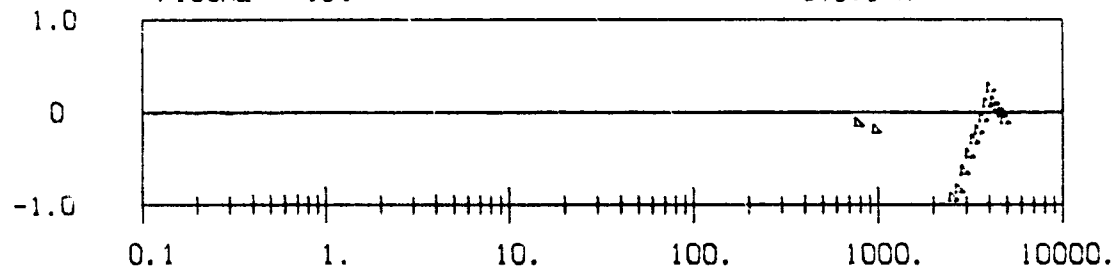


FIGURE 185

973.5 K

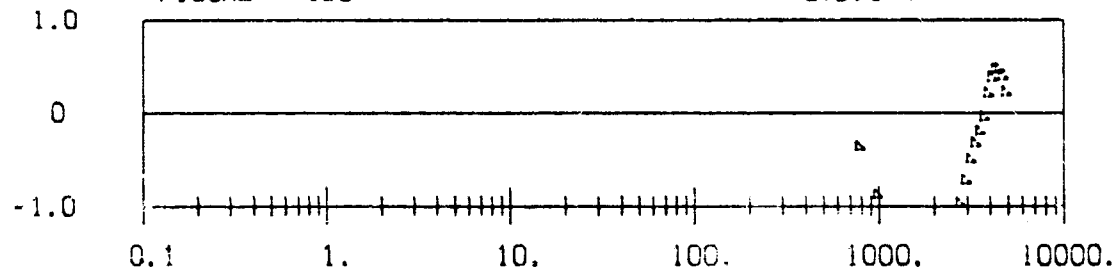
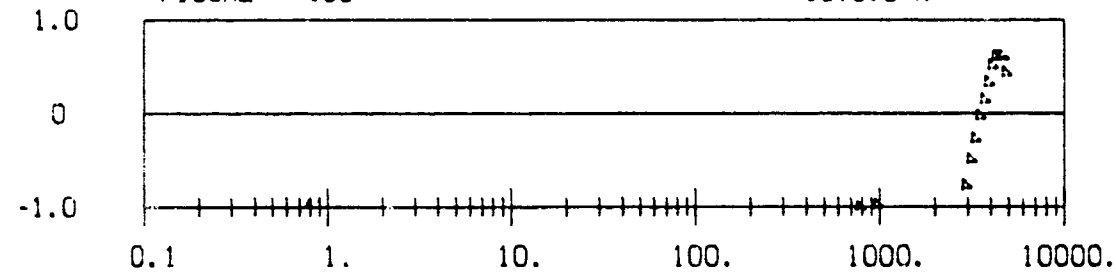


FIGURE 186

1073.8 K



PRESSURE (ATM)

▲ MALBRUNOT [17]

Density Deviations of Equation (22) from Data of References Indicated.

PERCENT DENSITY DEVIATION

FIGURE 187

1174.1 K

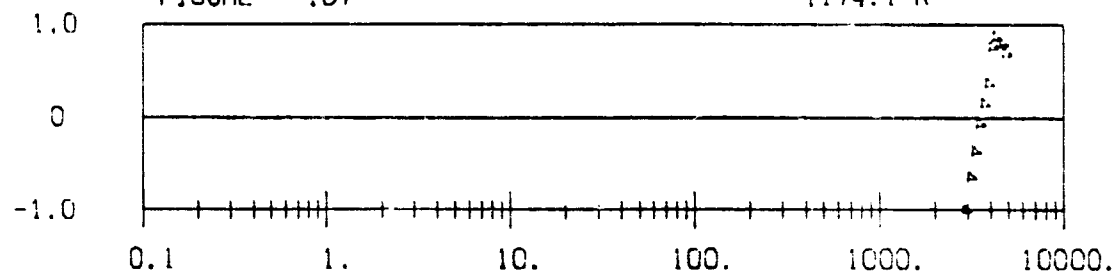


FIGURE 188

1274.4 K

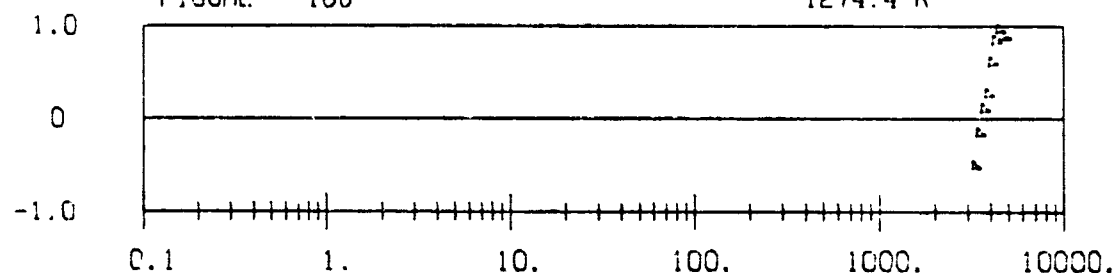


FIGURE 189

473.2 K

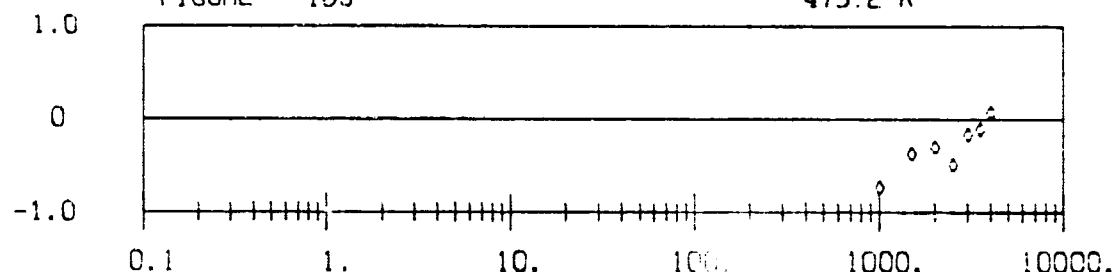
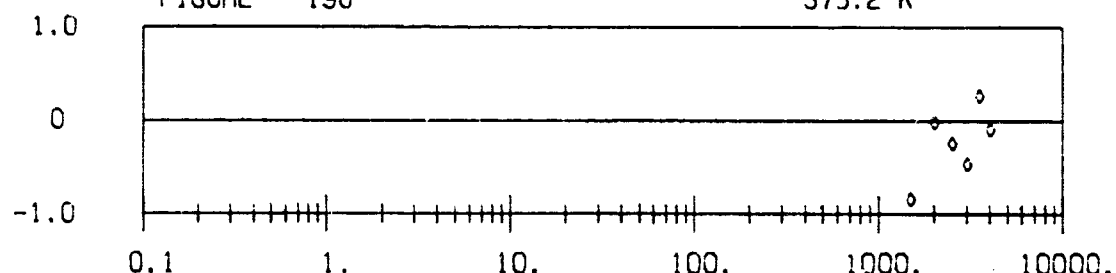


FIGURE 190

573.2 K



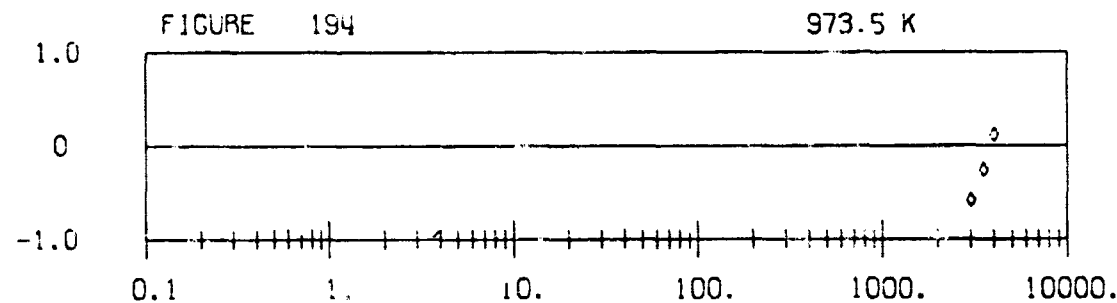
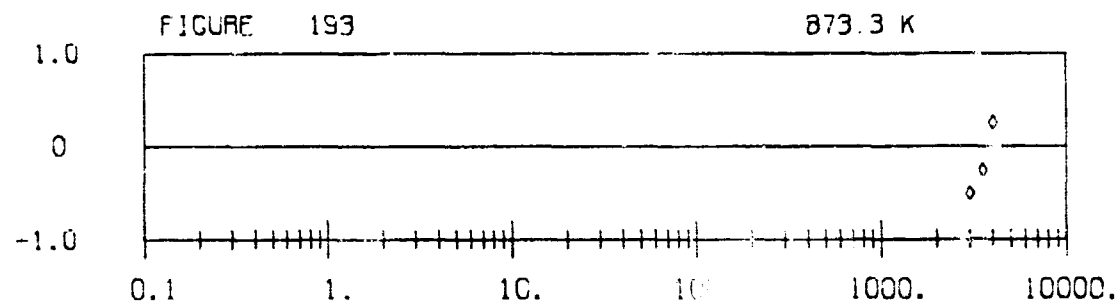
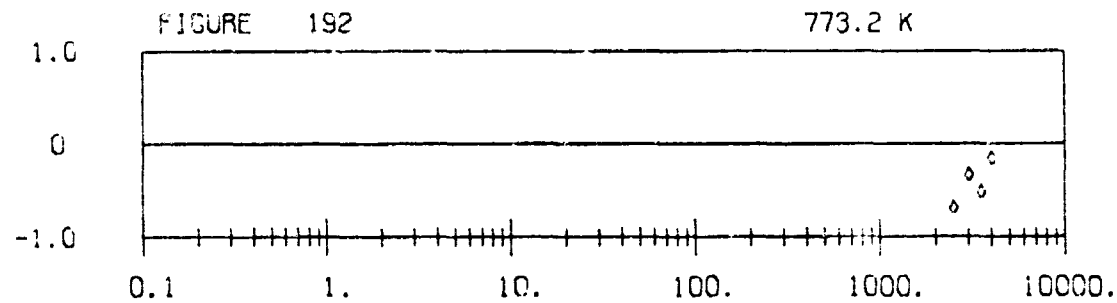
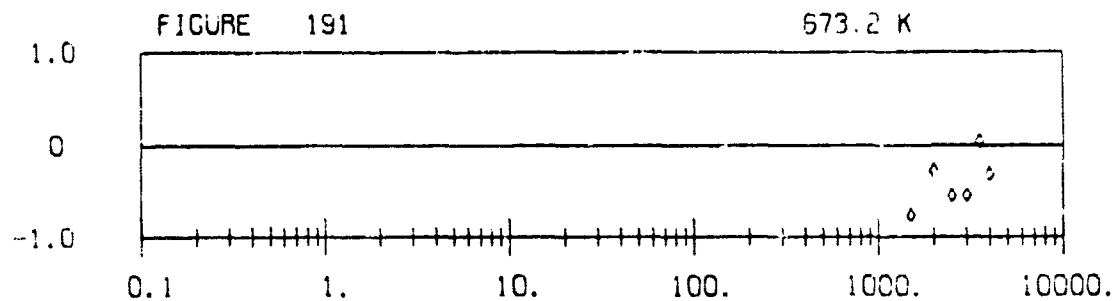
PRESSURE (ATM)

▲ MALBRUNOT [17]

◆ MALBRUNOT [18]

Density Deviations of Equation (22) from Data of References Indicated.

PERCENT DENSITY DEVIATION



PRESSURE (ATM)

◆ MALBRUNOT [18]

Density Deviations of Equation (22) from Data of References Indicated:

PERCENT DENSITY DEVIATION

FIGURE 195

1073.8 K

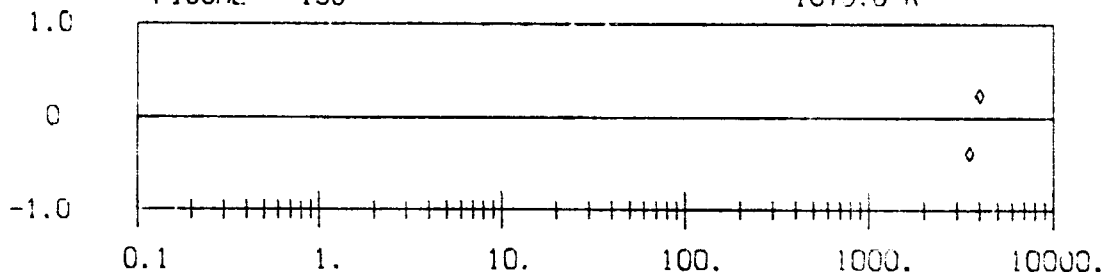


FIGURE 196

1174.1 K

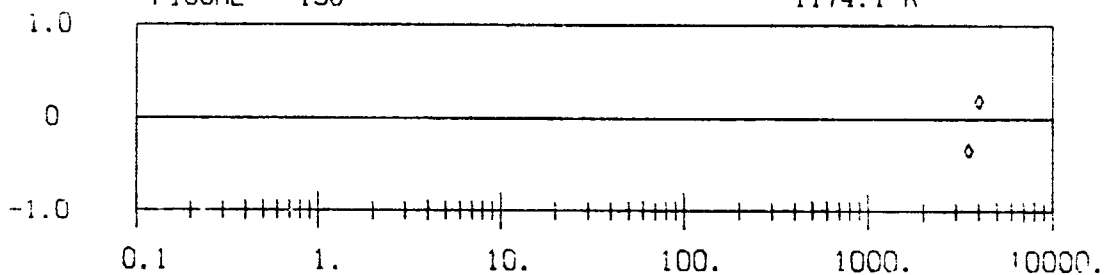


FIGURE 197

1274.4 K

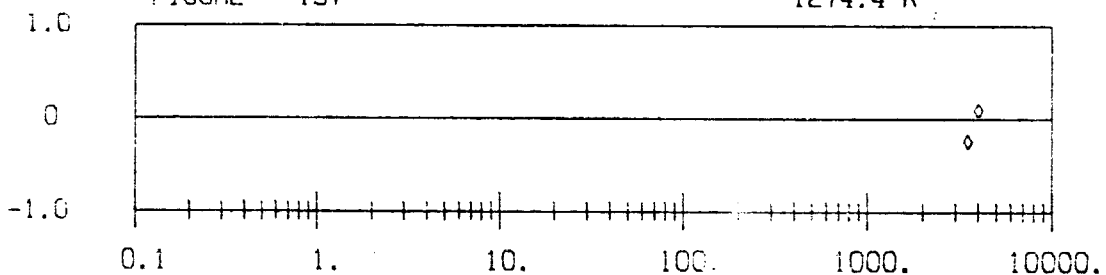
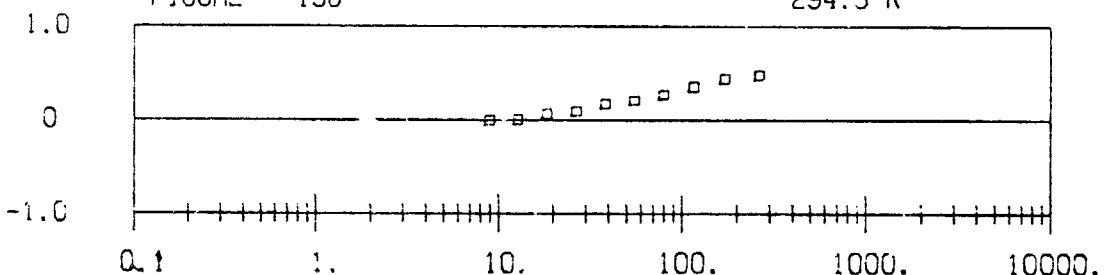


FIGURE 198

294.3 K



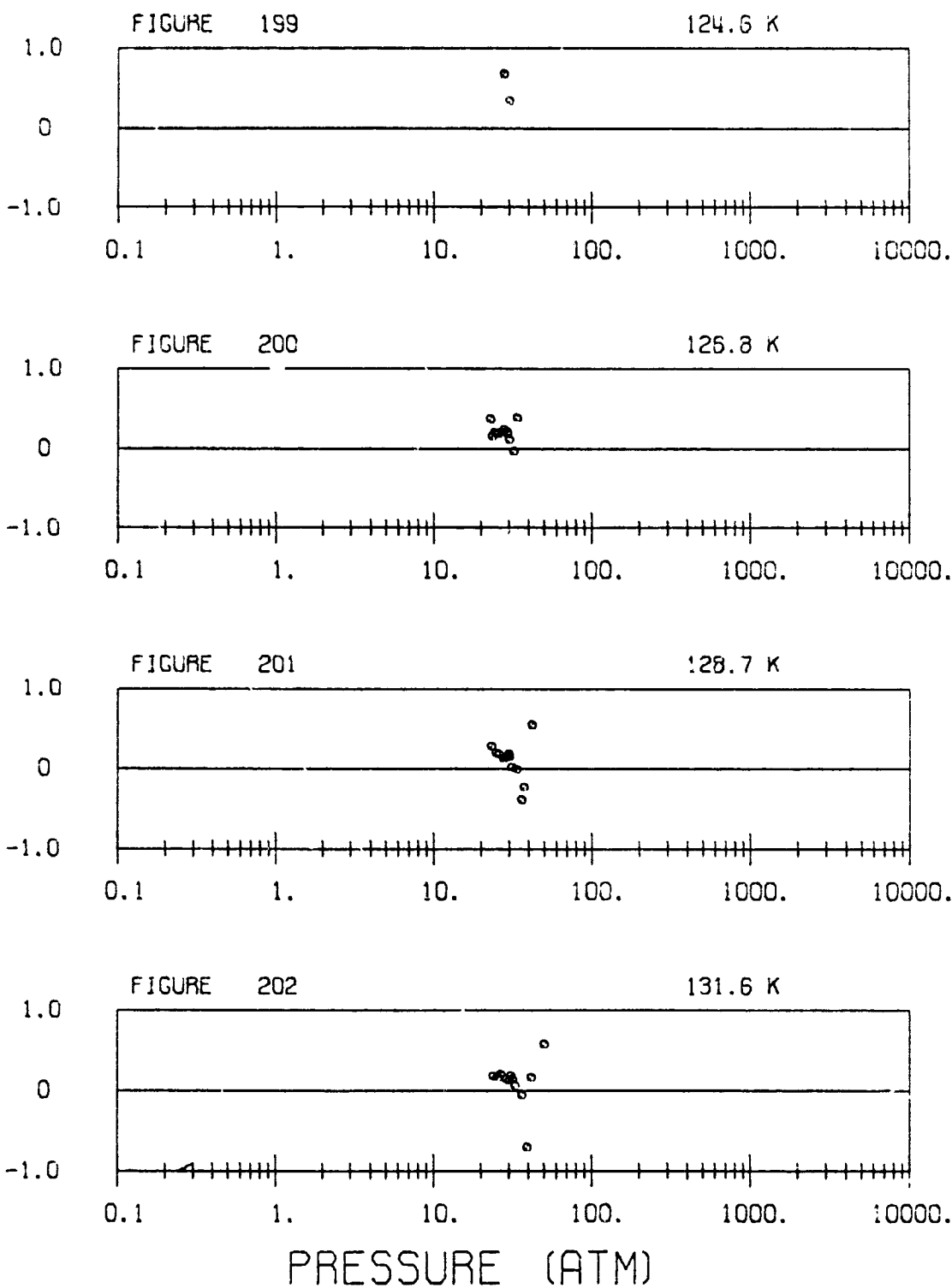
PRESSURE (ATM)

◊ MALBRUNOT [18]

◻ MILLER [21]

Density Deviations of Equation (22) from Data of References Indicated.

PERCENT DENSITY DEVIATION

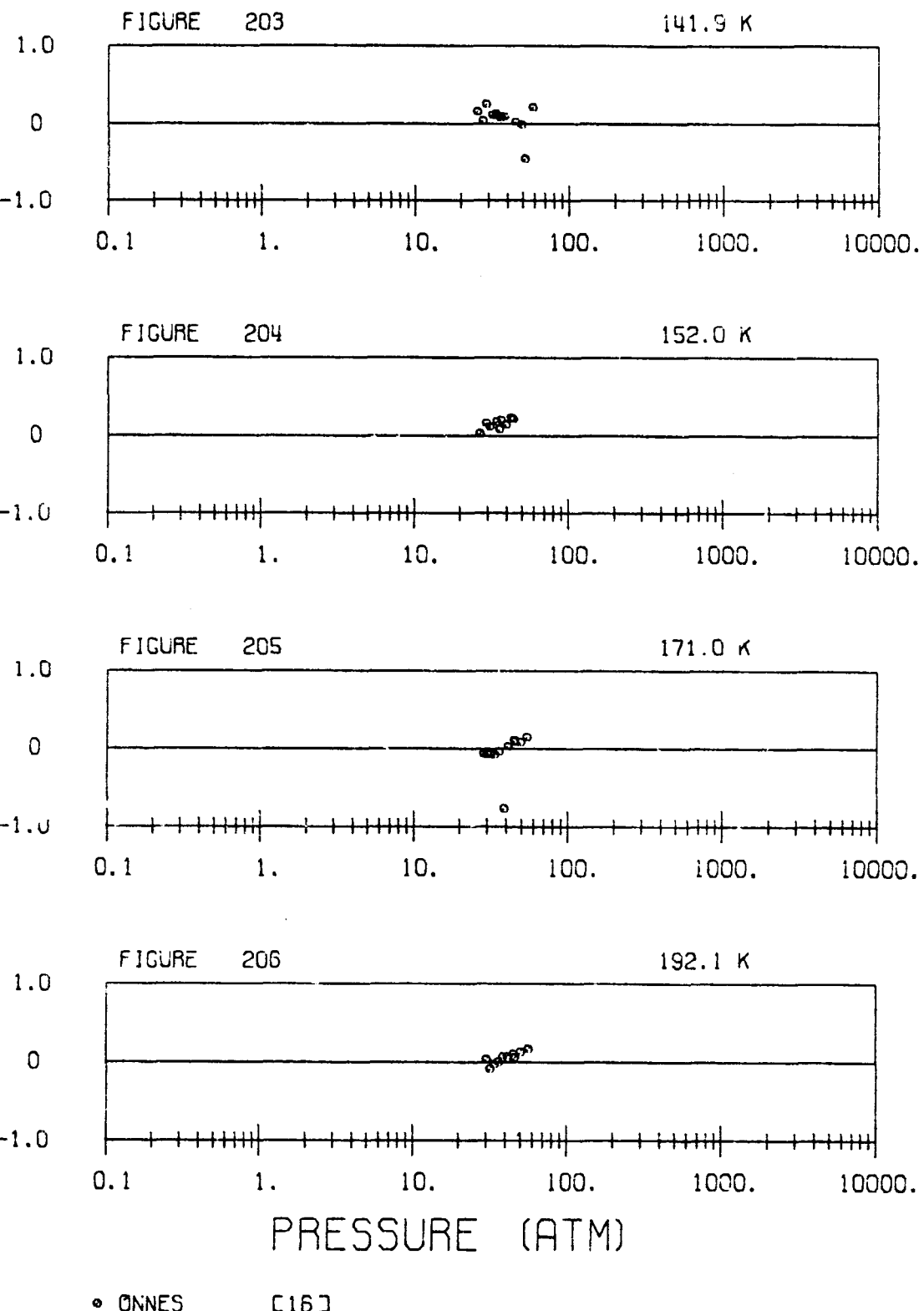


• ONNES

[16]

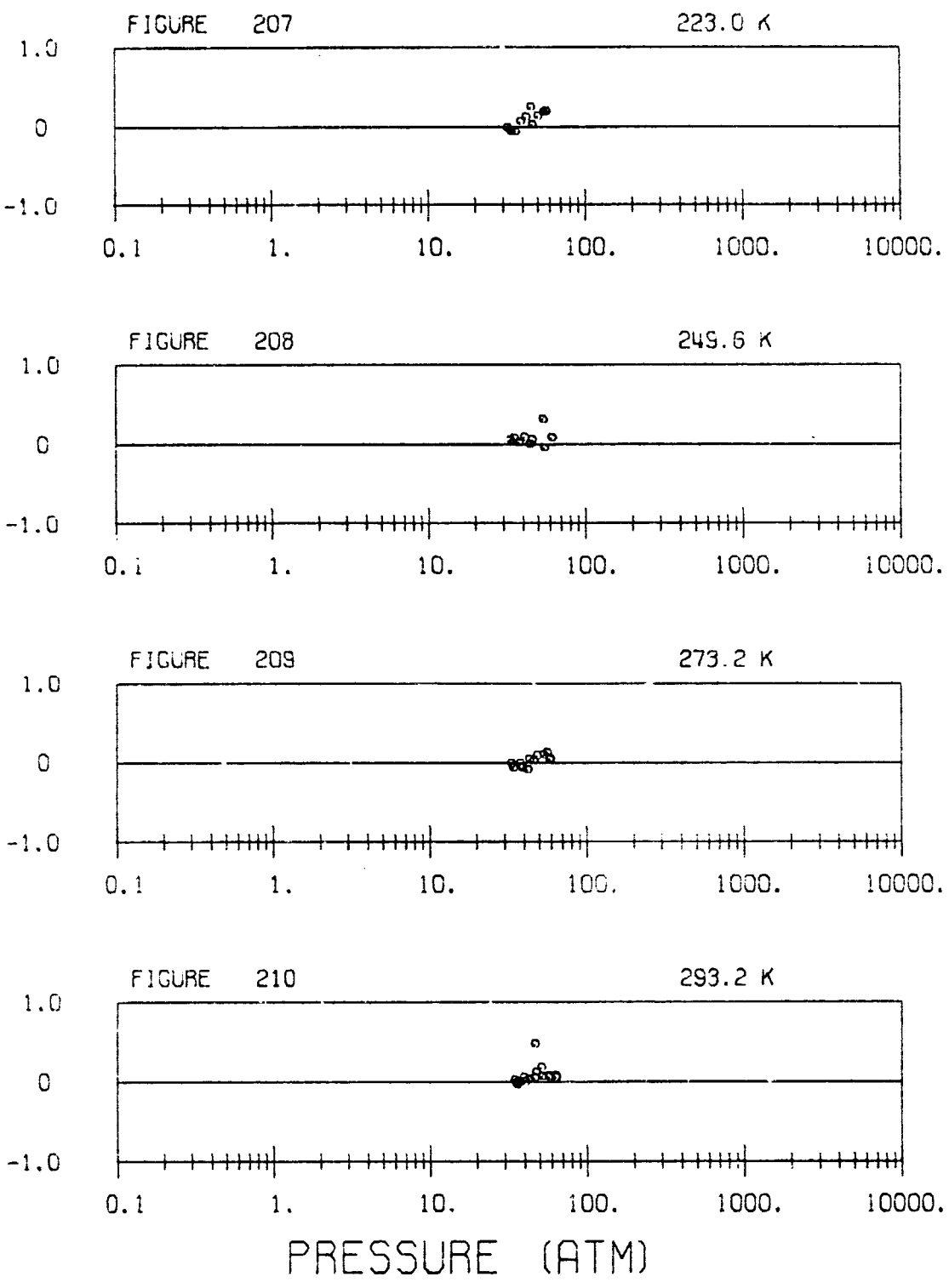
Density Deviations of Equation (22) from Data of References Indicated.

PERCENT DENSITY DEVIATION



Density Deviations of Equation (22) from Data of References Indicated.

PERCENT DENSITY DEVIATION



Density Deviations of Equation (22) from Data of References Indicated.

PERCENT DENSITY DEVIATION

FIGURE 211

77.4 K

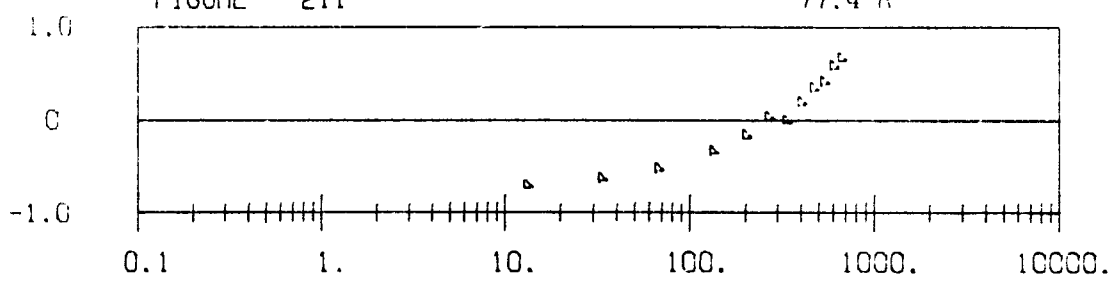


FIGURE 212

90.6 K

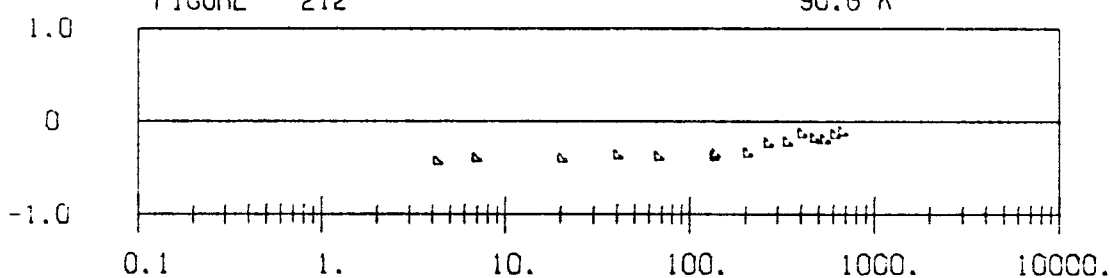


FIGURE 213

95.6 K

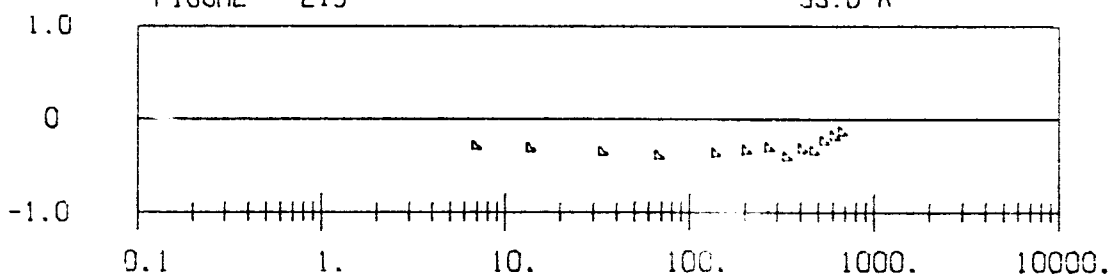
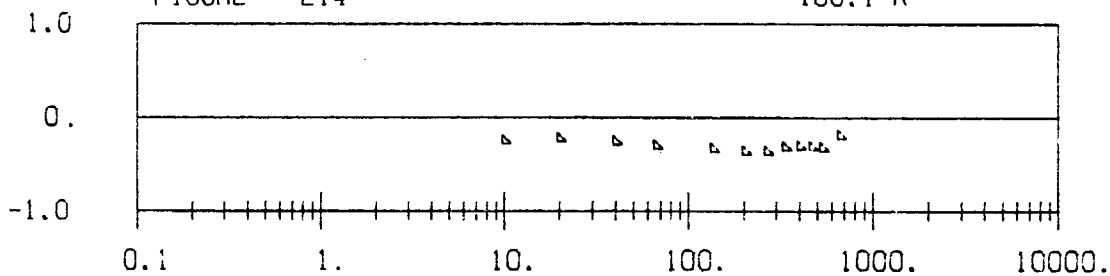


FIGURE 214

100.1 K



PRESSURE (ATM)

▲ STREETT [33]

Density Deviations of Equation (22) from Data of References Indicated.

PERCENT DENSITY DEVIATION

FIGURE 215

104.7 K

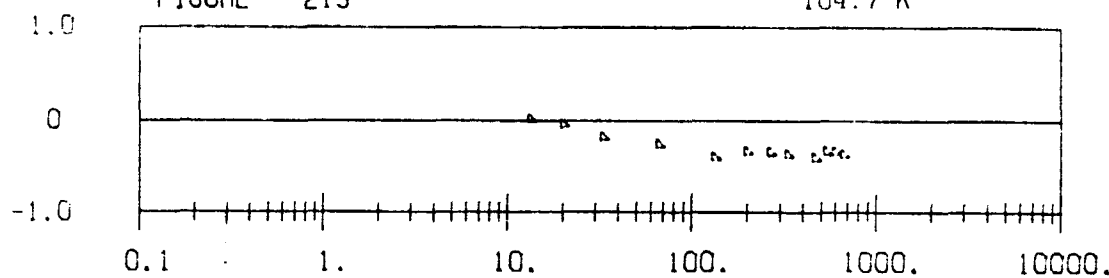


FIGURE 216

110.0 K

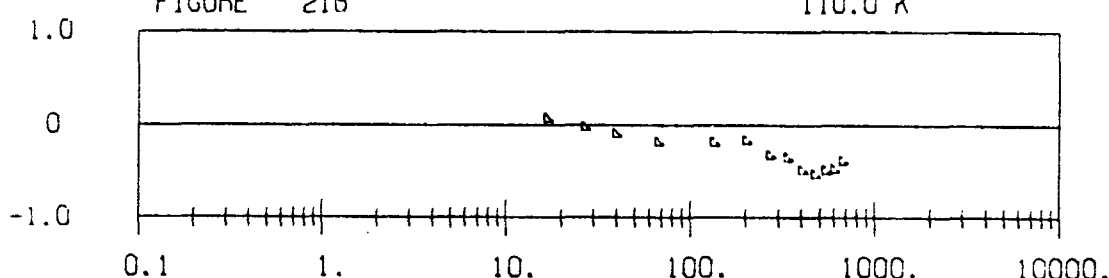


FIGURE 217

114.9 K

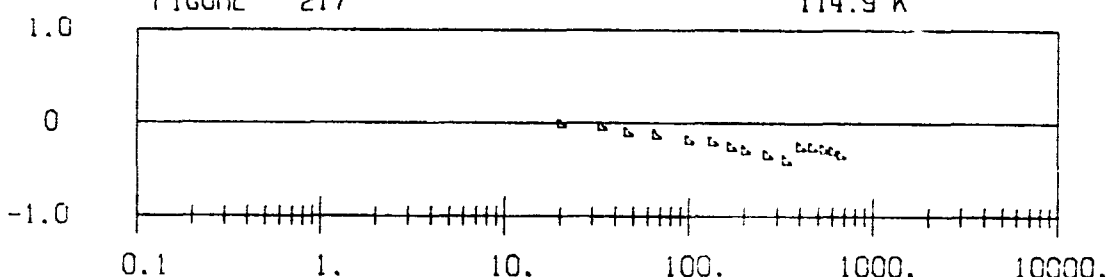
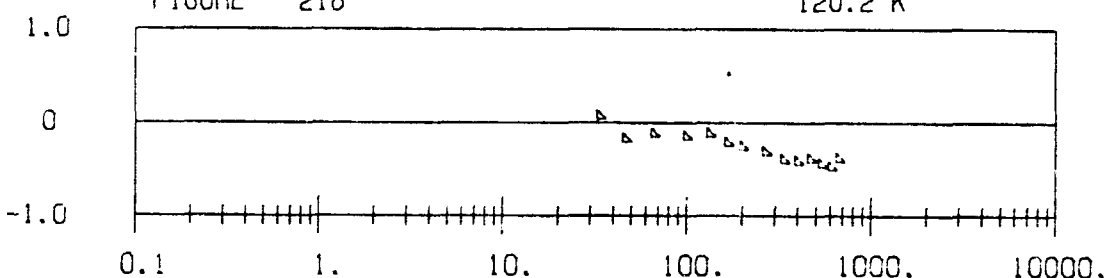


FIGURE 218

120.2 K

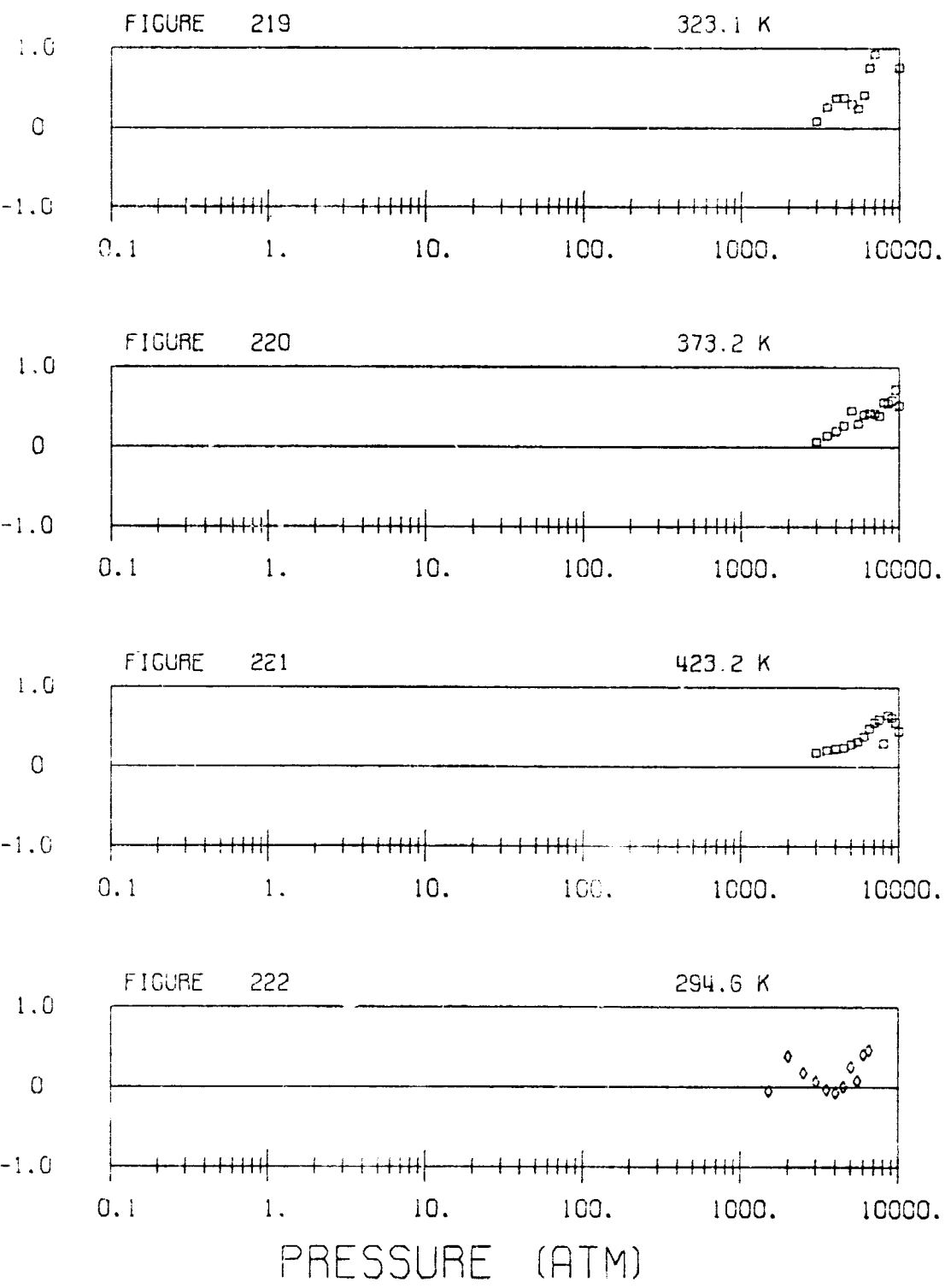


PRESSURE (ATM)

▲ STREETT [33]

Density Deviations of Equation (22) from Data of References Indicated.

PERCENT DENSITY DEVIATION



PRESSURE (ATM)

♦ TSIKLIS

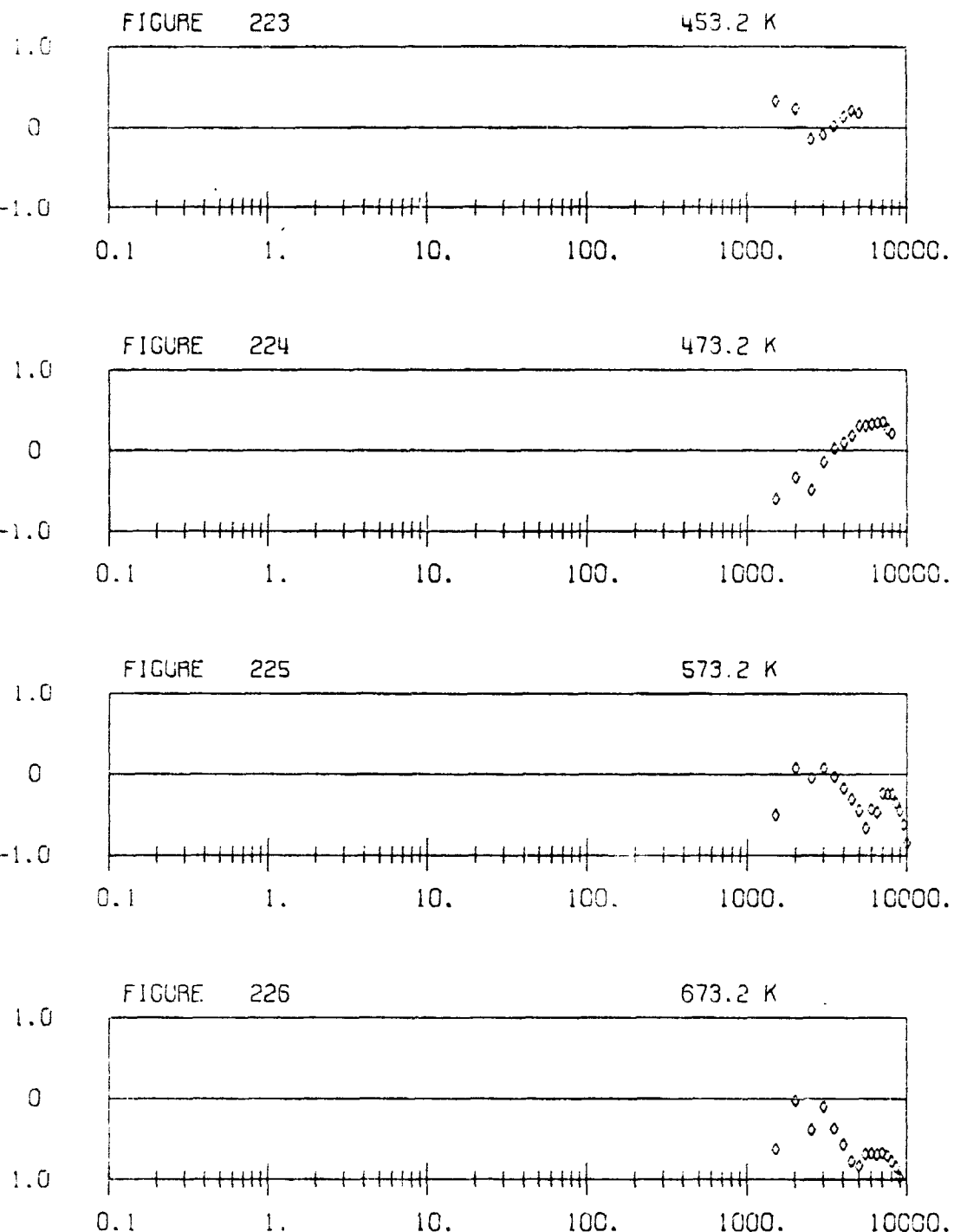
[27]

♦ TSIKLIS

[28]

Density Deviations of Equation (22) from Data of References Indicated.

PERCENT DENSITY DEVIATION



♦ TSIKLIS [27]

Density Deviations of Equation (22) from Data of References Indicated.

PERCENT DENSITY DEVIATION

FIGURE 227

65.9 K

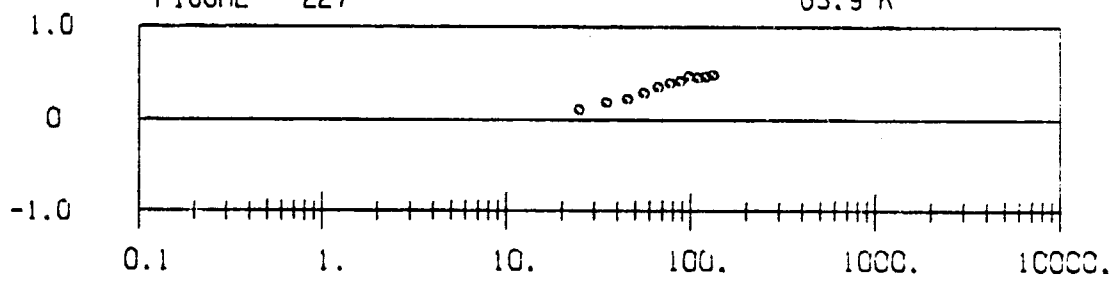


FIGURE 228

72.3 K

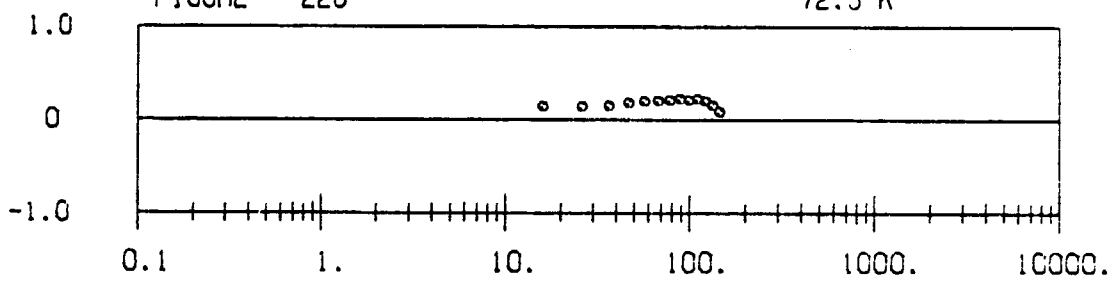


FIGURE 229

77.9 K

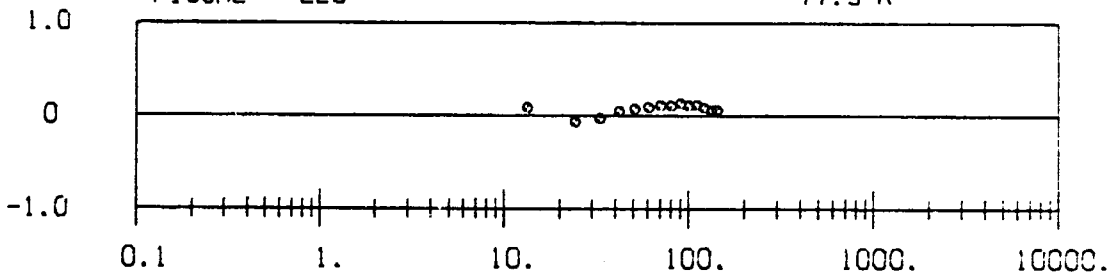
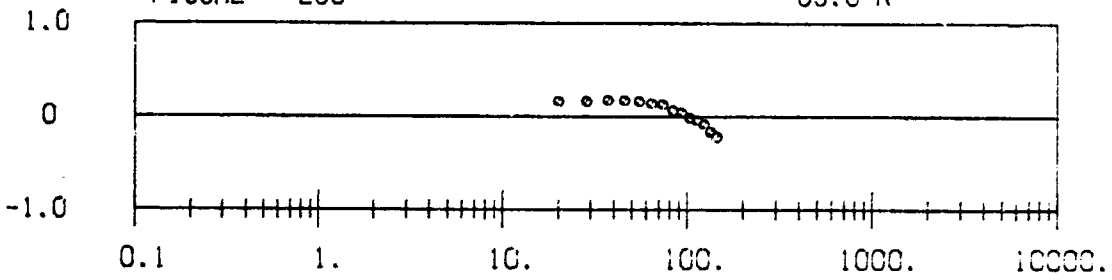


FIGURE 230

85.0 K



PRESSURE (ATM)

• ITTERBEEK C343

Density Deviations of Equation (22) from Data of References Indicated.

PERCENT DENSITY DEVIATION

FIGURE 231

90.6 K

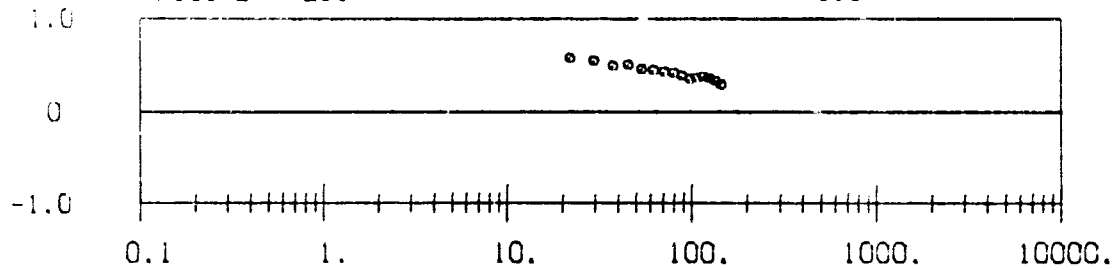


FIGURE 232

90.3 K

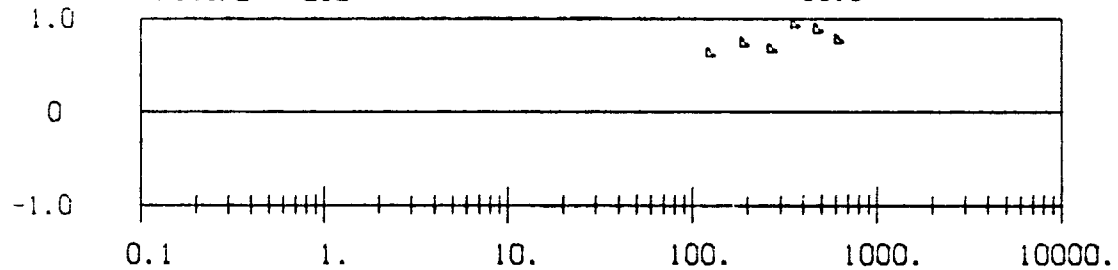


FIGURE 233

77.3 K

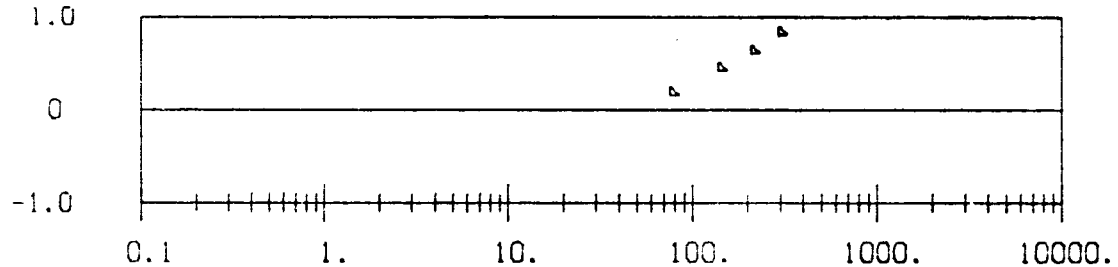
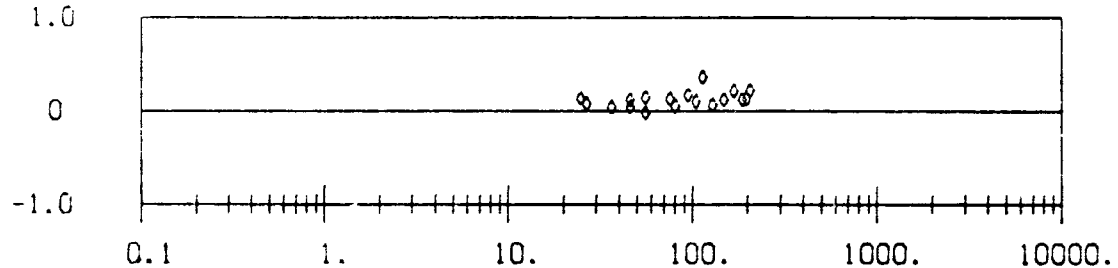


FIGURE 234

273.2 K



PRESSURE (ATM)

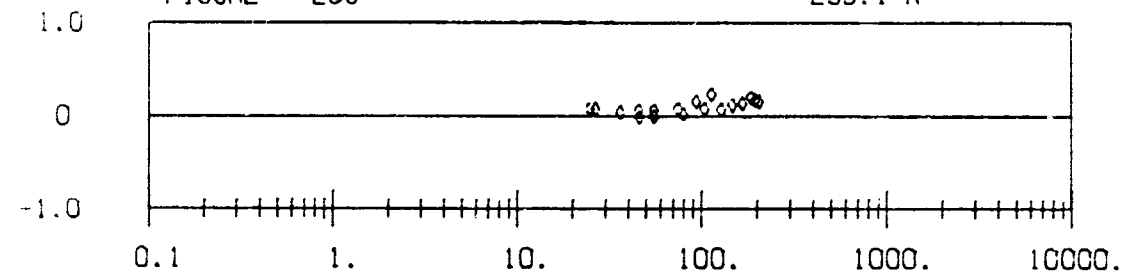
• ITTERBEEK [34] □ VERSCHOYLE [29]
▲ ITTERBEEK [35]

Density Deviations of Equation (22) from Data of References Indicated.

PERCENT DENSITY DEVIATION

FIGURE 235

293.1 K

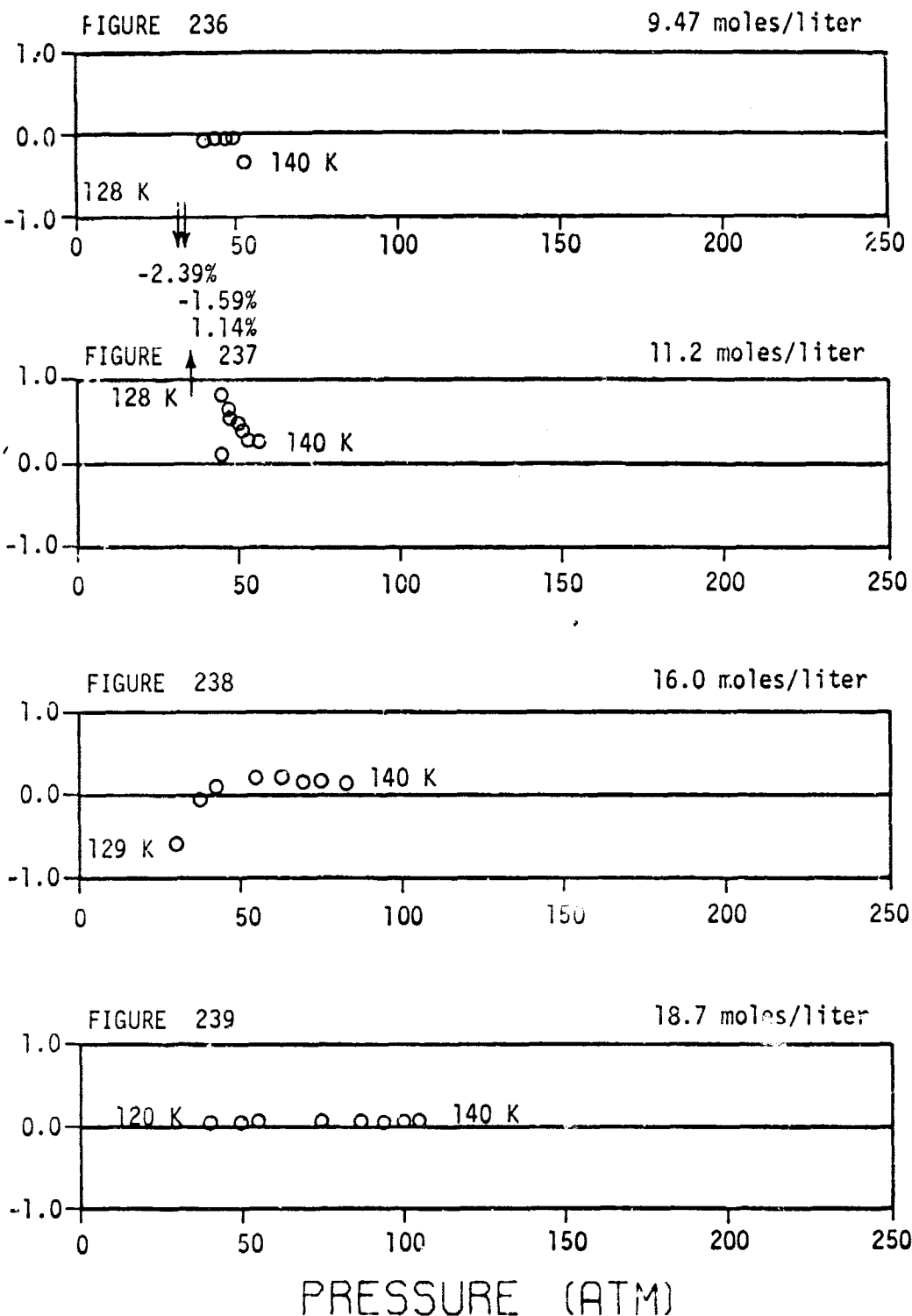


PRESSURE (ATM)

◊ VERSCHOYLE [29]

Density Deviations of Equation (22) from Data of References Indicated.

PERCENT DENSITY DEVIATION



Density Deviations of Equation (22) from Isochoric Data of
Weber [36].

PERCENT DENSITY DEVIATION

FIGURE 240

26.5 moles/liter

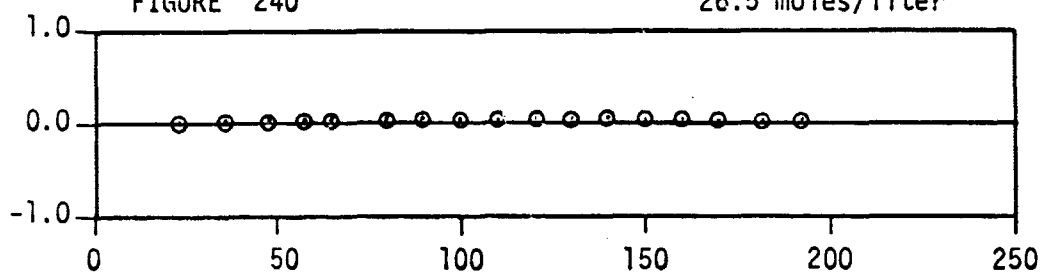
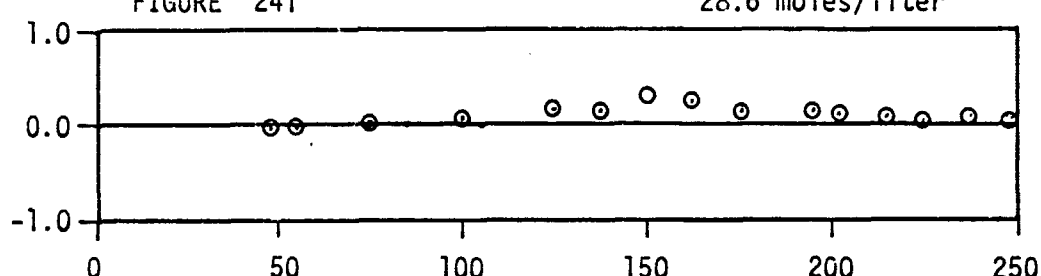


FIGURE 241

28.6 moles/liter



PRESSURE (ATM)

Density Deviations of Equation (22) from Isochoric Data of
Weber [36].

TABLE 12

P-ρ-T DATA WITH DENSITY DEVIATIONS IN
EXCESS OF ± 1 PERCENT

Figure	Temperature (K)	Pressure (atm)	Density Deviation (Percent)	Reference
3	133.14	40.74	-1.11	[8]*
24	110.02	8.91	-1.24	[10]*
25	120.01	4.84	-51.22	[10]
26	125.21	31.67	-1.37	[10]*
27	125.73	32.12	-1.99	[10]*
27	125.73	32.77	-5.54	[10]*
27	125.73	31.66	-1.43	[10]*
27	125.73	31.20	-1.93	[10]*
30	126.17	33.17	-1.43	[10]*
30	126.17	33.08	-1.27	[10]*
30	126.17	33.46	-1.09	[10]*
30	126.17	33.51	-1.18	[10]*
123	128.00	36.03	-2.39	[36]*
123	128.00	36.51	1.24	[36]*
124	128.00	36.52	1.14	[36]*
125	130.00	38.74	-1.59	[36]*
126	132.00	41.43	-1.15	[36]*
134	472.69	900.00	2.11	[1]
153	148.35	99.89	-5.34	[6]
158	123.14	3423.53	1.17	[7]
159	148.15	5387.77	1.09	[7]
179	143.14	65.97	2.01	[15]
179	143.12	67.41	1.80	[15]
180	473.19	4145.07	1.18	[17]
181	573.22	986.92	-1.66	[17]
181	573.22	1184.31	-1.34	[17]
182	673.23	1184.31	-1.43	[17]
182	673.23	1381.69	-1.03	[17]
183	773.23	1184.31	-1.65	[17]
183	773.23	1381.69	-2.08	[17]
183	773.23	1776.46	-1.18	[17]
184	873.30	1184.31	-1.91	[17]
184	873.30	1381.69	-2.55	[17]
184	873.30	1579.08	-2.66	[17]
184	873.30	1776.46	-2.36	[17]
184	873.30	1973.85	-1.94	[17]
184	873.30	2171.23	-1.60	[17]
185	973.54	1184.31	-2.59	[17]
185	973.54	1381.69	-3.27	[17]
185	973.54	1579.08	-3.00	[17]

TABLE 12--continued

Figure	Temperature (K)	Pressure (atm)	Density Deviation (Percent)	Reference
185	973.54	1776.46	-2.70	[17]
185	973.54	1973.85	-2.05	[17]
185	973.54	2171.23	-1.56	[17]
185	973.54	2368.62	-1.25	[17]
185	973.54	2566.00	-1.01	[17]
186	1073.82	1184.31	-2.75	[17]
186	1073.82	1381.69	-3.54	[17]
186	1073.82	1579.08	-3.56	[17]
186	1073.82	1776.46	-3.25	[17]
186	1073.82	1973.85	-2.76	[17]
186	1073.82	2171.23	-2.18	[17]
186	1073.82	2368.62	-1.69	[17]
186	1073.82	2566.00	-1.32	[17]
186	1073.82	2763.39	-1.08	[17]
187	1174.10	789.54	-2.24	[17]
187	1174.10	986.92	-1.84	[17]
187	1174.10	1184.31	-3.68	[17]
187	1174.10	1381.69	-4.16	[17]
187	1174.10	1579.08	-4.32	[17]
187	1174.10	1776.46	-3.99	[17]
187	1174.10	1973.85	-2.97	[17]
187	1174.10	2368.62	-2.42	[17]
187	1174.10	2566.00	-1.89	[17]
187	1174.10	2763.39	-1.40	[17]
188	1274.39	789.54	-4.30	[17]
188	1274.39	986.92	-3.96	[17]
188	1274.39	1184.31	-4.59	[17]
188	1274.39	1579.08	-5.29	[17]
188	1274.39	1776.46	-4.77	[17]
188	1274.39	1973.85	-4.32	[17]
188	1274.39	2171.23	-3.83	[17]
188	1274.39	2368.62	-3.34	[17]
188	1274.39	2763.39	-2.09	[17]
188	1274.39	2960.77	-1.54	[17]
188	1274.39	3158.15	-1.07	[17]
190	573.22	1000.00	-1.51	[18]
191	673.23	1000.00	-2.62	[18]
192	773.23	1000.00	-7.66	[18]
192	773.23	1500.00	-2.53	[18]
192	773.23	2000.00	-1.60	[18]

TABLE 12--continued

Figure	Temperature (K)	Pressure (atm)	Density Deviation (Percent)	Reference
193	873.30	1000.00	-6.94	[18]
193	873.30	1500.00	-3.58	[18]
193	873.30	2000.00	-2.22	[18]
193	873.30	2500.00	-1.30	[18]
194	973.54	1000.00	-7.12	[18]
194	973.54	1500.00	-4.48	[18]
194	973.54	2000.00	-2.47	[18]
194	973.54	2500.00	-1.34	[18]
195	1073.82	1000.00	-8.72	[18]
195	1073.82	1500.00	-5.51	[18]
195	1073.82	2000.00	-3.48	[18]
195	1073.82	2500.00	-2.08	[18]
195	1073.82	3000.00	-1.05	[18]
196	1174.10	1000.00	-10.00	[18]
196	1174.10	1500.00	-7.22	[18]
196	1174.10	2000.00	-4.26	[18]
196	1174.10	2500.00	-2.34	[18]
196	1174.10	3000.00	-1.16	[18]
197	1274.40	1000.00	-12.47	[18]
197	1274.40	1500.00	-8.86	[18]
197	1274.40	2000.00	-5.25	[18]
197	1274.40	2500.00	-3.00	[18]
197	1274.40	3000.00	-1.59	[18]
199	124.59	30.92	67.10	[16]
200	126.85	34.44	13.68	[16]
201	126.85	34.44	14.28	[16]
201	126.85	34.47	12.85	[16]
201	126.85	34.47	13.14	[16]
201	126.85	34.67	7.65	[16]
201	126.85	35.13	3.41	[16]
201	126.85	36.49	1.07	[16]
202	128.71	38.79	2.10	[16]
203	131.64	44.25	2.04	[16]
205	152.00	54.25	1.97	[16]
207	192.12	54.60	1.27	[16]
209	249.58	47.33	1.04	[16]
210	273.19	35.98	1.43	[16]
215	104.70	480.95	-2.17	[33]
219	323.14	7500.00	1.06	[28]
219	323.14	8000.00	1.16	[28]

TABLE 12--continued

Figure	Temperature (K)	Pressure (atm)	Density Deviation (Percent)	Reference
219	323.14	8500.00	1.17	[28]
219	323.14	9000.00	1.22	[28]
219	323.14	9500.00	1.26	[28]
226	673.23	10000.00	-1.46	[27]
226	673.23	9500.00	-1.24	[27]
232	90.26	815.21	1.21	[35]
233	77.31	555.73	1.21	[35]
233	77.31	417.14	1.25	[35]

NOTE: See Figures 3 through 235.

*p-ρ-T data used in determining equation of state (22).

TABLE 13

 ROOT MEAN SQUARE DEVIATIONS IN DENSITY
 AND PRESSURE OF P- ρ -T DATA FROM
 THE EQUATION OF STATE

Source	RMS Deviation in Density (percent)	RMS Deviation in Pressure (percent)
Data used in the Determination of the Equation of State		
Canfield [8]	0.14	0.22
Cockett et al. [30]	0.25	7.12
Crain [9]	0.08	0.11
Friedman [10]	0.24	0.14
Golubev and Dobrovolskii [32]	0.35	5.52
Gibbons [31]	0.16	7.90
Holborn and Otto [14]	0.07	0.07
Michels et al. [19]	0.02	0.02
Michels et al. [20]	0.05	0.15
Otto et al. [22]	0.01	0.01
Robertson and Babb [23]	0.08	0.22
Saurel [24]	0.07	0.09
Weber [36]	0.30	0.84
Data not used in the Determination of the Equation of State		
Amagat [1]	0.17	0.21
Amagat [2]	0.14	0.40
Bartlett et al. [4]	0.32	0.48
Bartlett et al. [5]	0.15	0.42
Benedict [6]	0.31	3.29
Benedict [7]	0.24	1.34
Hali and Canfield [11]	0.42	0.36
Heuse and Otto [12]	0.01	0.01
Holborn and Otto [13]	0.08	0.08
Holborn and Otto [15]	0.42	0.33
Malbrunot [18]	0.46	0.89
Malbrunot and Vodar [17]	0.40	0.83
Miller et al. [21]	0.26	0.30
Kamerlingh Onnes and van Urk [16]	0.20	0.14
Streett and Staveley [33]	0.31	28.90
Tsiklis [28]	0.47	1.81
Tsiklis and Polyakov [27]	0.29	1.08
Van Itterbeek and Verbeke [34], [35]	0.37	19.63
Verschoyle [29]	0.13	0.14

CHAPTER 8

EXTRAPOLATION OF THE EQUATION OF STATE

The coefficients of the equation of state (22) in Table 10 were determined by a least squares fit to selected, weighted data as described in Chapter 5. The data for the saturated liquid of [37] and [38] and the freezing line data of [39] were excluded in the determination of these coefficients because the data are not sufficient for inclusion as P- ρ -T points (i.e., the reported data are temperature and density, and the pressure must be determined from an independent measurement of the vapor pressure or the melting pressure). It is of interest to examine the extrapolation of the equation of state determined by a fit to data in the single phase region to the saturated liquid and saturated solid lines.

The comparison of the saturated liquid data of [37] and [38] was made by using the vapor pressure equation (29) with coefficients from Table 11 to calculate the pressure corresponding to the data temperature. The equation of state (22) was then solved for the density corresponding to the saturation temperature and pressure determined in this manner. The percent density deviation was calculated as $[(\rho_{\text{exp}} - \rho_{\text{calc}})/\rho_{\text{exp}}] \times 100$, where ρ_{exp} is the experimental density and ρ_{calc} is the density calculated from the equation of state at the saturation temperature and pressure. This comparison is illustrated in Figure 242. The deviations of the equation of state from liquid P- ρ -T data at the vapor pressure are systematic. The calculated values are greater than the experimental values except at 105 K where the density deviation is + 0.006 percent. These comparisons are dependent upon the vapor pressure equation used.

The extrapolation of the equation of state to the melting curve was made by employing the Simon melting curve equation as reported by Grilly and Mills [39] with appropriate temperature corrections. The equation used to calculate the pressure at the experimental temperature corresponding to the melting density data was

$$P = a + bT^c \quad (30)$$

where

$$a = -1579.08$$

$$b = 0.926302$$

$$c = 1.795$$

Densities calculated from the equation of state at the melting temperature and pressure are compared to the measured values of Grilly and Mills [39] in Figure 243.

In addition to the extrapolation of the equation in the liquid range it is also desirable to extrapolate the vapor data to higher and lower temperatures. At both high and low temperatures, it is notable that the terms in the equation of state which contribute the most to the pressure calculated by the equation are the ideal gas term and the terms in the temperature polynomial which represent the second virial coefficient of equation (22) when this equation is expanded to the virial form. The contribution for the ideal gas and second virial terms taken from equation (22) is as follows:

$$\text{Percent } P = (P/P_{\text{eqn}}) \times 100 \quad (31)$$

where

P is the contribution to the calculated pressure attributed to the sum of the first nine terms of the equation of state [$P = \rho RT + B(T)\rho^2$], $B(T)$

is given in equation (33) below,

and P_{eqn} is the pressure calculated from equation (22) at specified temperature, T, and density, ρ .

Figures 244 and 245 illustrate the contribution of these terms. Figure 246 is a similar comparison showing the percentage contribution of the first virial (ideal gas) term for the low temperature vapor. The contribution here is determined from (22) as:

$$\text{Percent } P = (\rho RT/P_{eqn}) \times 100 \quad (32)$$

where

Percent P is the percentage contribution of the ideal gas term to the total pressure calculated from equation (22),

and ρ , T, and P_{eqn} are as defined above.

Examination of Figures 244, 245, and 246 indicates that the extrapolation of the equation of state for the vapor at high and low temperatures is reasonable and limited only by the accuracy of the second virial coefficient as predicted by equation (22), i.e.,

$$B(T) = N_1 T + N_2 T^{1/2} + N_3 + N_4/T^{1/2} + N_5/T + N_6/T^2 + N_7/T^3 + N_8/T^4 \quad (33)$$

Figure 247 is a comparison of values from equation (33) with the experimental second virial coefficients from [9], [10], [19], [22], [59], [60], and [61]. Values of the second virial coefficient determined by the use of the Lennard-Jones potential function with parameters from Ziegler and Mullins [122] for temperatures from 70 K to 200 K agree with the calculated values from (33) within the accuracy of the plot in Figure 247.

With the apparent accuracy of the second virial coefficient from equation (22), Figure 244 suggests that it is reasonable to extrapolate the equa-

tion of state from 1000 K to 2000 K for pressures to 300 atmospheres. Figures 245 and 246 demonstrate that equation (22) may be extrapolated to lower temperatures for the gas, since the pressures below the range for which data are available are very low.

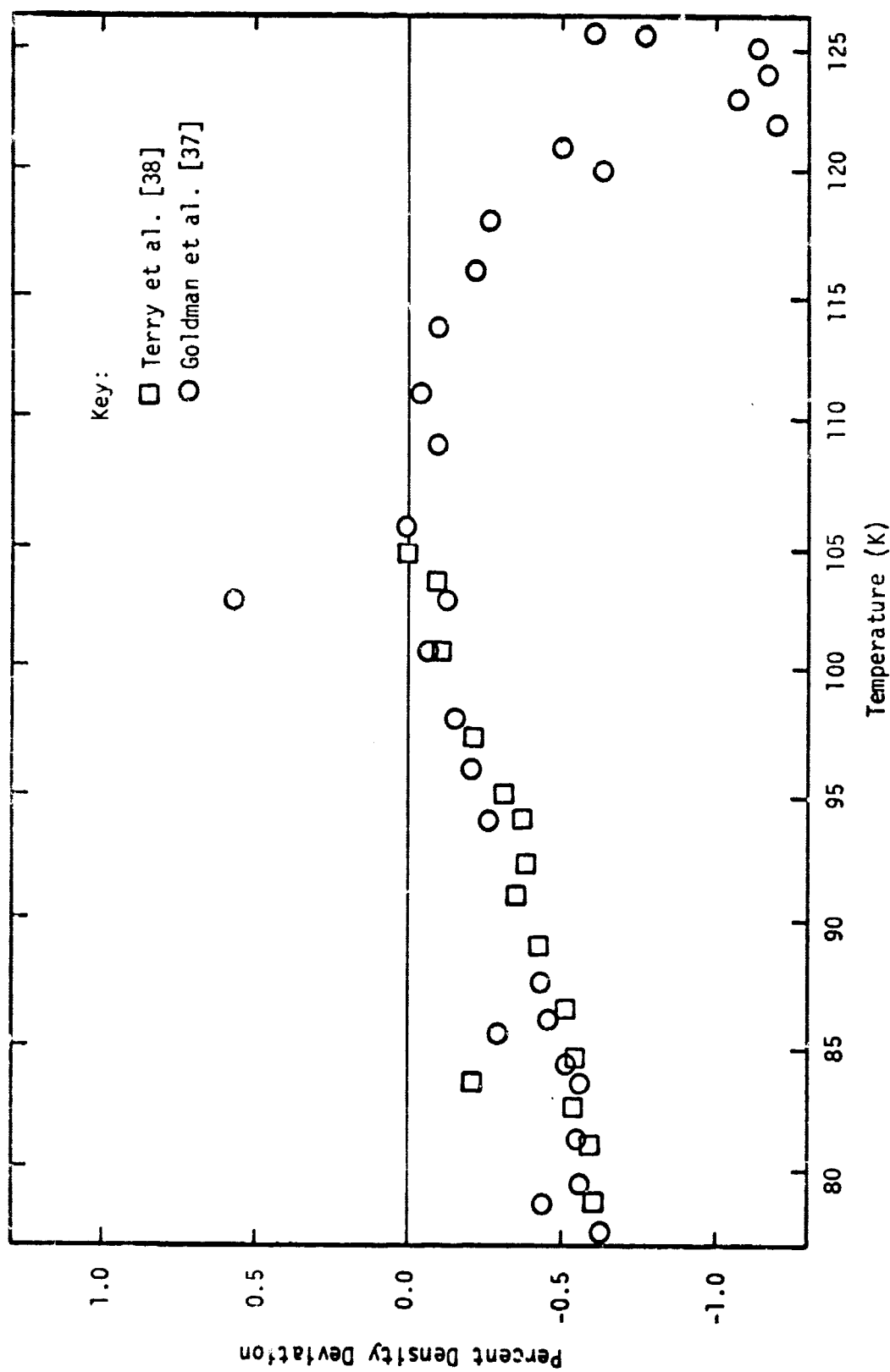


Figure 242.--Deviations of Equation of State from Liquid P- ρ -T Data at the Vapor Pressure.

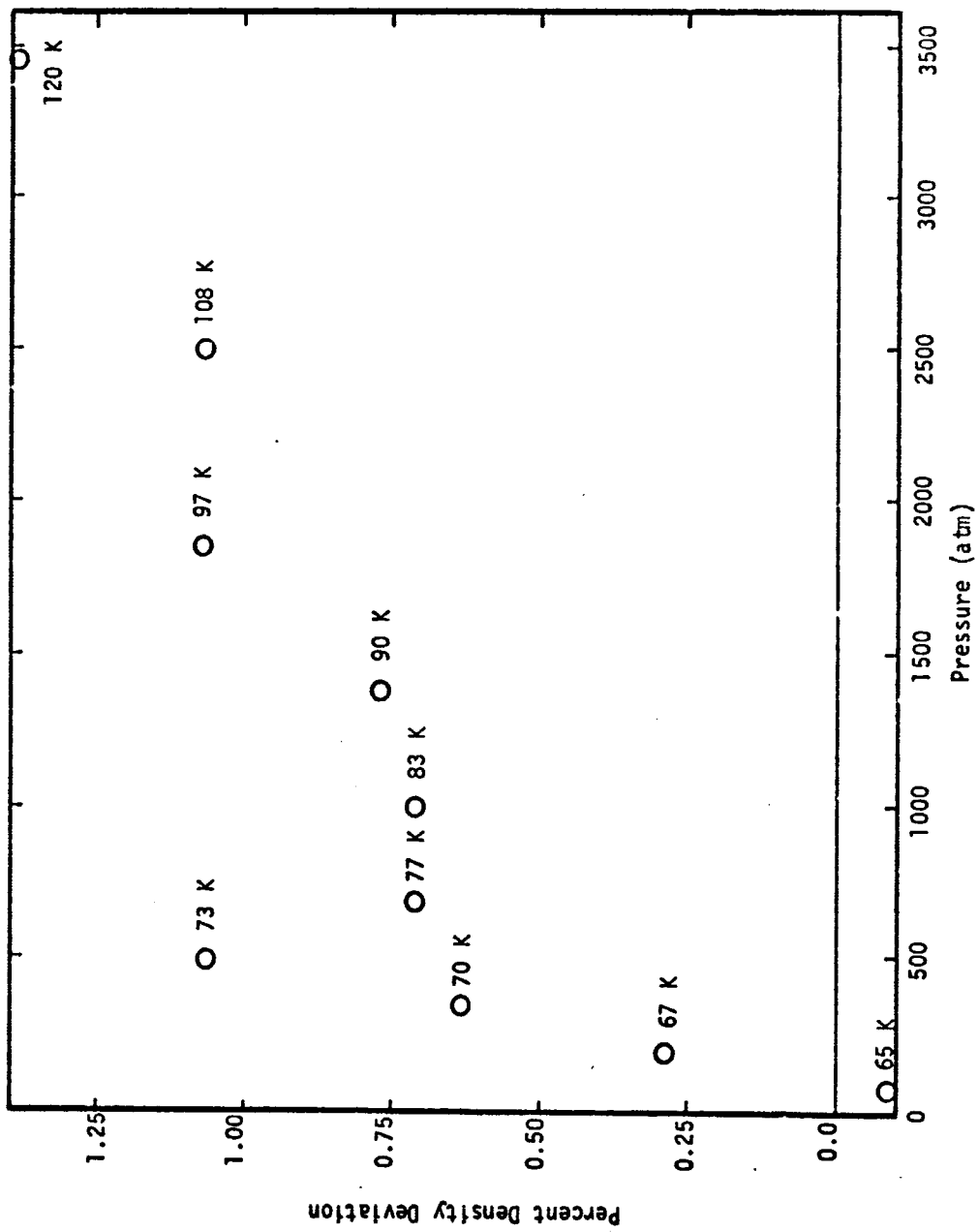


Figure 243.--Deviations of Equation (22) from Liquid P-p-T Data on the Freezing Line from [39] (Nominal Temperatures are given below each point).

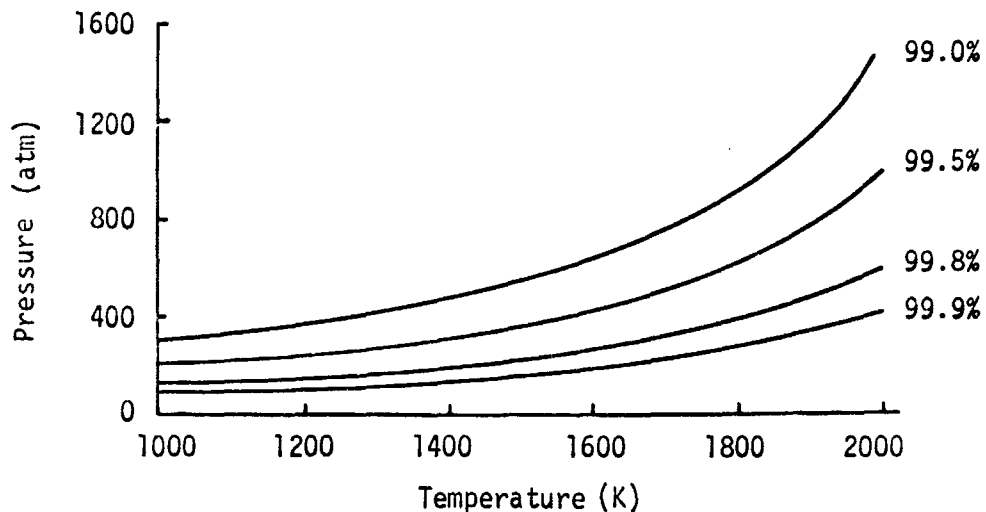


Figure 244.--Percentage Contribution of First and Second Virial Terms to Pressure from Eqn. (22) at High Temperature.

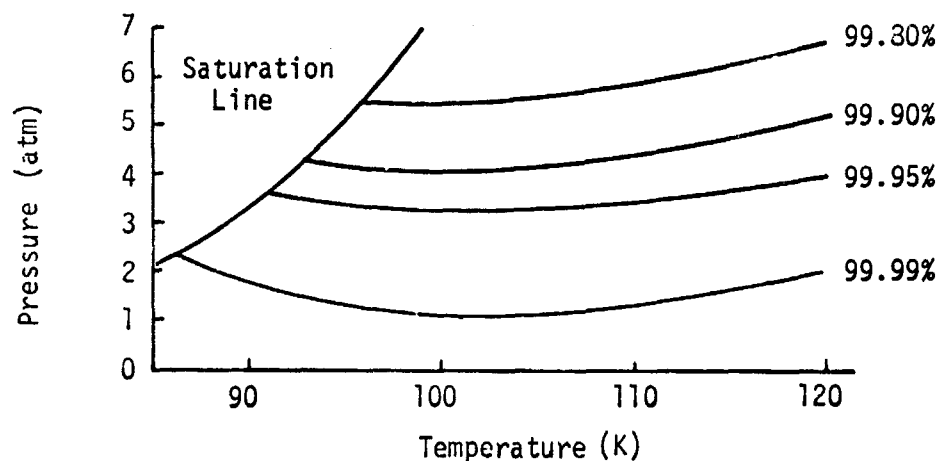


Figure 245.--Percentage Contribution of First and Second Virial Terms to Pressure from Eqn. (22) at Low Temperature.

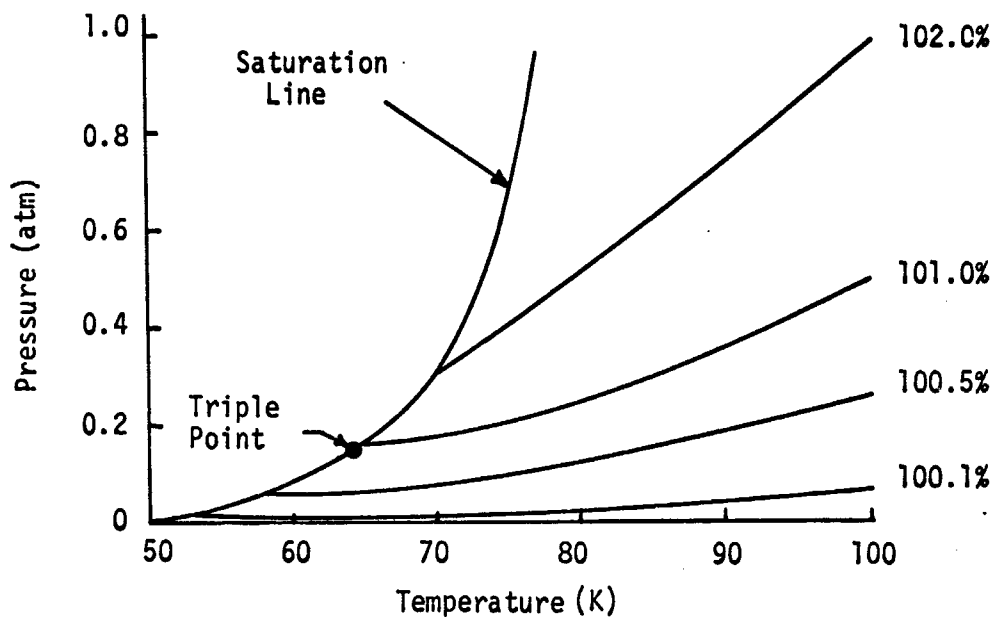


Figure 246.--Percentage Contribution of First Virial (ideal gas) Term to Pressure from Eqn. (22) at Low Temperature.

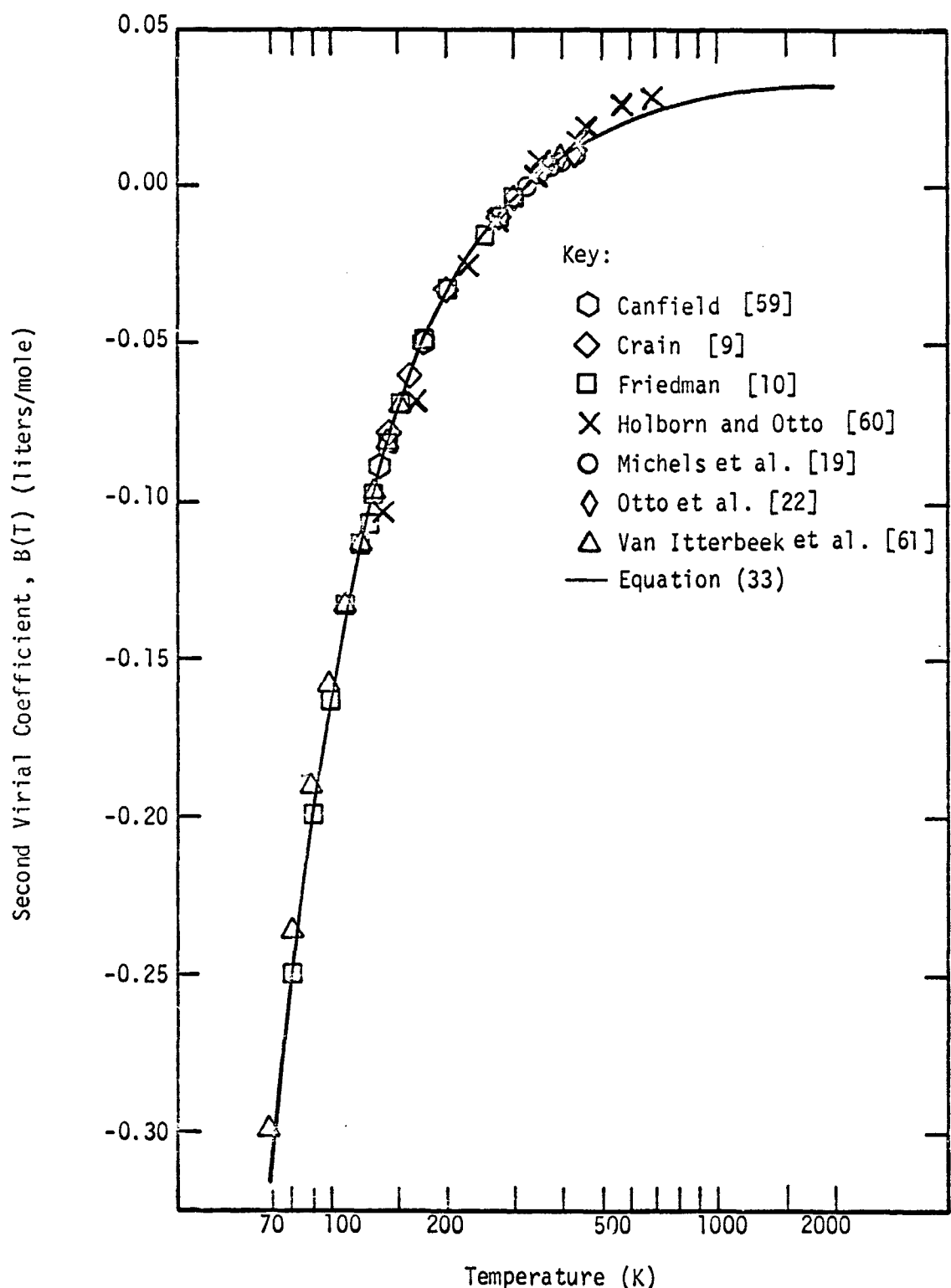


Figure 247.--Comparison of Second Virial Coefficient from Equation (22) to Experimental Values from the Sources Indicated.

CHAPTER 9

IDEAL GAS HEAT CAPACITY

In the earlier work of Coleman and Stewart [95], ideal gas heat capacity values were calculated from an equation that was fitted to preliminary results of a calculation by Woolley [86]. New values for the ideal gas heat capacity are now available from [84] and [85]. These values appear to be the most accurate to date, and will be used for the tables produced in this work.

The equation suggested by Barieau [87], and Barieau and Tully [88], which was used previously in [95] and [117], has been fitted to the data from [84]. This equation is

$$\begin{aligned} C_p^0/R = & N_1/T^3 + N_2/T^2 + N_3/T + N_4 + N_5T + N_6T^2 + N_7T^3 \\ & + N_8u^2e^u/(e^u - 1)^2 \end{aligned} \quad (34)$$

where

C_p^0 is the ideal gas heat capacity,

T the temperature,

and $u = N_9/T$.

The coefficients for equation (34) with values of T in degrees Kelvin are given in Table 14.

TABLE 14

COEFFICIENTS FOR THE IDEAL HEAT CAPACITY EQUATION (34)
FOR NITROGEN

Coefficients	Numerical Value	Coefficients	Numerical Value
N_1	$-0.7352104012 \times 10^{-3}$	N_6	$0.1746508498 \times 10^{-7}$
N_2	$0.3422399804 \times 10^{-2}$	N_7	$-0.3568920335 \times 10^{-11}$
N_3	-0.5576482846	N_8	$0.1005387228 \times 10^{-1}$
N_4	$0.3504042283 \times 10^{-1}$	N_9	3353.4061
N_5	$-0.1733901851 \times 10^{-4}$		

Table 15 is a listing of the ideal gas heat capacity values (C_p^0/R) as a function of temperature as reported in [84]. A comparison between these values from [84] and values calculated from equation (34) indicates exact agreement within the number of figures reported, except above 1200 K. Above 1200 K the differences between the values from equation (34) and from [84] is no more than $\pm .0001$. Equation (34) with coefficients from Table 14 has been used in the calculation of the property tables in this work.

TABLE 15

VALUES OF IDEAL GAS HEAT CAPACITY, C_p^0/R ,
FROM BAEHR ET AL. [84]

Temperature (K)	C_p^0/R	Temperature (K)	C_p^0/R
50.0	3.4999	450.0	3.5308
60.0	3.4998	460.0	3.5349
70.0	3.4998	470.0	3.5392
80.0	3.4997	480.0	3.5438
90.0	3.4997	490.0	3.5487
100.0	3.4996	500.0	3.5538
110.0	3.4996	510.0	3.5591
120.0	3.4995	520.0	3.5647
130.0	3.4995	530.0	3.5705
140.0	3.4994	540.0	3.5765
150.0	3.4994	550.0	3.5828
160.0	3.4994	560.0	3.5892
170.0	3.4993	570.0	3.5958
180.0	3.4993	580.0	3.6026
190.0	3.4992	590.0	3.6095
200.0	3.4992	600.0	3.6166
210.0	3.4992	610.0	3.6239
220.0	3.4992	620.0	3.6312
230.0	3.4992	630.0	3.6387
240.0	3.4992	640.0	3.6463
250.0	3.4993	650.0	3.6539
260.0	3.4994	660.0	3.6617
270.0	3.4995	670.0	3.6695
280.0	3.4998	680.0	3.6774
290.0	3.5001	690.0	3.6854
300.0	3.5006	700.0	3.6934
310.0	3.5011	710.0	3.7014
320.0	3.5018	720.0	3.7095
330.0	3.5027	730.0	3.7176
340.0	3.5038	740.0	3.7257
350.0	3.5050	750.0	3.7338
360.0	3.5065	760.0	3.7419
370.0	3.5081	770.0	3.7500
380.0	3.5101	780.0	3.7581
390.0	3.5122	790.0	3.7662
400.0	3.5147	800.0	3.7742
410.0	3.5174	810.0	3.7822
420.0	3.5203	820.0	3.7902
430.0	3.5235	830.0	3.7982
440.0	3.5270	840.0	3.8061

TABLE 15--continued

Temperature (K)	C_p^0/R	Temperature (K)	C_p^0/R
850.0	3.8139	1250.0	4.0724
860.0	3.8217	1300.0	4.0966
870.0	3.8295	1350.0	4.1192
880.0	3.8372	1400.0	4.1404
890.0	3.8448	1450.0	4.1601
900.0	3.8524	1500.0	4.1786
910.0	3.8599	1550.0	4.1959
920.0	3.8674	1600.0	4.2120
930.0	3.8748	1650.0	4.2271
940.0	3.8821	1700.0	4.2413
950.0	3.8894	1750.0	4.2546
960.0	3.8966	1800.0	4.2671
970.0	3.9037	1850.0	4.2789
980.0	3.9107	1900.0	4.2899
990.0	3.9177	1950.0	4.3003
1000.0	3.9246	2000.0	4.3101
1050.0	3.9579		
1100.0	3.9893		
1150.0	4.0188		
1200.0	4.0465		

CHAPTER 10

DERIVED THERMODYNAMIC PROPERTIES

The values of entropy, enthalpy, internal energy, and heat capacity at various state points are calculated from the pressure-explicit equation of state (22), and the ideal gas heat capacity equation (34). The vapor pressure equation (29) and the Simon melting curve equation (30) were used to identify the temperature of the phase changes from solid to liquid, and liquid to vapor, respectively, for each isobar. The integral representations for the properties are continuously integrated through the two-phase region to calculate properties in the liquid range. This is made possible by the fitting procedures employed in the development of the equation of state as described in Chapter 5 in which the conditions for two-phase equilibrium were included in the least squares determination of the coefficients for the equation of state (22). The thermodynamic formulations for the calculation of the thermodynamic property tables of Appendix E were taken from [118]. These relations are summarized in the following paragraphs. Functions for the integrals and derivatives of the equation of state required to perform these calculations are given in Appendix D.

The entropy of any thermodynamic state was calculated from

$$\begin{aligned}
 S(T, \rho) = & S_{T_0}^0 + \int_{T_0}^T (C_p^0/T)dT - R\ln(RT\rho) \\
 & + \int_0^\rho [R/\rho - (1/\rho^2)(\partial P/\partial T)_P]_T d\rho. \tag{35}
 \end{aligned}$$

The ideal gas specific heat, C_p^0 , is from equation (34). The reference entropy of the ideal gas at $T_0 = 298.15$ K and $P_0 = 1$ atmosphere, $S_{T_0}^0 = 191.502 \pm 0.025$ joules/mole-K is taken from [94]. The functions for evaluation of the integrals $\int (C_p^0/T) dT$ and $\int [(R/\rho) - (1/\rho^2)(\partial P/\partial T)\rho]_T d\rho$ are given in Appendix D. The functions for the isochore derivative $(\partial P/\partial T)_\rho$ of the equation of state are included in Appendix D.

The enthalpy of any state may be calculated from

$$H(T, \rho) = H_{T_0}^0 + T \int_0^\rho [(P/T\rho^2) - (1/\rho^2)(\partial P/\partial T)_\rho]_T d\rho + (P - \rho RT)/\rho + \int_{T_0}^T C_p^0 dT. \quad (36)$$

However, it is convenient to replace the first integral term in (36) as follows:

$$\begin{aligned} & T \int_0^\rho [(P/T\rho^2) - (1/\rho^2)(\partial P/\partial T)_\rho]_T d\rho \\ & \equiv T \int_0^\rho [(R/\rho) - (1/\rho^2)(\partial P/\partial T)_\rho]_T d\rho \\ & + \int_0^\rho [(P/\rho^2) - (RT/\rho)]_T d\rho \end{aligned} \quad (37)$$

By substitution of the identity of (37) in equation (36), the expression for enthalpy is given as

$$\begin{aligned} H(T, \rho) = H_{T_0}^0 & + T \int_0^\rho [(R/\rho) - (1/\rho^2)(\partial P/\partial T)_\rho]_T d\rho \\ & + \int_0^\rho [(P/\rho^2) - (RT/\rho)]_T d\rho + (P - \rho RT)/\rho \\ & + \int_{T_0}^T C_p^0 dT. \end{aligned} \quad (38)$$

The reference enthalpy of the ideal gas at $T_0 = 298.15$ K of $H_{T_0}^0 = 8669$ ± 3 joules/mole was taken from the value of $(H^0 - H_0^0)$ in [94] with $H_0^0 = 0.0$. The evaluations of the integrals and isochore derivative are given in Appendix D. The internal energy of a fluid state was calculated from

$$U(T,\rho) = H(T,\rho) - P/\rho. \quad (39)$$

The specific heat at constant volume, C_v , of liquid and gas phase points was calculated using the relation

$$C_v(T,\rho) = (C_p^0 - R) - \int_0^\rho (T/\rho^2) [(\partial^2 P/\partial T^2)_\rho] d\rho \quad (40)$$

where C_p^0 at temperature, T , is calculated from equation (34). The specific heat at constant pressure, C_p , is given by

$$C_p(T,\rho) = C_v(T,\rho) + [(T/\rho^2)(\partial P/\partial T)_\rho^2 / (\partial P/\partial \rho)_T]. \quad (41)$$

It is notable that the calculation of properties from the equation developed in this work is considerably simplified from the prior methods of [95] and [118] by the continuous integration along isotherms through the two phase region due to the imposing of the requirements for phase equilibrium in the determination of the equation of state as suggested in [92].

A sample table of thermodynamic properties of nitrogen illustrating the results of the property calculations outlined above is presented in Appendix E. This appendix also includes a table of properties of the saturated liquid and vapor states on two degree intervals between the triple point and the critical point.

CHAPTER 11

COMPARISONS OF THE EQUATION OF STATE WITH
DERIVED THERMODYNAMIC DATA

Experimental measurements of properties of nitrogen in addition to the P- ρ -T data are available for comparison to values calculated using the equation of state developed in this work. Comparisons of the experimental specific heats, latent heats of vaporization, enthalpies, and sonic velocities calculated using the equation of state (22) are reported here. The thermodynamic property formulations used in the calculation of various properties from the equation of state are presented in Chapter 10.

Calculated Heat Capacity Values

Values of C_p and C_v for nitrogen calculated by integration along isotherms using equation (22) with coefficients from Table 10 are illustrated in Figures 248 and 249 for isobars of 1, 10, 50, 100, and 400 atmospheres. The behavior of the calculated values of C_v below 75 K as indicated in Figure 249 is questionable.

Comparisons of the Specific Heat Data

Comparisons of isobaric heat capacity values calculated from the equation of state (22) and the ideal gas heat capacity equation (34) to measured values from [54] and [55] are given in Tables 16 and 17, respectively. The measurements reported by Faulkner [51] are included in the table of values reported by Jones [53]. The data of Jones from [53] including the values from [51] are also included in the measured values reported in [55], eliminating the necessity for separate comparisons to the data of [51] and [53].

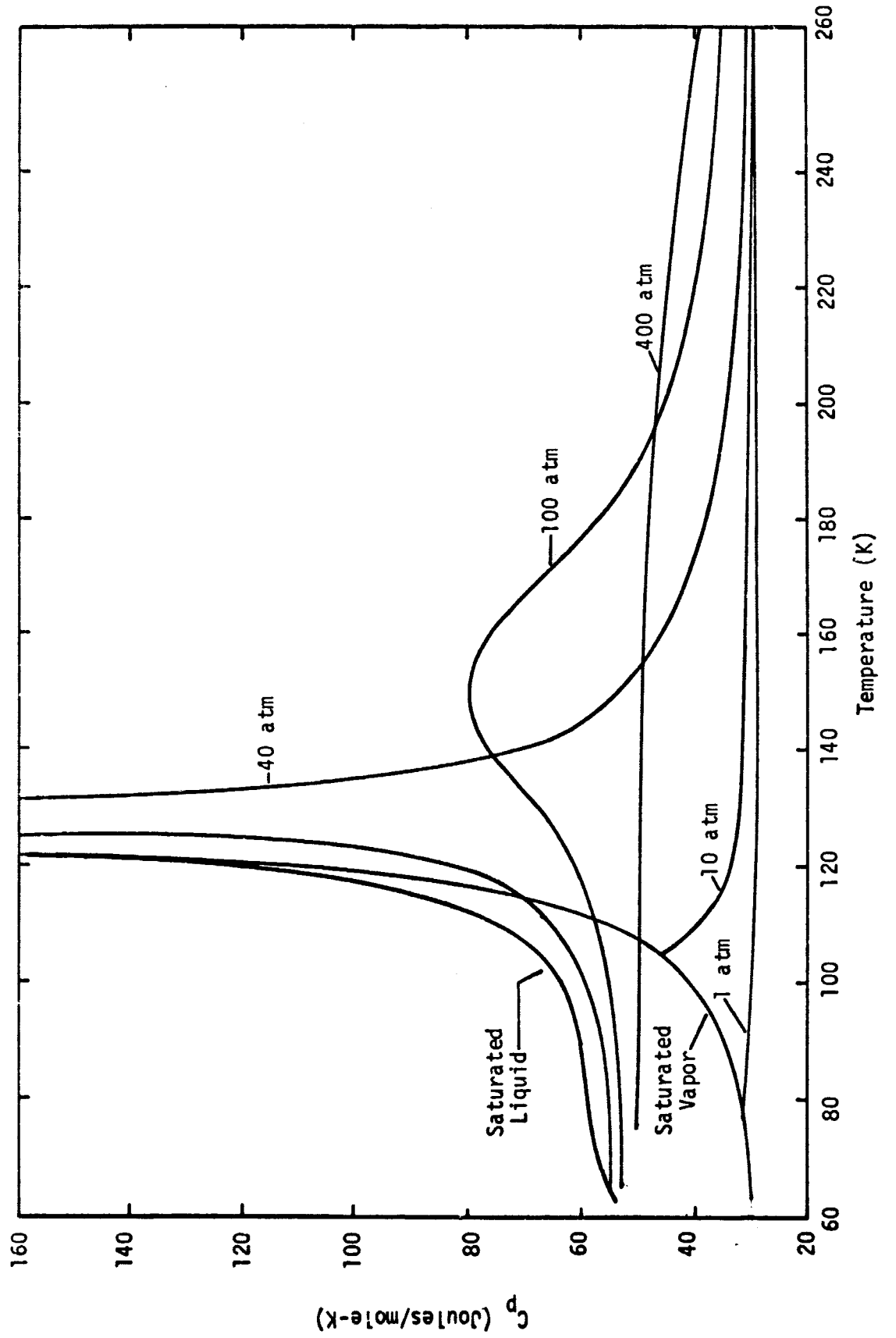


Figure 248.--Constant Pressure Heat Capacity (C_p) of Nitrogen Calculated from Equation of State (22) with Coefficients of Table 10_p.

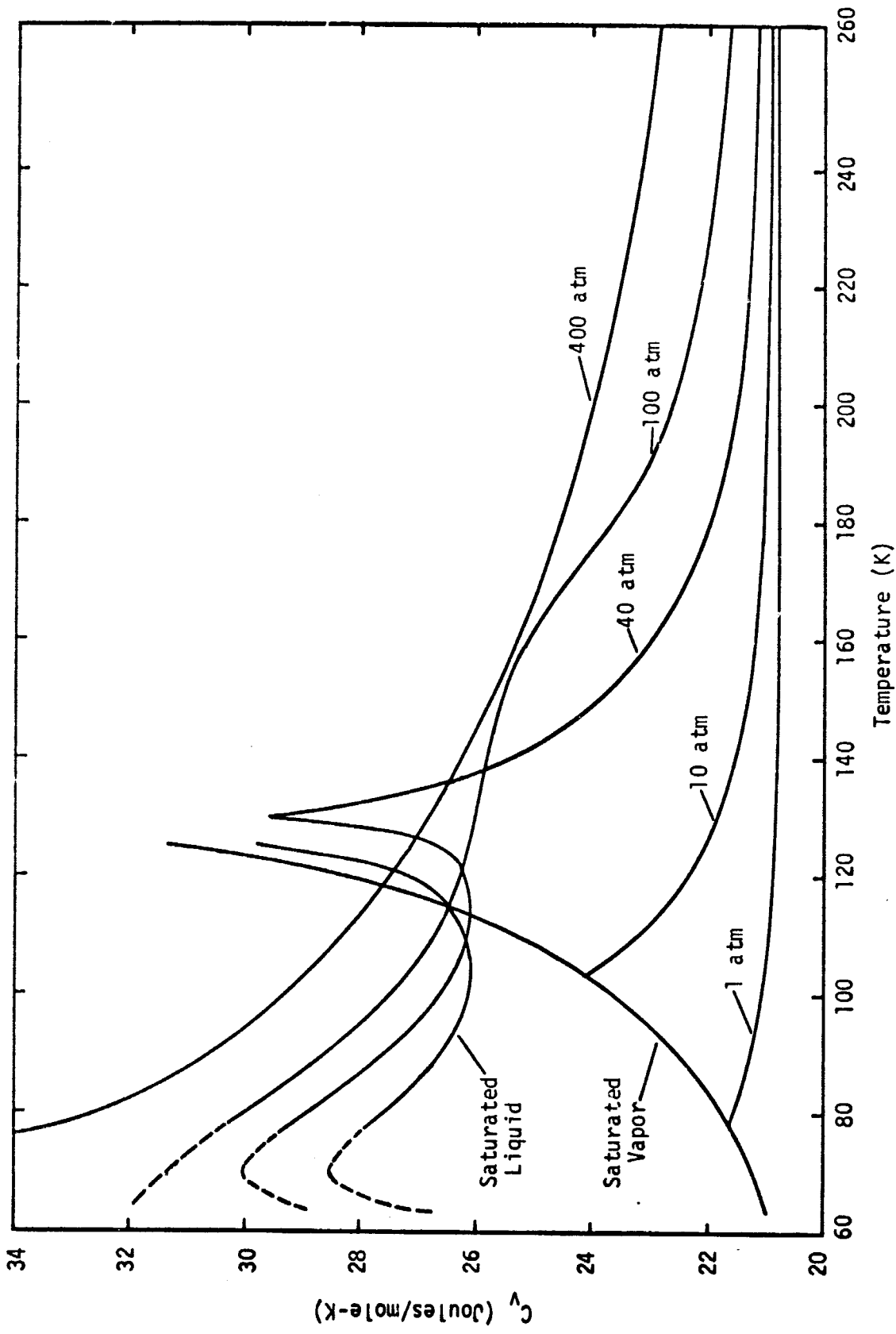


Figure 249.--Constant Volume Heat Capacity (C_V) of Nitrogen Calculated from Equation of State (22) with Coefficients of Table 10.

TABLE 16

COMPARISONS OF HEAT CAPACITY DATA OF KRASE AND MACKEY [54]
 WITH VALUES CALCULATED FROM THE EQUATION OF STATE (22)
 AND THE IDEAL GAS HEAT CAPACITY EQUATION (34)

Temperature (K)	Pressure (atm)	$C_p[54]$ (joules/mole-K)	$C_p[54] - C_{p,calc}$ (joules/mole-K)
303.1	1	28.94	-0.22
303.1	50	31.03	-0.31
303.1	100	33.17	-0.20
303.1	200	36.18	-0.10
303.1	300	37.44	-0.22
303.1	400	37.98	-0.13
303.1	500	38.19	0.02
303.1	600	38.27	0.17
303.1	700	38.36	0.35
323.1	1	28.98	-0.18
323.1	100	32.33	-0.40
323.1	200	34.84	-0.41
323.1	300	36.43	-0.16
323.1	400	36.89	-0.26
323.1	500	37.06	-0.28
323.1	600	37.10	-0.27
323.1	700	37.19	-0.15
323.1	800	37.23	-0.05
373.2	1	29.06	-0.14
373.2	50	30.19	-0.32
373.2	100	31.32	-0.38
373.2	200	33.17	-0.38
373.2	300	34.46	-0.23
373.2	400	34.97	-0.38
373.2	500	35.13	-0.56
373.2	600	35.30	-0.57
373.2	700	35.39	-0.57
398.2	1	29.10	-0.14
398.2	50	30.15	-0.22
398.2	100	30.99	-0.40
398.2	200	32.50	-0.49
398.2	300	33.54	-0.50
398.2	400	34.21	-0.47
398.2	500	34.59	-0.47
398.2	600	34.76	-0.52

TABLE 16--continued

Temperature (K)	Pressure (atm)	$C_p[54]$ (joules/mole-K)	$C_p[54] - C_{p\text{calc}}$ (joules/mole-K)
398.2	700	34.97	-0.44
423.2	1	29.15	-0.15
423.2	50	30.11	-0.16
423.2	100	30.82	-0.34
423.2	200	32.08	-0.49
423.2	300	33.04	-0.48
423.2	400	33.58	-0.56
423.2	500	34.04	-0.50
423.2	600	34.34	-0.45
423.2	700	34.55	-0.39

TABLE 17

COMPARISONS OF HEAT CAPACITY DATA OF MAGE ET AL. [55] WITH
VALUES CALCULATED FROM THE EQUATION OF STATE (22) AND
THE IDEAL GAS HEAT CAPACITY EQUATION (34)

Temperature Range (K)	Pressure (atm)	$C_p[55]$ (joules/mole-K)	$C_p[55] - C_{p\text{calc}}$ (joules/mole-K)
268.3 - 279.6	10.0	29.58	-0.09
222.7 - 233.9	10.0	29.87	-0.13
194.3 - 205.0	10.0	30.23	-0.17
166.6 - 177.7	10.0	31.02	-0.06
267.7 - 279.0	20.0	30.19	-0.07
222.7 - 233.9	20.0	30.85	-0.11
194.3 - 205.3	20.0	31.62	-0.20
166.6 - 177.6	20.0	33.53	0.05
116.5 - 119.2	27.2	94.76	2.48
122.5 - 124.7	33.6	166.32	25.25
122.5 - 125.6	33.6	265.07	99.49
122.5 - 125.7	33.6	496.48	323.99
122.5 - 128.0	33.6	499.22	-1.38
122.5 - 153.0	33.6	128.31	-0.35
267.8 - 279.0	40.0	31.35	-0.09
222.7 - 234.0	40.0	32.86	-0.19
194.3 - 205.3	40.0	34.98	-0.08
166.6 - 177.7	40.0	39.85	-0.04
119.3 - 125.1	40.0	96.50	0.81
267.8 - 279.2	80.0	33.67	-0.04
222.8 - 234.1	80.0	37.19	0.07
194.3 - 205.3	80.0	42.32	-0.15
166.6 - 177.7	80.0	57.19	-0.72
119.3 - 125.0	80.0	66.63	-0.23
267.8 - 279.0	136.1	36.48	0.06
222.9 - 234.2	136.1	41.78	-0.06
194.3 - 205.4	136.1	49.36	-0.16
166.6 - 177.6	136.1	61.38	-0.13
146.0 - 148.0	136.1	64.90	0.35
146.0 - 150.3	136.1	65.17	0.40
146.0 - 154.6	136.1	65.58	0.49
146.0 - 156.4	136.1	65.51	0.41
126.9 - 129.1	136.1	59.82	0.27
126.9 - 131.3	136.1	60.23	0.41
126.9 - 135.4	136.1	60.85	0.51
119.3 - 125.1	136.1	58.01	-0.20

The heat capacities reported in Table 16 agree with the values calculated from the equation of state generally within 1 percent, while the data of Mage et al. [55] exhibit an average deviation of less than 0.5 percent except in the region of the critical point where one point shows a deviation of 65.3 percent. This behavior of calculated C_p values reflects the imprecision of the experimental data and the fitting problems in the critical region.

Comparisons of the isochoric heat capacity values, C_v , calculated from the equation of state (22) and the ideal gas heat capacity equation (34) to measured values along the critical isochore published by Voronel et al. [56] are given in Table 18. (The value of the critical density determined in this work is 11.21 moles/liter while that of [56] is 11.1 moles/liter.)

The calculated values of C_v do not exhibit the large increase in value near the critical point that is evident in the data of [56], and no attempt was made to introduce this behavior into the equation of state. Although experiments have shown that C_v does behave in the manner indicated by [56], the few measurements of the properties of nitrogen near the critical point now available do not appear to be sufficient to provide for the correct characteristics of second derivatives of an equation of state determined by a least squares fit.

It should be noted that the data at temperatures below 126.20 K reported in [56] are for the two phase fluid. Above the critical temperature up to 135 K the calculated values of C_v do not exhibit the behavior indicated by the data of [56]. The range of densities for which this second derivative behavior should be found for nitrogen is unknown since the C_v values reported in [56] are for a single density of 11.21 moles/liter.

Comparisons of Latent Heat Data

Furukawa and McCoskey [52] have published measured latent heats of vaporization at low temperatures (67 K - 78 K), and Jones [53] has presented five measurements of the latent heat of nitrogen for the range from 119 K to 124 K. The comparisons of calculated values from equations (22) and (29) to these measured values are given in Table 19. The data of [52] and the calculated values show an agreement within 0.7 percent while that of [53] exhibits deviations of up to 2.3 percent from the calculated values at temperatures near the critical temperature.

TABLE 18

COMPARISONS OF ISOCHORIC HEAT CAPACITY DATA AT 11.1 MOLES/LITER
 OF VORONEL ET AL. [56] WITH VALUES CALCULATED FROM THE
 EQUATION OF STATE (22) AND THE IDEAL GAS
 HEAT CAPACITY EQUATION (34)

Temperature (K)	C_V [56] (joules/mole-K)	C_V _{calc} (joules/mole-K)
105.877	83.1	39.6
106.206	80.6	39.4
109.443	84.0	37.5
117.872	95.5	33.5
121.896	105.6	32.1
122.352	106.8	31.9
122.841	108.8	31.7
123.329	111.5	31.6
123.817	114.0	31.4
124.298	117.5	31.3
124.743	124.9	31.1
124.749	120.7	31.1
125.195	126.2	31.0
125.628	136.6	30.9
125.847	142.1	30.8
125.931	154.9	30.8
126.988	154.1	30.8
126.009	153.2	30.8
126.078	169.8	30.8
126.114	175.8	30.7
126.120	168.5	30.7
126.121	160.2	30.7
126.145	180.3	30.7
126.146	170.9	30.7
126.155	190.3	30.7
126.158	212.7	30.7
126.169	209.9	30.7
126.171	204.1	30.7
126.192	110.3	30.7
126.194	105.1	30.7
126.197	103.3	30.7
126.206	95.7	30.7
126.216	94.8	30.7
126.225	85.6	30.7
126.230	87.9	30.7

TABLE 18--continued

Temperature (K)	C_v [56] (joules/mole-K)	C_v _{calc} (joules/mole-K)
126.232	79.5	30.7
126.245	79.7	30.7
126.249	84.2	30.7
126.261	76.6	30.7
126.270	77.8	30.7
126.288	75.7	30.7
126.291	71.0	30.7
126.333	65.3	30.7
126.341	67.9	30.7
126.340	65.6	30.7
126.383	65.0	30.7
126.383	61.5	30.7
126.445	58.8	30.6
126.396	58.8	30.7
126.470	56.6	30.6
126.567	54.7	30.6
126.725	50.5	30.6
126.872	49.2	30.5
126.967	47.1	30.5
127.055	45.8	30.5
127.346	43.8	30.4
127.910	40.4	30.2
128.752	37.6	30.0
129.794	35.7	29.8
130.868	34.0	29.5
131.974	32.8	29.2
133.100	31.8	29.0
135.357	29.9	28.5
136.340	30.0	28.3
142.178	28.1	27.3
143.050	27.8	27.1
155.658	26.4	25.6
156.716	26.1	25.5
167.040	26.1	24.6

TABLE 19

COMPARISON OF LATENT HEATS OF EVAPORATION FROM
 [52] and [53] TO VALUES FROM
 EQUATIONS (22) AND (29)

Comparison to Data of Furukawa and McCoskey [52]			
Temperature (K)	Pressure (atm)	Latent Heat [52] (joules/mole)	$\frac{L[52] - L_{\text{calc}}}{L[52]} \times 100$ (percent)
67.96	0.28	5901.6	0.29
67.96	0.28	5899.0	0.24
73.09	0.59	5739.1	0.40
73.09	0.59	5732.1	0.28
78.02	1.08	5579.4	0.70
78.01	1.08	5563.1	0.41

Comparison to Data of Jones [53]			
Temperature (K)	Pressure (atm)	Latent Heat [53] (joules/mole)	$\frac{L[53] - L_{\text{calc}}}{L[53]} \times 100$ (percent)
119.20	23.80	2702.3	-1.10
119.16	23.80	2678.2	-2.04
119.19	27.18	2220.4	-2.33
121.89	30.61	1681.3	0.56
124.29	23.80	2714.7	-0.82

Comparison of Experimental Enthalpy Values

Wiener [57] has reported measurements of the enthalpy of nitrogen made prior to measuring hydrocarbon enthalpy values. A comparison of the measured enthalpy values by Wiener to values calculated from the equation of state (22) is presented in Table 20. The values of [57] have been adjusted to the ideal gas reference enthalpy of 8669 joules/mole at 298.15 K from the published datum of 0.0 Btu/lb_m at 75 F and 14.7 psia. Wiener has estimated the accuracy of the measured values of [57] as ± 130 joules/mole. The calculated values of enthalpy at the experimental temperature and pressure are well within this uncertainty with the exception of two points which the author cites as in doubt.

Comparisons of the Entropy of the Saturated Liquid

The vapor pressure equation (29) was tested using calculations employing the saturated liquid heat capacity data of Clusius [50] and Wiebe and Brevoort [58]. The results are summarized in Table 21 which compares values of saturated liquid entropy S_c'' and S_σ'' . S_c'' was calculated using the datum value for entropy of the ideal gas at 298.15 K, the equation of state, the ideal gas heat capacity equation, and the vapor pressure equation for values of the slope (dP/dT) as required by the Clapeyron equation. S_σ'' was determined by the calculation of differences in the saturated liquid entropy along the saturated liquid line, from an equation for saturated liquid heat capacity data determined by a least squares fit to the data reported in [50] and [58]. The datum state in the calculation of S_σ'' was the value of the saturated liquid entropy S_c'' at 100 K.

TABLE 20

COMPARISON OF ENTHALPY DATA BY WEINER [57] WITH VALUES
CALCULATED FROM THE EQUATION OF STATE (22) AND THE
IDEAL GAS HEAT CAPACITY EQUATION (34)

Temperature (K)	Pressure (atm)	H[57] (joules/mole)	H[57] - H _{calc} (joules/mole)
138.71	67.37	621	-248
142.59	52.06	1988	-107
142.04	29.26	3551	323
145.93	28.58	3421	- 10
143.15	21.78	3551	8
142.04	17.69	3616	- 16
158.71	28.92	3877	- 69
159.26	28.58	4072	96
199.82	51.72	5049	- 22
202.04	28.99	5505	33
207.59	65.32	5179	- 1
310.93	34.02	8826	- 24
322.59	27.90	9151	- 85
359.26	40.83	10258	- 33
421.48	47.63	12146	- 10
422.04	40.83	12146	- 41
449.26	47.63	12993	- 3

TABLE 21

COMPARISON OF SATURATED LIQUID ENTROPY CALCULATED FROM
 (1) EQUATION OF STATE AND IDEAL GAS HEAT CAPACITY
 EQUATION, AND (2) SATURATED LIQUID HEAT
 CAPACITY DATA OF CLUSIUS [50] AND
 WIEBE AND BREVOORT [58]

Temperature (K)	Pressure (atm)	(1) S_c''' (joules/mole-K)	(2) S_σ''' (joules/mole-K)
70	0.38	73.80	73.68
71	0.44	74.61	74.49
72	0.51	75.41	75.28
73	0.58	76.20	76.07
74	0.66	76.98	76.85
75	0.75	77.75	77.62
76	0.85	78.51	78.38
77	0.96	79.27	79.13
78	1.08	80.01	79.87
79	1.21	80.74	80.61
80	1.35	81.47	81.34
81	1.51	82.19	82.06
82	1.67	82.90	82.77
83	1.86	83.60	83.48
84	2.05	84.30	84.18
85	2.26	84.99	84.87
86	2.49	85.67	85.56
87	2.73	86.34	86.24
88	2.99	87.01	86.92
89	3.27	87.68	87.59
90	3.56	88.34	88.26
91	3.88	88.99	88.92
92	4.21	89.64	89.58
93	4.51	90.29	90.24
94	4.94	90.93	90.89
95	5.34	91.57	91.53
96	5.76	92.21	92.18
97	6.21	92.84	92.82
98	6.68	93.47	93.46
99	7.17	94.10	94.09
100	7.69	94.73	94.73
101	8.24	95.35	95.36
102	8.81	95.98	95.99
103	9.41	96.60	96.62
104	10.04	97.23	97.25
105	10.70	97.85	97.88

TABLE 21--continued

Temperature (K)	Pressure (atm)	(1) S_c'' (joules/mole-K)	(2) S_σ'' (joules/mole-K)
106	11.39	98.48	98.51
107	12.11	99.10	99.14
108	12.87	99.73	99.77
109	13.66	100.36	100.40
110	14.48	101.00	101.03
111	15.34	101.63	101.67
112	16.23	102.28	102.31
113	17.16	102.93	102.95
114	18.13	103.58	103.60
115	19.14	104.25	104.25

NOTE:

T - Temperature of comparison.

P - Vapor pressure from vapor pressure equation at temperature T.

 S_c'' - Entropy of saturated liquid from equation of state, vapor pressure equation, and ideal gas heat capacity equation using Clapeyron equation with the derivative of the vapor pressure equation. S_σ'' - Entropy of saturated liquid from a fit to saturated liquid heat capacity data

$$S_\sigma'' = S_0 + \int_{T_0}^T (C_\sigma/T) dT \text{ where } T_0 = 100 \text{ K and } S_0 = S'' \text{ at}$$

100 K.

Comparison of Selected Velocity of Sound Data

The velocity of sound data from references [62] through [83] have been reviewed, and the data from [73], [74], [75], and [83] have been selected for comparison with sonic velocities calculated from the equation of state. A large proportion of the data not included in these comparisons is for pressures of 1 atmosphere or less. Although this analysis of velocity of sound data is not complete, the sample of the data compared to sonic velocity values calculated from the equation of state includes data for the liquid, the vapor to high pressures, and values for the saturated liquid and the saturated vapor. These comparisons are given in Table 22.

The calculated values of the velocity of sound for the vapor phase including the saturated vapor and the high pressure region above the critical temperature are generally within 1 percent of the measured values. However, deviations for the calculated sonic velocities in the low temperature liquid region are as large as 12 percent, while the saturated liquid values indicate differences of nearly 30 percent at pressures below 0.5 atmosphere and near the critical point.

TABLE 22

REPRESENTATIVE COMPARISONS OF CALCULATED SONIC VELOCITIES
TO EXPERIMENTAL VALUES

Pressure (atm)	Temperature (K)	Experimental Velocity of Sound (meters/sec)	$\frac{W_{data} - W_{calc}}{W_{data}} \times 100$ (percent)
Low Temperature Liquid Data of [73]			
84.3	113.6	589	0.22
68.3	109.2	617	2.02
104.7	113.4	634	2.15
104.7	113.6	631	1.95
42.2	104.8	614	0.66
43.6	105.0	616	1.00
57.1	105.9	629	1.23
94.8	110.2	646	1.81
126.8	113.8	659	1.82
104.7	109.5	666	1.84
8.5	90.6	725	- 2.38
8.5	90.6	726	- 2.24
46.9	85.5	819	- 2.89
86.0	87.6	836	- 1.17
136.9	91.0	850	0.16
38.4	84.3	822	- 3.72
84.3	87.7	834	- 1.12
134.3	90.6	853	0.30
8.2	81.0	826	- 6.76
1.6	77.6	851	- 9.89
8.1	75.3	883	-10.87
52.0	77.5	897	- 6.64
116.6	81.0	917	- 2.39
61.5	77.6	902	- 6.30
121.9	80.9	920	- 2.47
1.7	73.6	896	-12.82
112.6	75.0	959	- 5.97
111.5	75.0	959	- 5.93
120.0	73.8	975	- 6.35
Saturated Liquid Data of [74]			
0.18	65.4	968	-27.17
0.22	66.4	959	-24.81
0.29	68.1	942	-21.37
0.38	70.0	924	-18.21
0.50	71.9	905	-15.64

TABLE 22--continued

Pressure (atm)	Temperature (K)	Experimental Velocity of Sound (meters/sec)	$\frac{W_{\text{data}} - W_{\text{calc}}}{W_{\text{data}}} \times 100$ (percent)
0.68	74.2	881	-13.17
0.85	76.0	864	-11.44
1.26	79.3	831	-8.99
1.29	79.6	829	-8.77
1.39	80.3	822	-8.31
1.81	82.7	796	-6.95
1.89	83.2	791	-6.70
2.25	84.9	772	-5.85
2.66	86.7	755	-4.93
2.70	86.9	753	-4.79
2.82	87.4	748	-4.54
3.05	88.2	739	-4.26
3.96	91.3	705	-3.27
4.61	93.1	685	-2.72
6.39	97.4	636	-1.74
7.38	99.4	612	-1.47
8.34	101.2	590	-1.36
9.86	103.7	559	-1.22
13.4	108.7	493	-1.50
14.7	110.2	472	-1.73
17.1	112.9	434	-2.32
19.1	115.0	403	-3.05
21.4	117.1	369	-4.22
23.9	119.3	329	-6.31
24.1	119.4	327	-6.12
25.0	120.2	313	-6.92
26.4	121.2	290	-9.09
28.0	122.4	265	-10.49
30.6	124.3	220	-14.77
30.7	124.3	219	-14.79
31.9	125.1	191	-20.16
32.4	125.5	183	-19.51

Saturated Vapor Data of [75]

1.24	79.2	177	0.46
1.13	78.4	177	0.78
1.07	78.0	176	0.39
0.50	71.9	171	0.45

TABLE 22--continued

Pressure (atm)	Temperature (K)	Experimental Velocity of Sound (meters/sec)	$\frac{W_{\text{data}} - W_{\text{calc}}}{W_{\text{data}}} \times 100$ (percent)
High Pressure Data of [83]			
600	298.14	655	- 0.90
1000	298.14	844	- 0.36
1500	298.14	1030	0.35
2000	298.14	1170	- 0.03
2500	298.14	1296	0.39
3000	298.14	1398	0.23
3250	298.14	1445	0.23
3500	298.14	1500	0.94
3750	298.14	1545	1.11
200	323.14	440	0.37
600	323.14	650	- 0.59
1000	323.14	830	- 0.38
1500	323.14	1010	0.08
2000	323.14	1160	0.69
2500	323.14	1280	0.59
3000	323.14	1380	0.23
3500	323.14	1480	0.75
600	348.14	655	0.73
1000	348.14	825	0.26
1500	348.14	1000	0.46
2000	348.14	1140	0.30
2500	348.14	1262	0.42
3000	348.14	1370	0.64
3500	348.14	1433	0.63
200	373.15	462	0.02
600	373.15	648	- 0.19
1000	373.15	820	0.57
1500	373.15	985	0.08
2200	373.15	1130	- 3.90
2500	373.15	1248	0.40
3000	373.15	1354	0.48
3500	373.15	1442	0.12
200	398.16	476	0.55
600	398.16	654	0.60
1000	398.16	818	0.98
1500	398.16	978	0.29
2200	398.16	1115	- 4.20
2500	398.16	1232	0.05
3000	398.16	1338	0.19
200	423.17	486	0.30

TABLE 22--continued

Pressure (atm)	Temperature (K)	Experimental Velocity of Sound (meters/sec)	$\frac{W_{\text{data}} - W_{\text{calc}}}{W_{\text{data}}} \times 100$ (percent)
600	423.17	658	0.86
1000	423.17	810	0.43
1500	423.17	972	0.41
2200	423.17	1107	- 4.12
2500	423.17	1223	0.15
3000	423.17	1330	0.39
3500	423.17	1420	0.16
4000	423.17	1480	- 1.47
200	448.18	500	0.92
600	448.18	660	0.68
1000	448.18	810	0.69
1500	448.18	960	- 0.25
2200	448.18	1098	- 4.23
2500	448.18	1216	0.29
3000	448.18	1325	0.72
3500	448.18	1410	0.13
4000	448.18	1435	- 4.00

CHAPTER 12

CONCLUSIONS AND RECOMMENDATIONS

The results of this study are summarized below:

1. The equation of state (22) developed in this work represents the experimental P- ρ -T data in the liquid and vapor phases for pressures from 0 to 10,000 atmospheres and for temperatures of 65 K to 1073 K. The equation may be extrapolated to 2000 K at pressures below 300 atmospheres with an accuracy of at least ± 1 percent. The equation may also be extrapolated to lower temperatures for the vapor with an accuracy of at least ± 2 percent down to 20 K at very low pressures. It is estimated that the accuracy of the equation of state is within 0.5 percent in the liquid region, except in the vicinity of the critical point. At temperatures above the critical temperature for pressures up to 1000 atmospheres, the accuracy is generally within 0.1 percent except in the region near the critical point between temperatures of 126.2 K and 150 K and at pressures between 30 and 150 atmospheres where the density deviations from experimental data are as large as 0.7 percent. In the range from 1000 to 10,000 atmospheres the accuracy is estimated to be within 0.3 percent of the data used in the formulation, but deviations in density as large as 12 percent are evident in comparisons to other data in this range.
2. The vapor pressure equation (29) represents the selected data used in the formulation of the equation generally within an accuracy of ± 0.01 K between the triple point and the critical point.
3. The equation for the ideal gas specific heat (34) has been used to represent the recent values of C_p/R from [55] with an accuracy of $\pm .00001$ for values to 1200 K, and within ± 0.0001 above 1200 K.
4. Values of the heat capacity, enthalpy, and latent heats of vaporization are presented with comparisons to available measured calorimetric data. Although the paucity of these measurements make it difficult to define the accuracy of the equation of state (22) for the calculation of heat capacity values, these comparisons further indicate that the behavior of the isobaric calculated values is thermodynamically correct.
5. The least squares techniques used in the formulation presented here include the simultaneous fitting of P- ρ -T data, C_p data, and the criteria for phase equilibrium to allow for continuous integration along isotherms through the two-phase region.

Suggestions for further research are presented below:

1. The work reported here is essentially complete within the limits imposed by the availability of experimental data to describe the thermodynamic properties of nitrogen. However, the lack of agreement of the various P- ρ -T data in the liquid region suggests the need for further measurement of the properties of the liquid.
2. The use of a single equation of state for the P- ρ -T surface appears to be accompanied by fitting problems near the critical point which propagate to temperatures above the critical value. It is suggested that new methods of accomodating the requirements of the P- ρ -T surface in this region for the least squares determination of the equation of state be explored.
3. When precise experimental heat capacity data become available for nitrogen for the saturated liquid and vapor phases to define the derivative behavior and saturation conditions more accurately, the equation of state may be improved.
4. The consistency of the vapor pressure equation, melting equation, and equation of state in the region of the triple point should be investigated.
5. The simultaneous fitting procedures developed in this work are applicable to other fluids for which the appropriate data are available.
6. A detailed study of the sonic velocity data should be made to complete the analysis of this data and to identify the cause of the large deviations of calculated velocity of sound values from experimental measurements in the liquid region.

BIBLIOGRAPHY

References Containing Experimental
Data for Nitrogen

Pressure-Density-Temperature Data

Vapor

- [1] Amagat, E. H., Mémoire sur la compressibilité des gaz a des pressions élevées, Ann. Chim. et Phys. 19, 345-385 (1880).
- [2] Amagat, E. H., Compressibilité des gaz: oxygène, hydrogène, azote et air jusqu' à 3000 atm., Compt. Rend. 107, 522-524 (1888).
- [3] Bartlett, E. P., The compressibility isotherms of hydrogen, nitrogen, and mixtures of these gases at 0 degree and pressures to 1000 atmospheres. A correction, J. Am. Chem. Soc. 49, 1955-1957 (1927).
- [4] Bartlett, E. P., H. L. Cupples, and T. H. Tremearne, The compressibility isotherms of hydrogen, nitrogen, and a 3:1 mixture of these gases at temperatures between 0 degrees and 400 degrees and at pressures to 1000 atmospheres, J. Am. Chem. Soc. 50, 1275-1288 (1928).
- [5] Bartlett, E. P., N. C. Hetherington, H. M. Kvalnes, and T. H. Tremearne, The compressibility isotherms of hydrogen, nitrogen, and a mixture of these gases at temperatures of -70, -50, -25, and -20 degrees and at pressures to 1000 atmospheres, J. Am. Chem. Soc. 52, 1363-1373 (1930).
- [6] Benedict, M., Pressure, volume, temperature properties of nitrogen at high density. I. Results obtained with a weight piezometer, J. Am. Chem. Soc. 59, 2224-2233 (1937).
- [7] Benedict, M., Pressure, volume, temperature properties of nitrogen at high density. II. Results obtained by a piston displacement method, J. Am. Chem. Soc. 59, 2233-2242 (1937).
- [8] Canfield, F. B., Jr., The Compressibility Factors and Second Virial Coefficients for Helium-Nitrogen Mixtures at Low Temperature and High Pressure, Rice University, Houston, Texas, Ph.D. Thesis (1962).
- [9] Crain, R. W., Jr., P-V-T Behavior in the Argon-Nitrogen System, University of Michigan, Ann Arbor, Michigan, Ph.D. Thesis (1965).

- [10] Friedman, A. S., Pressure-Volume-Temperature Relationships of Gaseous Hydrogen, Nitrogen, and a Hydrogen-Nitrogen Mixture, Ohio State University, Columbus, Ohio, Ph.D. Thesis (1950).
- [11] Hall, K. R., and F. B. Canfield, Isotherms for the He-N₂ system at -190 degrees C, -170 degrees C, and -160 degrees C up to 700 atmospheres, *Physica* 47, 219-226 (1970).
- [12] Heuse, W., and J. Otto, Über eine Neubestimmung des Grenzwertes der Ausdehnungs- und Spannungskoeffizienten von Helium, Wasserstoff und Stickstoff, *Ann. Physik* 2, 1012-1030 (1929).
- [13] Holborn, L., and J. Otto, Über die Isothermen von Stickstoff, Sauerstoff und Helium, *Z. Physik* 10, 367-377 (1922).
- [14] Holborn, L. and J. Otto, Über die Isothermen einiger Gase bis 400° und ihre Bedeutung für das Gasthermometer, *Z. Physik* 23, 77-94 (1924).
- [15] Holborn, L. and J. Otto, Über die Isothermen von Helium, Stickstoff und Argon unterhalb 0°, *Z. Physik* 30, 320-328 (1924).
- [16] Kamerlingh Onnes, H., and A. Th. van Urk, Isotherms of diatomic substances and their binary mixtures XXVIII. On the isotherms of nitrogen at low temperatures, *Communs. Phys. Lab. Univ. of Leiden* No. 169-D (1924).
- [17] Malbrunot, P., and B. Vodar, Détermination expérimentale de la densité de l'azote jusqu'à 4000 atm et 1000°C, *C. R. Acad. Paris, Series B* 268, 1337-1340 (1969).
- [18] Malbrunot, P., Measure des Paramètres d'Etat des Gaz Denses à Températures Eleveés. Application à l'Azote, University of Paris, Paris, France, Ph.D. Thesis (1970).
- [19] Michels, A., H. Wouters, and J. DeBoer, Isotherms of nitrogen between 0 degrees and 150 degrees and at pressures from 20 to 80 atmospheres, *Physica* 1, 587-594 (1934).
- [20] Michels, A., H. Wouters, and J. DeBoer, Isotherms of nitrogen between 200 and 3000 atmospheres and 0 degrees and 150 degrees, *Physica* 3, 585-589 (1936).
- [21] Miller, J. E., L. Stroud, and L. W. Brandt, Compressibility of helium-nitrogen mixtures, *J. Chem. and Engr. Data* 5, 6-9 (1960).
- [22] Otto, J., A. Michels, and H. Wouters, Über Isothermen des Stickstoffes zwischen 0° und 150° bei Drucken bis zu 400 Atmosphären, *Physik Z.* 35, 97-101 (1934).
- [23] Robertson, S. L., and S. E. Babb, Jr., Isotherms of nitrogen to 400 degrees C and 1000 bar, *J. Chem. Phys.* 50, 4560-4564 (1969).

- [24] Saurel, J. R., Determination of the equations of state of compressed gases at elevated temperatures. Application to the study of nitrogen to 1000 kg/CM² and 1000 degrees, *J. Recherches Centre Natl. Recherches Sci.* 42, 21-60 (1958).
- [25] Smith, L. B., and R. S. Taylor, The equation of state for pure nitrogen, gas phase, *J. Am. Chem. Soc.* 45, 2107-2124 (1923).
- [26] Townsend, P. W., *Pressure-Volume-Temperature Relationships of Binary Gaseous Mixtures*, Columbia University, New York, New York, Ph.D. Thesis (1956).
- [27] Tsiklis, D. S., and E. V. Polyakov, Measuring the compressibility of gases by the displacement method. Nitrogen compressibility at pressures up to 10,000 atmospheres and temperatures to 400 degrees, *Soviet Physics--Doklady* 12, 901-904 (1968).
- [28] Tsiklis, D. S., Compressibility of nitrogen at pressures up to 10,000 atmospheres, *Doklady Akad. Nauk. SSSR* 89, 289-290 (1951).
- [29] Verschoyle, T. T. H., Isotherms of hydrogen, of nitrogen, and of hydrogen-nitrogen mixtures, at 0 degrees and 20 degrees C, up to a pressure of 200 atmospheres, *Proc. Royal Soc. A* 111, 552-576 (1926).

Liquid

- [30] Cockett, A. H., K. Goldman, and N. G. Scrase, The Density of Liquid Nitrogen from 85 to 120 Degrees K and from the Saturation Boundary to 200 Atmospheres, *Proceedings of the Second International Cryogenic Engineering Conference*, Iliffe Science and Technology Publications, Ltd., Guildford, England, 1968, pp. 276-280.
- [31] Gibbons, R. M., The equation of state of neon between 27 and 70 K, *Cryogenics* 9, 251-260 (1969).
- [32] Golubev, I. F., and O. A. Dobrovolskii, Measurement of the density of nitrogen and hydrogen at low temperatures and high pressures by the method of hydrostatic weighing, *Gasovaia Promyshlen* 9, 43-47 (1964).
- [33] Streett, W. B., and L. A. K. Staveley, The P-V-T behavior of liquid nitrogen at temperatures from 77 to 120 degrees K and pressures to 680 atmospheres, *Advances in Cryogenic Engineering* 13, 363-374 (1968).
- [34] Van Itterbeek, A., and O. Verbeke, Density of liquid nitrogen and argon as a function of pressure and temperature, *Physica* 26, 931-938 (1960).
- [35] Van Itterbeek, A., and O. Verbeke, The variation of the density of liquid nitrogen and liquid oxygen as a function of pressure, *Cryogenics* 2, 79-80 (1961).
- [36] Weber, L. A., Some vapor pressure and P-V-T data on nitrogen in the range 65 to 140 K, *J. Chem. Thermodyn.* 2, 839-846 (1970).

Saturated Liquid

- [37] Goldman, K., and N. G. Scrase, Densities of saturated liquid oxygen and nitrogen, *Physica* 44, 555-586 (1969).
- [38] Terry, M. J., J. T. Lynch, M. Bunclark, K. R. Mansell, and L. A. K. Staveley, The densities of liquid argon, krypton, xenon, oxygen, nitrogen, carbon monoxide, methane, and carbon tetrafluoride along the orthobaric liquid curve, *J. Chem. Thermodyn.* 1, 413-424 (1969).

Liquid on the Freezing Line

- [39] Grilly, E. R., and R. L. Mills, Volume change on melting of N₂ up to 3500 kg/cm², *Physical Review* 105, 1140-1145 (1957).

Vapor Pressure Data

- [40] Armstrong, G. T., Vapor pressure of nitrogen, *Journal of Research of the National Bureau of Standards* 53, 263-266 (1954).
- [41] Cath, P. G., On the measurement of very low temperatures. XXIX. Vapor pressures of oxygen and nitrogen for obtaining fixed points on the temperature scale below 0 degrees C, *Communs. Phys. Lab. Univ. of Leiden* No. 152-D, 45-53 (1918).
- [42] Crommelin, C. A., Isotherms for diatomic gases and for their binary mixtures. XVI. Vapor pressure for nitrogen between critical and boiling temperatures, *Communs. Phys. Lab. Univ. of Leiden* No. 145-D (1915).
- [43] Dodge, B. F., and H. N. Davis, Vapor pressure of liquid oxygen and nitrogen, *J. Chem. Soc.* 49, 610-620 (1927).
- [44] Friedman, A. S., and D. White, The vapor pressure of liquid nitrogen, *J. Am. Chem. Soc.* 72, 3931-3932 (1950).
- [45] Giauque, W. F., and J. O. Clayton, The heat capacity and entropy of nitrogen. Heat of vaporization. Vapor pressures of solid and liquid. The reaction $\frac{1}{2}\text{N}_2 + \frac{1}{2}\text{O}_2 = \text{NO}$ from spectroscopic data, *J. Am. Chem. Soc.* 55, 4875-4880 (1933).
- [46] Keesom, W. H., and A. Bijl, Determination of the vapor pressure of liquid nitrogen below one atmosphere and of solid nitrogen beta. Boiling point and triple point of nitrogen, *Physica* 4, 305-310 (1937).
- [47] Michels, A., T. Wassenaar, W. DeGraaff, and Chr. Prins, Vapor pressure of liquid nitrogen, *Physica* 19, 26-28 (1953).
- [48] Moussa, M. R., R. Muijlwijk, and H. Van Dijk, The vapour pressure of liquid nitrogen, *Physica* 32, 900-912 (1966).

- [49] Porter, F., and J. H. Perry, High vapor pressures of nitrogen, J. Am. Chem. Soc. 48, 2059-2060 (1926).

NOTE: Reference 36 above also contains Vapor Pressure Data.

Calorimetric Data

- [50] Clusius, K., Über die spezifische Wärme einiger kondensierter Gase zwischen 10° abs. und ihrem Tripelpunkt, Z. Physik Chem. B3, 41-79 (1929).
- [51] Faulkner, R. C., Jr., Experimental Determination of the Thermodynamic Properties of Gases at Low Temperatures and High Pressures, University of Michigan, Ann Arbor, Michigan, Ph.D. Thesis (1959).
- [52] Furukawa, G. T., and R. E. McCoskey, Condensation Line of Air and the Heats of Vaporization of Oxygen, National Advisory Comm. Aeronaut. Tech. Note No. 2969 (1953).
- [53] Jones, M. L., Jr., Thermodynamic Properties of Methane and Nitrogen at Low Temperatures and High Pressures, University of Michigan, Ann Arbor, Michigan, Ph.D. Thesis (1961).
- [54] Kruse, N. W., and B. H. Mackey, The specific heats of gases at high pressures. II. Method and apparatus at high temperatures, Industrial and Engr. Chem. 22, 1060-1062 (1930).
- [55] Mage, D. T., M. L. Jones, D. L. Katz, and J. R. Roebuck, Experimental enthalpies for nitrogen, Chemical Engineering Progress Symposium Series 59, 61-65 (1963).
- [56] Voronel', A. V., V. G. Gorbunova, Yu. R. Chaskin, and V. V. Shchekochikhina, Specific heat of nitrogen near the critical point, Soviet Physics JETP 23, 597-601 (1966).
- [57] Weiner, L. D., Hydrocarbon enthalpies by means of a high-pressure flow calorimeter, Preprint 9C, Presented at the Symposium on Thermodynamics of Fluids, Part II--Fifty Eighth National Meeting, Dallas, Texas, American Institute of Chemical Engineers (1966).
- [58] Wiebe, R., and M. J. Brevoort, The heat capacity of saturated liquid nitrogen and methane from the boiling point to the critical temperature, J. Am. Chem. Soc. 52, 622-633 (1930).

Sources of Experimental Second Virial Coefficients

- [59] Canfield, F. B., T. W. Leland, and R. Kobayashi, Volumetric behavior of gas mixtures at low temperatures by the Burnett method: the helium-nitrogen system, 0 degrees to -140 degrees C, Adv. in Cryogenic Engr. 8, 146-157 (1962).

- [60] Holborn, L., and J. Otto, Über die Isothermen einiger Gase zwischen +400° und -183°, Z. Physik 33, 1-11 (1925).
- [61] Van Itterbeek, A., Miss H. Lambert, and G. Fovrey, Measurements on the second virial coefficient of nitrogen between 90 and 65 degrees K with use of ultrasonics, Appl. Sci. Research A6, 15-20 (1956).

NOTE: References 9, 10, 19, and 22 above are also sources of Experimental Second Virial Coefficients.

Velocity of Sound Data

- [62] Blagoi, Yu. P., A. E. Butko, S. A. Mikhailenko, and V. V. Yakuba, Velocity of sound in liquid nitrogen, oxygen, and argon in the temperature range above the normal boiling points, Soviet Physics--Acoustics 12, 355-359 (1967).
- [63] Boyer, R. A., Ultrasonic velocities in gases at low temperatures, J. Acoust. Soc. Am. 23, 176-178 (1951).
- [64] Colwell, R. C., and L. H. Gibson, Sound velocities in gases under different pressures, J. Acoust. Soc. Am. 12, 436-437 (1941).
- [65] Dixon, H. B., C. Campbell, and A. Parker, On the velocity of sound in gases at high temperatures, and the ratio of the specific heats, Proc. Roy. Soc. (London) A100, 1-26 (1921).
- [66] Dobbs, E. R., and L. Finegold, Measurement of the velocity of sound in liquid argon and liquid nitrogen at high pressures, J. Acoust. Soc. Am. 32, 1215-1220 (1960).
- [67] El-Hakeem, A. S., Velocity of sound in nitrogen and argon at high pressures, J. Chem. Phys. 42, 3132-3133 (1965).
- [68] Keesom, W. H., and J. A. V. Lammeren, Measurements of the velocity of sound in nitrogen, Proc. Acad. Sci. Amsterdam 35, 727-736 (1932).
- [69] Lestz, S. S., Acoustic isotherms for nitrogen, argon, and krypton, J. Chem. Phys. 38, 2830-2834 (1963).
- [70] Liepmann, H. W., Über die Messung der Schallgeschwindigkeit in flüssigem Argon, Helv. Phys. Acta. 12, 421-442 (1939).
- [71] Pine, A. S., Velocity and attenuation of hypersonic waves in liquid nitrogen, J. Chem. Phys. 51, 5171-5173 (1969).
- [72] Schilling, W. G., and J. R. Partington, Measurements of the velocity of sound in air, nitrogen, and oxygen with special reference to the temperature coefficients of molecular heats, Phil. Mag. 6, 920-939 (1928).
- [73] Singer, J. R., and J. H. Lunsford, Ultrasonic attenuation and volume viscosity in liquid nitrogen, J. Chem. Phys. 47, 811-814 (1967).

- [74] Van Dael, W., A. Van Itterbeek, A. Cops, and J. Thoen, Sound velocity measurements in liquid argon, oxygen, and nitrogen, *Physica* 32, 611-620 (1966).
- [75] Van Itterbeek, A., Déterminations des grandeurs thermodynamiques et cinétiques des gaz et des gaz condensés aux basses températures, *Nuovo Cimento* 7, 218-228 (1950).
- [76] Van Itterbeek, A., A. DeBock, and L. Verhaegen, Velocity of sound in liquid nitrogen, *Physica* 15, 624-626 (1949).
- [77] Van Itterbeek, A., W. DeRop, and G. Forrey, Measurements on the velocity of sound in nitrogen under high pressure, *Appl. Sci. Res.* 6, 421-432 (1957).
- [78] Van Itterbeek, A., and W. Van Dael, Measurements on the velocity of sound in liquid oxygen and nitrogen and mixtures of nitrogen and oxygen under high pressures, *Bull. IIR* 1958-1, 295-306 (1958).
- [79] Van Itterbeek, A., and W. Van Dael, The velocity of sound in liquid argon and liquid nitrogen at high pressures, *Cryogenics* 1, 226-228 (1961).
- [80] Van Itterbeek, A., and W. Van Dael, Velocity of sound in liquid oxygen and liquid nitrogen as a function of temperature and pressure, *Physica* 28, 861-870 (1962).
- [81] Vasserman, A. A., and V. I. Selevanyuk, Velocity of sound in nitrogen, *Soviet Physics--Acoustics* 13, 104-106 (1967).
- [82] Verhagen, L., Measurements of the speed of propagation of sound in some liquefied gases, *Verhandel. Koninkl. Vlaam. Acad. Wetenschap. Belg. Kl. Wetenschap* No. 38, (1952).
- [83] Voronov, F. F., L. L. Pitaevokaya, and A. V. Bilevich, Rate of propagation of ultrasound in nitrogen at pressures up to 4 kbar and temperatures in the range 25-175°C, *Russian Journal of Physical Chemistry* 43, 321-324 (1969).

Ideal Gas Specific Heat Data

- [84] Baehr, H. D., H. Hartmann, H. C. Pohl, and H. Schomacker, *Thermodynamische Funktionen idealer Gase für Temperaturen bis 6000°K*, (Springer-Verlag, Berlin, Germany, 1968).
- [85] Pohl, H. C., Die genaue Berechnung Thermodynamischer Funktionen zweiatomiger idealer Gase durch direkte Summierung der Zustandssummen, der Technischen Hochschule Carolo-Wilhelmina Zu Braunschweig, Germany, Ph.D. Thesis (1965).
- [86] Private Communication from H. W. Woolley, National Bureau of Standards (1970).

General References

- [87] Barieau, R. E., Analytical expressions for the zero pressure thermodynamic properties of nitrogen gas including corrections for the latest values of the atomic constants and the new carbon-12 atomic weight scale, *J. Phys. Chem.* 69, 495-499 (1965).
- [88] Barieau, R. E., and P. C. Tully, Zero Pressure Thermodynamic Properties of Nitrogen Gas, Bureau of Mines Information Circular 8319 (1967).
- [89] Bedford, R. E., M. Durieux, R. Muijlwijk, and C. R. Barber, Relationships between the international practical temperature scale of 1968 and the NBS-55, NPL-61, PRMI-54, and PSU-54 temperature scales in the range from 13.81 to 90.188 K, *Metrologia* 5, 47-49 (1969).
- [90] Bedford, R. E., H. Preston-Thomas, M. Durieux, and R. Muijlwijk, Derivation of the CCT-68 reference function of the international practical temperature scale of 1968, *Metrologia* 5, 45-47 (1969).
- [91] Benedict, M., G. B. Webb, and L. C. Rubin, An empirical equation for thermodynamic properties of light hydrocarbons and their mixtures, *J. Chem. Phys.* 8, 334-345 (1940).
- [92] Bender, E., Equations of state exactly representing the phase behavior of pure substances, Proceedings of the Fifth Symposium on Thermophysical Properties, pp. 227-235 (1970).
- [93] Bibliography of References, Thermodynamic Properties of Nitrogen in Solid, Liquid, and Gaseous Phases, Private communication from the National Bureau of Standards (1971).
- [94] CODATA Bulletin 5, International Council of Scientific Unions, Committee on Data for Science and Technology (December 1971).
- [95] Coleman, T. C., and R. B. Stewart, The Thermodynamic Properties of Nitrogen, University of Idaho, Engineering Experiment Station, Research Report No. 11 (1970).
- [96] Din, F., Thermodynamic Functions of Gases, Vol. 3, (Butterworths Scientific Publications, London, 1961).
- [97] Diller, D. E., The specific heat. (C_V) of dense simple fluids, *Cryogenics* 11, 186-191 (1971).
- [98] Douglas, T. B., Conversion of existing calorimetrically determined thermodynamic properties to the basis of the international practical temperature scale of 1968, *J. Res. NBS* 73A, 451-470 (1969).
- [99] Goodwin, R. D., and L. A. Weber, Specific heats of oxygen at coexistence, *J. Res. NBS* 73A, 1-13 (1969).

- [100] Hilsenrath, J., C. W. Beckett, W. S. Benedict, L. Fano, H. J. Hoge, J. F. Masi, R. L. Nutall, Y. S. Touloukian, and H. J. Woolley, Tables of Thermal Properties of Gases, NBS Circular No. 564 (November 1955), reprinted as Tables of Thermodynamic and Transport Properties of Air, Argon, Carbon Dioxide, Carbon Monoxide, Hydrogen, Nitrogen, Oxygen, and Steam, (Pergamon Press, Oxford, 1960).
- [101] Hust, J. G., A Compilation and Historical Review of Temperature Scale Differences, NBS Laboratory Note, Project No. 3150121, File No. 68-1 (1968).
- [102] Hust, J. G., A compilation and historical review of temperature scale differences, *Cryogenics* 9, 443-455 (1969).
- [103] Hust, J. G., and R. D. McCarty, Curve-fitting techniques and applications to thermodynamics, *Cryogenics* 7, 200-206 (1967).
- [104] Hust, J. G., and R. B. Stewart, Thermodynamic property computations for systems analysis, *ASHRAE Journal* 8, 64-68 (1966).
- [105] The international practical temperature scale of 1968, *Metrologia* 5, 34-55 (1969).
- [106] Ishkin, I. P., and M. G. Kaganer, Investigation of thermodynamic properties of air and nitrogen at high pressures and low temperatures. I. Thermodynamic diagrams of state for air and nitrogen, *Soviet Physics JETP* 1, 2263-2271 (1956).
- [107] Kamerlingh Onnes, H., Expression of the Equation of State of Gases and Liquids by Means of Series, *Communs. Phys. Lab. Univ. of Leiden* No. 71 (19⁰¹).
- [108] Mather, A. E., The Direct Determination of the Enthalpy of Fluids under Pressure, Univ. of Michigan, Ann Arbor, Michigan, Ph.D. Thesis (1967).
- [109] Private Communication from R. D. McCarty, National Bureau of Standards (1971).
- [110] Mechty, E. A., The International System of Units, Physical Constants and Conversion Factors, Revised, Scientific and Technical Information Division Office of Technology Utilization, National Aeronautics and Space Administration (NASA SP-7012), Washington, D.C. (1969).
- [111] Myers, A. F., R. T. Jacobsen, and R. B. Stewart, A vapor pressure equation for oxygen, paper presented to the XIII International Congress of Refrigeration, Washington, D.C. (1971).
- [112] Prydz, R., and R. Goodwin, Specific heats, C_p , of compressed liquids and gaseous fluorine, *J. Res. NBS* 74A, 661 (1970).
- [113] Prydz, R. and G. C. Straty, The Thermodynamic Properties of Compressed Gaseous and Liquid Fluorine, *NBS Tech. Note* 392 (1970).

- [114] Rose, G. L., A Critical Review of Least Squares Procedures for Determination of Thermodynamic Equations of State, University of Idaho, Moscow, Idaho, M.S. Thesis (in progress).
- [115] Sengers, J. M. H. L., in Physics of High Pressures and the Condensed Phase, Van Itterbeek, Editor (North Holland Publishing Company, Amsterdam, 1965).
- [116] Stewart, R. B., The Thermodynamic Properties of Oxygen, University of Iowa, Iowa City, Iowa, Ph.D. Thesis (1966).
- [117] Stewart, R. B., and R. T. Jacobsen, The Thermodynamic Properties of Nitrogen II, University of Idaho, Engineering Experiment Station, Research Report No. 12 (1971).
- [118] Stewart, R. B., R. T. Jacobsen, and A. F. Myers, An Equation of State for Oxygen and Nitrogen, University of Idaho, Engineering Experiment Station, Research Report No. 13 (1971).
- [119] Strobridge, T. R., The Thermodynamic Properties of Nitrogen from 114 to 540 R between 1.0 and 3000 psia, NBS Tech. Note 129A (1963).
- [120] Vasserman, A. A., and V. A. Rabinovich, Thermophysical Properties of Liquid Air and its Components, Committee of Standards, Measures, and Measuring Instruments of the USSR Council of Ministers, Government Standards Service, Series of Monographs, No. 3, Moscow (1968). [Translation--published for the U.S. Department of Commerce and the National Science Foundation by the Israel Program for Scientific Translations (1970), available from Clearinghouse for Federal Scientific and Technical Information, Springfield, Va. 22151.]
- [121] Vasserman, A. A., Ya. Z. Kazavchinskii, and V. A. Rabinovich, Thermophysical Properties of Air and its Components, Akademiya Nauk S.S.R., Moscow (1966). [Translation--published for the U.S. Department of Commerce and the National Science Foundation by the Israel Program for Scientific Translations (1970), available from Clearinghouse for Federal Scientific and Technical Information, Springfield, Va. 22151].
- [122] White, D., A. S. Friedman, and H. L. Johnston, The critical temperature and critical pressure of nitrogen, J. Am. Chem. Soc. 73, 5713-5715 (1951).
- [123] Ziegler, W. T., and J. C. Mullins, Calculation of the Vapor Pressure and Heats of Vaporization and Sublimation of Liquids and Solids, Especially below One Atmosphere. IV. Nitrogen and Fluorine, Georgia Institute of Technology, Engineering Experiment Station, Tech. Report No. 1, Project No. A-663 (1963).
- [124] Ziegler, W. T., J. C. Mullins, and B. S. Kirk, Calculation of the Vapor Pressure and Heats of Vaporization and Sublimation of Liquids and Solids, Especially below One Atmosphere Pressure. I. Ethylene, Georgia Institute of Technology, Engineering Experiment Station, Tech. Report No. 1, Project No. A-460 (1962).

APPENDIX A

THE SELECTION OF P- ρ -T AND VAPOR PRESSURE DATA FOR
THE DETERMINATION OF EQUATIONS (22) AND (29)

APPENDIX A

THE SELECTION OF P- ρ -T AND VAPOR PRESSURE DATA FOR
THE DETERMINATION OF EQUATIONS (22) AND (29)Selection of P- ρ -T Data

Low Temperature Liquid Data

A careful examination of the density deviation plots of figures 3 through 241 indicates a lack of agreement among the various data in the liquid region of the P- ρ -T surface.

The least squares formulations of equations (20) and (22) indicate the isochoric data of Weber [36] as the most precise of all the data sets for the liquid. The two publications by Van Itterbeek and Verbeke, [34] and [35], contain data sets which are not consistent with one another. The data of [34] appear to be in closer agreement with other data in the same region than those of [35].

The measurements of Golubev [32] for temperatures between 77 K and 133 K have been used in the development of the equation of state despite the systematic deviations of the equation from the data. The data of Streett and Staveley [33] for temperatures between 77 K and 120 K exhibit systematic trends which are contradictory to the trends of the values of Golubev [32]. In addition, the systematic nature of the deviations of the data of Streett and Staveley from the equation of state is not consistent from isotherm to isotherm. Consequently, the data from [33] were not used in the fit of equation (22).

The data of Gibbons at 72 K and 77 K, with the exception of one point at 77 K, are consistent with the equation of state within 0.2 percent. These low temperature data were used in the fit to determine the coefficients of the equation of state. The data of Cockett [30] appear to be a self consistent data set with the exception of the points on the 120 K isotherm, which are not in agreement with other data at this temperature. These data with the exception of the 120 K values were incorporated in the fit.

High Pressure Data

The lack of agreement of the high pressure data for nitrogen is notable. The difficulty in experimental procedures for pressures above 1000 atmospheres undoubtedly accounts for some of the imprecision exhibited by the various data at these extreme pressures. A selection of data for use in the determination of the equation of state was made on the basis of consistency with data in adjacent regions of the surface and on the agreement of the data with trends established by lower pressure data at the various experimental temperatures.

The analysis of the high pressure data indicates that the data of Michels [20] and those of Robertson and Babb [23] agree closely with the trends established by the data of Saurel [24] and of Michels [19] at pressures below 1000 atmospheres. The systematic deviations of the equation from the data of [23] are smaller in magnitude than those exhibited by any other data at pressures above 3000 atmospheres. The isothermal data by experimenters for pressures above 1000 atmospheres are discussed below.

373 K.--The data of Michels [20] and Robertson and Babb [23] are in agreement at this temperature. The densities of Tsiklis [27] and [28] are as much as 1 percent lower than those of [20] and [23] and those of Benedict [7] are lower by as much as 0.3 percent. The data of Tsiklis are in closer agreement (within 0.5 percent) at pressures below 6000 atmospheres than at pressures above this value.

398 K.--The only measurements are those of Michels [20] which are in agreement with the equation of state to within 0.2 percent.

423 K.--The data of Saurel [24] and those of Michels [19] differ by as much as 0.2 percent at pressures between 100 and 500 atmospheres. The data of Michels [20] and Benedict [7] are in good agreement above 1000 atmospheres, but the densities of Tsiklis [27] and [28] are as much as 1 percent lower than those indicated by the equation of state.

473 K.--The data of [7], [23], [27], [28], [17], and [18] at this temperature are in agreement with one exception. The densities reported by Tsiklis [27] and [28] are again consistently lower than those of other data sets.

573 K.--At this temperature the densities of Tsiklis [27] and [28] are up to 1 percent higher than those of Robertson and Babb [23]. The data of Malbrunot [18] and those of Malbrunot and Vodar [17], which represent the results from the same experimental apparatus show a lack of agreement at pressures below 3000 atmospheres of up to 0.5 percent.

673 K.--The data of Malbrunot [18] and those of Malbrunot and Vodar [17] again exhibit a lack of agreement. It is noticed that the later data of [17] are in agreement with the data of Saurel [24] at pressures near 1000 atmospheres, and discrepancies exceed 1.5 percent on this isotherm.

773 K to 1274 K.--The data of [17] and [18] exhibit a clear lack of agreement at lower pressures. This discrepancy is more pronounced at the higher temperatures. These considerations suggested that the equation of state be fitted to the data of Saurel [24], Robertson and Babb [23], and Michels [20], to define the surface at high pressures and temperatures. The equation of state must be considered an extrapolation above 773 K, since no data above 1000 atmospheres and 773 K were used in the least squares fit. Further discussion of the validity of the extrapolation of the equation of state is included in Chapter 8.

Selection of Vapor Pressure Data

In the development of the vapor pressure equation it was found that the various data sets listed in Table 2 were not sufficiently concordant to produce an equation which was consistent with all the data within the estimated experimental uncertainty. It was found that the data of Armstrong [40] and Weber [36] could be represented to within about 0.01 K. These data appear to be among the most precise nitrogen vapor pressure data available and extend from the triple point to the critical point. The data of [36] and [40] were used in the determination of the coefficients listed in Table 11.

APPENDIX B

DERIVATION OF FUNCTIONS FOR THE USE OF PHASE
EQUILIBRIUM CRITERIA IN SIMULTANEOUS
LEAST SQUARES FITTING

APPENDIX B

DERIVATION OF FUNCTIONS FOR THE USE OF PHASE
EQUILIBRIUM CRITERIA IN SIMULTANEOUS
LEAST SQUARES FITTING

The implementation of the relations (23), (24), (25), and (26) as given in Chapter 5 for use in the simultaneous least squares procedures for the determination of the coefficients of the equation of state, includes the requirement that the conditions for two phase equilibrium of a pure substance be satisfied. Using the equation of state and the definition of C_V [equations (23) and (24) respectively], and the terminology of Chapter 5, the derivations are presented here for equations (25) and (26). These equations represent the equality of the pressures for saturated liquid and saturated vapor at a temperature, T_S , and the equality of the Gibbs function, G , of the saturated liquid and saturated vapor states at equilibrium.

For (25):

$$P_{SL} = P_{SV}$$

$$P(\rho, T) = \sum N_i P_i(\rho, T) + \rho RT$$

$$P_{SL} = P(\rho_{SL}, T_S) = \sum N_i P_i(\rho_{SL}, T_S) + \rho_{SL} RT_S$$

$$P_{SV} = P(\rho_{SV}, T_S) = \sum N_i P_i(\rho_{SV}, T_S) + \rho_{SV} RT_S$$

$$\sum N_i P_i(\rho_{SL}, T_S) + \rho_{SL} RT_S = \sum N_i P_i(\rho_{SV}, T_S) + \rho_{SV} RT_S$$

$$\sum N_i P_i(\rho_{SL}, T_S) - \sum N_i P_i(\rho_{SV}, T_S) = \rho_{SV} RT_S - \rho_{SL} RT_S$$

$$\sum N_i P_i(\rho_{SL}, T_S) - \sum N_i P_i(\rho_{SV}, T_S) = RT_S (\rho_{SV} - \rho_{SL}). \quad (25)$$

For (26):

$$G = H - TS$$

$$\Delta G_{SV-SL} = \Delta H - \Delta(T_S S_{SV-SL})$$

$$H(T, \rho) = H_{T_0}^0 + T \int_0^\rho [R/\rho - 1/\rho^2 (\partial P/\partial T)_\rho]_T d\rho$$

$$+ \int_0^\rho [P/\rho^2 - RT/\rho]_T d\rho + [(P - \rho RT)/\rho] + \int_{T_0}^T C_p^0 dT$$

$$S(T, \rho) = S_{T_0}^0 + \int_{T_0}^T C_p^0 dT/T - R \ln(RT\rho) + \int_0^\rho [R/\rho - 1/\rho^2 (\partial P/\partial T)_\rho]_{T_S} d\rho$$

$$\begin{aligned}
H(T_S, \rho_{SV}) - H(T_S, \rho_{SL}) &= H_{T_0}^0 + T_S \int_0^{\rho_{SV}} [R/\rho - 1/\rho^2(\partial P/\partial T)_P]_{T_S} d\rho \\
&\quad + \int_0^{\rho_{SV}} [P/\rho^2 - RT/\rho]_T d\rho + [(P_S - \rho_{SV}RT_S)/\rho_{SV}] + \int_{T_0}^{T_S} C_p^0 dT \\
&- H_{T_0}^0 - T_S \int_0^{\rho_{SL}} [R/\rho - 1/\rho^2(\partial P/\partial T)_P]_{T_S} d\rho - \int_0^{\rho_{SL}} [P/\rho^2 - RT/\rho]_T d\rho \\
&- [(P_S - \rho_{SL}RT_S)/\rho_{SL}] - \int_{T_0}^{T_S} C_p^0 dT \\
S(T_S, \rho_{SV}) - S(T_S, \rho_{SL}) &= S_{T_0}^0 + \int_{T_0}^{T_S} C_p^0 dT/T - R \ln(RT\rho_{SV}) \\
&\quad + \int_0^{\rho_{SV}} [R/\rho - 1/\rho^2(\partial P/\partial T)_P]_{T_S} d\rho - S_{T_0}^0 - \int_{T_0}^{T_S} C_p^0 dT/T \\
&\quad + R \ln(RT\rho_{SL}) - \int_0^{\rho_{SL}} [R/\rho - 1/\rho^2(\partial P/\partial T)_P]_{T_S} d\rho \\
\Delta G_{SV-SL} &= T_S \int_{\rho_{SL}}^{\rho_{SV}} [R/\rho - 1/\rho^2(\partial P/\partial T)_P]_{T_S} d\rho + \int_{\rho_{SL}}^{\rho_{SV}} [P/\rho^2 - RT_S/\rho]_{T_S} d\rho \\
&\quad + [(P_S - \rho_{SV}RT_S)/\rho_{SV} - (P_S - \rho_{SL}RT_S)/\rho_{SL}] + RT_S \ln(RT\rho_{SV}) \\
&\quad - RT_S \ln(RT\rho_{SL}) - T_S \int_{\rho_{SL}}^{\rho_{SV}} [R/\rho - 1/\rho^2(\partial P/\partial T)_P]_{T_S} d\rho \\
\Delta G_{SV-SL} &= \int_{\rho_{SL}}^{\rho_{SV}} [P/\rho^2 - RT_S/\rho]_{T_S} d\rho + P_S(1/\rho_{SV} - 1/\rho_{SL}) \\
&\quad + RT_S \ln RT + RT_S \ln \rho_{SV} - RT_S \ln RT - RT_S \ln \rho_{SL} \\
\Delta G_{SV-SL} &= \int_{\rho_{SL}}^{\rho_{SV}} [P/\rho^2 - RT_S/\rho]_{T_S} d\rho + P_S(1/\rho_{SV} - 1/\rho_{SL}) \\
&\quad + RT_S \ln(\rho_{SV}/\rho_{SL}) = 0 \text{ for equilibrium}
\end{aligned}$$

$$\begin{aligned}
\int_{\rho_{SL}}^{\rho_{SV}} [P/\rho^2 - RT_S/\rho]_{T_S} d\rho &\equiv \sum N_i G_i = -P_S(1/\rho_{SV} - 1/\rho_{SL}) \\
&\quad - RT_S \ln(\rho_{SV}/\rho_{SL})
\end{aligned}$$

$$\Sigma N_i G_i = P_S(1/\rho_{SL} - 1/\rho_{SV}) + RT_S \ln(\rho_{SL}/\rho_{SV}). \quad (26)$$

APPENDIX C

HEAT CAPACITY VALUES CALCULATED USING THE
PRINCIPLE OF CORRESPONDING STATES

APPENDIX C

HEAT CAPACITY VALUES CALCULATED USING THE
PRINCIPLE OF CORRESPONDING STATES

The principle of corresponding states was used to calculate C_v values for nitrogen from the oxygen equation for C_v (equation 4 of [99]), as suggested in [97], for use in the determination of the equation of state for nitrogen as described in Chapter 5.

To establish the validity of the corresponding states analysis employed in this work, the method described above was utilized in the calculation of C_v values for fluorine which were then compared to the experimental data of [112]. Critical parameters for fluorine were taken from [113]. Figures 250 through 257 illustrate the results of this comparison.

Although the systematic deviations of the calculated values from the data are clearly evident, it was felt that the accuracy of the corresponding states heat capacity values was adequate to justify their use as described in Chapter 5 to enhance the behavior of the derivatives of the equation of state.

The values used in simultaneous fitting to determine the coefficients of equation (22) given in Table 10 were calculated from equation (4) of [99]. Comparisons of calculated values from the final equation of state exhibited an overall agreement of about ± 5 percent with the C_v values determined using the principle of corresponding states.

FIGURE 250

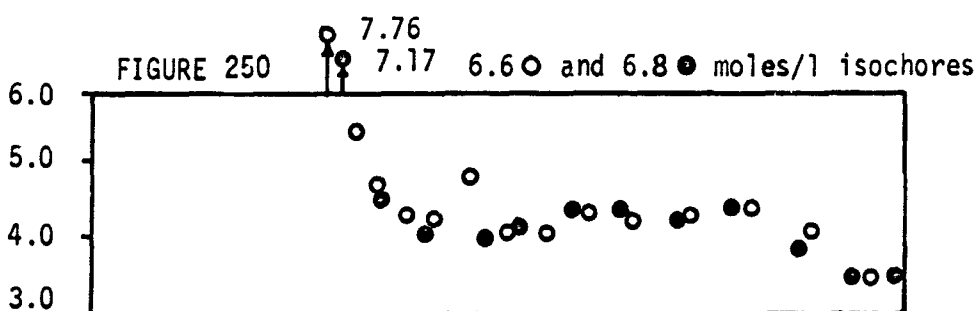


FIGURE 251

8.7 moles/l isochore

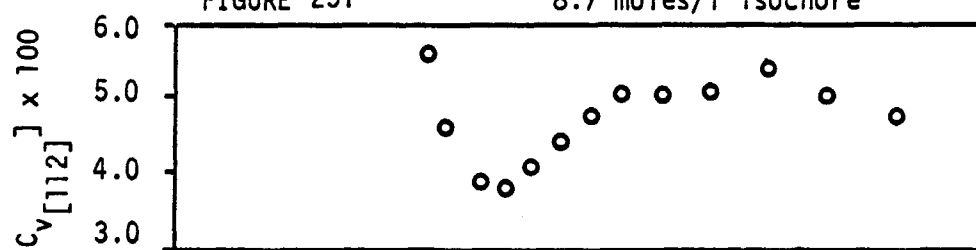


FIGURE 252

9.8 moles/l isochore

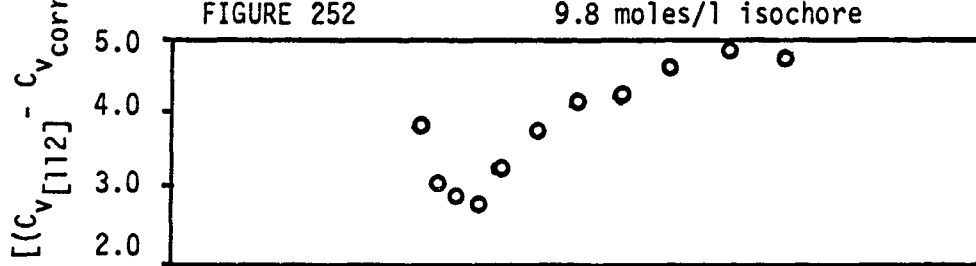
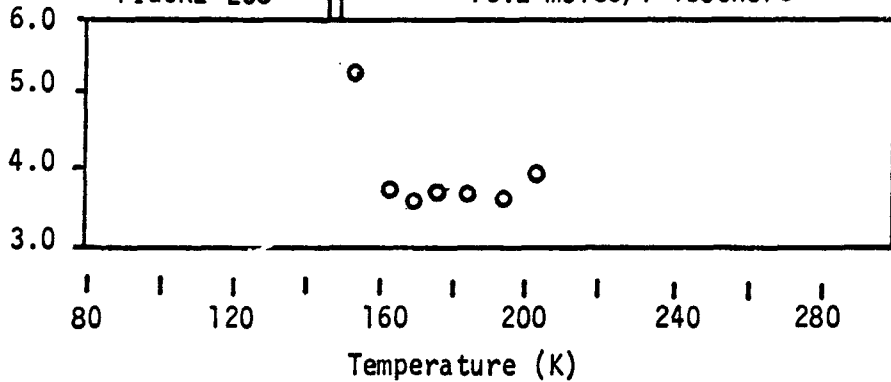


FIGURE 253

15.2 moles/l isochore



Comparisons of C_V Data for Fluorine from [112] with Values Predicted from Oxygen Equation of [99] using the Principle of Corresponding States (Data are for approximate isochores).

FIGURE 254 21.3 O and 26.3 O moles/l isochores

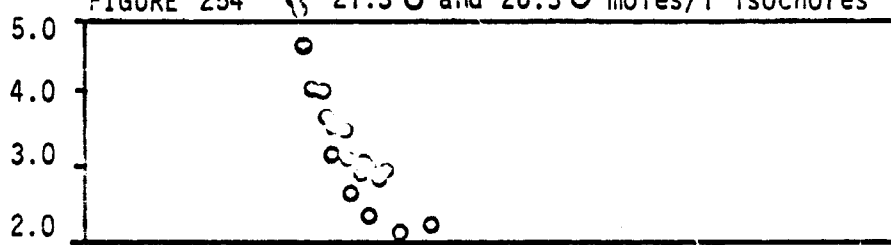


FIGURE 255 26.6 O and 30.0 O moles/l isochores

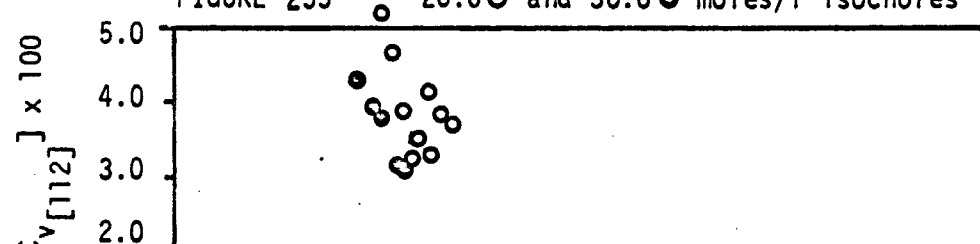


FIGURE 256 34 O and 36 O moles/l isochores

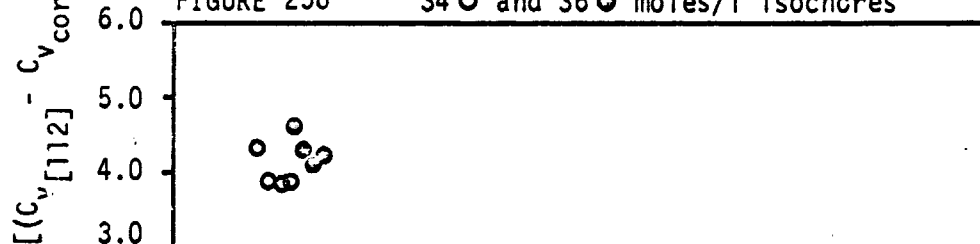
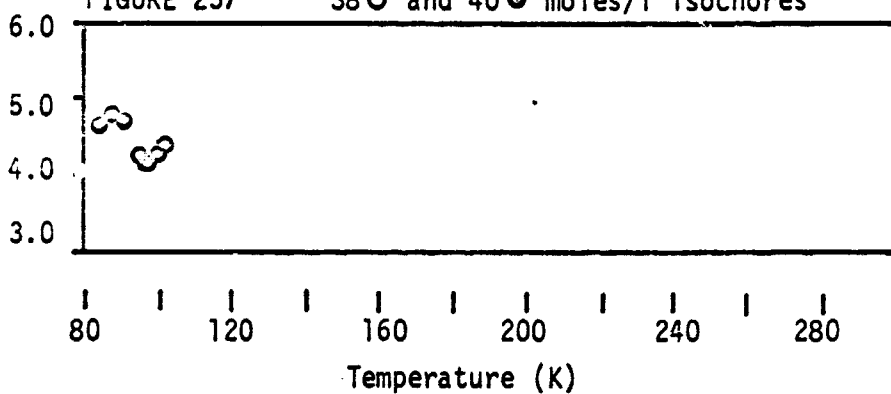


FIGURE 257 38 O and 40 O moles/l isochores



Comparisons of C_V Data for Fluorine from [112] with Values Predicted from Oxygen Equation of [99] using the Principle of Corresponding States (Data are for approximate isochores).

APPENDIX D

**FUNCTIONS FOR THE CALCULATION OF THERMODYNAMIC
PROPERTIES FROM THE EQUATION OF STATE (22)**

The Equation of State

Equation (22) may be written in the form:

$$P = \rho RT + \sum_{i=1}^{32} N_i X_i \quad (42)$$

where the N_i are listed in Table 10 and the X_i are as follows:

$X_1 = \rho^2 T$	$X_{12} = \rho^4 / T$	$X_{23} = \rho^5 F / T^4$
$X_2 = \rho^2 T^{1/2}$	$X_{13} = \rho^5$	$X_{24} = \rho^7 F / T^2$
$X_3 = \rho^2$	$X_{14} = \rho^6 / T$	$X_{25} = \rho^7 F / T^3$
$X_4 = \rho^2 / T$	$X_{15} = \rho^6 / T^2$	$X_{26} = \rho^9 F / T^2$
$X_5 = \rho^2 / T^2$	$X_{16} = \rho^7 / T$	$X_{27} = \rho^9 F / T^4$
$X_6 = \rho^3 T$	$X_{17} = \rho^8 / T$	$X_{28} = \rho^{11} F / T^2$
$X_7 = \rho^3$	$X_{18} = \rho^8 / T^2$	$X_{29} = \rho^{11} F / T^3$
$X_8 = \rho^3 / T$	$X_{19} = \rho^9 / T^2$	$X_{30} = \rho^{13} F / T^2$
$X_9 = \rho^3 / T^2$	$X_{20} = \rho^3 F / T^2$	$X_{31} = \rho^{13} F / T^3$
$X_{10} = \rho^4 T$	$X_{21} = \rho^3 F / T^3$	$X_{32} = \rho^{13} F / T^4$
$X_{11} = \rho^4$	$X_{22} = \rho^5 F / T^2$	

$$F = \exp(-0.0056 \rho^2)$$

The Isotherm Derivative

The isotherm derivative of the equation of state (22) may be represented as:

$$(\partial P / \partial \rho)_T = RT + \sum_{i=1}^{32} N_i X_i \quad (43)$$

where the N_i are given in Table 10 and the X_i are as follows:

$X_1 = 2\rho T$	$X_{12} = 4\rho^3/T$	$X_{23} = F_{22}/T^4$
$X_2 = 2\rho T^2$	$X_{13} = 5\rho^4$	$X_{24} = F_{23}/T^2$
$X_3 = 2\rho$	$X_{14} = 6\rho^5/T$	$X_{25} = F_{23}/T^3$
$X_4 = 2\rho/T$	$X_{15} = 6\rho^5/T^2$	$X_{26} = F_{24}/T^2$
$X_5 = 2\rho/T^2$	$X_{16} = 7\rho^6/T$	$X_{27} = F_{24}/T^4$
$X_6 = 3\rho^2 T$	$X_{17} = 8\rho^7/T$	$X_{28} = F_{25}/T^2$
$X_7 = 3\rho^2$	$X_{18} = 8\rho^7/T^2$	$X_{29} = F_{25}/T^3$
$X_8 = 3\rho^2/T$	$X_{19} = 9\rho^8/T^2$	$X_{30} = F_{26}/T^2$
$X_9 = 3\rho^2/T^2$	$X_{20} = F_{21}/T^2$	$X_{31} = F_{26}/T^3$
$X_{10} = 4\rho^3 T$	$X_{21} = F_{21}/T^3$	$X_{32} = F_{26}/T^4$
$X_{11} = 4\rho^3$	$X_{22} = F_{22}/T^2$	

$$F = \exp(-0.0056 \rho^2)$$

$$F_1 = 2F\rho(-0.0056)$$

$$F_{21} = 3F\rho^2 + F_1\rho^3$$

$$F_{22} = 5F\rho^4 + F_1\rho^5$$

$$F_{23} = 7F\rho^6 + F_1\rho^7$$

$$F_{24} = 9F\rho^8 + F_1\rho^9$$

$$F_{25} = 11F\rho^{10} + F_1\rho^{11}$$

$$F_{26} = 13F\rho^{12} + F_1\rho^{13}$$

The Isochore Derivative

The isochore derivative of the equation of state (22) may be written as:

$$(\partial P / \partial T)_\rho = \rho R + \sum_{i=1}^{32} N_i X_i \quad (44)$$

where the N_i are given in Table 10 and the X_i are as follows:

$X_1 = \rho^2$	$X_{12} = -\rho^4/T^2$	$X_{23} = -4\rho^5 F/T^5$
$X_2 = \rho^2/(2T^2)$	$X_{13} = 0.0$	$X_{24} = -2\rho^7 F/T^3$
$X_3 = 0.0$	$X_{14} = -\rho^6/T^2$	$X_{25} = -3\rho^7 F/T^4$
$X_4 = -\rho^2/T^2$	$X_{15} = -2\rho^6/T^3$	$X_{26} = -2\rho^9 F/T^3$
$X_5 = -2F^2/T^3$	$X_{16} = -\rho^7/T^2$	$X_{27} = -4\rho^9 F/T^5$
$X_6 = \rho^3$	$X_{17} = -\rho^8/T^2$	$X_{28} = -2\rho^{11} F/T^3$
$X_7 = 0.0$	$X_{18} = -2\rho^8/T^3$	$X_{29} = -3\rho^{11} F/T^4$
$X_8 = -\rho^3/T^2$	$X_{19} = -2\rho^9/T^3$	$X_{30} = -2\rho^{13} F/T^3$
$X_9 = -2\rho^3/T^3$	$X_{20} = -2\rho^3 F/T^3$	$X_{31} = -3\rho^{13} F/T^4$
$X_{10} = \rho^4$	$X_{21} = -3\rho^3 F/T^4$	$X_{32} = -4\rho^{13} F/T^5$
$X_{11} = 0.0$	$X_{22} = -2\rho^5 F/T^3$	

$$F = \exp(-0.0056 \rho^2)$$

The Evaluation of Integrals

The integral, $\int [R/\rho - (1/\rho^2)(\partial P/\partial T)_\rho]_T d\rho$ may be written as:

$$\sum_{i=1}^{32} N_i Y_i \quad (45)$$

where the N_i are listed in Table 10 and the Y_i are listed below:

$Y_1 = -\rho$	$Y_{12} = \rho^3/(3T^2)$	$Y_{23} = 4G_2/T^5$
$Y_2 = -\rho/(2T^2)$	$Y_{13} = 0.0$	$Y_{24} = 2G_3/T^3$
$Y_3 = 0.0$	$Y_{14} = \rho^5/(5T^2)$	$Y_{25} = 3G_3/T^4$
$Y_4 = \rho/T^2$	$Y_{15} = 2\rho^5/(5T^3)$	$Y_{26} = 2G_4/T^3$
$Y_5 = 2\rho/T^3$	$Y_{16} = \rho^6/(6T^2)$	$Y_{27} = 4G_4/T^5$
$Y_6 = -\rho^2/2$	$Y_{17} = \rho^7/(7T^2)$	$Y_{28} = 2G_5/T^3$
$Y_7 = 0.0$	$Y_{18} = 2\rho^7/(7T^3)$	$Y_{29} = 3G_5/T^4$
$Y_8 = \rho^2/(2T^2)$	$Y_{19} = \rho^8/(4T^3)$	$Y_{30} = 2G_6/T^3$
$Y_9 = \rho^2/T^3$	$Y_{20} = 2G_1/T^3$	$Y_{31} = 3G_6/T^4$
$Y_{10} = -\rho^3/3$	$Y_{21} = 3G_1/T^4$	$Y_{32} = 4G_6/T^5$
$Y_{11} = 0.0$	$Y_{22} = 2G_2/T^3$	

$$F = \exp(-0.0056\rho^2)$$

$$\begin{aligned}
 G_1 &= F/[2(-0.0056)] \\
 G_2 &= (F\rho^2 - 2G_1)/[2(-0.0056)] \\
 G_3 &= (F\rho^4 - 4G_2)/[2(-0.0056)] \\
 G_4 &= (F\rho^6 - 6G_3)/[2(-0.0056)] \\
 G_5 &= (F\rho^8 - 8G_4)/[2(-0.0056)] \\
 G_6 &= (F\rho^{10} - 10G_5)/[2(-0.0056)]
 \end{aligned}$$

The integral $\int [(\rho/\rho^2) - (RT/\rho)]_T d\rho$ may be written as:

$$\sum_{i=1}^{32} N_i Y_i \quad (46)$$

where the N_i are listed in Table 10 and the Y_i are listed below:

$Y_1 = \rho T$	$Y_{12} = \rho^3/(3T)$	$Y_{23} = G_2/T^4$
$Y_2 = \rho T^{1/2}$	$Y_{13} = \rho^4/4$	$Y_{24} = G_3/T^2$
$Y_3 = \rho$	$Y_{14} = \rho^5/(5T)$	$Y_{25} = G_3/T^3$
$Y_4 = \rho/T$	$Y_{15} = \rho^5/(5T^2)$	$Y_{26} = G_4/T^2$
$Y_5 = \rho/T^2$	$Y_{16} = \rho^6/(6T)$	$Y_{27} = G_4/T^4$
$Y_6 = \rho^2 T/2$	$Y_{17} = \rho^7/(7T)$	$Y_{28} = G_5/T^2$
$Y_7 = \rho^2/2$	$Y_{18} = \rho^7/(7T^2)$	$Y_{29} = G_5/T^3$
$Y_8 = \rho^2/(2T)$	$Y_{19} = \rho^8/(8T^2)$	$Y_{30} = G_6/T^2$
$Y_9 = \rho^2/(2T^2)$	$Y_{20} = G_1/T^2$	$Y_{31} = G_6/T^3$
$Y_{10} = \rho^3 T/3$	$Y_{21} = G_1/T^3$	$Y_{32} = G_6/T^4$
$Y_{11} = \rho^3/3$	$Y_{22} = G_2/T^2$	

$$F = \exp(-0.0056\rho^2)$$

$$G_1 = F/[2(-0.0056)]$$

$$G_2 = (F\rho^2 - 2G_1)/[2(-0.0056)]$$

$$G_3 = (F\rho^4 - 4G_2)/[2(-0.0056)]$$

$$G_4 = (F\rho^6 - 6G_3)/[2(-0.0056)]$$

$$G_5 = (F\rho^8 - 8G_4)/[2(-0.0056)]$$

$$G_6 = (F\rho^{10} - 10G_5)/[2(-0.0056)]$$

The integral, $\int [(T/\rho^2)(\partial^2 P/\partial T^2)]_T d\rho$ may be written as:

$$\sum_{i=1}^{32} N_i Y_i \quad (47)$$

where the N_i are listed in Table 10 and the Y_i are listed below:

$Y_1 = 0.0$	$Y_{12} = (2\rho^3)/(3T^2)$	$Y_{23} = 20G_2/T^5$
$Y_2 = \rho/(4T^2)$	$Y_{13} = 0.0$	$Y_{24} = 6G_3/T^3$
$Y_3 = 0.0$	$Y_{14} = (2\rho^5)/(5T^2)$	$Y_{25} = 12G_3/T^4$
$Y_4 = 2\rho/T^2$	$Y_{15} = (6\rho^5)/(5T^3)$	$Y_{26} = 6G_4/T^3$
$Y_5 = 6\rho/T^3$	$Y_{16} = \rho^6/(3T^2)$	$Y_{27} = 20G_4/T^5$
$Y_6 = 0.0$	$Y_{17} = (2\rho^7)/(7T^2)$	$Y_{28} = 6G_5/T^3$
$Y_7 = 0.0$	$Y_{18} = (6\rho^7)/(7T^3)$	$Y_{29} = 12G_5/T^4$
$Y_8 = \rho^2/T^2$	$Y_{19} = (3\rho^8)/(4T^3)$	$Y_{30} = 6G_6/T^3$
$Y_9 = 3\rho^2/T^3$	$Y_{20} = 6G_1/T^3$	$Y_{31} = 12G_6/T^4$
$Y_{10} = 0.0$	$Y_{21} = 12G_1/T^4$	$Y_{32} = 20G_6/T^5$
$Y_{11} = 0.0$	$Y_{22} = 6G_2/T^3$	

$$F = \exp(-0.0056\rho^2)$$

$$G_1 = F/[2(-0.0056)]$$

$$G_2 = (F\rho^2 - 2G_1)/[2(-0.0056)]$$

$$G_3 = (F\rho^4 - 4G_2)/[2(-0.0056)]$$

$$G_4 = (F\rho^6 - 6G_3)/[2(-0.0056)]$$

$$G_5 = (F\rho^8 - 8G_4)/[2(-0.0056)]$$

$$G_6 = (F\rho^{10} - 10G_5)/[2(-0.0056)]$$

The integral $\int C_p^0 dT$ may be written as:

$$\sum_{i=1}^{32} N_i Y_i \quad (48)$$

where the N_i are listed in Table 14 and the Y_i are given below:

$$\begin{array}{ll} Y_1 = -1/(2T^2) & Y_5 = T^2/2 \\ Y_2 = -1/T & Y_6 = T^3/3 \\ Y_3 = \ln(T) & Y_7 = T^4/4 \\ Y_4 = T & Y_8 = UT/[\exp(U)-1] \end{array}$$

$$U = N_g/T \quad (N_g \text{ from Table 14})$$

The integral $\int (C_p^0/T) dT$ may be written as:

$$\sum_{i=1}^{32} N_i Y_i \quad (49)$$

where the N_i are listed in Table 14 and the Y_i are given below:

$$\begin{array}{ll} Y_1 = -1/(3T^3) & Y_5 = T \\ Y_2 = -1/(2T^2) & Y_6 = T^2/2 \\ Y_3 = -1/T & Y_7 = T^3/3 \\ Y_4 = \ln(T) & Y_8 = U/(EU-1) - \ln[1-(1/EU)] \end{array}$$

$$U = N_g/T \quad (N_g \text{ from Table 14})$$

$$EU = \exp(U)$$

APPENDIX E
TABLES OF THERMODYNAMIC PROPERTIES OF NITROGEN

THERMODYNAMIC PROPERTIES OF SATURATED NITROGEN.

TEMPERATURE DEG KELVIN	PRESSURE ATM	DENSITY MOLE/L	INTERNAL ENERGY J/MOL	ENTHALPY J/MOL	ENTROPY J/MOL-K	CV J/MOL-K	CP J/MOL-K	VELOCITY OF SOUND M/SEC
63.148	0.1237	30.977	-4212.	-4212.	68.01	26.69	56.68	1326.
		0.02410	1296.	1816.	163.56	21.00	29.64	161.
64	0.1443	30.863	-4165.	-4165.	68.74	27.23	55.25	1298.
	0.02777	1313.	1839.	162.65	21.02	29.70	162.	
66	0.2037	30.589	-4054.	-4053.	70.48	28.05	56.21	1210.
	0.03613	1351.	1892.	160.63	21.08	29.87	164.	
68	0.2813	30.306	-3941.	-3940.	72.14	28.42	56.81	1147.
	0.05130	1388.	1943.	158.75	21.15	30.06	166.	
70	0.3807	30.013	-3827.	-3826.	73.80	28.50	57.19	1092.
	0.06774	1424.	1993.	157.01	21.23	30.29	168.	
72	0.5059	29.712	-3713.	-3711.	75.41	28.41	57.42	1045.
	0.08796	1459.	2042.	155.39	21.31	30.55	170.	
74	0.6610	29.402	-3598.	-3596.	76.98	28.23	57.58	1002.
	0.1125	1493.	2089.	153.87	21.41	30.85	172.	
76	0.8506	29.086	-3483.	-3480.	78.51	27.99	57.71	964.
	0.1418	1526.	2134.	152.45	21.51	31.20	174.	
77.347	1.0000	28.865	-3405.	-3402.	79.53	27.82	57.80	939.
	0.1647	1548.	2163.	151.54	21.59	31.45	175.	
78	1.0793	28.758	-3368.	-3364.	80.01	27.74	57.84	928.
	0.1767	1558.	2177.	151.11	21.62	31.58	175.	
80	1.3520	28.424	-3252.	-3248.	81.47	27.49	58.01	894.
	0.2176	1588.	2218.	149.85	21.75	32.02	177.	
82	1.6739	28.082	-3137.	-3131.	82.90	27.26	58.23	862.
	0.2652	1617.	2256.	148.65	21.88	32.52	178.	
84	2.0503	27.732	-3021.	-3013.	84.30	27.05	58.52	832.
	0.3203	1644.	2292.	147.51	22.02	33.08	179.	
86	2.4865	27.373	-2904.	-2895.	85.67	26.87	58.89	802.
	0.3836	1669.	2326.	146.42	22.18	33.71	180.	
88	2.9882	27.006	-2788.	-2776.	87.01	26.71	59.35	773.
	0.4561	1692.	2356.	145.37	22.34	34.41	181.	
90	3.5607	26.630	-2670.	-2656.	88.34	26.57	59.92	746.
	0.5385	1713.	2383.	144.37	22.51	35.22	182.	
92	4.2099	26.244	-2551.	-2535.	89.64	26.46	60.59	718.
	0.6319	1732.	2407.	143.39	22.70	36.13	182.	
94	4.9415	25.847	-2432.	-2412.	90.93	26.37	61.40	692.
	0.7374	1749.	2428.	142.45	22.90	37.16	183.	

THERMODYNAMIC PROPERTIES OF SATURATED NITROGEN

TEMPERATURE DEG KELVIN	PRESSURE ATM	DENSITY MOLE/L	INTERNAL ENERGY J/MOL	ENTHALPY J/MOL	ENTROPY J/MOL-K	CV J/MOL-K	CP J/MOL-K	VELOCITY OF SOUND MI/SEC
98	6.6746	25.018 0.9900	-2189. 1774.	-2162. 2457.	93.47 140.62	26.24 23.34	63.44 39.71	639. 183.
100	7.6685	24.583 1.140	-2065. 1782.	-2033. 2465.	94.73 139.72	26.19 23.58	64.73 41.29	613. 183.
102	8.8083	24.133 1.309	-1939. 1786.	-1902. 2468.	95.98 138.83	26.17 23.84	66.24 43.15	587. 183.
104	10.041	23.665 1.499	-1811. 1787.	-1768. 2466.	97.23 137.94	26.15 24.13	68.02 45.35	562. 183.
106	11.392	23.178 1.713	-1681. 1783.	-1631. 2457.	98.48 137.05	26.16 24.43	70.15 46.00	536. 183.
108	12.870	22.669 1.954	-1548. 1774.	-1491. 2441.	99.73 136.14	26.17 24.76	72.73 51.25	510. 182.
110	14.461	22.133 2.228	-1412. 1759.	-1345. 2417.	100.99 135.20	26.21 25.12	75.92 55.32	484. 191.
112	16.233	21.566 2.542	-1271. 1737.	-1195. 2384.	102.28 134.23	26.26 25.52	79.98 60.56	457. 181.
114	18.133	20.960 2.903	-1126. 1707.	-1038. 2340.	103.58 133.21	26.35 25.96	85.36 67.54	429. 179.
116	20.190	20.302 3.326	-974. 1666.	-873. 2281.	104.93 132.12	26.46 26.45	92.75 77.29	400. 178.
118	22.411	19.575 3.828	-813. 1611.	-697. 2205.	106.34 130.92	26.62 27.01	103.72 91.85	370. 177.
120	24.806	18.745 4.444	-639. 1537.	-505. 2103.	107.85 129.57	26.86 27.66	121.74 115.84	338. 176.
122	27.386	17.745 5.239	-443. 1434.	-286. 1963.	109.54 127.97	27.23 26.43	157.06 162.77	302. 174.
124	30.174	16.388 6.392	-200. 1272.	-14. 1750.	111.62 125.84	27.86 29.40	259.24 296.19	259. 173.
126	33.227	13.270 9.237	272. 867.	526. 1211.	115.76 121.20	29.73 30.80	29.73 30.80	29.73 30.80
128.200	33.555	11.210	559.	863.	118.41	30.68		

0.10 ATMOSPHERE ISOBAR THERMODYNAMIC PROPERTIES OF NITROGEN

TEMPERATURE DEG KELVIN	DENSITY MOLE/L	INTERNAL ENERGY J/MOL	ENTHALPY J/MOL	ENTROPY J/MOL-K	CV	CP	VELOCITY OF SOUND M/SEC
• 63.151	0.01965	1298.	1819.	165.36	20.96	29.53	161.
65	0.01888	1337.	1874.	166.21	20.94	29.49	154.
70	0.01751	1442.	2021.	168.39	20.90	29.40	170.
75	0.01632	1567.	2168.	170.42	20.87	25.33	176.
80	0.01529	1652.	2315.	172.31	20.85	21.28	182.
85	0.01438	1756.	2461.	177.08	20.83	29.25	188.
90	0.01358	1861.	2607.	175.75	20.82	29.22	193.
100	0.01221	2069.	2899.	174.83	20.81	29.18	204.
110	0.01110	2278.	3191.	181.61	20.80	29.16	217.
120	0.01017	2486.	3482.	184.15	20.79	23.15	223.
130	0.009383	2694.	3774.	189.48	20.79	29.14	232.
140	0.008711	2902.	4065.	198.64	20.79	29.13	241.
150	0.008129	3110.	4355.	190.65	20.79	29.12	250.
160	0.007621	3318.	4667.	192.53	20.78	29.12	258.
180	0.006773	3734.	5230.	199.96	20.78	29.11	273.
200	0.006095	4149.	5812.	199.02	20.78	29.11	288.
220	0.005510	4565.	6394.	201.80	20.78	29.10	302.
240	0.005078	4981.	6976.	204.33	20.78	29.10	316.
260	0.004687	5396.	7558.	206.66	20.78	29.10	329.
280	0.004353	5812.	8140.	208.82	20.78	29.10	341.
300	0.004062	6228.	8722.	210.82	20.79	29.11	353.
350	0.003482	7268.	10178.	215.31	20.83	29.14	381.
400	0.003047	8312.	11637.	219.21	20.91	29.22	407.
450	0.002708	9360.	13102.	222.66	21.04	29.36	432.
500	0.002437	10417.	14574.	225.76	21.23	29.55	454.
600	0.002031	12565.	17554.	231.19	21.76	30.07	496.
700	0.001741	14772.	20592.	235.88	22.39	30.71	534.
800	0.001523	17045.	23697.	240.02	23.07	31.38	566.
900	0.001354	19384.	26667.	243.75	23.72	32.03	601.
1000	0.001219	21787.	30101.	247.16	24.32	32.63	631.
1200	0.001016	26755.	35132.	253.20	25.33	33.64	688.
1400	0.000871	31903.	42543.	258.45	26.11	34.42	740.
1600	0.000762	37187.	50490.	263.09	26.71	35.02	769.
1800	0.000677	42576.	57562.	267.24	27.16	35.48	835.
2000	0.000609	48046.	64675.	271.00	27.52	35.83	879.

• INDICATES TWO PHASE BOUNDARY

0.40 ATMOSPHERE ISOBAR

THERMODYNAMIC PROPERTIES OF NITROGEN

TEMPERATURE DEG KELVIN	DENSITY MOLE/L	INTERNAL ENERGY J/MOL	ENTHALPY J/MOL	ENTROPY J/MOL-K	CV	CP	VELOCITY OF SOUND M/SEC
• 63.157	30.98	-4212.	-4211.	68.01	26.71	54.68	1325.
65	30.73	-4110.	-4109.	69.60	27.72	55.78	1247.
70	30.01	-3827.	-3826.	73.79	28.50	57.19	1092.
• 70.339	29.76	-3808.	-3806.	76.07	28.50	57.23	1084.
73	0.07089	1430.	2022.	156.73	21.24	30.33	169.
80	0.06621	1530.	2142.	158.67	21.13	30.07	175.
85	0.06187	1637.	2292.	160.60	21.05	29.87	181.
90	0.05809	1743.	2441.	162.41	20.72	187.	
100	0.04913	1849.	2590.	164.10	20.95	29.61	192.
110	0.04458	2060.	2885.	167.21	20.89	29.46	203.
120	0.04081	2270.	3179.	170.01	20.85	29.36	213.
130	0.03764	2479.	3472.	172.57	20.83	29.30	223.
140	0.03492	2688.	3765.	174.91	20.82	29.25	232.
150	0.03258	3105.	4349.	179.09	20.80	29.20	249.
160	0.03073	3314.	4621.	180.98	20.80	29.18	258.
160	0.02712	3730.	5225.	184.41	20.79	29.16	273.
200	0.02440	4146.	5808.	187.48	20.79	29.14	286.
225	0.02217	4562.	6390.	190.26	20.79	29.13	302.
240	0.02032	4978.	6973.	192.79	20.78	29.13	316.
260	0.01875	5394.	7555.	195.13	20.78	29.12	329.
280	0.01761	5810.	8138.	197.28	20.79	29.12	341.
300	0.01625	6226.	8720.	199.29	20.79	29.12	353.
350	0.01393	7267.	10177.	203.78	20.83	29.15	381.
400	0.01219	8310.	11637.	207.68	20.91	29.23	407.
450	0.01083	9359.	13101.	211.13	21.04	29.36	432.
500	0.009748	10416.	14574.	214.23	21.23	29.55	455.
600	0.008123	12564.	17554.	219.67	21.76	30.07	496.
700	0.006963	14771.	20592.	226.35	22.39	30.71	534.
800	0.006093	17045.	23697.	228.49	23.07	31.38	564.
900	0.00516	19304.	26869.	232.23	23.72	32.03	601.
1000	0.004814	21766.	30102.	235.63	24.32	32.63	631.
1200	0.004062	26755.	36733.	241.68	25.33	33.64	688.
1400	0.003482	31902.	43544.	246.92	26.11	34.42	740.
1600	0.003046	37187.	50491.	251.56	26.71	35.02	789.
1600	0.002708	42516.	57543.	255.71	27.16	35.48	835.
2000	0.002317	48066.	54676.	259.47	27.52	35.83	879.

• INDICATES TWO PHASE BOUNDARY

0.70 ATMOSPHERE (50 BAR) THERMODYNAMIC PROPERTIES OF NITROGEN

TEMPERATURE DEG KELVIN	DENSITY MOL/L	INTERNAL ENERGY J/MOL	ENTHALPY J/MOL	ENTROPY J/MOL-K	CV J/MOL-K	CP J/MOL-K	VELOCITY OF SOUND M/SEC
• 63.164	30.98	-4212.	-4210.	68.01	26.73	54.68	1325.
65	30.73	-4111.	-4108.	69.60	27.73	55.77	1247.
• 70	30.01	-3828.	-3825.	73.79	28.52	57.18	1092.
74.444	29.33	-3572.	-3570.	153.55	21.43	30.93	172.
75	0.116	1501.	2099.	153.78	21.41	30.87	173.
80	0.096	1622.	2270.	155.76	21.26	30.49	180.
85	0.1027	1130.	2421.	157.60	21.15	30.22	186.
90	0.09661	1038.	2572.	159.32	21.07	30.01	191.
100	0.0651	2050.	2870.	162.46	20.97	29.74	202.
110	0.07837	2262.	3167.	165.29	20.91	29.56	213.
120	0.0167	2872.	3462.	167.86	20.87	29.45	222.
130	0.06604	2682.	3756.	170.21	20.85	29.38	232.
140	0.06125	2891.	4049.	172.39	20.83	29.32	241.
150	6.05711	3100.	4342.	174.41	20.82	29.28	249.
160	0.05350	3309.	4635.	176.30	20.81	29.25	257.
180	0.06750	3726.	5220.	179.74	20.80	29.21	273.
200	0.04272	4143.	5804.	182.81	20.79	29.18	288.
220	0.0882	4260.	6387.	185.59	20.79	29.16	302.
240	0.03557	4676.	6970.	188.13	20.79	29.15	316.
260	0.0283	5392.	7553.	190.46	20.79	29.14	329.
280	0.03048	5808.	8136.	192.62	20.79	29.14	341.
300	0.0284	6224.	87..	194.63	20.80	29.14	353.
350	0.02637	7266.	10.76.	199.13	20.83	29.16	381.
400	0.02132	8309.	11626.	203.03	20.91	29.24	408.
450	0.01695	9358.	13101.	206.49	21.04	29.37	432.
500	0.01706	10415.	14574.	209.58	21.23	29.56	455.
600	0.01423	12864.	17554.	215.01	21.76	30.08	496.
700	0.01213	1471.	20593.	219.70	22.40	30.71	534.
800	0.01046	17044.	23697.	223.84	23.07	31.38	569.
900	0.009476	19384.	26869.	227.57	22.72	32.03	601.
1000	0.008529	2176.	30102.	230.98	22.32	32.63	631.
1200	0.00108	26755.	36734.	237.02	23.33	33.64	688.
1400	0.0006092	31002.	43545.	242.27	26.11	34.42	740.
1600	0.005331	37187.	50492.	246.91	26.71	35.02	789.
1800	0.004739	42376.	57546.	251.06	27.16	35.48	835.
2000	0.00265	4846.	64677.	254.82	27.52	35.84	879.

• INDICATES TWO PHASE BOUNDARY

1 ATMOSPHERE ISOBAR THERMODYNAMIC PROPERTIES OF NITROGEN

TEMPERATURE DEG KELVIN	DENSITY MOLE/L	INTERNAL ENERGY J/MOL	ENTHALPY J/MOL	ENTROPY J/MOL-K	CV J/MOL-K	CP J/MOL-K	VELOCITY OF SOUND M/SEC
• 63.171	30.98	-4212.	-4209.	68.01	26.75	54.68	1325.
65	30.73	-4111.	-4107.	69.59	27.75	55.77	1277.
70	30.02	-3828.	-3824.	73.78	28.53	57.17	1092.
75	29.25	-3561.	-3537.	77.75	28.12	57.63	983.
• 77.347	28.87	-3405.	-3402.	79.53	27.92	57.80	930.
80	0.1667	1548.	2113.	151.56	21.59	31.45	175.
80	0.1595	1601.	2246.	152.59	21.48	31.17	176.
85	0.1482	1717.	2401.	154.47	21.32	30.74	184.
90	0.1392	1826.	2554.	156.22	21.10	30.44	190.
100	0.1243	2041.	2856.	159.40	21.05	30.02	204.
110	0.1125	2254.	3155.	162.25	20.97	29.77	212.
120	0.1027	2465.	3452.	164.83	20.91	29.61	222.
130	0.0946	2676.	3747.	167.20	20.88	29.50	231.
140	0.0876	2886.	4042.	169.38	20.85	29.42	240.
150	0.0817	3096.	4336.	171.41	20.84	29.36	249.
160	0.0765	3305.	4629.	173.30	20.82	29.32	257.
180	0.0679	3723.	5215.	176.75	20.81	29.26	273.
200	0.0610	4140.	5799.	179.83	20.80	29.22	288.
220	0.0554	4557.	6383.	182.62	20.79	29.19	302.
240	0.0503	4974.	6967.	185.16	20.79	29.17	316.
260	0.0460	5390.	7550.	187.49	20.79	29.16	329.
280	0.0435	5806.	8133.	189.65	20.75	29.15	341.
300	0.0406	6223.	8717.	191.66	20.80	29.15	353.
350	0.0348	7264.	10174.	196.16	20.83	29.17	381.
400	0.0304	8308.	11635.	200.06	20.91	29.25	408.
450	0.0270	9357.	13100.	203.51	21.05	29.37	432.
500	0.0243	10414.	14573.	206.61	21.24	29.56	455.
600	0.0203	12563.	17554.	212.05	21.76	30.08	496.
700	0.0174	14770.	20593.	216.73	22.40	30.71	534.
800	0.0152	17044.	23698.	220.87	23.07	31.38	569.
900	0.0135	19383.	26669.	224.61	23.72	32.03	601.
1000	0.0121	21786.	30103.	228.02	24.32	32.63	631.
1200	0.0101	26755.	36132.	234.06	25.23	33.64	698.
1400	0.0087	31902.	43345.	239.31	26.11	34.43	740.
1600	0.0076	37187.	50493.	243.94	26.71	35.02	789.
1800	0.0067	42576.	57345.	248.10	27.16	35.48	835.
2000	0.0060	48046.	64573.	251.85	27.52	35.84	879.

• INDICATES TWO PHASE BOUNDARY

4 ATMOSPHERE ISOBAR THERMODYNAMIC PROPERTIES OF NITROGEN

TEMPERATURE DEG KELVIN	DENSITY MOLE/L	INTERNAL ENERGY J/MOL	ENTHALPY J/MOL	ENTROPY J/MOL-K	CV J/MOL-K	CP J/MOL-K	VELOCITY OF SOUND M/SEC
* 63.238	30.98	-4211.	-4193.	68.03	26.94	54.66	1320.
* 65.	30.75	-4114.	-4100.	69.55	27.89	55.69	1246.
70	30.03	-3831.	-3818.	77.73	28.05	57.08	1012.
75	29.27	-3555.	-3531.	77.69	28.23	57.53	983.
80	28.45	-3257.	-3243.	81.41	27.58	57.90	895.
85	27.57	-2966.	-2952.	84.94	27.01	58.60	818.
90	26.64	-2671.	-2656.	88.33	26.58	59.88	746.
* 91.380	26.16	-2588.	-2573.	89.24	26.49	60.37	727.
* 91.380	0.6017	1771.	2400.	143.69	22.64	35.83	182.
100	0.5223	1937.	2699.	146.82	22.00	33.63	194.
110	0.4216	2170.	3027.	149.95	21.38	32.21	207.
120	0.4665	2391.	3345.	152.71	21.33	31.37	218.
130	0.3894	2615.	3656.	155.20	21.18	30.84	228.
140	0.3587	2832.	3962.	157.47	21.08	30.47	238.
150	0.3228	3048.	4266.	159.56	21.01	30.21	247.
160	0.3106	3262.	4567.	161.51	20.96	30.02	256.
180	0.2143	3637.	5164.	165.03	20.90	29.76	272.
200	0.2459	4101.	5758.	168.15	20.46	29.60	288.
220	0.2229	4530.	6348.	170.97	20.84	29.49	302.
240	0.2039	4950.	6937.	173.53	20.83	29.41	316.
260	0.1880	5369.	7525.	175.88	20.82	29.36	327.
280	0.1744	5787.	8112.	178.06	20.82	29.32	342.
300	0.1626	6201.	8698.	180.08	20.82	29.29	355.
350	0.1392	7250.	10161.	184.59	20.85	29.27	382.
400	0.1217	8296.	11626.	188.50	20.92	29.32	408.
450	0.1082	9367.	13094.	191.96	21.06	29.43	433.
500	0.0934	10406.	14570.	195.07	21.24	29.60	455.
600	0.0811	12557.	17554.	200.51	21.76	30.11	497.
700	0.06952	14765.	20595.	205.20	22.40	30.73	535.
800	0.06084	17040.	23702.	209.34	23.07	31.40	569.
900	0.05098	19380.	26874.	213.06	23.72	32.04	602.
1000	0.04868	21783.	30109.	216.49	24.32	32.64	632.
1200	0.04057	26753.	36742.	222.53	25.33	33.65	689.
1400	0.03478	31901.	43554.	227.78	26.11	34.43	741.
1600	0.03064	37186.	50501.	232.42	26.71	35.02	790.
1800	0.02706	42576.	57554.	236.57	27.17	35.48	836.
2000	0.02436	48046.	646687.	240.33	27.52	35.84	886.

* INDICATES TWO PHASE BOUNDARY

7 ATMOSPHERE ISOBAR **THERMODYNAMIC PROPERTIES OF NITROGEN**

TEMPERATURE DEG KELVIN	DENSITY MOLE/L	INTERNAL ENERGY J/MOLE	ENTHALPY J/MOLE	ENTROPY J/MOLE-K	CV	CP	VELOCITY OF SOUND M/SEC
• 63.304	30.99	-4210.	-4187.	68.06	27.13	54.66	1215.
65	30.76	-4116.	-4093.	69.50	28.03	55.62	1245.
70	30.05	-3835.	-3811.	73.69	26.78	56.99	1092.
75	29.29	-3549.	-3525.	77.63	24.34	57.43	984.
80	28.48	-3262.	-3237.	81.35	27.67	57.78	897.
85	27.61	-2972.	-2947.	84.87	27.09	58.44	820.
90	26.68	-2678.	-2652.	88.24	26.66	59.66	749.
• 98.664	24.87	-2148.	-2119.	93.89	26.22	63.85	630.
• 98.664	1.038	1777.	2460.	140.32	23.42	40.21	183.
100	1.014	1814.	2513.	140.45	23.24	39.40	186.
110	0.8755	2076.	2896.	144.40	22.32	35.54	201.
120	0.7775	2318.	3230.	147.40	21.81	33.57	213.
130	0.7027	2550.	3500.	150.04	21.51	32.61	225.
140	0.6428	2776.	3880.	152.41	21.31	31.66	235.
150	0.5934	2998.	4174.	154.58	21.18	31.14	245.
160	0.5517	3218.	4203.	156.58	21.10	30.77	254.
180	0.4848	3650.	5113.	160.17	20.99	30.44	271.
200	0.4331	4078.	5716.	163.34	20.92	29.98	287.
220	0.3918	4503.	6313.	166.19	20.89	29.76	302.
240	0.3579	4926.	6908.	168.78	20.86	29.65	316.
260	0.3295	5347.	7500.	171.15	20.85	29.55	329.
280	0.3054	5768.	8099.	173.33	20.84	29.48	342.
300	0.2847	6188.	8679.	175.37	20.84	29.43	354.
350	0.2435	7236.	10148.	179.90	20.86	29.37	383.
400	0.2128	8284.	11617.	183.82	20.94	29.39	409.
450	0.1891	9337.	13088.	187.29	21.06	29.48	433.
500	0.1701	10397.	14566.	190.40	21.25	29.65	456.
600	0.1418	12550.	17554.	195.85	21.77	30.13	498.
700	0.1215	14760.	20598.	200.54	22.41	30.75	536.
800	0.1063	17036.	23706.	204.69	23.08	31.41	570.
900	0.09454	19377.	26880.	208.42	23.72	32.05	602.
1000	0.08510	21781.	30115.	211.83	24.32	32.65	633.
1200	0.07094	26751.	36700.	217.88	25.33	33.66	689.
1400	0.06082	31900.	43562.	223.13	26.11	34.43	742.
1600	0.05323	37185.	50510.	227.76	26.71	35.03	790.
1800	0.04732	42573.	57563.	231.92	27.17	35.48	837.
2000	0.04260	48046.	64696.	235.67	27.52	35.84	880.

• INDICATES TWO PHASE BOUNDARY

10 ATMOSPHERE ISOBAR

THERMODYNAMIC PROPERTIES OF NITROGEN

TEMPERATURE DEG KELVIN	DENSITY MOLE/L	INTERNAL ENERGY J/MOL	ENTHALPY J/MOL	ENTROPY J/MOL-K	CV J/MOL-K	CP J/MOL-K	VELOCITY OF SOUND M/SEC
* 63.371	30.99	-4209.	-4176.	68.06	27.32	54.62	1311.
65	30.77	-4119.	-4086.	69.46	28.16	55.55	1244.
70	30.07	-3818.	-3805.	73.64	28.90	56.91	1092.
75	29.31	-3533.	-3519.	77.58	28.45	57.33	985.
80	28.51	-3267.	-3231.	81.29	27.77	57.65	898.
85	27.64	-2978.	-2942.	84.80	27.17	58.28	823.
90	26.72	-2666.	-2648.	88.16	26.73	59.44	752.
100	24.64	-2074.	-2032.	94.64	26.23	64.34	617.
* 103.937	23.68	-1815.	-1773.	97.19	26.15	67.96	562.
* 103.937	1.492	1777.	2466.	137.97	24.12	45.28	183.
110	1.339	1997.	2724.	140.39	23.22	46.43	194.
120	1.163	2244.	3106.	143.71	22.36	36.39	209.
130	1.038	2442.	3458.	146.53	21.87	34.28	221.
140	0.9415	2718.	3794.	149.02	21.57	33.01	233.
150	0.8643	2967.	4120.	151.27	21.37	32.17	243.
160	0.8013	3112.	4388.	153.33	21.14	31.58	253.
180	0.6994	3613.	5062.	157.00	21.08	30.83	271.
200	0.6228	4047.	5674.	160.22	20.99	30.39	287.
220	0.5621	4476.	6278.	163.10	20.93	30.09	302.
240	0.5127	4902.	6878.	165.71	20.90	29.89	316.
260	0.4716	5326.	7474.	168.10	20.88	29.75	330.
280	0.368	5748.	8068.	170.30	20.87	29.64	342.
300	0.4069	6170.	8660.	172.34	20.85	29.57	355.
350	0.3477	7221.	10136.	176.89	20.48	29.46	383.
400	0.3038	8273.	11608.	180.82	20.95	29.46	410.
450	0.2718	9321.	13081.	184.30	21.07	29.54	434.
500	0.2427	10369.	14563.	187.42	21.26	29.69	457.
600	0.2022	12564.	17554.	192.87	21.78	30.16	499.
700	0.1734	14755.	20600.	197.56	22.44	30.77	536.
800	0.1517	17022.	23710.	201.71	23.08	31.43	571.
900	0.1349	19374.	26885.	205.45	23.73	32.07	603.
1000	0.1214	21778.	30121.	208.86	24.33	32.66	633.
1200	0.1013	2650.	36757.	214.91	25.34	33.66	690.
1400	0.08682	31899.	43570.	220.16	26.12	34.44	742.
1600	0.07599	37185.	50519.	224.80	26.71	35.03	791.
1800	0.06756	42575.	57572.	228.95	27.17	35.48	837.
2000	0.06082	48046.	64706.	232.71	27.52	35.84	881.

* INDICATES TWO PHASE BOUNDARY

20 ATMOSPHERE ISOBAR **THERMODYNAMIC PROPERTIES OF NITROGEN**

TEMPERATURE DEG KELVIN	DENSITY MOLE/L	INTERNAL ENERGY J/MOL	ENTHALPY J/MOL	ENTROPY J/MOL-K	CV J/MOL-K	CP J/MOL-K	VELOCITY OF SOUND M/SEC
* 63.593	31.00	-4205.	-4140.	68.11	27.92	54.54	1206.
* 65	30.92	-4128.	-4063.	69.32	28.61	55.31	120.
70	30.13	-3849.	-3782.	73.47	29.29	56.63	1093.
75	29.39	-3561.	-3498.	77.40	28.07	57.01	988.
80	28.60	-3283.	-3212.	81.08	28.07	57.26	904.
85	27.76	-2990.	-2925.	84.57	27.43	57.78	830.
90	26.86	-2709.	-2634.	87.90	26.95	58.76	792.
100	24.96	-2110.	-2029.	94.27	26.39	62.84	633.
110	22.17	-1444.	-1358.	100.65	26.23	73.16	499.
* 115.822	20.36	-988.	-888.	104.81	26.45	91.97	403.
* 115.822	3.285	1670.	2287.	132.22	26.40	76.27	178.
120	2.693	1862.	2562.	134.55	25.04	58.48	190.
130	2.176	2210.	3063.	138.57	23.41	44.51	209.
140	2.070	2500.	3479.	141.65	22.56	39.26	226.
150	1.854	2763.	3856.	144.26	22.07	36.49	237.
160	1.689	3012.	4212.	146.55	21.75	34.80	248.
180	1.446	3483.	4885.	150.53	21.38	32.86	266.
200	1.273	3900.	5332.	153.93	21.19	31.80	286.
220	1.140	4384.	6161.	156.93	21.09	31.15	302.
240	1.035	4821.	6780.	159.62	21.02	30.72	317.
260	0.9984	5254.	7391.	162.07	20.97	30.42	331.
280	0.8762	5664.	7997.	164.31	20.44	30.19	344.
300	0.8147	6112.	8599.	166.39	20.93	30.03	357.
350	0.6943	7174.	10933.	171.00	20.93	29.78	386.
400	0.6057	8234.	11580.	174.97	20.99	29.69	412.
450	0.5316	9296.	13064.	178.46	21.11	29.71	437.
500	0.434	10361.	14552.	181.60	21.29	29.83	460.
600	0.4027	12522.	17555.	187.07	21.80	30.25	502.
700	0.3553	14759.	20608.	191.78	22.43	30.84	533.
800	0.3023	17019.	23723.	195.94	23.09	31.47	573.
900	0.2688	19263.	26902.	199.68	23.74	32.10	605.
1000	0.2221	21770.	30142.	203.09	24.34	32.68	636.
1200	0.2019	26744.	36782.	209.14	25.34	33.68	692.
1400	0.1732	31896.	43598.	214.39	26.12	34.45	744.
1600	0.1516	37193.	50548.	219.03	26.72	35.04	793.
1800	0.1348	42574.	57603.	223.19	27.17	35.49	839.
2000	0.1214	48046.	64737.	226.95	27.53	35.84	882.

* INDICATES TWO PHASE BOUNDARY

30 ATMOSPHERE ISOBAR THERMODYNAMIC PROPERTIES OF NITROGEN

TEMPERATURE DEG KELVIN	DENSITY MOL/L	INTERNAL ENERGY J/MOL	ENTHALPY J/MOL	ENTROPY J/MOL-K	CV	CP	VELOCITY OF SOUND M/SFC
* 63.814	31.02	-4202.	-4106.	68.17	28.50	54.47	1283.
65	30.86	-4137.	-4039.	69.18	29.05	55.08	1238.
70	30.19	-3860.	-3760.	73.32	29.68	56.36	1093.
75	29.46	-3580.	-3477.	77.22	29.13	56.70	991.
80	28.69	-3299.	-3133.	80.88	28.36	56.90	909.
85	27.86	-3017.	-2901.	84.34	27.68	57.32	837.
90	26.99	-2732.	-2619.	87.64	27.17	58.14	772.
100	25.07	-2144.	-2023.	93.92	26.54	61.57	648.
110	22.74	-1507.	-1374.	100.10	26.29	69.42	524.
120	19.36	-729.	-572.	107.06	26.62	100.82	369.
* 123.890	16.49	-217.	-13.	111.47	27.81	247.92	262.
* 123.880	6.305	1284.	1767.	125.99	29.34	281.38	173.
130	4.419	1810.	2488.	131.78	25.88	75.67	195.
140	3.502	2230.	3098.	136.24	23.87	50.68	216.
150	3.015	2552.	3561.	139.64	22.89	47.90	231.
160	2.686	2837.	3988.	142.07	22.32	39.03	244.
180	2.244	3351.	4703.	146.47	21.70	35.21	267.
200	1.950	3830.	5389.	150.02	21.40	33.35	286.
220	1.733	4291.	6055.	153.14	21.23	32.27	303.
240	1.565	4740.	6662.	155.92	21.13	31.57	318.
260	1.430	5182.	7309.	158.43	21.06	31.09	332.
280	1.318	5620.	7921.	160.72	21.02	30.75	346.
300	1.223	6053.	8559.	162.83	20.99	30.49	359.
350	1.039	7128.	10053.	167.49	20.98	30.09	368.
400	0.9055	8195.	11552.	171.50	21.02	29.92	415.
450	0.8031	9262.	13047.	175.02	21.14	29.89	440.
500	0.7221	10333.	14543.	178.17	21.31	29.96	463.
600	0.6014	12501.	17556.	183.66	21.82	30.34	504.
700	0.5157	14722.	20617.	188.38	22.44	30.90	542.
800	0.4516	17006.	23731.	192.55	23.11	31.52	576.
900	0.4017	19353.	26920.	196.30	23.75	32.13	608.
1000	0.3618	21761.	30163.	199.71	24.35	32.71	638.
1200	0.3019	26739.	36807.	205.77	25.35	33.69	694.
1400	0.2591	31892.	43625.	211.02	26.13	34.46	746.
1600	0.2269	37181.	50578.	215.66	26.72	35.04	795.
1800	0.2018	42573.	57633.	219.82	27.18	35.49	841.
2000	0.1818	46046.	64759.	223.57	27.53	35.85	884.

* INDICATES TWO PHASE BOUNDARY

40 ATMOSPHERE ISOBAR THERMODYNAMIC PROPERTIES OF NITROGEN

TEMPERATURE DEG KELVIN	DENSITY MOLE/L	INTERNAL ENERGY J/MOL	ENTHALPY J/MOL	ENTROPY J/MOL-K	CV	CP	VELOCITY OF SOUND M/SEC
* 64.035	31.03	-4198.	-4063.	68.22	29.05	54.38	1271.
65	30.91	-4146.	-4015.	69.04	29.47	54.86	1235.
70	30.25	-3871.	-3737.	73.16	30.05	56.11	1094.
75	29.53	-3593.	-3455.	77.05	29.45	56.40	993.
80	28.77	-3314.	-3173.	80.69	28.64	56.55	914.
85	27.97	-3035.	-2890.	84.13	27.92	56.89	846.
90	27.12	-2753.	-2604.	87.40	27.37	57.59	781.
100	25.26	-2176.	-2015.	93.59	26.68	60.49	662.
110	23.07	-1559.	-1383.	99.61	26.35	66.68	545.
120	20.18	-849.	-648.	106.00	26.40	86.12	414.
130	11.39	649.	1005.	119.07	29.64	424.56	196.
140	5.508	1868.	2603.	131.05	25.60	76.06	209.
150	4.416	2305.	3223.	135.33	23.86	52.84	227.
160	3.814	2642.	3705.	138.45	22.95	44.66	242.
180	3.096	3211.	4520.	143.25	22.03	37.92	266.
200	2.653	3718.	5246.	147.08	21.61	35.01	286.
220	2.340	4197.	5929.	150.36	21.38	33.42	304.
240	2.103	4659.	6587.	155.20	21.24	32.44	320.
260	1.914	5111.	7229.	155.77	21.15	31.77	334.
280	1.760	5556.	7859.	158.10	21.09	31.30	348.
300	1.631	5996.	8481.	160.25	21.06	30.95	361.
350	1.383	7082.	10013.	164.98	21.02	30.40	391.
400	1.203	8157.	11526.	169.02	21.06	30.14	418.
450	1.066	9230.	13030.	172.56	21.17	30.05	443.
500	0.9586	10305.	14533.	175.73	21.34	30.09	465.
600	0.7984	12480.	17557.	181.24	21.84	30.43	507.
700	0.6847	14706.	20625.	185.97	22.46	30.96	544.
800	0.5997	16993.	23751.	190.14	23.12	31.50	579.
900	0.5336	19343.	2693d.	193.89	23.76	32.17	610.
1000	0.4808	21753.	3083.	197.31	24.35	32.74	640.
1200	0.4014	26733.	36832.	203.37	25.36	33.71	696.
1400	0.3445	31889.	42653.	208.63	26.13	34.47	748.
1600	0.3018	37179.	50607.	213.27	26.73	35.05	797.
1800	0.2686	42572.	57664.	217.42	27.18	35.50	842.
2000	0.2419	48045.	64800.	221.18	27.53	35.85	886.

* INDICATES TWO PHASE BOUNDARY

TO ATMOSPHERE 150 BAR THERMODYNAMIC PROPERTIES OF NITROGEN

TEMPERATURE DEG KELVIN	DENSITY MOLE/L	INTERNAL ENERGY J/MOL	ENTHALPY J/MOL	ENTROPY J/MOL-K	CV J/MOL-K	CP J/MOL-K	VELOCITY OF SOUND M/SEC
• 64.693	31.07	-4187.	-3959.	68.39	30.56	54.12	1241.
65	31.06	-4171.	-3942.	68.65	30.67	54.25	1230.
70	30.41	-3901.	-3668.	72.72	31.09	55.38	1096.
75	29.74	-3629.	-3390.	76.55	30.34	55.59	1002.
80	29.02	-3350.	-3112.	80.14	29.40	55.62	939.
85	28.27	-3081.	-2834.	83.51	28.37	55.77	867.
90	27.48	-2812.	-2554.	86.71	27.93	56.18	807.
90	25.78	-2255.	-1984.	92.71	27.07	58.01	700.
100	23.87	-1688.	-1388.	98.39	26.37	61.47	559.
110	21.65	-1073.	-745.	103.98	26.27	67.81	499.
120	18.92	-384.	-8.	109.88	26.23	81.88	391.
130	14.72	466.	947.	116.94	26.66	109.16	286.
140	10.49	1333.	2009.	124.27	26.19	95.15	248.
150	8.112	1967.	2821.	129.52	24.77	69.19	251.
160	5.956	2756.	3947.	136.18	23.00	47.81	272.
180	4.893	3370.	4820.	140.78	22.20	40.51	293.
200	4.221	3911.	5592.	144.46	21.79	37.04	311.
220	3.742	4415.	6311.	147.59	21.55	35.05	327.
240	3.377	4898.	6998.	150.35	21.40	33.78	342.
260	3.066	5366.	7665.	152.81	21.30	32.90	356.
280	2.847	5825.	8316.	155.06	21.23	32.27	370.
300	2.399	6945.	9902.	159.95	21.15	31.29	400.
350	2.081	8045.	11453.	164.10	21.17	30.78	427.
400	1.842	9135.	12985.	167.70	21.16	30.54	451.
450	1.655	10224.	14509.	170.92	21.42	30.47	476.
500	1.378	12419.	17564.	176.49	21.70	30.68	516.
600	1.163	14658.	20654.	181.25	22.21	31.13	552.
700	1.037	16954.	23794.	185.44	23.16	31.69	586.
800	0.9235	19312.	26992.	189.21	23.79	32.26	618.
900	0.8327	21728.	30246.	192.64	24.38	32.81	648.
1000	0.6961	26717.	36907.	198.70	25.38	33.76	703.
1200	0.5982	31879.	43735.	203.97	26.15	34.50	754.
1400	0.5245	37173.	50695.	208.61	26.74	35.07	802.
1600	0.4671	42569.	57756.	212.77	27.19	35.51	848.
1800	0.4210	48045.	64894.	216.53	27.55	35.86	891.

• INDICATES TWO PHASE BOUNDARY

100 ATMOSPHERE ISOBAR THERMODYNAMIC PROPERTIES OF NITROGEN

TEMPERATURE DEG KELVIN	DENSITY MOL/L	INTERNAL ENERGY J/MOL	ENTHALPY J/MOL	ENTROPY J/MOL-K	CV J/MOL-K	CP J/MOL-K	VELOCITY OF SOUND M/SEC
* 65.346	31.12	-4176.	-3860.	68.56	31.87	53.82	1217.
70	30.57	-3929.	-3597.	72.30	32.03	54.73	1101.
75	29.93	-3661.	-3327.	76.09	31.14	54.86	1012.
80	29.25	-3395.	-3049.	79.63	30.08	54.91	943.
85	28.54	-3130.	-2775.	82.95	29.14	54.96	884.
90	27.80	-2864.	-2500.	86.09	28.41	55.07	831.
100	26.22	-2331.	-1944.	91.94	27.41	56.23	733.
110	24.50	-1786.	-1372.	97.40	26.79	58.39	643.
120	22.60	-1221.	-773.	102.61	26.34	61.70	557.
130	20.44	-628.	-132.	107.73	26.00	66.83	474.
140	17.93	7.	572.	112.95	25.77	74.21	394.
150	15.08	676.	1347.	118.29	25.58	79.33	332.
160	12.44	1308.	2123.	123.30	25.12	74.28	301.
180	9.008	2295.	3420.	130.96	23.67	56.15	295.
200	7.217	3022.	4426.	136.27	22.68	45.72	308.
220	6.129	3630.	5233.	140.36	22.13	40.47	324.
240	5.382	4177.	6000.	143.74	21.81	37.51	339.
260	4.826	4691.	6700.	146.67	21.61	35.65	354.
280	4.392	5183.	7430.	149.26	21.48	34.39	367.
300	4.040	5660.	8168.	151.60	21.39	33.59	380.
350	3.389	6814.	9804.	156.65	21.27	32.10	410.
400	2.935	7936.	11369.	160.88	21.26	31.37	437.
450	2.596	9043.	12947.	164.55	21.34	30.99	461.
500	2.331	10145.	14422.	167.80	21.49	30.83	484.
600	1.942	12359.	17575.	173.43	21.95	30.91	524.
700	1.668	14611.	20666.	178.22	22.55	31.30	561.
800	1.464	16917.	23880.	182.43	23.20	31.81	594.
900	1.305	19202.	27048.	186.21	23.83	32.36	625.
1000	1.177	21704.	30311.	189.65	24.41	32.88	655.
1200	0.9856	26701.	36983.	195.73	25.40	33.80	709.
1400	0.8479	31868.	43819.	200.99	26.17	34.53	760.
1600	0.7441	37167.	50784.	205.64	26.75	35.09	808.
1800	0.6631	42567.	57848.	209.80	27.21	35.53	853.
2000	0.5980	48045.	64989.	213.56	27.56	35.87	896.

* INDICATES TWO PHASE BOUNDARY

200 ATMOSPHERE ISOBAR THERMODYNAMIC PROPERTIES OF NITROGEN

TEMPERATURE DEG KELVIN	DENSITY MOLE/L	INTERNAL ENERGY J/MOL	ENTHALPY J/MOL	ENTROPY J/MOL-K	CV J/MOL-K	CP J/MOL-K	VELOCITY OF SOUND M/SEC
• 67.486	31.30	-4131.	-3486.	69.16	34.96	52.65	1170.
70	31.04	-4006.	-3353.	71.09	34.59	52.85	1121.
75	30.50	-3753.	-3089.	74.74	33.27	52.82	1066.
80	29.32	-3502.	-2825.	78.14	31.85	52.65	989.
85	29.32	-3223.	-2562.	81.33	30.62	52.52	962.
90	28.69	-3008.	-2300.	84.33	29.44	52.47	900.
100	27.38	-2514.	-1774.	89.87	28.78	52.68	824.
110	26.01	-2024.	-1245.	94.91	27.40	53.22	755.
120	24.60	-1533.	-709.	99.57	26.75	53.94	690.
130	23.14	-1022.	-166.	103.92	26.19	54.69	631.
140	21.66	-552.	386.	108.00	25.69	55.36	578.
150	20.12	-67.	940.	111.83	25.22	55.83	521.
160	18.61	410.	1499.	115.44	24.78	55.86	492.
170	15.77	1316.	2601.	121.93	24.00	53.84	437.
200	13.42	2128.	3639.	127.40	23.33	49.78	412.
220	11.61	2866.	4592.	131.95	22.91	45.64	404.
240	10.24	3411.	5470.	135.77	22.42	42.28	405.
260	9.196	4083.	6289.	139.05	22.15	39.75	411.
280	8.352	4338.	7064.	141.92	21.96	37.88	419.
300	7.676	5167.	7807.	144.49	21.82	36.47	428.
350	6.429	6517.	9569.	149.92	21.62	34.21	451.
400	5.568	7605.	11245.	154.40	21.55	32.95	474.
450	4.929	8761.	12873.	158.23	21.59	32.22	496.
500	4.433	9801.	14473.	161.61	21.70	31.82	517.
600	3.707	1271.	17638.	167.38	22.12	31.59	555.
700	3.195	1463.	20805.	172.26	22.69	31.79	589.
800	2.813	16799.	24003.	176.53	23.31	32.18	621.
900	2.515	1986.	27244.	180.35	23.93	32.64	651.
1000	2.276	2126.	30532.	183.81	24.50	33.11	679.
1200	1.914	26550.	37240.	189.92	25.47	33.95	732.
1400	1.652	31836.	44100.	195.21	26.22	34.63	781.
1600	1.454	37448.	51081.	199.87	26.80	35.16	827.
1800	1.299	42557.	58156.	204.04	27.25	35.58	871.
2000	1.174	48043.	65306.	207.80	27.59	35.90	913.

• INDICATES TWO PHASE BOUNDARY

100 ATMOSPHERE ISOBAR THERMODYNAMIC PROPERTIES OF NITROGEN

TEMPERATURE DEG KELVIN	DENSITY MOLE/L	INTERNAL ENERGY J/MOL	ENTHALPY J/MOL	ENTROPY J/MOL-K	CV J/MOL-K	CP J/MOL-K	VELOCITY OF SOUND M/SEC
* 69.576	31.49	-6086.	-1121.	69.77	36.58	51.28	1154.
70	31.45	-4666.	-3099.	70.09	36.46	51.28	1147.
75	30.99	-3824.	-2843.	73.62	34.78	51.12	1082.
80	30.49	-3585.	-2588.	76.91	33.07	50.92	1033.
85	29.96	-3348.	-2334.	80.00	31.63	50.78	994.
90	29.40	-3116.	-2080.	82.90	30.48	50.71	959.
100	28.26	-2649.	-1573.	88.24	28.89	50.68	897.
110	27.08	-2158.	-1066.	93.07	27.88	50.77	839.
120	25.89	-1732.	-558.	97.49	27.15	50.88	784.
130	24.69	-1280.	-49.	101.57	26.55	50.94	734.
140	23.48	-834.	-461.	105.34	26.02	50.88	689.
150	22.29	-395.	-969.	108.85	25.53	50.67	649.
160	21.12	34.	1474.	112.11	25.08	50.30	614.
180	16.89	859.	2468.	117.96	24.30	49.04	558.
200	16.86	1630.	3431.	122.04	23.67	47.14	521.
220	15.15	2346.	4352.	127.43	23.19	46.92	499.
240	13.70	3009.	5228.	132.24	22.81	42.74	487.
260	12.49	3629.	6063.	135.58	22.53	40.81	483.
280	11.48	4215.	6862.	137.55	22.32	39.18	483.
300	10.63	4773.	7632.	140.20	22.15	37.84	486.
350	9.07	6085.	9460.	145.84	21.90	35.46	500.
400	7.852	7322.	11193.	150.47	21.79	34.00	517.
450	6.984	8516.	12869.	154.42	21.60	33.10	535.
500	6.304	9687.	14509.	157.88	21.89	32.55	553.
600	5.302	1203.	17737.	163.77	22.28	32.13	587.
700	4.591	14329.	20951.	168.72	22.82	32.19	619.
800	4.056	16690.	24184.	173.04	23.42	32.49	648.
900	3.638	19097.	27452.	176.89	24.02	32.89	676.
1000	3.201	21553.	30762.	180.37	24.58	33.30	703.
1200	2.799	26601.	37502.	186.51	25.54	34.08	754.
1400	2.416	31806.	44384.	191.82	26.28	34.72	801.
1600	2.113	37129.	51380.	196.49	26.85	35.22	846.
1800	1.910	42548.	58466.	200.66	27.28	35.62	889.
2000	1.729	48042.	65624.	204.43	27.62	35.94	929.

400 ATMOSPHERE ISOBAR THERMODYNAMIC PROPERTIES OF NITROGEN

TEMPERATURE DEG KELVIN	DENSITY MOLE/L	INTERNAL ENERGY J/MOL	ENTHALPY J/MOL	ENTROPY J/MOL-K	CV J/MOL-K	CP J/MOL-K	VELOCITY OF SOUND M/SEC
• 71.413	31.69	-4036.	-2157.	70.38	37.20	49.80	1155.
75	31.41	-3879.	-2589.	72.68	35.83	49.59	1118.
80	30.97	-3650.	-2342.	75.87	33.92	49.39	1075.
85	30.50	-3424.	-2095.	78.86	32.33	49.31	1041.
90	30.01	-3199.	-1848.	81.64	31.07	49.39	1012.
100	28.98	-2754.	-1355.	86.87	29.35	49.30	959.
110	27.93	-2314.	-9663.	91.57	28.26	49.26	909.
120	26.87	-1879.	-70.	95.85	27.50	49.17	861.
130	25.81	-1450.	121.	99.78	26.89	49.00	816.
140	24.76	-1027.	603.	103.41	26.36	48.73	775.
150	23.74	-613.	1095.	106.76	25.88	48.35	738.
160	22.73	-207.	1576.	109.86	25.44	47.87	705.
180	20.82	575.	2522.	115.43	24.67	46.67	651.
200	19.07	1316.	3441.	120.28	24.05	45.23	612.
220	17.50	2015.	4331.	122.52	23.55	43.69	584.
240	16.12	2676.	5189.	128.25	23.17	42.14	566.
260	14.91	3299.	6017.	131.57	22.87	40.70	555.
280	13.87	3895.	6818.	135.54	22.63	39.40	549.
300	12.96	4466.	7594.	137.21	22.45	38.27	547.
350	11.15	5813.	9450.	142.94	22.15	36.09	551.
400	9.807	7083.	11215.	147.66	22.01	34.64	561.
450	8.778	8305.	12922.	151.68	21.99	33.69	575.
500	7.962	9479.	14590.	155.19	22.06	33.09	590.
600	6.741	11853.	17666.	161.17	22.61	32.55	620.
700	5.866	14207.	21116.	161.18	22.94	32.52	648.
800	5.204	16590.	23379.	170.53	23.52	32.76	676.
900	4.682	19015.	27671.	174.41	24.11	33.10	702.
1000	4.260	21485.	31000.	177.92	24.66	33.48	728.
1100	3.910	24000.	34367.	181.13	25.16	33.85	752.
1200	3.614	26595.	37169.	184.09	25.40	34.20	776.

• INDICATES TWO PHASE BOUNDARY

700 ATMOSPHERE ISOBAR

THE THERMODYNAMIC PROPERTIES OF NITROGEN

TEMPERATURE DEG KELVIN	DENSITY MOLE/L	INTERNAL ENERGY J/MOL	ENTHALPY J/MOL	ENTROPY J/MOL-K	CV J/MOL-K	CP J/MOL-K	VELOCITY OF SOUND M/SEC
• 77.471	32.29	-3879.	-1683.	72.05	36.04	45.30	1208.
80	32.13	-3776.	-1568.	73.51	34.99	45.24	1192.
85	31.79	-3573.	-1342.	76.25	33.23	45.39	1167.
90	31.41	-3372.	-1114.	78.85	31.90	45.73	1145.
100	30.61	-2970.	-653.	83.71	30.13	46.40	1103.
110	29.77	-2570.	-181.	84.15	29.07	46.70	1071.
120	28.93	-2172.	280.	92.21	28.35	46.65	1034.
130	28.10	-1779.	745.	95.94	27.79	46.41	998.
140	27.29	-1392.	1207.	99.37	27.31	46.03	964.
150	26.50	-1012.	1665.	102.53	26.88	45.57	932.
160	25.73	-638.	2119.	105.45	26.47	45.05	903.
180	24.26	-85.	3009.	110.69	25.74	43.93	852.
200	22.90	779.	3875.	115.26	25.12	42.78	812.
220	21.65	1444.	4727.	119.29	24.59	41.68	780.
240	20.50	2083.	5543.	122.87	24.15	40.66	756.
260	19.44	2698.	634.	126.09	23.79	39.73	736.
280	18.48	3294.	7133.	129.00	23.49	38.88	722.
300	17.59	3871.	7903.	131.65	23.25	38.12	711.
350	15.71	5551.	9761.	137.41	22.82	36.54	697.
400	14.19	6564.	11566.	142.25	22.59	35.37	693.
450	12.94	7830.	13310.	146.32	22.49	34.52	695.
500	11.91	9066.	15020.	149.92	22.51	33.94	701.
600	10.30	11493.	18379.	156.05	22.78	33.33	717.
700	9.098	13907.	21703.	161.17	23.24	33.21	737.
800	8.163	16339.	25028.	165.61	23.79	33.36	758.
900	7.412	18005.	28376.	169.55	24.34	33.59	779.
1000	6.795	23309.	31749.	173.11	24.84	33.89	800.
1100	6.277	23853.	35153.	176.35	25.34	34.20	821.
1200	5.836	26334.	38588.	179.34	25.76	34.50	842.

• INDICATES TWO PHASE BOUNDARY

1000 ATMOSPHERE ISOBAR **THERMODYNAMIC PROPERTIES OF NITROGEN**

TEMPERATURE DEG KELVIN	DENSITY MOL/L.	INTERNAL ENERGY J/MOL	ENTHALPY J/MOL	ENTROPY J/MOL-K	CV	CP	VELOCITY OF SOUND M/SEC
* 82.997	32.85	-3725.	-640.	73.42	33.68	41.54	1285.
85	32.74	-3621.	-557.	74.41	33.07	41.72	1277.
90	32.45	-3469.	-346.	76.81	31.87	42.40	1258.
100	31.80	-3101.	85.	81.36	30.39	43.93	1226.
110	31.10	-2726.	530.	85.60	29.56	44.95	1195.
120	30.37	-2354.	982.	89.53	28.99	45.36	1163.
130	29.66	-1980.	1436.	93.17	28.54	45.33	1131.
140	28.96	-1611.	1888.	96.52	28.14	45.04	1101.
150	28.28	-1447.	2336.	99.61	27.75	44.62	1072.
160	27.62	-889.	2780.	102.47	27.38	44.12	1045.
180	26.37	-191.	3652.	107.61	26.68	43.05	998.
200	25.20	481.	4502.	112.09	26.05	41.98	956.
220	24.11	1129.	5332.	116.06	25.49	40.97	925.
240	23.10	1756.	6142.	119.57	25.01	40.06	899.
260	22.16	2263.	6935.	122.74	24.60	39.23	877.
280	21.29	2953.	7712.	125.62	24.25	38.50	860.
300	20.48	3557.	8475.	128.25	23.96	37.84	846.
350	16.69	4710.	10332.	133.98	23.42	36.51	822.
400	17.18	6224.	12131.	138.79	23.09	35.51	810.
450	15.90	7516.	13888.	142.93	22.93	34.79	804.
500	14.81	8770.	15614.	146.56	22.89	34.28	803.
600	13.03	11334.	19010.	152.76	23.09	33.74	810.
700	11.66	13683.	22375.	157.95	23.50	33.61	822.
800	10.56	16146.	25740.	162.44	24.01	33.71	836.
900	9.667	18846.	29121.	166.42	24.54	33.93	853.
1000	8.921	21169.	32528.	170.01	25.04	34.20	870.
1100	8.287	23335.	35962.	173.28	25.50	34.48	888.
1200	7.742	26315.	39423.	176.29	25.91	34.74	906.

* INDICATES TWO PHASE BOUNDARY

2000 ATMOSPHERE ISOBAR

THERMODYNAMIC PROPERTIES OF NITROGEN

TEMPERATURE DEG KELVIN	DENSITY MOL/L	INTERNAL ENERGY J/MOL	ENTHALPY J/MOL	ENTROPY J/MOL-K	CV J/MOL-K	CP J/MOL-K	VELOCITY OF SOUND M/SEC
* 99.618	34.36	-3253.	2645.	76.42	28.98	35.29	1530.
100	36.34	-3242.	2659.	76.56	29.00	35.43	1525.
110	33.93	-2943.	3031.	80.10	29.59	38.84	1496.
120	32.45	-2835.	3433.	83.60	30.02	41.37	1465.
130	32.95	-296.	3855.	86.98	30.21	42.90	1435.
140	32.44	-1660.	4288.	90.19	30.20	43.63	1408.
150	31.93	-1622.	4725.	93.20	30.06	43.80	1363.
160	31.43	-1885.	5163.	96.03	29.82	43.64	1360.
160	30.48	-621.	6029.	101.12	29.21	42.82	1319.
170	29.59	26.	6874.	115.58	28.55	41.81	1286.
220	28.76	655.	7700.	109.52	27.90	40.81	1254.
240	27.98	1265.	8507.	113.03	27.30	39.89	1228.
260	27.25	1861.	9297.	116.19	26.76	39.08	1205.
280	26.56	2641.	10071.	119.06	26.28	38.37	1186.
300	25.91	3010.	10832.	121.69	25.86	37.75	1169.
350	26.41	4385.	12687.	127.41	25.03	36.51	1136.
400	23.09	5711.	14490.	132.22	26.47	35.64	1112.
450	23.90	7003.	16256.	136.38	24.12	35.04	1096.
500	20.84	8271.	17997.	140.05	23.94	34.63	1084.
600	19.00	10773.	21437.	146.33	23.92	34.25	1071.
700	17.48	13265.	24858.	151.60	24.20	34.22	1066.
800	16.20	15773.	28286.	156.18	24.61	34.36	1067.
900	15.10	18311.	31733.	160.24	25.06	34.58	1072.
1000	14.15	20883.	35206.	163.89	25.51	34.83	1080.
1100	13.32	23448.	38699.	167.22	25.92	35.08	1089.
1200	12.59	2626.	42218.	170.29	26.29	35.30	1100.

* INDICATES TWO PHASE BOUNDARY

4000 ATMOSPHERE ISOBAR THERMODYNAMIC PROPERTIES OF NITROGEN

TEMPERATURE DEG KELVIN	DENSITY MOL/L	INTERNAL ENERGY J/MOL	ENTHALPY J/MOL	ENTROPY J/MOL-K	CV J/MOL-K	CP J/MOL-K	VELOCITY OF SOUND M/SEC
127.569	36.51	-2335.	8766.	80.05	29.12	33.62	1850.
130	36.45	-2270.	8849.	80.69	29.59	34.53	1840.
140	36.18	-1991.	9211.	83.37	31.08	37.71	1803.
150	35.88	-1695.	9800.	86.06	31.98	40.00	1771.
160	35.56	-1390.	10003.	88.69	32.40	41.50	1744.
180	34.89	-763.	10654.	93.67	32.47	42.78	1699.
200	34.22	-133.	11710.	98.18	31.97	42.70	1665.
220	33.58	488.	12558.	102.22	31.27	42.03	1638.
240	32.97	1096.	13390.	105.84	30.53	41.15	1616.
260	32.39	1690.	14204.	109.10	29.81	40.26	1597.
280	31.84	2270.	15001.	112.05	29.15	39.43	1581.
300	31.32	2839.	15782.	114.75	28.55	38.58	1566.
350	30.11	4213.	17676.	120.59	27.33	37.18	1536.
400	29.01	5538.	19507.	125.48	26.45	36.14	1511.
450	28.01	6828.	21293.	129.70	25.85	35.45	1492.
500	27.09	8095.	23056.	133.41	25.45	35.01	1475.
600	25.43	10597.	26534.	139.75	25.14	36.63	1450.
700	23.98	13094.	29996.	145.09	25.20	34.66	1433.
800	22.70	15613.	33472.	149.73	25.67	34.87	1422.
900	21.55	18166.	36972.	153.85	25.81	35.15	1415.
1000	20.53	20756.	40501.	157.57	26.17	35.43	1413.
1100	19.60	23382.	44058.	160.96	26.52	35.70	1413.
1200	18.76	26041.	47640.	164.07	26.84	35.94	1415.

* INDICATES TWO PHASE BOUNDARY

7000 ATMOSPHERIC ISOBAR THERMODYNAMIC PROPERTIES OF NITROGEN

TEMPERATURE DEG KELVIN	DENSITY MOL/L	INTERNAL ENERGY J/MOL	ENTHALPY J/MOL	ENTROPY J/MOL-K	CV J/MOL-K	CP J/MOL-K	VELOCITY OF SOUND M/SEC
4162.127	36.88	-828.	17417.	84.17	30.63	33.10	2163.
180	3d.5%	-334.	18047.	87.85	32.79	37.13	2102.
200	38.19	248.	16813.	91.91	33.71	39.80	2053.
220	37.76	843.	19630.	95.78	33.73	41.05	2016.
240	37.30	1439.	20455.	99.37	33.29	41.38	1989.
260	36.84	2029.	21281.	102.67	32.65	41.17	1968.
280	36.39	2610.	22100.	107.71	31.95	40.68	1952.
300	35.96	3181.	22908.	108.49	31.25	42.06	1939.
350	34.93	4563.	24871.	111.55	29.70	38.49	1914.
400	33.99	5891.	26762.	119.60	28.51	37.21	1896.
450	33.12	7181.	28598.	123.93	27.64	36.30	1881.
500	32.31	8444.	30397.	127.72	27.04	35.69	1866.
600	30.86	10932.	31930.	136.16	26.42	35.11	1844.
700	29.52	13412.	31436.	139.57	26.27	35.06	1825.
800	28.33	15914.	40950.	146.26	26.38	35.26	1809.
900	27.24	18452.	44490.	148.43	26.61	35.56	1797.
1000	26.24	21030.	48062.	152.19	26.88	35.88	1788.
1100	25.32	23647.	51665.	155.62	27.16	36.18	1782.
1200	24.46	26301.	55297.	158.78	27.42	36.45	1779.

♦ INDICATES TWO PHASE BOUNDARY

10000 ATMOSPHERE 150 BAR THERMODYNAMIC PROPERTIES OF NITROGEN

TEMPERATURE DEG KELVIN	DENSITY MOLE/L	INTERNAL ENERGY J/MOL	ENTHALPY J/MOL	ENTROPY J/MOL-K	CV	CP	VELOCITY OF SOUND M/SEC
*191.605	40.76	773.	25634.	87.49	30.22	31.52	2404.
200	40.68	997.	25906.	88.87	31.30	33.19	2374.
220	40.44	1545.	26602.	92.19	32.87	36.24	2319.
240	40.14	2107.	27149.	95.43	33.47	38.19	2280.
260	39.81	2674.	28124.	98.54	33.49	39.30	2251.
280	39.46	3240.	28915.	101.47	33.18	39.79	2230.
300	39.11	3802.	29713.	104.22	32.69	39.87	2214.
320	38.21	5175.	31693.	110.33	31.27	39.16	2188.
350	37.36	6502.	33624.	115.49	29.98	38.10	2172.
400	36.56	7790.	35504.	119.92	28.96	37.15	2160.
450	35.81	9050.	37543.	123.79	28.22	36.44	2151.
500	34.45	11525.	40942.	130.36	27.37	35.66	2134.
600	33.21	13986.	44495.	135.83	27.06	35.47	2118.
700	32.09	16467.	48046.	140.57	27.06	35.59	2104.
800	31.05	18983.	51618.	146.78	27.20	35.86	2092.
900	30.09	21540.	55219.	148.58	27.41	36.18	2082.
1000	29.19	24139.	58853.	152.04	27.64	36.49	2074.
1100	28.35	26775.	62316.	155.23	27.86	36.78	2068.
1200							